Universitat Autònoma de Barcelona

Design and development of molecularly imprinted polymers for electronic tongues and biosensing

Anna Herrera Chacón

Universitat Autònoma de Barcelona

Design and development of molecularly imprinted polymers for electronic tongues and biosensing

Anna Herrera Chacón

Doctoral Thesis

Doctoral Studies in Chemistry

Director: Prof. Manel del Valle Zafra

Departament de Química

Unitat de Química Analítica

Facultat de Ciències

2021

Declaration

Thesis submitted to aspire for the doctoral degree

Anna Herrera Chacón

Director's approval:

Prof. Manel del Valle Zafra

Bellaterra (Cerdanyola del Vallès), 28 October 2021

Funding Acknowledgement

This present Thesis has been carried out in the laboratories of the Group of Sensors and Biosensors of the Chemistry Department in the *Universitat Autònoma de Barcelona,* with the financial support of the Ministry of Economy and Innovation (MINECO), which funded the projects:

- "Electronic tongue fingerprinting: aplicaciones en el campo alimentario y de seguridad" MCINN, CTQ2013-41577-P.
- "Lenguas electrónicas con transducción electroquímica. Explorando nuevas aplicaciones" MCINN, CTQ2016-800170-P.
- "Lenguas electrónicas con sistemas de reconocimiento mejorados" MCINN, PID2019-107102RB-C21

Grup de Sensors i Biosensors

Unitat de Química Analítica

Departament de Química

Universitat Autònoma de Barcelona

Edifici, Cn 08193, Bellaterra

“To Manel for giving me the opportunity to start the PhD.

To my mother and parents in law, for their help and support.

To Andreu, for always being there”

The research produced during this thesis has produced the following publications included in the compendium:

- Article 1 - Herrera-Chacon, A., González-Calabuig, A., Campos, I., & del Valle, M. (2018). Bioelectronic tongue using MIP sensors for the resolution of volatile phenolic compounds. Sensors and Actuators B: Chemical, 258, 665-671.
- Article 2 - Herrera-Chacón, A., Dinç-Zor, Ş., & del Valle, M. (2020). Integrating molecularly imprinted polymer beads in graphite-epoxy electrodes for the voltammetric biosensing of histamine in wines. Talanta, 208, 120348.
- Article 3 - Herrera-Chacon, A., Gonzalez-Calabuig, A., & del Valle, M. (2021). Dummy Molecularly Imprinted Polymers Using DNP as a Template Molecule for Explosive Sensing and Nitroaromatic Compound Discrimination. Chemosensors, 9(9), 255.

The research produced during this thesis has produced the following publications included out the compendium:

- Proceedings 1 -Herrera-Chacon, A., González-Calabuig, A., Bates, F., Campos, I., & del Valle, M. (2017, May). Novel voltammetric electronic tongue approach using polyelectrolyte modifiers to detect charged species. In 2017 ISOCS/IEEE International Symposium on Olfaction and Electronic Nose (ISOEN) (pp. 1-3). IEEE.
- Article 4 -Herrera-Chacón, A., Torabi, F., Faridbod, F., Ghasemi, J. B., González-Calabuig, A., & Del Valle, M. (2019). Voltammetric electronic tongue for the simultaneous determination of three benzodiazepines. Sensors, 19(22), 5002.
- Review 1 - Herrera-Chacón, A., Cetó, X., & Del Valle, M. (2021). Molecularly imprinted polymers-towards electrochemical sensors and electronic tongues. Analytical and Bioanalytical Chemistry, 1-24.
- Article 5 - Herrera-Chacón, A., Rodríguez-Franch, E., Borrego-Muñoz, C., Cetó, X., & Del Valle, M. (202X). Biomimetic electronic tongue using MIP sensors for the quantification of biogenic amines (Manuscript submitted).

Summary

ABSTRACT

This doctoral thesis aims to unite three fields of scientific knowledge: molecular imprinting technology, the use of electrochemical sensors and the development of chemometric tools, specifically the electronic tongue approach (ET). This combination makes it possible to process and discern useful data from redundant data in order to obtain unequivocal analytical parameters for the development of applications with a real impact on the improvement of society. This work has been carried out in the Group of Sensors and Biosensors (GSB) of the Autonomous University of Barcelona (UAB) continuing the research path focused on the application of electronic tongues for the resolution of complex mixtures for different applications.

Versatility, portability and energy and time efficiency have been a constant in the established and thriving world of sensors and biosensors. Compared to conventional methods, sensors provide us with a wide range of features that make it easier to obtain real analytical information. When combined with the sensing performance, their own response can have added value by improving analytical parameters such as linear range, sensitivity or limits of detection and quantification. At the same time, electrochemistry offers an array of benefits by presenting large data acquisition in a small-time frame, easily and in a portable manner. However, this response can be non-specific, superfluous and requires planning and further data processing to obtain useful and clear analytical information. Therefore, the use of chemometric tools in addition to the performance of electrochemical sensing helps us to discern important data from redundant data, making their combination a valuable ally.

Sensing performance can be limited by the construction of the sensor itself, so the improvement of the different components of a sensor is constantly evolving.

The inclusion of new materials to improve the performance of these sensors generates a wide field of study, either by the incorporation of materials of a synthetic or biological nature.

In this compendium, the use of molecularly imprinted polymers is presented as the main focus of the manuscript to improve the response in the field of electrochemical sensors, specifically in the specificity of the sensor. Such polymers can be used as biomimetic recognition elements improving the baseline performance of a common sensor in different fields of application in a robust way over a wide period of time, not limited only to strict physiological conditions.

This manuscript presents applications in three distinct fields: (1) in beverage production to detect and quantify ethylphenols during winemaking; (2) in the conservation and preservation of food products with the aim of determining the presence and proliferation of histamine in wines; and finally, (3) in the field of safety and environment for the detection and quantification of TNT and its nitroaromatic derivatives as emerging contaminants.

RESUMEN

Esta tesis doctoral pretende unir tres campos del conocimiento científico: la tecnología de impresión molecular, el uso de sensores electroquímicos y el desarrollo de herramientas quimiométricas, especialmente la aplicación de lengua electrónica. Esta combinación permite procesar y discernir los datos útiles de los redundantes con la finalidad de obtener parámetros analíticos inequívocos para el desarrollo de aplicaciones con impacto real en la mejora de la sociedad. Este trabajo se ha realizado en el Grupo de Sensores y Biosensores (GSB) de la Universidad Autónoma de Barcelona (UAB) continuando la senda investigadora focalizada en la aplicación de lenguas electrónicas para la resolución de mezclas complejas para diferentes aplicaciones.

La versatilidad, portabilidad, la eficiencia energética y temporal han sido una constante en el asentado y pujante mundo de los sensores y biosensores. En comparación con los métodos convencionales los sensores nos aportan un amplio abanico de prestaciones que nos facilitan la obtención real de información analítica. Si esta se combina con las prestaciones del sensado, su propia respuesta puede tener un valor añadido al mejorar los parámetros analíticos como serian el rango lineal, la sensibilidad o los límites de detección y cuantificación. Al mismo tiempo, la electroquímica ofrece un conjunto de prestaciones al presentar una gran adquisición de datos en un espacio temporal reducido, fácilmente y de manera portátil. Sin embargo, esta respuesta puede ser inespecífica, superflua y requiere de una planificación y un posterior tratamiento de datos para obtener información analítica útil y nítida. Por ello, el uso de herramientas quimiométricas además de las prestaciones del sensado electroquímico nos ayuda a discernir aquellos datos importantes de los redundantes, siendo así, su combinación una valiosa aliada.

Las prestaciones del sensado pueden verse limitadas por la propia construcción del sensor, por ello, la constante mejora del principal componente de un sensor está en permanente evolución. La inclusión de nuevos materiales para mejorar las prestaciones de dichos sensores genera un amplio campo de estudio, ya sea por la incorporación de materiales de naturaleza sintética o biológica.

En el presente compendio, se presenta el uso de los polímeros molecularmente impresos como eje conductor del manuscrito para mejorar la respuesta en el campo de los sensores electroquímicos, especialmente en la especificidad del sensor. Dichos polímeros, pueden usarse como elementos de reconocimiento biomiméticos mejorando las prestaciones basales de un sensor común en diferentes campos de aplicación de un modo robusto en un amplio periodo de tiempo, sin limitarse solamente a las estrictas condiciones fisiológicas.

En este manuscrito se presentan aplicaciones en tres campos diferenciados: (1) en la producción de bebidas para detectar y cuantificar etilfenoles durante la elaboración de vino; (2) en la conservación y preservación de productos alimentarios con el objetivo de determinar la presencia y proliferación de histamina en vinos; y finalmente, (3) en el campo de la seguridad y el medio ambiente para la detección y cuantificación de TNT y sus derivados nitroaromáticos como contaminantes emergentes.

RESUM

En aquesta tesi doctoral convergeixen tres camps del coneixement científic: la tecnologia d'impronta molecular, l'ús de sensors electroquímics i el desenvolupament d'eines quimiomètriques, especialment en l'aplicació de la llengua electrònica. Aquesta combinació permet processar i discernir les dades útils de les redundants amb la finalitat d'obtenir paràmetres analítics inequívocs pel desenvolupament d'aplicacions amb un impacte real en la millora de la societat. Aquest treball s'ha realitzat al Grup de Sensors i Biosensors (GSB) de la Universitat Autònoma de Barcelona (UAB) continuant el curs de la investigació focalitzada en l'aplicació de llengües electròniques per la resolució de mescles complexes en diferents aplicacions.

La versatilitat, portabilitat i eficiència energètica i temporal han estat una constant en el consolidat i creixent món dels sensors i biosensors. En comparació amb els mètodes convencionals, els sensors ens aporten un ampli ventall de prestacions que ens faciliten l'obtenció real d'informació analítica. Si aquesta es combina amb les prestacions del sensat, la seva resposta pot tenir un valor afegit que millori els paràmetres analítics com ara el rang lineal, la sensibilitat i els límits de detecció o quantificació. Alhora l'electroquímica ofereix un conjunt de possibilitats en presentar una gran adquisició de dades en un espai temporal reduït, de manera fàcil i portàtil. No obstant això, la seva resposta pot ser inespecífica, supèrflua i requereix una planificació i posterior tractament de dades per obtenir informació analítica útil i nítida. Per tant, l'ús d'eines quimiomètriques sumat a les prestacions dels sensors electroquímics ens ajuda a discernir aquelles dades importants de les redundants, essent així, llur combinació una valuosa aliada.

Les prestacions del sensat poden ésser limitades per la pròpia construcció i muntatge del sensor, per tant, la millora constant del principal component d'un sensor està en permanent evolució. La inclusió de nous materials per millorar les prestacions del sensors genera un ampli camp d'estudi, ja sigui per la incorporació de materials de naturalesa sintètica o biològica.

En el present compendi, es presenta l'ús de polímers molecularment impresos com a eix conductor del manuscrit per millorar la resposta en el camp dels sensors electroquímics, especialment, en l'especificitat del sensor. Aquests polímers poden emprar-se com a elements de reconeixement biomimètics millorant les prestacions basals d'un sensor comú en diferents aplicacions de manera robusta, en un ampli període de temps, sense limitar-se a les estrictes condicions fisiològiques.

En aquest manuscrit es presenten aplicacions en tres camps diferenciats: (1) en la producció de begudes per detectar i quantificar etilfenols durant l'elaboració del vi; (2) en la conservació i preservació de productes alimentaris amb l'objectiu de determinar la presència i proliferació d'histamina en vins; i finalment, (3) en el camp de la seguretat i el medi ambient per a la detecció i quantificació de TNT i els seus derivats nitroaromàtics, com a contaminats emergents.

Table of Contents

Abbreviations

AIVN	2.2'-azobis(2,4-dimethylvaleronitrile)
ANNs	Artificial Neural Networks
AP	Acetaminophen
ATRP	Atomic Transfer Radical Polymerisation
AUX	Auxiliary
BDNF	Brain Derived Neurotrophic Factor
BioET	Bioelectronic tongue
CE	Counter Electrode
COD	Chemical Oxygen Demand
CM	Confocal Microscopy
COFs	Covalent Organic Frameworks
CPEs	Carbon Paste Electrodes
CRP	Control Radical Polymerisation
CV	Cyclic Voltammetry
DEHP	Di(2-ethylhexyl)Pthalate
DFT	Density Functional Theory
1,3-DNB	1,3-dinitrobenzene
2,4-DNP	2,4-dinitrophenol
2,4-DNT	2,4-dinitrotoluene
2,6-DNT	2,6-dinitrotoluene
DOE	Design of Experiments
DPV	Differential Pulse Voltammetry
DVB	Divinylbenzene
EAP	Potential Anodic Peak
ECP	Potential Cathodic Peak
EE	Electronic Eye
EGDMA	Ethylene Glycol Dimethacrylate
4-EG	4-ethylguaiacol
EN	Electronic Nose
4-EP	4-ethylphenol

EtOH	Ethanol
ETs	Electronic Tongues
FRP	Free Radical Polymerisation
FT-IR	Fourier transform infrared spectroscopy
GCE	Glassy Carbon Electrodes
GECs	Graphite Epoxy Composites
GSB	Sensors and Biosensors Group
HCl	Hydrochloric acid
HPLC	High Performance Chromatography
ICS	International Chemometrics Society
IPA	Intensity Peak Anodic
IPC	Intensity Peak Cathodic
IR	Infrared spectroscopy
IUPAC	International Union of Pure and Applied Chemistry
LOD	Limit of Detection
LRP	Living Radical Polymerisation
LSV	Linear Sweep Voltammetry
MAA	Methacrylic Acid
MeOH	Methanol
MIPs	Molecularly Imprinted Polymers
MLP	Multi-Layered Perceptron
MOFs	Metallic Organic Frameworks
MWCNTs	Multi-wallet carbon nanotubes
1-NB	1-nitrobenzene
NIPs	Non-imprinted Polymers
NMP	Nitroxide-mediated Polymerisation
NPs	Nanoparticles
2-NT	2-nitrotoluene
4-NT	4-nitrotoluene
OPA	O-phtaladialdehyde

oPD	o-Phenylenediamine
PCA	Principal Component Analysis
PCs	Principal Component
PECs	Polyelectrolytes
PMMA	Poly(methyl methacrylate)
PSA	Prostate-specific Antigen
Py	Pyrrole
QCM	Quartz Crystal Microbalance
RAFT	Reversible Addition Fragmentation Chain Transfer Polymerisation
RE	Reference Electrode
SAM	Self-Assembled Monolayers
SDS	Sodium Dodecyl Sulphate
SEM	Scanning electron microscopy
SER	Serotonin
SWV	Square Wave Voltammetry
TEOS	Tetramethyl orthosilicate
TLC	Thin Layer Chromatography
2,4,6-TNT	2,4,6-trinitrotoluene
TRYPT	Tryptamine
TV	Triangular voltammetry
WE	Working Electrode

Figures and tables

1. Introduction

1. INTRODUCTION

The role of analytical chemistry in daily life is exponentially growing and society is getting conscious about how sensor and biosensors devices can improve our lifestyle. The request to identify, detect and quantify or classify chemicals and biological species has become a necessity. A more educated society requires from the stakeholders and policy makers a better control, understand and monitor the composition of daily lives products, environmental parameters, checkpoint border control or simply daily tests to prevent the dissemination of diseases, among others. Some examples can be found in the environmental field, where new emerging contaminants have been increasing with over 100.000 new chemicals listed [1,2]; in foodstuff monitoring, where analytical methods are key to ensure its quality and its traceability [3]; in clinical

diagnostics, where biomarker identification allows the detection and diagnostic of pathologies [4]; in homeland security, to prevent and/or avoid terrorist attacks, as well as control areas in blast or post-blast scenarios [5–7]; and forensic applications to aid during crime investigation or to detect substances that may be used against human will (*e.g.* illegal substances) [8–10]. These challenges cannot be solved only using analytical chemistry, in fact, the intervention of different knowledge areas is needed to obtain a real-world solution. Towards this direction, in the last decade the field of sensors and biosensors has been incorporating new materials such as nanomaterials or biomimetic artificial receptors as well as the use of multivariate data analysis tools to surpass the inherent limitations of the sensing and biosensing field.

This PhD thesis explores the suitability of the molecularly imprinted polymers (MIPs) combined with electrochemical techniques and chemometric tools through the use of voltammetric sensors to study different kind of analytes relevant to the following areas: food and beverage, homeland security and environmental field. The aim of this research was the synthesis and immobilisation of the aforementioned biomimetic artificial receptors, named MIPs, for the development of the first electronic tongue (ET) that incorporates MIPs as recognition elements in an array of electrochemical sensors to solve a mixture of species employing advanced chemometric tools. Consequently, as happened through the incorporation of biosensors as part of the ET sensor array, the combination of MIP-based sensors and chemometrics can unleash a new research area in the ET field [11].

In the last decades, sensors and biosensors, biomimetic receptors and advanced chemometric tools had the attention of numerous scientists. This can be

perceived in the increasing number of publications regarding these topics in different science disciplines over the past years, as can be seen in Figure 1.1. For that reason, the merge of artificial neural networks, electrochemical sensors and imprinting techniques are proposed in this thesis manuscript.

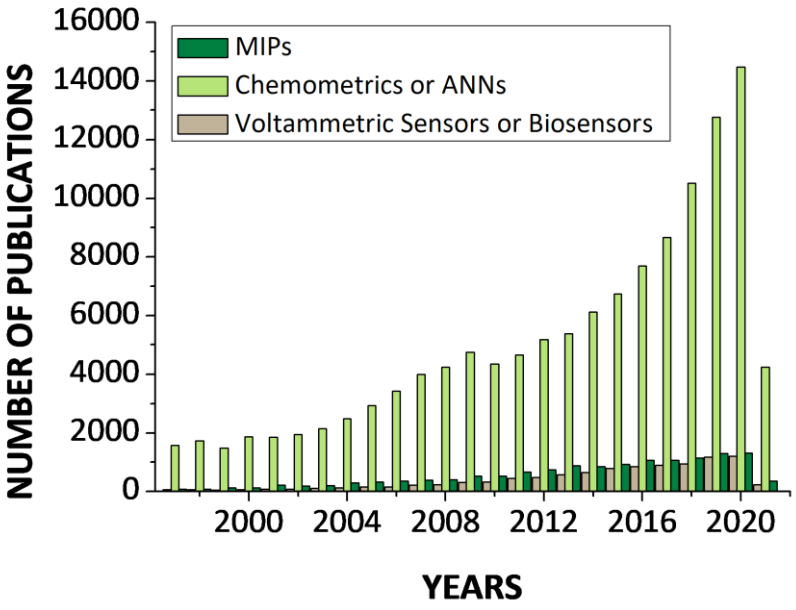

Figure 1.1. Number of publications over the last 25 years regarding molecularly imprinted polymers (dark green), artificial neural networks (ANN) or chemometrics (light green) and voltammetric sensors or biosensors (light brown). Data obtained from web of knowledge database on May 9th, 2021.

The combination of the aforementioned scientific areas is a challenging endeavour due to the nature of MIPs and electrochemical techniques. However, these polymers are usually synthesised in an organic media which yields a non-conductive material. The preferred medium to perform electrochemical measurements is the aqueous media with conductive materials allowing an optimal electrical transduction. Additionally, depending on the electrochemical technique employed, a huge amount of data might be generated. This data volume must be processed to avoid unnecessary or redundant information. Finally, the required system selectivity and sensitivity is highly demanding in

terms of a low detection limit, it must be able to work on complex matrices and to produce a unique and invariable response over the time.

1.1. Molecularly Imprinted polymers

1.1.1. Historical perspective

The concept of MIP encompasses various scientific fields of knowledge such as chemistry, biology, physics, mathematics and the more recent fields such as biochemistry, nanoscience and nanotechnology, among others [12]. Therefore, besides including different scientific advances, polymer imprinting technology was discovered by more than one scientist at a time without being fully aware of each other. What nowadays is understood as MIP has been developed from the early concepts disclosed by Polyakov in 1931 [13,14], who described the unusual properties shown by silica particles prepared with an innovative procedure based on the using of several additives and solvents during its elaboration. At the same time, the immune system and the antibodies' selectivity mechanism was under debate as reported by Brenil [15] and Pauling [16]. A few years later, Dickey, a Pauling's former student, described a similar procedure as Polyakov. His study described for the very first time a polymerisation synthesis of silica in presence of orange methyl dye. Then, the silica was treated with acetic acid and different organic solvents in order to obtain a material that presented an increase in selectivity towards the dye [17].

In 1952, in line with Dickey's and Polyakov's studies, Martin and Synge published their own work wherein methyl orange dye was used as an indicator ligand during the segregation of amino acid based molecules. It was found that this process was inducing selective 'footprints' for such dye. Later, Martin and Synge were laureated with Nobel price for these studies [18].

These publications lay the foundations of molecular imprinting technique. Then, it was in the 70's when Wulff and Klotz [19,20] published their work with molecular imprinting solvents and Sagiv worked on the concept of imprinting in silica particles [21]. Finally, in the 80's, Moscbach's group explored the idea of employing the imprinting of dyes containing several groups such as amino, phenyl, dodecyl and glycidoxyl functionalities onto silica [22]. The following Figure 1.2. shows the MIP timeline.

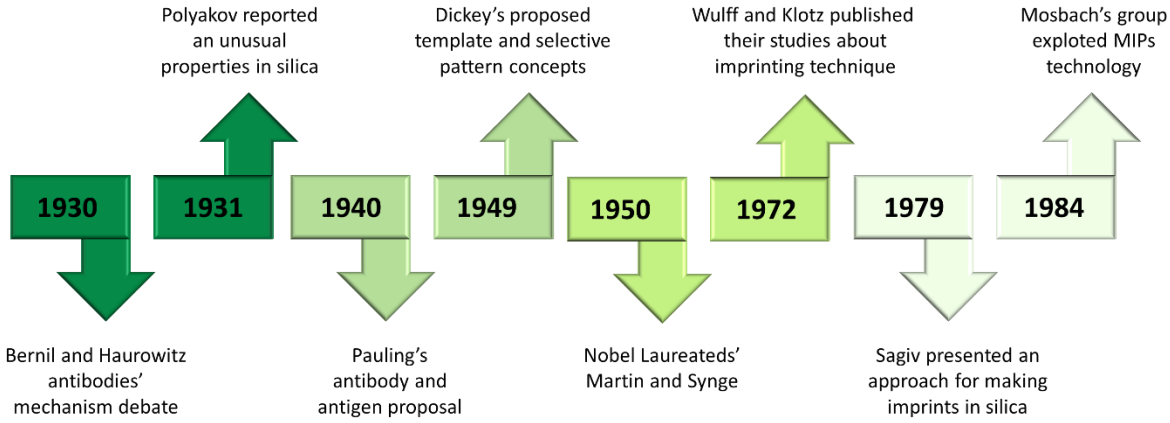

Figure 1.2. Timeline of MIPs development from early concepts to nowadays.

The molecular imprinting technique has evolved over the years, incorporating new scientific advances and becoming increasingly popular. From its origins based on silica-organic systems, new approaches have been reported including the use of larger templates and new type of inorganic matrices extending the original concept described by Polyakov and Dickey [12]. Consequently, the applicability of silica MIPs was first described for chromatographic applications and it was also reported on catalysis purposes. The former gave place to column and thin layer chromatography and it was also employed in structural determination techniques. It is needed to be mentioned that the imprinting process is based on natural biological processes. Then, the concept of imprinting has moved to organic and posterior inorganic synthesis disciplines. Recently, it has also incorporated new advances in material and technological fields, making

the imprinting technique a versatile option that has dramatically improved over time.

1.1.2. Definition

Understanding how nature works is a longed-for goal of the scientific community. There are a myriad of natural processes and mechanisms that are yet not possible to mimic. Complex molecular annealing processes such as ligand and receptor interaction, substrate-enzyme binding and transcription and translation of the DNA and RNA code are unmatched biological processes. Therefore, they are scientific universal interests [9]. As it was discussed in the previous section, MIP definition needed some decades to be clarified, understood and most importantly, accepted by the scientific community. The idea of mimicking molecular recognition changed over the time into new synthetic routes, incorporating materials and technological advances into the emerging discipline.

A widely accepted MIP definition was coined by Alexander *et al.* in 2005: "*The construction of ligand selective recognition sites in synthetic polymers where a template (atom, ion, molecule, complex or a molecular, ionic or macromolecular assembly, including micro-organisms) is employed in order to facilitate recognition site formation during the covalent assembly of the bulk phase by a polymerisation or polycondensation process, with subsequent removal of some or all of the template being necessary for recognition to occur in the spaces vacated by the templating species*" [12].

A more recent definition of MIPs was written by Garcia-Soto et al. in 2017: "*Molecularly imprinted polymers (MIPs), also known as "antibody mimics", are*

synthetic materials bearing binding sites with recognition properties on a par with those of antibodies, hormone receptors, and enzymes. During their synthesis a target molecule, or a derivative thereof, acts as a template and coordinates functional monomers which upon polymerisation with a crosslinker produce a cast-like shell. The subsequent removal of the template leaves binding sites complementary to the target in terms of the size, shape, and position of functional groups. This attribute allows the polymer to recognize its target with high affinity and specificity, thus making MIPs ideal candidates for technological applications involving recognition processes" [23].

Target molecules are used as the template to create recognition binding sites in the polymers. The resulting sites are complementary in terms of shape, size and functionality to the target molecule. Thus, the imprinted memory of the template into the MIP has been compared with the lock and key theory proposed by Fischer. This analogy is used to explain the preferential behaviour of enzymatic reactions [24].

Non-imprinted polymers (NIPs) are synthesised with the same procedure without adding the template. NIPs act as a baseline to compare binding capacity against MIPs. NIPs are polymers without specific imprinting (against the template molecule) and therefore have less functional cavities. It is important to mention that NIP polymer will have unspecific cavities due to its three-dimensional design and can therefore capture some of the template molecules even though this is not its purpose. That is why NIP will act as a control in comparison with MIP. In the following Figure it is depicted the MIP and NIP synthetic process, see Figure 1.3.

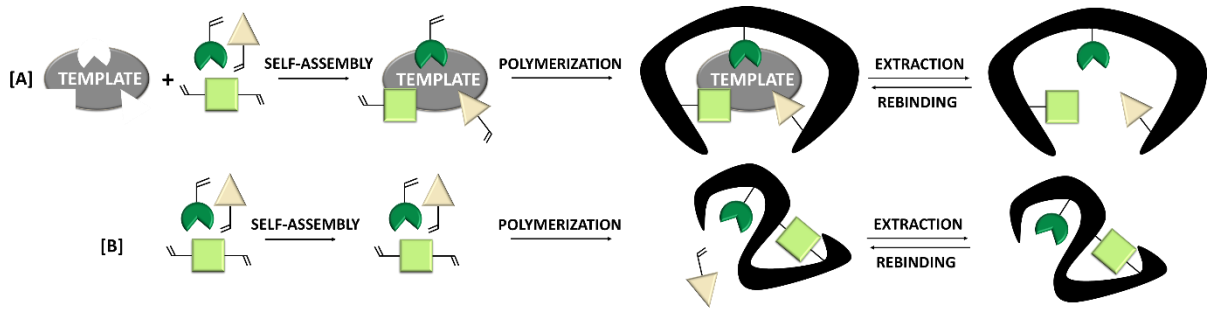

Figure 1.3. Depicted scheme of [A] MIP and [B] NIP synthesis.

As a general idea, it should be understood that these biomimetic polymers emulate the host-guest functionality of their biological counterparts such as antibodies, enzymes or aptamers. Which means, that the MIPs' cavities provide the polymer with affinity and recognition properties versus the template, so they can act as an artificial receptor. The synthetic nature of these materials allows for superb and exquisite properties in terms of tuneability (to suit almost any type of (bio)molecule, robustness, durability, low-cost, reusability and the possibility to work outside of physiological conditions, on a broader range of pH, temperature, etc. [11]. Section 1.2.5. explains the role of MIPs in sensing and biosensing.

Depending on the final application, the synthesis procedure can be tuned to obtain a material more or less adequate. Different polymerisation methodology or type that can be used to obtain different materials approaches (see Section 1.1.3.3.). Noteworthy the immobilisation is a key step in the final application as sensor and it will be discussed in Section 1.2.5.

1.1.3. Synthesis

In this section, a summary of the principal synthetic consideration will be presented. Imprinting technology combines the design and synthesis of MIPs and NIPs comprising several synthetic alternatives. As it was depicted in Figure 1.3., the imprinting strategy is firstly based on the generation of the pre-polymerisation complex, called self-assembly. This first step is crucial for the final capacity binding of the polymer; thus, the tailored-made cavity creation is related with the interaction between the template and the functional monomer(s). This process organises a complex with a fixed space disposition and chemical functionalities orientation for future reactions involved. The next step is the polymer formation around the pre-polymerisation complex in the surroundings of its functionalities, *i.e.*, double bounds or weak interactions. At that time is when the crosslinker and the initiator are added and the polymerisation is started (in an inert atmosphere). Finally, the template and the unreactive reagents are removed [12,25]. Precisely, the main differences among the set of synthesis approaches are: (1) the type of the interactions in the pre-polymerisation complex; (2) its union with surrounding functional monomer(s) and crosslinking agent (to obtain the polymer); and consequently, the template removal. In this section, MIP synthesis approaches will be explained and their main advantages and drawbacks will be pointed out. Once all the steps involved in the design and synthesis of MIPs are completed, they can be used for the development of the electrochemical sensors with MIP polymers in Section 1.2.4.

1.1.3.1. Elements in a MIP synthesis

Prior to move into different synthesis approaches, the main elements involved in the process are described. Those are the template, the functional monomer(s), the crosslinker, the solvent, the initiator and the so-called pre-

polymerisation complex [26–28]. Not all of the elements are strictly necessary to synthesise a MIP, especially in the electrochemical field. Nevertheless, all the chemicals presented in this section are used in the vast majority of synthesis procedures.

The template is commonly referred as an analyte in analytical chemistry. It is our object of study and the key to this synthesis strategy. Not all analytes are directly amenable to templating, the ability of the template to generate a pre-polymer complex that latter will be stabilized during the polymerisation step is required for the process to be successful. Template candidates for synthetic processes may ideally: (1) not be reactive in polymerisation conditions; (2) be completely soluble in the porogen (porosity generator) solvent; and (3) be moderately stable at elevated temperatures or under UV irradiation. It is necessary to be mentioned that the more functionalities the template has, including double bonds and functional groups able to generate different intermolecular interactions, the better imprinting chance the MIP will have.

The functional monomer(s) have a dual purpose, on one hand, it is the reagent that will be binding the template molecule in the imprinted binding locations, often using at least one double free bound. On the other hand, it is creating the pre-polymerisation complex in union with the template, which will originate the tailor-made cavities into the MIP matrix. In theory, this compound matches the functionality of the template in a complementary manner to maximise complex formation and thus the imprinting effect. Additionally, more than one functional monomer(s) can be used as a co-monomer(s) mixture or a “cocktail” of monomers. Finally, the pre-polymerisation complex is formed with the union between the template and the functional monomer. It is important that the

template only reacts with the functional monomer(s) fragments, in this manner the complex interactions are prevented, and the cavity remains tailored for the template molecule and its posterior polymerisation with other reagents that are going to be used for continuing polymer synthesis.

Another important element is the crosslinker, which is used as a linker with the template free regions of the functional monomer(s), normally through the chemical bonding derived from the radical polymerisation that unites free double bound functionalities. So, it has relevant functions such as (1) controlling the morphology of the polymer matrix, (2) stabilising the imprinted cavities and (3) giving mechanical stability and robustness.

Then, the porogen solvent, or simply solvent, is the phase where all the synthesis process takes place. The solvent also controls the creation of pores when working with macroporous polymers, controlling the morphology and total pore volume. In other words, it has an effect on the quality of the pore structure and the specific surface area. In some synthetic approaches, it could be purposely chosen due to the direct influence that has in the pre-polymerisation complex.

The polymerisation process, of the polymer matrix, is started by an initiator, which can be triggered by thermal, photochemical, or electrochemical reactions, depending on the template reactivity. For example, if the template is unstable at a certain temperature, the initiator might be induced with a photochemical reaction. Once the main elements that can be used for MIPs synthesis have been introduced, it is the time to present the different synthesis approaches.

1.1.3.2. Synthesis approaches

The imprinting technique survived over the years thanks to its renewal capacity, scientists are replicating, adapting and evolving synthetic routes for MIP production in laboratories worldwide [26]. The imprinting technique can be simplified in three stages: the self-assembly, the polymerisation and finally, the template removal. These steps are used to describe MIPs and NIPs synthesis (see Figure 1.3). In this section, different approaches to take each step will be described. The different synthesis approaches are the covalent, the semi-covalent, the non-covalent and the metal ion-exchange approach [12,27]. In Figure 1.4. the different synthetic approaches are summarised.

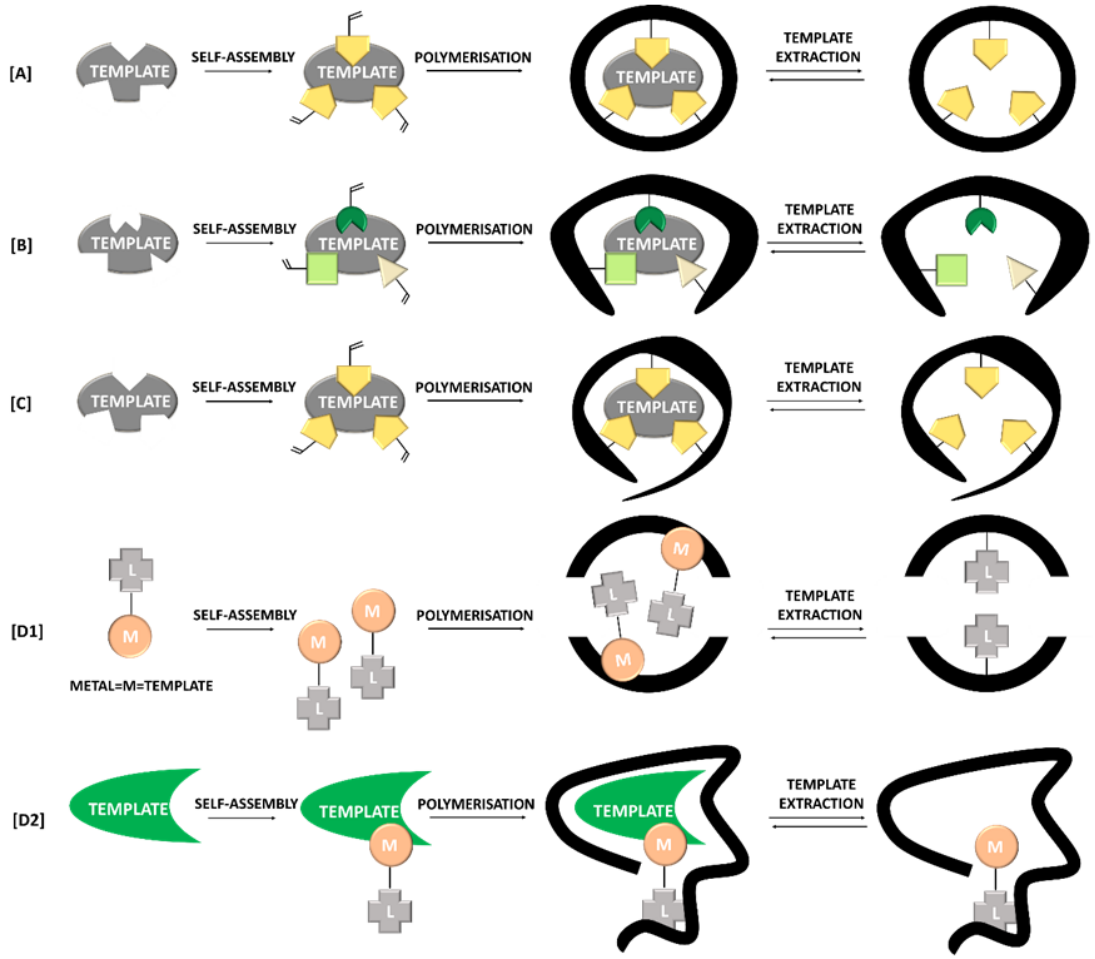

Figure 1.4. Diagram of the main MIP synthesis representing the different approaches: (A) covalent, (B) non-covalent, (C) semi-covalent, (D1) and (D2) are referring to the metal ion-approach and respectively the ionic species imprinting and the metal-ion mediated imprinting.

Covalent approach

The molecular imprinting technique via covalent bonding (see, Figure 1.4. [A]) was firstly reported for the design of these artificial receptors. It distinguishes the use of templates covalently bound to at least one polymerisable functional group. Therefore, this approach utilises polymerisable template derivatives. Then, the template cleavage is done in harsher environments, to remove this union, and the cavity is formed ready to be used for the re-establishment of the covalent bond.

This strategy provides precise and high affinity cavities. The reason of this is the high stability of the pre-polymerisation complex between the template and the functional monomer(s). Nevertheless, this high stability complex may be a major drawback. This approach normally provides bulky materials which need to be grinded and sieved before its reuse. During this process the polymer structure may be damaged resulting in a posterior poor recovery, low yields and slower kinetics. Another inconvenient that can be attributed to this approach is the extra step needed to chemically modify the template together with the limited species able to be combined to reversible covalent bonds.

Some considerations that it is need to be taking into account are: (1) the equimolar ratio between the template and the functional monomer(s); (2) normally, the covalent approach includes carboxylic [29,30], Schiff's base [31,32], ketals [33], boronate esters [34], among others; (3) in order to incorporate the template into the polymer matrix, some of the common functional groups that template must have in order to be able to be derivatized are alcohols, aldehydes, ketones, amines or carboxylic acids, which limits the number of compounds that this approach can be used on.

The imprinting of D-glyceric acid was reported by Wulff and Sarhan [19,31] employing the covalent approach. Their strategy used molecules with polymerisable vinyl moieties, amine moieties and boronic acid; this groups acted functional monomers providing the imprinting mechanism along a crosslinker such as divinylbenzene and a further monomer. Thus, this approach presented an organic polymer with imprinting properties to selective capture of the template and its analogues.

Non-covalent approach

The most preferred synthesis is the non-covalent approach (see, Figure 1.4. [B]) and it is by far the most widespread methodology to study and exploit the exquisite molecular recognition properties. The key to success is its few limitations, easy procedure, non-specialist equipment nor highly trained personnel to produce the polymer synthesis. The nature of the prearrangement in non-covalent imprinting became the key point in the imprinting technique, it allowed for a wide array of applications over several scientific fields as non-covalent interactions allowed the use of imprinting molecules with a humongous number of chemical species.

A non-equimolar ratio of the template and the functional monomer(s) is self-organised in solution to form a pre-polymerisation non-covalent network. In the non/approach the predominant interactions are Van der Waals forces, dipole-dipole, charge-dipole, cation-π, π-stacking, hydrogen bonds or electrostatic (charge-charge), among others. In the synthesis of MIPs, functional monounsaturated monomers are used, e.g., vinylic [35–37], acrylic [38,39] or methacrylic [22,40–42]; together with a high number of cross-linkers with similar functional groups. One of the most widely reproduced systems

worldwide is using (meth)acrylic acid (MAA) as the functional monomer and ethylene glycol dimethacrylate (EGDMA) as the crosslinker. This system can be easily reproduced with several templates without complexities. The final organic network material is preferably obtained by free radical polymerisation (FRP) thermally or UV-induced. For other mechanisms of polymerisation initiation, see Section 1.1.3.3.1.

The major disadvantage of this strategy is heterogeneity of the tailored-made cavities, that is clearly compromised due to the several interactions that take place in the pre-polymerisations stage, the direct competition from the solvent, the high crosslinked medium or the erratic polymerisation by the FRP.

This approach can be applied for small molecules up to supramolecular complexes, e.g., proteins, and cells; in other words, from simple chemical structures to complex biological ones. The stronger the pre-polymerisation complex interaction is, the better binding sites are generated. Another interesting point is that analytes containing multiple binding functionalities per molecule lead to favourable self-assembly. However, the resultant binding sites will be heterogenous. Given the great variety of non-covalent interactions, it can be considered that almost any species can be used as template as long as it contains at least one functional group able to bind the functional monomer active moieties.

Finally, it should be noted that this approach was originated in the 80's in the prolific Mosbach's laboratory, responsible for most of the advancement of molecular imprinting [43–45]. Furthermore, this approach caused a great popularization of the imprinting techniques and a skyrocketing growth in the

number of publications over the las two decades; nowadays it is still increasing at similar rates [46].

Semi-covalent approach

Covalent and non-covalent synthesis are diametrically opposed in terms of cavity functionality, affinity and specificity. It should be noted that if the polymer is imprinted too strongly, it will be too difficult to access the cavities, resulting in a slower and more inefficient template removal and subsequent re-uptake (or binding). Therefore, it is not difficult to understand the synthetic effort that was made to try to combine the before-mentioned approaches creating the semi-covalent synthesis (see, Figure 1.4. [C]), seeking to combine the advantages of both approaches, while counterbalancing their disadvantages.

The strategy is based in creating a covalent pre-polymerisation complex while the final polymerisation is performed among non-covalent functionalities. In this way, cavities can be synthesised like the covalent approach while the whole polymer is more versatile, resembling the non-covalent approach. This hybrid approach has the advantages of obtaining highly precise cavities from a covalent imprinting, together with a more favourable template rebinding process from a non-covalent polymerisation.

Nevertheless, this approach may present some disadvantages. Crowding and steric hindrance may occur during the pre-polymerization between the polymer and the template causing a loss in the polymer binding capacity and decreasing the affinity of the polymer. In order to overcome this drawback, a linker group may be used to connect the template and the functional monomer(s), this spacer will be eliminated at a later step, e.g., during the template extraction.

Thus, the spacer binds to covalently attach the template and the functional monomer(s) during pre-polymerisation while at the same manner prevents steric effects. Some examples of spacers include carbonate esters [47–50], carbamates [51,52], urea [53], salicylamides [53,54] or silyl ethers [55–57]. The use of spacers limits the possible candidates for imprinting, adds an additional step in the synthesis that will need to be addressed and yields a less effective polymer if the interaction between the target molecule and the monomer is insufficient.

The semi-covalent approach seems to have its origins in the laboratory of one of the founding fathers of molecular imprinting in the 70s, Gunter Wulff [19,31]. But it was not until 1995, when Whitcombe *et al.* reported a method that includes the terminology of sacrificial spacer [58]. In this work, 4-vinylphenyl carbonate ester were employed to covalently imprint cholesterol. Cholesterol was removed from the polymer via hydrolytic cleavage, the remaining carboxylic group was protonated to obtain a carbonyl group capable of forming dipole and hydrogen bonds with cholesterol molecules. This work was revolutionary because for the first time a polymer with uniform cavities created in a non-purely covalent assembly. This opened the door to future applications regarding small molecules with absence of functional groups or with difficulty to form stable pre-polymerisation complexes.

Metal ion approach

Another approach that allows us to modulate the interaction strength of the pre-polymerisation complex is by using ionic metals. This synthesis can be carried out using two strategies: the one employing (a) ionic species imprinting (see Figure 1.4. [D1]) and another option is the (b) metal ion-mediated

imprinting (see Figure 1.4. [D2]). The former forms a complex between the metal ion and the polymerisable ligand which subsequently polymerises with the crosslinker. While the other, the complex is used for printing polymerisable ligand(s) to form a complex with the metal ion (usually a transition metal ion) which in turn coordinates with the template acting as a mediator.

To sum up, this approach uses metal ions to make ionic bonds in two manners: (a) as a functional monomer(s) (b) or acting as a template making coordinative bonds with metals. An important advantage, which makes this strategy very interesting compared to the others described, is that the strength of the pre-polymer complex can be adjusted, for example, by changing the metal, the metal's oxidation or the ligand properties.

Therefore, the advantages of this approach come from the metal ion use and their inherent properties. Metal ions can bind to a wide range of functional groups by donating electrons from the heteroatoms present in the ligands or from the metal's outer coordination sphere. This allows them to interact with a wide variety of templates, such as molecules, peptides and proteins, making them comparable to the non-covalent approach as long as they contain metal complexing groups.

This was first proposed by Fujii *et al.* for the promising application of discriminating between stereoisomers of an amino acid, demonstrating the enormous potential of MIPs and this particular approach [59].

Moreover the use of different metals can be found in literature such as the synthesis of selective polymers using the following templates: bisimidazoles

[60,61], carbohydrate [62–64], amino acids [65,66], peptides [67] and proteins [68,69].

Finally, in order to have a global view of the different synthetic approaches and their main advantages and drawbacks, they have been summarized in table 1.1. below. There is no superior synthetic approach as each of the options presented in this section have different strong points which made them suitable for specific applications.

Table 1.1. Molecularly Imprinted technologies. Main advantages and drawbacks of each synthetic approach.

Synthesis approach	Advantages	Drawbacks
Covalent	Simple synthesis Precise and high affinity cavities Homogenous cavities Rigid polymer	Need to use a polymerizable template derivatives Wide particle size and distribution Harsher template removal Poor template re-uptake Low yields Slower kinetics
Non-covalent	Easy synthesis procedure Suitable for several template types Flexible polymer Higher yields Faster kinetics	Heterogeneous cavities due to the high amount of interactions It might be difficult to reproduce
Semi-covalent	Homogeneous cavities due to the nature of the bond Less rigid polymer	Need to use a sacrificial spacer which means one extra step Medium template re-uptake Medium yields Intermediate kinetics
Metal ion imprinting	Metals act as functional monomer or as template Cavity-template bond can be tuned	Limitation in the use of metallic species Heterogeneous cavities due to the different amount of interactions

1.1.3.3. Polymerisation

Polymerisation is a powerful word that can be attributed to different processes or actions even in the same synthesis. For this reason, the use of this word can sometimes lead to confusion. In recent literature the word polymerisation has been used differently to address multiple concepts. In the present manuscript an attempt has been made to maintain a terminology to differentiate certain aspects of polymerisation. From now on, it must be differentiated between the pre-polymerisation process, the type of polymerisation and the method of polymerisation.

The pre-polymerisation process refers to the formation of the complex between template and functional monomer(s). It is created before the polymerisation step of the artificial receptor (or MIP polymer) and is extremely important as it is the key point in the formation of the cavities and its binding capacity. After the polymer formation this term is defined as the imprinting process.
The type of polymerisation refers to the exact mechanism to obtain the product and in the sub-section that will discuss types of polymerisation (see Section 1.1.3.3.1.) one will find previously mentioned concepts such as FRP, among others types.

Finally, the sub-section dedicated to the method of polymerisation (see Section 1.1.3.3.2.) is going to explain in the detail the final forms of the polymer, which may be determinant for the type of application to be used. The more widely used methodologies are depicted in Figure 1.5.

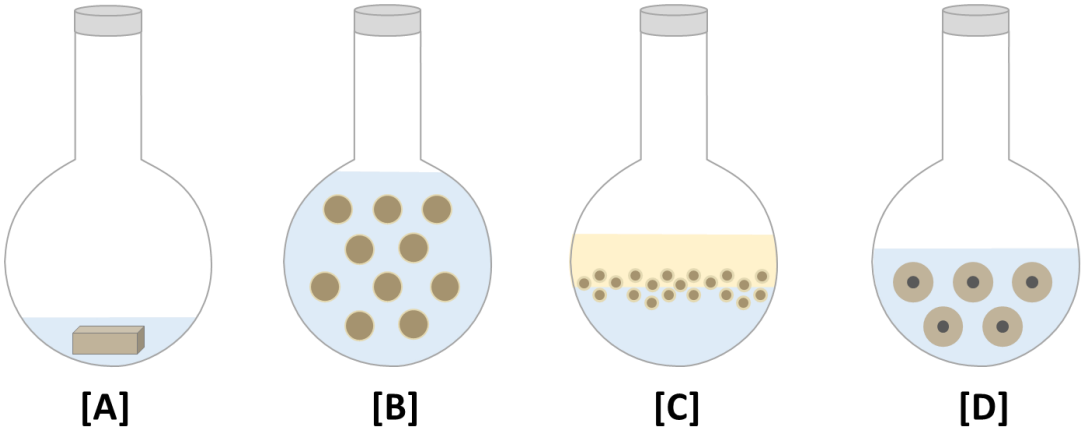

Figure 1.5. Depicted figure of the most used MIP polymerisation methods such as: (A) Bulk, (B) Precipitation, (C) Emulsion and (D) Core-shell.

Reproducing a MIP synthesis is not an easy feat, it also requires at least the basics of chemical equilibrium, molecular recognition theory, thermodynamics and polymer chemistry concepts, as well as being imbued by analytical chemistry and statistical mathematics [26].

1.1.3.3.1. Type of polymerisation

This section is focused on the radical addition polymerisation and the polymerisations materials that can be obtained using imprinting technology. Briefly, they are going to be described and some recent literature is going to be included.

Radical addition polymerisation describes the different mechanisms for initiating the polymerisation, that might be mainly employed in imprinting technology. The most employed source is the thermal and UV treatment, though others such as mid-IR, ionising photons, X- and gamma-rays can be used to modify the polymer properties. The different types of polymerisation are the FRP, controlled radical polymerisation (CRP), sol-gel process, photopolymerisation and electropolymerisation [70].

One of the most widespread type of polymerisation is FRP due to its rapidity, simplicity and easy-proceeding. Because of its versatility, it can be employed to synthesise monolith or bead polymers and it can be triggered by thermal or UV induction. As drawbacks, it is needed to be pointed out that FPR includes an irreversible termination reaction and uncontrolled atom transfers. For these reasons, polymers prepared using FRP usually present high-branching, broad molecular weight distribution and atactic structure [11,71].

More advanced alternatives that could tune the polymer or beads size, shape and molecular weight distribution are the CRP, also called living radical polymerisation (LRP). This strategy is an iteration of activation and deactivation cycles, which is a useful alternative to obtain a similar length chains in comparison with FRP. Using CRP is a versatile option because a plethora of chemical species can be used, and it also includes other strategies like atom transfer radical polymerisation (ATRP) [72–75], nitroxide-mediated polymerisation (NMP) [76], iniferter-mediated polymerisation [77] or reversible addition-fragmentation chain transfer polymerisation (RAFT) [78–82] .

Sol-gel is a common matrix to incorporate materials into a generated inorganic framework, in the field of (bio)sensing [83,84]. This process started with a “sol-formation”, an alkaloid precursor colloid liquid suspension. Thus, this “sol” is transformed into a “gel” by a step process that include hydrolysis and poly-condensation. Moreover, it can be used to obtain films with memory imprinting and be tuned by little modifications on its preparation proceedings [85].

Photopolymerisation is mainly employed either as initiator to obtain particle beads or to grow thin films with tuneable thickness, down to the nanoscale.

Although it is a suitable option when one wants to control the film growth or the particle size, the radiation's low penetrating power can be a limiting factor once the reaction is underway. Additionally, some templates may degrade under its exposure due to its poor stability [70].

Finally, electropolymerisation approach is intensively used to grown films onto the electrode surface (see Section 1.2.5.). Because is one-step synthesis where all the products are mixed in the same solution, this option has become very popular in the field of electrochemical sensors. As main advantages that can be attributed to this approach are its simple polymerisation process (in comparison to the previous methods), high reproducibility, the thickness control and the compatibility with aqueous media.

1.1.3.3.2. Method of polymerisation

Bulk or monolith

Bulk imprinted polymerisation is used to obtain a monolith block (see, Figure 1.5. [A]) and it is very useful due to its easy and fast synthetic procedure. However, the monolith is a bulky polymer that needs to be grinded and sieved to obtain a particle size distribution in different fractions. The grinding process usually damages the tailored-made cavities, which are mostly synthesised in the inner part of the polymer network. This material provides a robust polymer able to work in a broader range of solvents, under different pressure and temperature environments. The trade-off is that a lot of the material is lost in the process of grinding and sieving which is time-consuming and might affect the re-binding process by hindering the mass transport and diffusion.

This strategy was widely used in the early days of MIPs, so it is not surprising that chromatography was the application of choice for its final purpose. Some examples in literature include the use of conventional stationary phase, capillary columns, thin layer chromatography (TLC), solid phase extraction (SPE) and high-performance chromatography (HPLC) [75,86–89].

Precipitation polymerisation

Precipitation polymerisation is the widespread method due to its versatility, straightforward and fast strategy (see Figure 1.5. [B]). It can also be considered the more counter-balanced strategy to obtain uniform and structured (sub)micrometre particles with proper imprinting activity.

A non-equimolar template monomer ratio is dissolved in a highly crosslinked solvent and after degassing the mixture, an initiator is added. Normally, this approach is employed with the aforementioned FRP type. This combination of the method and type of polymerisation makes the most recurrent strategy to obtain an imprinted polymer with the desired properties.
The polymer grows in a diluted media with high proportion of the solvent, until it collapses upon reaching the critical size. Then the material precipitates until the initiator is depleted or deactivated.

Moreover, there is no need to modify the template, the monomer nor the pre-polymerisation complex. The aqueous environment helps in the creation of several weak interactions making a less rigid polymer, so the re-uptake process is more efficient. However, the diluted media facilitate the heterogenous cavity formation, reason why this approach presents low-affinity interactions that might interfere in the polymer selectivity.

Some examples that can be found in the literature employing this methodology are MIPs for purifying tylosine [90], theranostic application in cancer therapy [91], controlled release of rivastigmine tartrate [92] and fluorescent sensing of paracetamol [93].

Emulsion polymerisation

The emulsion strategy is the preferred to obtain nanometric-sized particles (see, Figure 1.5. [C]). Emulsion polymerisation uses an organic solvent solution where the template-conjugated functional monomers and organic crosslinking monomers are immersed. This method combines organic and aqueous media as well as the addition of emulsifier agents (e.g. sodium dodecyl sulphate, SDS) and co-stabilizers.

The emulsion methodology mixes the organic monomer(s), the template and the crosslinker solution with an aqueous surfactant media, obtaining a microemulsion. This method needs vigorously stirring and sonication. Moreover, several washing steps and purification processes are used to clean the polymer. Consequently, this application might be limited to *in vitro* applications and is excluded from *in vivo* applications.

The main disadvantage of the emulsion methodology is the binding sites heterogeneity, that directly impact the imprinting activity due to the use of water-surfactant mixtures. This reduces the stability of pre-polymerisation complex; moreover, the use of surfactants requires to add an extra steps during the synthesis. Therefore, this is not a very attractive technique for MIP synthesis.

Some works published recently employ this technique to create MIPs to purifying solasenol that is a pharmaceutical interest specie [94], determine Di(2-ethylhexyl)Pthalate (DEHP) an emergent water contaminant [95], applicating a renewal plant oil- based MIP biopesticide delivery systems [96], sorptive extraction of cis-diol-containing catechol [97] and determining L-cysteine [98].

Core-shell polymerisation

Core-shell polymerisation (see, Figure 1.5. [D]), as the name implies the polymer is synthetized around a central core. The "Core materials" may be selected from polymeric structures, silica or magnetic particles, this are further functionalised with a thin polymeric layer shell.

This methodology is often used with magnetic and metallic nanoparticles (taking advantage of the properties that these materials offer) or glass beads. This method produces a controlled imprinted polymer with grafting, chemical grafting or simply by drop-casting immobilisation.

The main point in favour of core-shell MIP particles taking into account the other strategies is the tuneable control of the thickness of the polymeric film. This fine control of the polymer shell allows for a better accessibility of the molecules to the tailor-made cavities and generally results in a higher binding performance. The main disadvantage is its complex and costly synthesis procedure.

Recent literature describes this methodology being used on: magnetic MIPs [99,100] , the recognition of polybrominated diphenyl ethers in aqueous media employing a dummy MIP [101], the extraction of antazoline and hydroxyantazoline from human plasma [102], the detection

organophosphorous insecticide fenamiphos [103] and determining tartrazine in soft drinks [104].

Solid-phase synthesis approach

The solid phase synthesis approach is one of the most promising and advanced techniques for working on *in vivo* applications. This approach is based on the preparation on glass-beads by activation and salinization, which act as a support for polymerisation reactions. The template is orientated and covalently bonded on the glass-beads, afterwards, the polymerisation take place and finally a purification step is needed to obtain the polymer imprinted material free of template or unreactive reagents.

The main advantages are the possibility of reuse of the templates immobilised onto the glass-bead support, a better control of the template orientation before the polymerisation and the final purification and elution of the polymer preserves homogeneously oriented binding sites. These polymers might be soluble in water, so they are more likely to be used as enzymes or antibody competitors. They are involved in interesting applications such as drug delivery, toxin scavenging and imaging. The main drawbacks are the high-cost equipment columns to perform this approach as well as the extra step of the preparation and activation of the glass-beads.

Some recent examples published studies the use of SPS for: bioimaging of glycans in cells [105], inhibiting cadherin-mediated cell-cell adhesion in cancer therapy [106] and optimizing the protocol of this approach for selective proteins [107].

Finally, in order to have a global view of the different method of polymerisations their main advantages and drawbacks, they have been summarized in table 1.2.

There is no superior methodology approach as each of the options presented in this section have different strong points which made them suitable for specific applications.

Table 1.2. Main advantages and drawbacks of each method of polymerisation for MIPs.

Polymerisation Method	Advantages	Drawbacks
Bulk	Simple synthesis Homogeneous cavities	Wide particle size and distribution Harsher template removal and Poor template re-uptake Low yields Slow kinetics
Precipitation polymerisation	Easy to proceed synthesis Easier template removal High yields High template re-bind Faster kinetics Versatile procedure in terms of applications	Diluted reagents media producing heterogeneous cavities It might be difficult to reproduce
Emulsion polymerisation	Small nano-MIPs	Emulsifier agent needed Hydrophilic initiator needed Difficult surfactant removal
Core-shell	Dual property material with outer imprinted layer	Inefficient imprinting if outer layer is not thick enough
Solid phase synthesis approach	Fully automatize process High affinity and selectivity Template can be easily recuperated on the glass-bead surface	Expensive laboratory equipment Glass-beads needed Purification step is needed

1.1.4. Improving strategies for molecular imprinting applications

As mentioned above, MIPs have an important market in the current scientific literature. This section has been added to the manuscript to highlight two approaches, which help in the design and synthesis of such polymers and their final application. These strategies will be divided into two sections: the use of computational models and the use of dummy MIPs.

Computational approaches for designing MIPs

Even if it is not considered a synthetic route on its own, the use of computational methods in designing and synthesising MIPs deserves a special mention. There is a wide variety of MIPs designs and syntheses. Therefore, computational methods are a helpful tool to guide us on which might be the most efficient path to our purpose. These approaches are used to facilitate and improve the affinity of these polymers through the rational design of their protocols [108–111] without the need for a new synthesis every iteration, saving us a lot of time, effort and money.

Computational tools were applied for this purpose in the 90s decade, but it was in 2001 when Piletsky *et al.* published accurate predictions without the need of synthetic effort in the laboratory [112]. These studies comprise the optimisation of the functional monomer and template ratio, the selection of the best crosslinker and solvent candidate. The computational tools use modelling of the different species that could be used as template, monomer, crosslinker or solvent and looking for the best combination and ratio among them. Thus, the advantages of applying this strategy are obtaining high-affinity polymers with better imprinted cavities saving time and resources.

Modelling approaches used in recent publications include molecular mechanics, molecular dynamics or quantum mechanics-based techniques (semi-empirical, *ab initio* or density functional theory (DFT)). Nevertheless, some chemometric studies have also been employed for the optimisation of such parameters [113,114].

The Dummy MIPs

One of the selling points of using MIPs is the versatility of being able to create artificial receptors for almost any chemical and/or biological species of complex nature. This presents a large number of possibilities, but there is always the exception that proves the rule.

The dummy term is referred to the use of a template analogue or similar chemical specie when the use of the template it is not possible because of different issues. Basically, when the template (i) is not-stable under the polymerisation conditions or has a poor solubility in the synthesis solvent, (ii) it is considered a hazard and/or there is substantial safety concerns arising from its manipulation, (iii) it has an exorbitant price or (iv) the template has leakage problems associated with its reactivity (i.e. evaporation) [11].

These are the scenarios in which the use of the so-called dummy template is highly recommended. This terminology was first used by Anderson *et al.* [115]. In the same direction, it can be found in recent literature the use of dummy MIPs towards compounds such as the explosive 2,4,6-trinitrotoluene (TNT) [116], or Bisphenol A due to its spillage [117] or employed in greener applications such as acrylamide extraction in food samples [118].

1.2. Sensors, biosensors and biomimetic sensors

The sensors and biosensors field is expanding continuously and it is one of the most productive research areas worldwide, it includes a vast number of publications that increases yearly. As a technology that begun in the last century, this field is permanently renewing new strategies and materials to detect, quantify and separate chemical and biological species in different matrices and being employed in a wide variety of applications. The high demand on consumption and the legislation to prevent and control the quality and the preservation of products makes sensors and biosensor devices the perfect tool.

Sensors were created as an analogy to our sensory perceiving organisms. A similarity that was also used for computers. The modern sensors are inspired on the complexity of sensory organs of a living organism. So, as can be seen in Figure 1.6., a sensor responds to stimuli received from the environment by changing some of its inherent properties; then, the transducer changes this information into a signal, typically an electrical signal. This signal is then processed and sent to the microcomputer working like the central nervous system of a living organism [119].

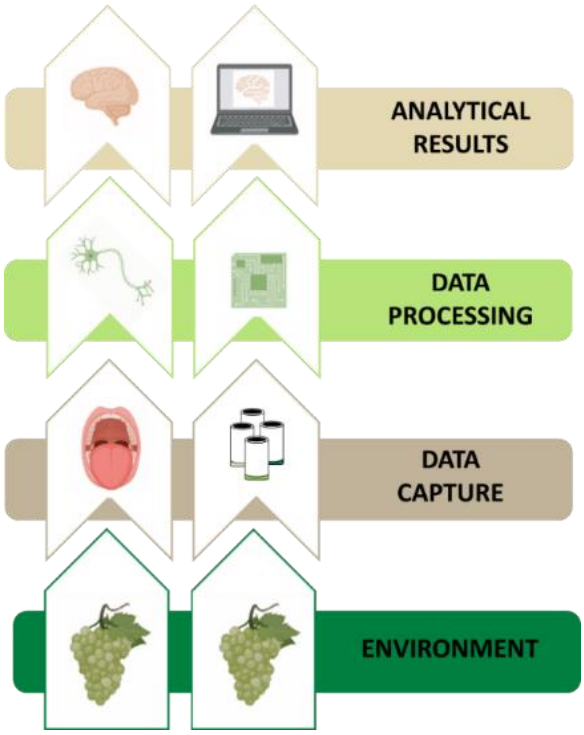

Figure 1.6. Analogy between computer signal processing systems *versus* biological organisms.

This concept will be the basis for the development of sensor arrays and the electronic tongue (ET) approach which will be extensively explained in the section 1.4.

1.2.1. Historical perspective

The first historical milestone is dated on 1906, Cremer proved that the electric potential between different acid solutions separated by a glass membrane is proportional to the acid concentration difference [120]. In the same decade, Sorensen reported the concept of pH (hydrogen ion-concentration). A few years later, in 1922, Hughes performed the first measurements with a pH electrode [121]. The first attempt to develop a biosensor was when Griffin and Nelson published the enzyme invertase immobilisation on aluminium hydroxide and charcoal [122].

But, it was in 1956 when the first biosensor was developed by Clark, father of biosensors, for oxygen detection [123]. The so-called Clark oxygen detector consists of a platinum cathode at which oxygen is reduced and silver chloride reference electrode. In 1962, Clark and Lyons combined the before-mentioned electrode with glucose oxidase integrated in a dialysis membrane to obtain an electrode able detect the concentration of glucose in solution.

This work was the basis to develop biosensor that used potentiometric technique to detect urea by Guilbault and Montalvo in 1969, which was based on urease immobilisation onto an ammonium-selective liquid membrane electrode [124]. In the same decade, Updike and Hicks reported an enzyme electrode to quantify glucose in solution and *in vitro* tissues through the immobilisation of glucose oxidase in a gelatine membrane that coated a polarographic oxygen electrode [125].

Since the first attempts, a broad range of sensors have been developed whose nature varies depending on the recognition element. Several elements have been employed such as enzymes, antibodies, polypeptides, aptamers or nucleic acids depending on the intended application and technologies available. More recently, nano- biosensors based on nanomaterials have been developed in the last decades. At this point, it should be noted that there is a new generation of materials, called biomimetics, within this classification are molecularly imprinted polymers.

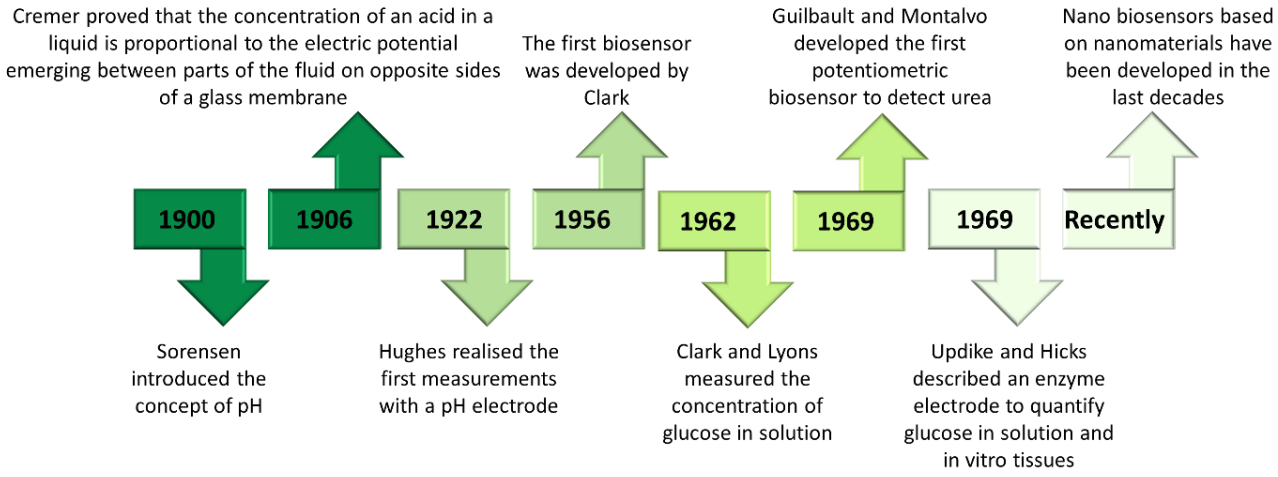

Figure 1.7. Timeline of sensing and biosensors development from early to nowadays.

1.2.2. Definition and classification

The word sensor came into use in the 1970s. Its popularity came hand in hand with technological advances and especially with developments in the field of microelectronics. The International Union of Pure and Applied Chemistry (IUPAC) defines: "*chemical sensor is a device that transforms chemical information, ranging from the concentration of specific sample component to total composition analysis, into an analytically useful signal*"[126]. In the analytical field the sensor must be able to selectively transform chemical, physical or biological information into a quantifiable signal.

Another definition that was proposed by Wolfbeis in 1990 defines: "*Chemical sensors are small-sized devices comprising a recognition element, a transduction element and a signal processor capable of continuously and reversibly reporting a chemical concentration*" [127].

The former is the classical definition, but one would have to clarify the statement in various ways. The term reversibility is quite important because it means that sensor signals should respond dynamically to changes in sample

concentration. Moreover, small, or miniaturised devices are increasingly in demand as they are easier to store and transport.

As can be seen in Figure 1.8., chemical sensors are composed of three main units: the receptor, the transducer, and the detector. Firstly, the receptor transforms the chemical information into a form of energy which may be measured by the transducer. This information is the primary signal. The receptor must provide selectivity to the sensor discriminating the target among interferants substances. Afterwards, the transducer transforms the primary signal generated by the receptor into a useful analytical signal, the secondary signal, generally an electric one. Optionally, a step of amplification might be necessary, and a signal processing takes place before displaying the results on the detector.

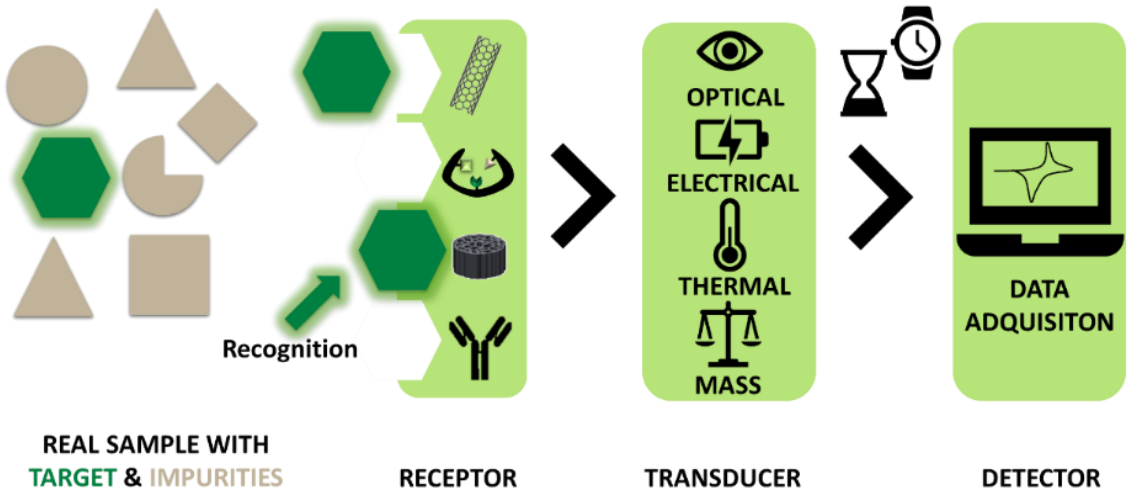

Figure 1.8. Depicted scheme of the sensor and biosensor components.

The main difference between a sensor and a biosensor is that in the latter its recognition element belongs in the biological world. Biosensors, have incorporated in their receptor a biological recognition element such as antibodies, enzymes, cells and DNA, among others. As MIP is considered as an artificial receptor, that acts as their analogues antibodies or enzymes, the more

accepted term to refer to sensors that incorporate them as recognition elements is biomimetic sensors [46].

In the case of sensing, tailored-made elements such as nanoparticles (NPs), polymers, polyelectrolytes, metal oxides, metals and carbon-derived materials such as graphene, multi-wallet carbon nanotubes (MWCNTs), mesoporous carbon or carbon black are incorporated either by physical adsorption or chemical bonding.

Moreover, sensors and biosensors should ideally behave in a certain manner, they must be [120]:

- Highly Selective: it must be able to specifically detect an analyte in a sample that contains mixtures of substances and interferents.
- Reproducible: it must be able to generate acceptable responses for a duplicated experimental set-up. Ideally, the responses have to be the same but a variability of 5 to 10% is generally accepted.
- Robust and stable: it must be able to withstand shifts of the operating conditions and still deliver an acceptable response over the time.
- Highly Sensitive: it must be able to detect and quantify low amounts of the target analyte.
- Linear response: the sensor must be able to operate within a specific range wherein the amount of detected analyte and the signal present a linear correlation.

To finish this section, a classification of sensors and biosensors is proposed. This classification is based on the recognition element and the transducer. All the qualities that defines an ideal sensor are mostly governed by the choice of the

recognition element and the transducer. Therefore, Figure 1.9. presents a general classification of sensors and biosensors based on the receptor and transducer categories.

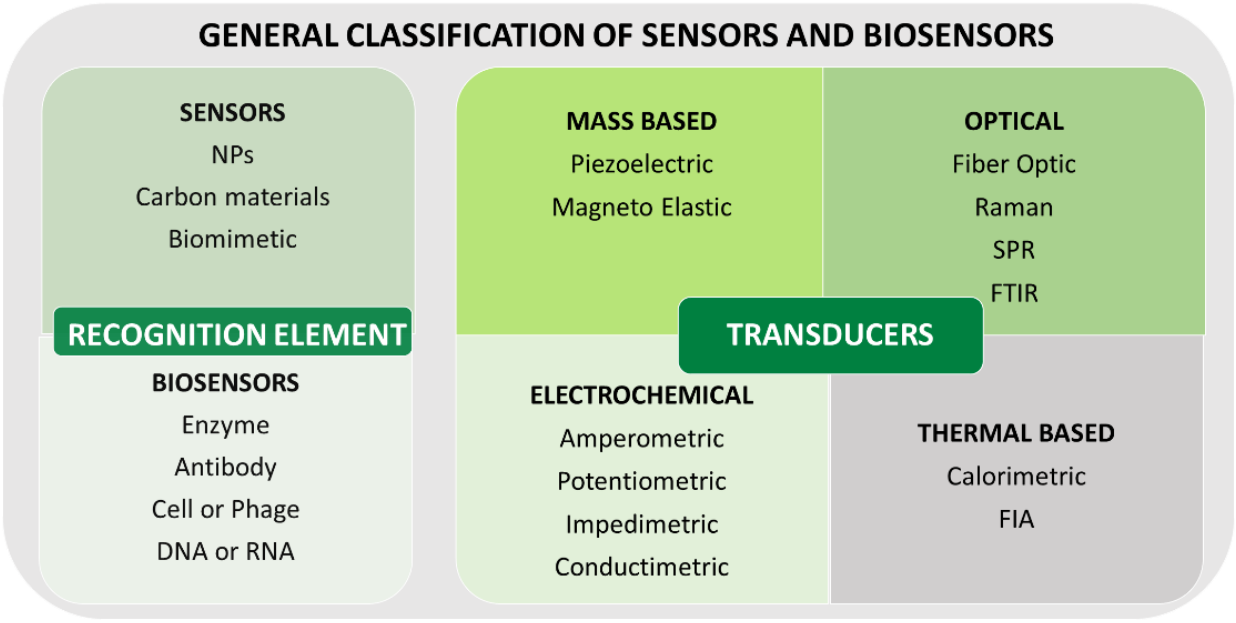

Figure 1.9. Schematic classification of sensors and biosensors, adapted from [128].

Electrochemical techniques

As mentioned in the first section of this manuscript, analytical chemistry is a science discipline that serves interdisciplinary purposes in many areas of knowledge. Moreover, its role is decisive and has a direct and daily impact on the lives of our fellow citizens. Quantitative analytical chemistry provides real information on the state of a chemical species in a sample, *e.g.* different ions in a blood sample such as potassium, calcium, among others [129].

Electroanalytical chemistry comprises a group of quantitative analytical methods based on electrical properties of an analyte solution when it is part of an analytical cell, which can be directly or indirectly related to the species of interest [129] .

Electroanalytical methods have a better response/performance compared to classical methods such as HPLC-UV, ICP-MS or GC-MS. The main advantages of electroanalytical methods are: easy protocols, fast measurements, quick cleaning procedures and the possibility of being portable, miniaturized and energy efficient.

However, they also present some drawbacks such as the measurement drift, the technique limitation in order to obtain low limit of detections or the lack of robustness due to the fouling of the electrode surface.

1.2.3. Voltammetry

Voltammetry is a technique included in the electroanalytical methods. Using this technique, the analyte information is obtained from the measured current intensity at different electrical potentials when a polarization is created at the working electrode. The recorded current is generated from the electronic transfer that takes place on the electrode surface between the electrode and the compounds in the solution when the potential is applied; depending on the applied potential the species are oxidized or reduced [129].

The electrochemical cell

The instrumentation required for this methodology involves the use of a three-electrode circuit typical of a potentiostat in the design of an electrochemical cell, see Figure 1.10. It is mandatory the usage of this configuration in order to apply the appropriate potential while measuring the relevant current intensity. The components are: a working electrode (WE), a reference electrode (RE) and an auxiliary electrode also known as a counter electrode (CE or AUX). The reaction of the analyte happens in the surface of the WE and, consequently, the change

of its potential over the time. While the RE is maintaining a controlled potential throughout the experiment and a complementary redox reaction is taking place in the CE. Thus, the potential is applied between the WE and the RE while the current between the WE and the CE is measured.

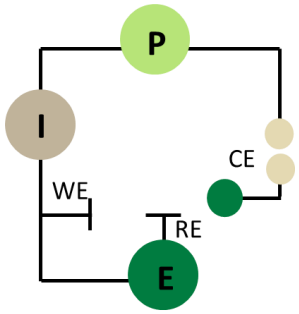

Figure 1.10. Three-electrode electrochemical cell configuration.

Voltammetric excitation signals

Voltammetric measurements can be classified according to the type of excitation signal applied, that will define the response obtained in the electrochemical cell. The different excitation signals gave name to the several voltammetric techniques, see Figure 1.11.:

- Linear sweep voltammetry (LSV): the applied potential is linearly dependant of a function of time.
- Differential pulse voltammetry (DPV): it is a derived method of the LSV where a pulse is applied while the potential increases linearly as a function of time. The current is measured before and after the pulse.
- Square wave voltammetry (SWV): it is also considered a derived method of the LSV. In the same direction of DPV, in this variation of the excitement signal the pulse applied changes in a stair shape, superimposing a SWV with LSV. As aforementioned, the current is measured before and after the potential change.

- Triangular voltammetry (TV): is the most widely used to obtain an electrochemical signal quickly. The potential is cycled between two values, first increasing linearly to the maximum and then decreasing with the same slope to the starting value. This is the so-called Cyclic Voltammetry (CV).

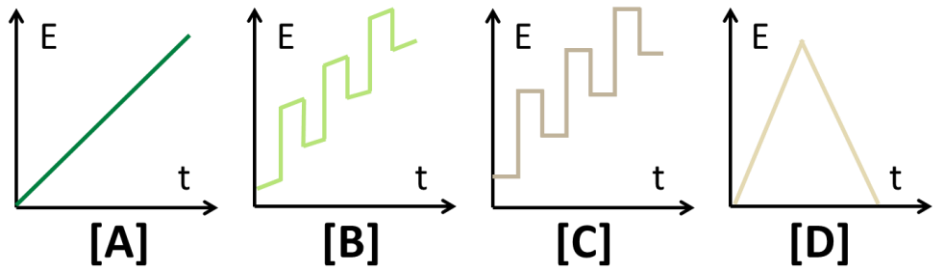

Figure 1.11. Representation of the before-mentioned excitement signals employed in voltammetry. [A] LSV, [B] DPV, [C] SWV and [D] CV.

Depending on the equipment and instrumentation, there are some parameters that can be tuned in order to obtain a better response for electrochemical performance. Some parameters are shared such as step potential (V) and scan rate ($V.s^{-1}$), others are specific for pulse ones like pulse frequency (Hz) and amplitude (V) and are only used for SWV or DPV [130].

CV is the most preferred excitement signal to obtain a quick view of the electrochemical performance of the transducer and the electroactive species that are in solution. However, DPV and SWV are the preferred excitations to obtain more sensitive and accurate responses. Especially, to obtain a lower lineal range and limit of detection (LOD), once the aforementioned parameters are optimised. There is a necessity to counter balance among: the time of the measurement, the behaviour of the electroactive species, the transducer response over the measurements, and the viability in use of the recognition element (*e.g.* stability of the species or sensor units without losing the signal or damage the electrode surface).

Voltammograms

CV excitation signal with a broad range of potential is the most common setting for a transducer to produce a voltammogram. A potential scan is performed by measuring at different potentials, then reversing the order finishing in the starting point as a complete cycle. The electrochemical response that can be obtained is depicted in (Figure 1.12.), where is shown the intensity (I) that circulates between the working and the CE as a function of the applied potential.

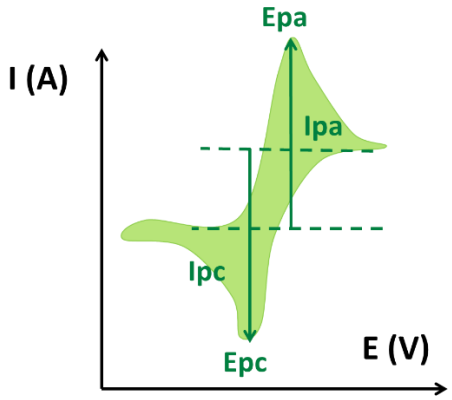

Figure 1.12. CV from a reversible redox system.

The working electrode is converted into an anode (oxidant) when is performing the scanning in positive potentials. Thus, if all the electroactive species are in their reduced form, the oxidation on the electrode surface is favoured. That is automatically translated in an increase in the anodic intensity (Ipa), until the specie in the surface of the electrode is totally consumed. Since, the measurements are conducted without stirring the solution, the species consumed increase the current, producing a current peak.

In the same direction, while the voltammogram is performed during the negative potential values, the electrode is converted in a cathode (reductor). That is automatically translated in an increase in the cathodic current (Ipc) until

all the specie is oxidised into the electrode surface and then the signal is decreasing again.

The important parameters to consider while performing a cyclic voltammetry are: the cathodic potential and intensity (Epc and Ipc) and the anodic ones (Epa and Ipa).

1.2.4. MIPs integration in voltammetric sensors a key step

As discussed in previous sections, electrodes have certain limitations that can be improved by modifying them. This is closely linked to immobilisation or how the aforementioned electrode can be modified. In our case, the sensor element is the graphite-epoxy composite (GECs), that can be modified by adding the recognition element (MIPs) (see section 3.2).

In order to improve sensor capabilities, specifically in terms of selectivity, sensitivity and lower limit of detection many different materials have been incorporated when developing electrochemical sensors nanoparticles and bio-materials [131,132].

Another example is the use of enzymes, their function is to change the target analyte into another product through a catalytic reaction, making easier and possible the analyte detection. Another variant is the use of electrocatalysts, that compounds acts as mediators promoting the electron exchange more efficient, i.e. making this reaction faster, efficiently or more sensible. [133]. The progress in material science gives the opportunity to work with a wide variety of new materials that are an alternative to the respective bulk metals given its higher surface to mass ratio and improved electrochemical properties [134].

Biochemical recognition elements, *i.e.,* enzymes, antibodies or oligonucleosides, that do not change the electrochemical signal directly are used to enhance the selectivity of the developed sensor. The biochemical recognition elements specifically bind to the desired analyte. Examples of sensors containing these elements are affinity biosensors, such as immunosensors, genosensors, etc, that have been commonly used in the last decades [135]. However, the high-performance of such biosensors have drawbacks such as its high cost or a low long-term stability outside physiological conditions, among other.

To tackle the drawbacks of biosensors, there is long felt need to obtain synthetic receptors that might replace their biological counterparts, e.g., antibodies or enzymes. Some of the advantages using these alternative artificial receptors are not only due to its low synthetic cost, it is also because of the versatility in working activity. They offer as the chance to work in a broader range of conditions (pH, temperature, solvents, etc) under non-physiological conditions. In the same direction, several synthetic alternative (bio)molecules such as aptamers (*i.e.,* aptasensors), molecularly imprinted polymers (MIPs), crown ethers or cyclodextrins; and recently, the use of metal-organic frameworks (MOFs) or covalent organic frameworks (COFs) have also become popular among the scientific community using them as artificial receptors.

From the before-mentioned list, aptamers and MIPs have clearly demonstrated a higher performance level. However, MIPs are a cost-effective and versatile option due to their operative working conditions with higher stability, robustness and specificityAdditionally, MIPs are a promising alternative due to their tailored-made binding sites, comparable performance to affinity bioreceptors and tuneability, as it is summarised in Figure 1.13.

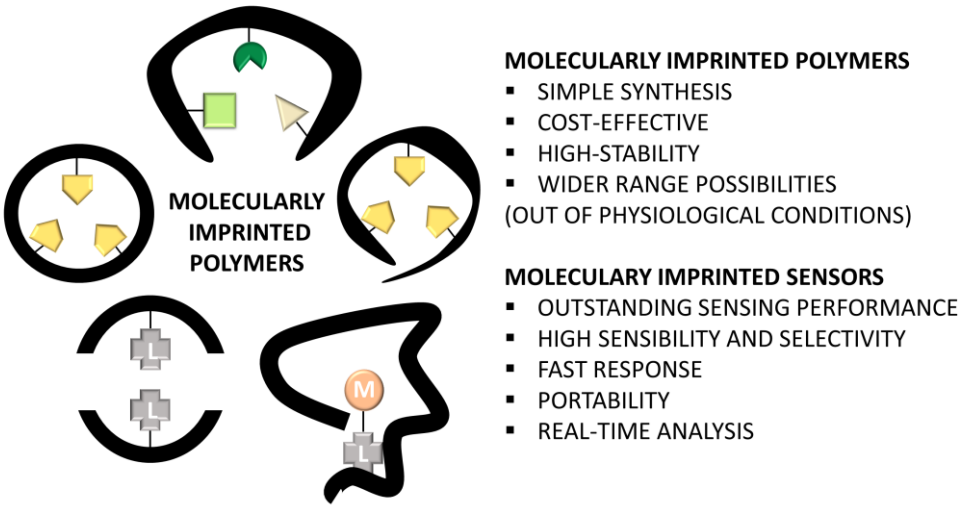

Figure 1.13. MIPs characteristics as a material and in sensing applications.

As it was explained in Section 1.1.3.3., MIPs can generate different types of materials due to different polymerisation methods. It is noteworthy to mention that at this point we must talk about a final sub-classification of polymerisation: (a) ex-*situ* polymerisation and (b) *in-situ* polymerisation. These have not been mentioned in previous sections because it is specific to sensors. The former decouples the synthesis and the immobilisation in order to enable a better optimisation of each one separately, making this option more versatile although specific immobilisation strategies are needed. The *in-situ* polymerisation consists in one-step method achieving the direct polymerisation of the MIP onto the electrode surface, which enables a better adherence and control of the film to the transducer surface. On the other hand, this strategy is closely dependant on the functional monomer(s) reactivity, specifically in front of the template desired.

Ex-situ polymerisation

The ex-situ polymerisation decouples the synthesis and the immobilisation to enable a better optimisation of each one separately. This approach allows the

synthesis and its subsequent characterisation to be undertaken in an independent manner from the measuring system, i.e., the sensor. Then, it is possible to select the optimal conditions to immobilise the polymer, *e.g.*, onto the surface electrode, and tune the electrochemical conditions to obtain the best electrochemical performance. Although chemical bonding is possible to incorporate polymeric material onto the sensor, physical entrapment is the most common solution. This is done with the use of a membrane or a framework to incorporate the polymeric material in the working electrode combining them before the final sensor is ready to be used.

MIP entrapment onto electrode surface

There are several ways to fix materials added onto the electrode or transducer surface, especially when physical adsorption is the employed technique, such as the use of sol-gel, Nafion®, chitosan or glutaraldehydes, among other options.

The idea is to preserve the properties and structure of the polymeric material by incorporating it onto a structure that allows its immobilization without modifying its intrinsic properties. To guarantee a homogeneous particle distribution over the electrode surface, several techniques can be implemented, including but not limited to drop-casting, spin- or spray-coating.

In section 1.1.3.3.1., the sol-gel process was described as a material that might be classified as a type of polymerisation. As itself, some works reported its imprinting properties, while in the sensing and biosensing field it is used as a framework material to incorporate different sized materials. In this direction several works were published in our group and are the main strategy used in this manuscript [83,84,136].

Nafion® is a convenient material to prepare modified sensing platforms as it is a non-electroactive, hydrophilic material that has an inexistent solubility in in water. Normally, its preparation consists of making an alcohol or water-based solution where the nanomaterials are resuspended. Thus, they can be physically suspended by drop-casting and then dried [137]. Following the previous procedures, a hemin-based co-polymerised MIP was synthesised by precipitation and immobilised onto a glassy carbon electrode (GCE) for the amperometric detection of 4-aminophenol [138]. In the same line, a voltammetric modified sensor was performed to detect tryptophan by drop-casting combining a mixture of prepared MWCNTs and nano-MIPs [139].

In the same direction than Nafion®, chitosan can be employed as a membrane because is a linear polysaccharide, obtained by deacetylation of chitin, with properties such as toxic-free, biocompatible and cost-effectiveness product. Roushani *et al.*, reported the development of a manganese voltammetric sensor based on the drop-casting deposition onto GCE of the synthesised MIP together with ioninc liquids and MWCNTs [140].

Poly(methyl methacrylate) (PMMA) is an acrylic synthetic based polymer that can act as a entrapment agent. As an example, volatile organic compounds QCM-based sensor was prepared by spin-coating a dispersion of MIP beads and the methyl methacrylate on the AT quartz crystal resonator [141].

Entrapment into electrode surface

Another strategy is the addition MIP beads distributing them directly into the electrode by including them in the material employed to build the electrode transducer. This is a common strategy when working with sensing platforms based on carbon paste electrodes (CPEs) or graphite-epoxy composites (GECs).

The strong point of this approach is its simplicity and high particle retention; however, in contrast to previous entrapment options, it may offer lower active areas in terms of MIP particles due to the non-homogenic distribution into the sensor. This is non-homogenic distribution will occur every time that the surface of the electrode is renovated, *i.e.*, by polishing the surface to clean or renovate the reactive surface. Even so, some studies were done using this approach, for example the voltammetric modified MIP sensor towards metronidazole was performed by combining graphite powder, n-eicosane and MIP beads [142]; another example includes the impedimetric sensing to determine digoxin [143]; and sensor for the determination of bisoprolol fumarate using potentiometric technique [144].

Although this may seem a rather rudimentary way of incorporating polymers, when combined with technological advances this approach can be very useful. For example by combining by inject printing, screen printing, soft lithography, contact printing, 3D printing and roll-to-roll processing or even with paper based technology [145].

In-situ polymerisation

This approach was proposed in order to permit a better integration and compatibility of the MIP and the transducer. The main goal is to promote the formation of tailor-made cavities as close as possible to the sensor surface by tuneable thin films in order to obtain better kinetics [146]. Herein, in this sub-section two strategy are going to be discussed: the grafting and the electropolymerisation.

Grafting of the MIP particles

Another alternative is to attach polymerisable functional groups in order to acquire ultra-thin MIP films [147]. Grafting may be performed to obtain self-assembled monolayers (SAM) using thiols on gold electrodes, silanes or diazonium salts. Thus, the main reagents: template, functional monomer(s), cross-linker and initiator are combined in a solution to add onto the electrode surface. In this approach, depending on the chemical structure one or another reagent will be covalently bonded onto the surface. Several studies can be found in recent literature such as: Khilfi *et al.* published the electrografting of-bezoylphenyl groups from the corresponding diazonium salts for melamine detection [148]. In the same direction, Kidakova *et al.* reported for the first time, a photochemical grafting of MIP receptors capable of selectively binding a clinically relevant protein [149].

Electropolymerisation

Polymerisable functional monomer(s) are solved into a solution, that contains the template and an electrolyte solution. Then, other elements such as co-monomer(s), crosslinker agents or different nanomaterials are added to achieve their incorporation into the polymetric matrix. Finally, the template removal could be achieved through the oxidation of the unwanted compound. In comparison with other template extraction methods used in other approaches, the strong point of oxidative removal is its relatively simple and quick procedure.

The first work involving an electropolymerised MIP modified sensor was published in 1999 by Malietista *et al.*, in this work Malietista employed a quartz crystal microbalance (QCM) to detect glucose [150]. The employed MIP was

obtained using a solution comprising o-phenylenediamine (oPD), an electropolymeritzable monomer. Özcam *et al.* reported a paracetamol voltammetric sensor based on electrochemically polymerized polypyrrole films, such films were obtained by the electropolymerisation of a solution consisting of pyrrole, paracetamol and a supporting electrolyte [151]. Even bacteria have been used as a templated polymer synthesised (*e.g*. S. aureus) [152]. In a more sophisticated approach, Ma. *et al.* published an interesting strategy that consists on a covalently binding a bacteria protein (template) and glutaraldehyde by means of an imine reaction. This approach was employed to quantify a prostate-specific antigen employing a graphite epoxy electrode modified with graphene nanoplates and gold nanoparticles that comprised the MIP [153].

Even if it is still not being considered yet a category per se of imprinting technologies [146], the use in (bio)sensing of electropolymerized MIPs had a great increase during the last decades. Recent published works appear to be inclined to use this strategy as it has some advantages when developing lab scale applications, e.g, obtention simplicity or its easy integration in the sensing platform. Some of the more common monomers employed in this approach include o-phenylenediamine, aniline, thiophene or thiophene derivatives, chitosan, acrylamide and the most widely used pyrrole, alone or in derivatized forms.

1.3. Chemometrics

1.3.1. Chemometrics analysis

The great technological advances of the last decades have allowed us to carry out analysis automatically, with a large volume of samples and even without the need for a technician to be present. Miniaturisation, automation, as well as technological advances in the field of computation and microelectronics have

allowed us to obtain instrumental machinery and devices that are increasingly efficient, autonomous, powerful and versatile.

In the framework of this Thesis, electrochemical techniques produce a enormous volume of analytical information that must be processed. Not all data will give us relevant and specific information for our purpose. Most of the information obtained experimentally may be redundant or unnecessary. The problem is how to treat this data and distinguish which is necessary and which is not. To paraphrase a colleague, data collection is not synonymous with information ownership. The data must be collected and put it in the right context to subsequently obtain the valid information. Moreover, the leap in information is even greater when we increase the number of sensors from working with a single sensor to a matrix of sensors (n+1). This inevitably increases the complexity and dimensionality of our data, and the use of single variable statistical methods is insufficient. It is needed the creation of multi-variated analysis to classify, quantify and/or modelling complex systems and/or mixture of samples untreatable by naked-eye or classical techniques. For this purpose, chemometrics will be the discipline that will serve as a tool to achieve our goal.

The International Chemometrics Society (ICS) defined in 1975 chemometrics as: "*the chemistry discipline that uses mathematical and statistical methods to design or select tailor-made methods and experiments, to provide maximum chemical information by means of data analysis*".

Chemometrics is widely used in different science areas, such as, medicine, engineering, biology and, chemistry. There are several classifications that are mainly focused on qualitative and quantitative methods or supervised and non-

supervised ones. As it is not the main topic in this manuscript, only the ones used in the compendium will be explained in following sections: they are de PCA and the ANNs.

1.3.2. Principal Component Analysis (PCA)

Principal Component Analysis (PCA) is one of the most employed mathematical tools in the field of chemometrics to evaluate the differences between samples. PCA is employed to reorganize the data samples according to its variability and to reveal any underling patterns in the data set, reducing the correlated raw data to a new variable without correlation. In other words, PCA is a chemometric treatment that allows us to visualize and recognise the similarities or discrepancies among samples, making it suitable and more understandable by simplifying the obtained data in clusters.

In fact, it is a method to obtain important variables, so-called Principal Components (PCs), from a set of data comprising a large number of variables.

PCA minimise the data dimensionality projecting this data into new coordinates (scores) maximising the differences between the recalculated values. In this manner, important information is discriminated from the insignificant or redundant one. Finally, these scores are depicted in a figure providing an understandable and easy to interpret plot. Nevertheless, it is important to mention that, the larger the data set is the more representative system is obtained.

In Figure 1.14., the new coordinates or PCs (Z_1, Z_2, Z_n) are calculated as lineal combination of the original variables (X_1, X_2, X_n).

$$Z_1 = a_{11}X_1 + a_{12}X_2 + \ldots + a_{1n}X_n \quad (1)$$

$$Z_2 = a_{21}X_1 + a_{22}X_2 + \ldots + a_{2n}X_n \quad (2)$$

$$\vdots$$

$$Z_n = a_{n1}X_1 + a_{n2}X_2 + \ldots + a_{nn}X_n \quad (n)$$

Figure 1.14. Mathematical treatment to obtain PCA new coordinates.

Ideally, as resulting of PCA treatment similar samples will end grouped in the same clusters, see Figure 1.15. The distance between each clusters will provide information of the sample differences.

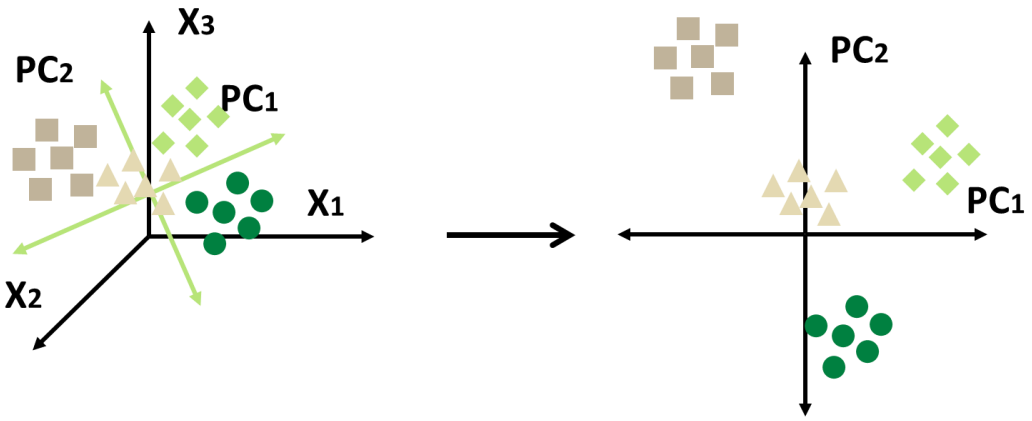

Figure 1.15. Scheme of data transformation by means of PCA.

PCA is an unsupervised method, which means that when performing this method, the generated PCs are identified in an unsupervised way, *i.e.,* the response variable (Y) is not employed to calculate the PC's components.

However, despite the advantages that PCA has regarding data set visualization it is important to mention that PCA it is not a classification tool, it only rearranges the data in a new set of coordinates. Therefore, in order to obtain a

classification tool would be necessary to feed the data obtained by PCA means with a chemometric classification tool such as Artificial Neural Networks.

1.3.1. Partial Least Squares (PLS)

Partial Least Squares (PLS) is a supervised chemometric tool that combine characteristics from PCA and multiple linear regression. Unlike PCA, that strives for maximum variance in samples, PLS focuses on the search of maximum predictive performance. This peak performance is obtained modelling simultaneously the sensor output, i.e., electrochemical response, and the target concentrations to calculate the Latent Variables. This LV achieve a similar function to the principal components in PC, they are new variables that correlate linearly manner with the target concentrations, see Figure 1.16.

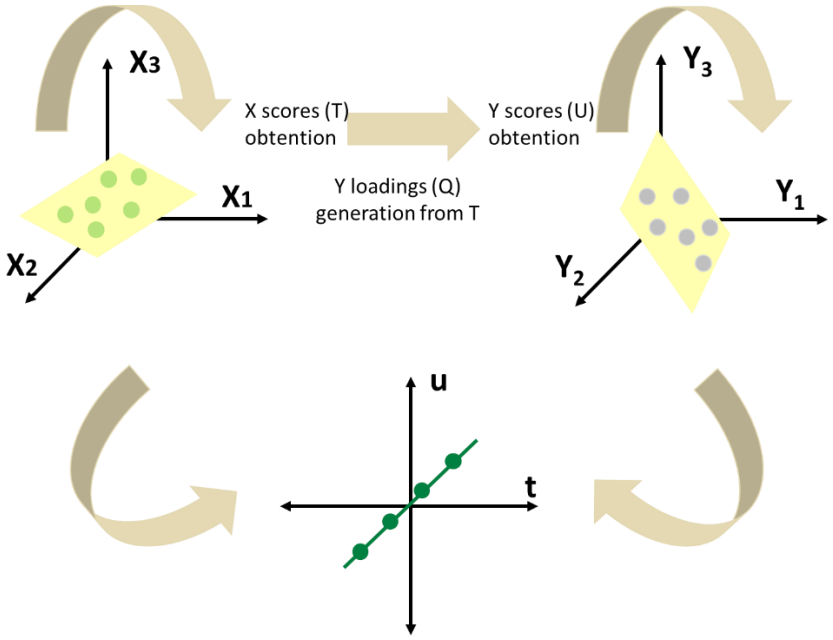

Figure 1.16. Schematic PLS data treatment to obtain the new coordinates.

PLS is widely used in chemometrics, probably the most employed, due its easy optimization. In order to build and optimize a PLS model, one has to select

enough number of LV that will contain a representative amount of the data set variance while maintaining the error at the minimum, see Figure 1.17.

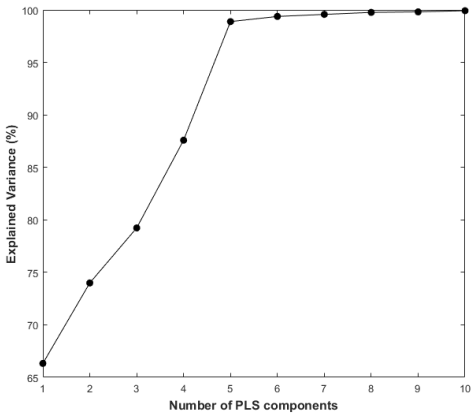

Figure 1.17. Plot of the explained variance vs. number of PLS components.

Being PLS the most widespread chemometric quantitative method it has been employed as a benchmark in certain applications presented herein.

1.3.2. Artificial Neural Networks (ANNs)

Artificial Neural Networks (ANNs) seek to mimic the human brain process of analysing information. ANNs are based in subunits called perceptron, see Figure 1.18. The perceptron is the most basic unit of an ANNs and consist of an input (X_1, …, X_n), a weight ($W_{1.i}$, …, $W_{n,i}$), a transfer function ($T_{1,i}$) and an output (a_k).

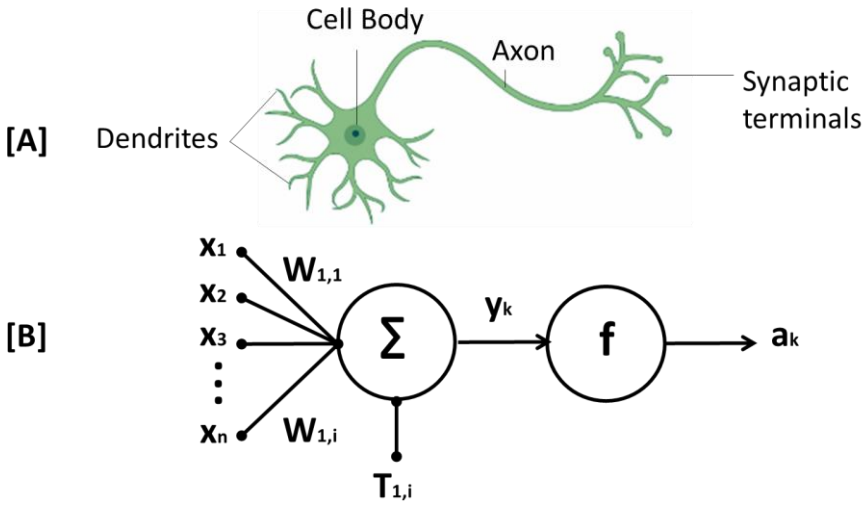

Figure 1.18. Diagram of neuron [A] versus. Perceptron [B].

However, with only a single perceptron is not enough to obtain the desired predictive capabilities, thus the multi-layered perceptron (MLP) model came to be useful, see Figure 1.19. The MLP is nothing more than an arrangement of perceptrons in mainly 3 different types of layers: the input layer, the hidden layer, and the output layer.

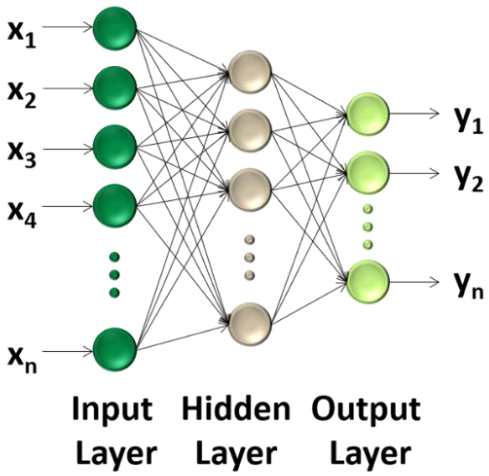

Figure 1.19. Multi-layered perceptron scheme depicting the input layer, the hidden layer and the output layer, this an artificial neuronal network.

The input and output layer are pretty self-explanatory, the input layer contains as much perceptrons as data points in the data set and its main function is to link the output to the hidden layer. The output layer contains as much perceptrons as the intended parameters to predict, *e.g*. if we are modelling mixtures of the X, Z and K compounds the output layer will have 3 perceptrons each one will give us the concentrations of X, Z or K.

However, it is in the hidden layer where the model does its prediction work, the architecture of these layer can be as complex as the model requires it. As a rule of thumb, the number of hidden layer's perceptrons for the applications of the present thesis ranges between 1 and 10. The number of neurons and transfer

functions of the hidden layer must be optimized by means of trial and error for each application.

ANNs are supervised methods, meaning that a training set of samples is required to teach the model how to perform its predictions. The model performance is then evaluated with an external set of samples usually named the test set. The ideal distribution of data points/samples for training and testing is around 30:70 ration.

Finally, the Electronic tongue (ET) approach seeks to mimic the human taste in two ways. First, mimics the human taste by employing different sensors with cross-selectivity. Second, it mimics the taste "processing" of the human brain by employing the mentioned ANN to analyse the data.

1.4. The Electronic Tongue

Several types of ETs exist. They can be classified according on the detection technique used, for example, potentiometric [154], amperometric [155], impedance based [156,157] and voltammetric [158].

In the research team led by Manel del Valle, there is a long tradition of employing ETs using voltammetric technique:

- To use different sensors modified with: enzymes [159] , NPs [160] , Polyelectrolytes (PECs) [161], Biochar [162], modified inks on screen-printed [163], MIPs [83], among others.
- To solve complexes mixtures such as: the determination of three benzodiazepines [164], ternary nitrophenol mixtures [165], analysis of amino acids [160], among others.

- To apply this technology in different cases: carbon oxygen demand (COD) [166], identify Brett Character in wine [167], for clustering metrics [168], to asses wine sensory descriptors [169], for nitro and peroxide explosive sensing [170], for photodegradation of phenolic compounds [171], among others.

The idea is to use a sensor array of efficient and low-cost electrochemical home-made sensors, so-called, graphite epoxy composites (GECs). These can be improved onto the surface by chemical or physical modification or in bulk.

Working with a sensor array provides us with a lot of raw data that must be processed in order to obtain analytical information, and this data must be processed accurately. Contrary to what one could think, the aim is not to obtain the best sensory performance. The main goal it to obtain a versatile transducer (transforming analytical information into electrical signal) that works as homogeneously as possible obtaining information through electrochemical techniques. The measurements must be stable and constant throughout the entire test. Moreover, the sensor array must be reusable, reproducible and as efficient as possible in terms of energy expenditure and cost-effective.

The ET has needed contributions from microelectronics, computer science, physics, mathematics, chemistry, among others to be developed. One of the most relevant points is that it has been able to adapt to the incorporation of the most outstanding scientific advances of the last few decades, and this is possibly one of its greatest successes. The incorporation of all kinds of recognition elements, whether they come from the areas of chemistry, biology or biomimetic and/or hybrid materials.

1.4.1. Historical perspective

ET application was first reported 1985 by Otto and Thomas to determine free metal ions using an array of non-specific ion selective electrodes (ISEs) [172]. However, it was not until a few years later that the term and definition of ET were coined [173]. Initial studies involving the use of ET were mainly based on potentiometric sensors, and exploited the potential of chemometric methods to improve the conventional ISEs in qualitative analysis [173]. However, soon after, the application of these systems in qualitative analysis for the recognition and discrimination of complex liquid analytes started to emerge [174]. Such applications demonstrated not only the potential of ET to derive the meaning from complex, imprecise or incomplete data, but also to accomplish novel applications not achievable by conventional approaches, such as mimicking the human taste perception.

Following, the advances in ET research, Winquist *et al.* reported the first voltammetric ET for the first time in 1997 [175]. The proposed system was composed by a double working electrode of gold and platinum. They used the principal component analysis (PCA) to allow the discrimination of different beverages.

However, the change in the measuring principle from potentiometry to voltammetry was very significant, because it removed the limitation of being able to detect only charged compounds and opened a new range of applications. Furthermore, voltammetric measurements present several advantages such a higher sensitivity, versatility, robustness and tuneability [175].

Over the next years, researchers in the field of ET evaluated different types of sensors to further improve the performance and potential of such systems. In

this manner, initial studies were based on the usage of different bare metals as working electrodes, but soon after, the usage of chemically modified electrodes was exploited to improve the performance of the former or to tackle the detection of different analytes.

More recently, Tonning *et al.* proposed the term Bio-ET to refer to the combination of one or more biosensors into the ET sensor array, usually sharing the same transduction principle to ensure their compatibility [176]. Bio-ET exploit the higher selectivity of biosensors to address the lack of selectivity and the capabilities of ET to extract relevant data from complex responses to compensate biosensors' interference problems and/or to allow the multidetermination of several species. In this manner, several systems based on such an approach have been reported [177,178], and despite the advantages that Bio-ET offer, they might still present some disadvantage in comparison to "conventional" ETs; these may be related to the potential higher cost of biosensors, their short-term stability and inoperability out of physiological conditions, or the lack of biological recognition elements suitable for any analytes of interest. That being said, the gain derived from the use of biosensors surpass those minor drawbacks, having in mind that there is still room for improvement. For that reason, the use of synthetic receptors analogous in function to natural bioreceptors counterparts would be of a great interest, specifically the artificial receptors like MIPs in electronic tongue application as Kutner published [179], see Figure 1.20.

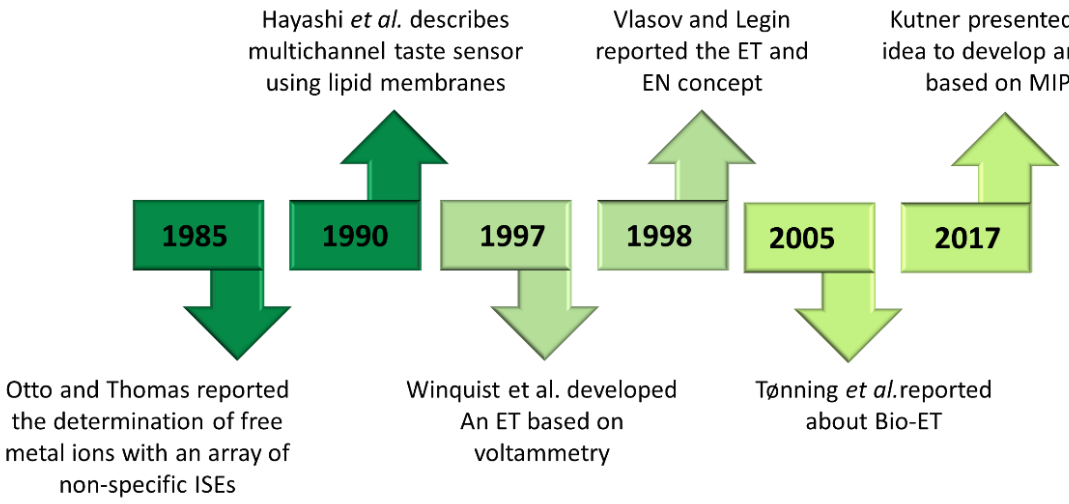

Figure 1.20. Timeline of ET history since early idea to the MIP-based ET concept.

1.4.2. Senses and biological processes

Since a long time ago, the perception of the real world and the senses living beings use are under debate, not only from scientific point of view but also from cultural and social one. It was in 1781 when Emmanuel Kant wrote in his masterpiece Critique of pure reason: *"All our knowledge begins with the senses, proceeds then to the understanding, and ends with reason. There is nothing higher than reason".*

Traditionally, there are five senses: hearing, touch, sight, smell and, taste. Although scientific community studies how senses work, there is not perfectly understood the mechanism that explains the stimulus or detection of receptor. However, it is accepted that sensations are perceived thanks to specific cells, which are filled with receptors and these are the ones that reacts to specific stimulus sending signal to the brain using nervous fibres. In the analytical field, there are systems combining physical sensors and mathematical treatments that draw inspiration from nature. These systems intend to mimic senses such as smell, sight and taste. This approach leaded to develop the Electronic Nose

(EN), the Electronic Eye (EE) and the above-mentioned ET, whose is going to be discussed in detail in the following section.

This work is going to be focused on the sense of taste as the ETs intend to be its man-made equivalent. Biology has discovered that mammals' sense of taste and human taste are based on specific taste receptors grouped in a sensory organ: the tongue, as can be seen in Figure 1.21. The bud receptors are formed by support and receptor cells, nerve fibres and microvilli, which maximise the contact surface and contain the specific receptor units for the different flavours. These receptors can be placed in different parts of the tongue and classified as circumvallate, foliate and fungiform taste buds. The different flavours: salty, sweet, sour and bitter can be detected by a specific group of receptors. They are localised in different areas of the tongue.

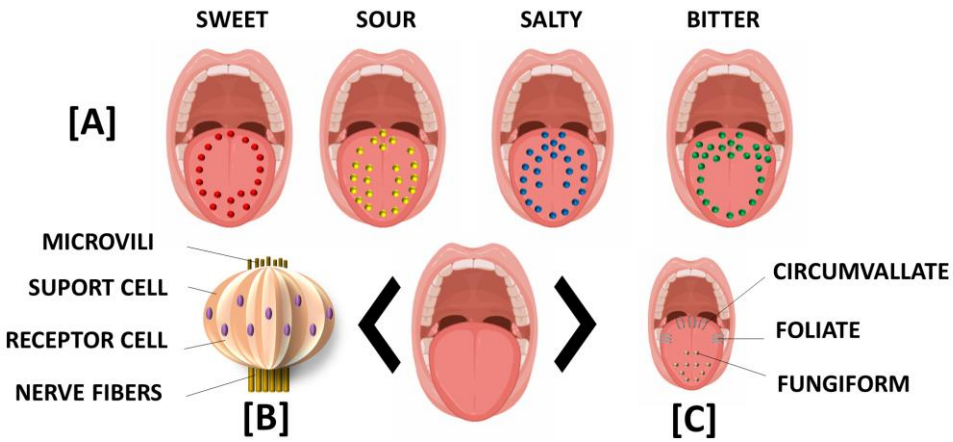

Figure 1.21. [A] Classical taste distribution, [B] representation of taste bud receptors and [C] different receptors.

Combinations of flavours, *e.g.* chocolate, are recognized through the specific electric signal pattern transmitted by bud tongues to the nervous system and interpreted by the brain comparing the unknown combination of flavours with the patterns already memorized.

Nevertheless, the above model is an oversimplification as recent studies seem to have demonstrated that the different receptors are not specific towards the different “flavours”. Is this cross-response that will be exploited to build the artificial models called ETs.

1.4.3. Definition

To mimic natural receptors senses it is needed to update the traditional univariate sensor approach and shift to the multivariate data responses provided by an array of sensors. The data obtained is then processed by a combination of mathematical statistics, several advances in informatics and the use of miniaturized devices. Furthermore, sensing technology is incorporating receptors which have an improved response against analytes of interest in complex matrices. However, it is also necessary to evaluate the possible redundancies of the huge data set obtained by using PCA and ANN approaches see Figure 1.22.

According to IUPAC definition: “The electronic tongue is a multisensor system that consists of a number of low-selective sensors and uses advanced mathematical procedures for signal processing based on the pattern recognition (PARC) and/or multivariate analysis (e.g., artificial neural networks (ANNs), principal component analysis (PCA))”.

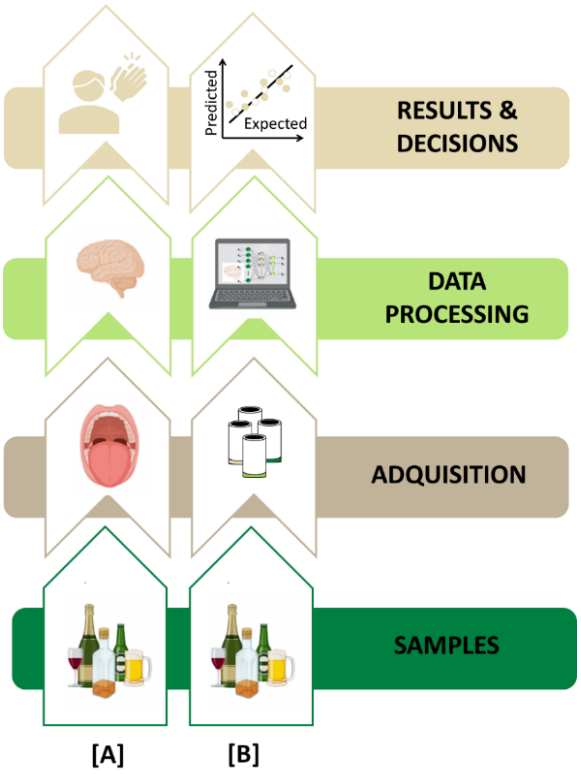

Figure 1.22. Samples recognition process comparison between: [A] Biological mechanism *versus* [B] Biomimetic process so-called Electronic Tongue Approach.

1.4.1. The electronic tongue-based MIPs paradigm

MIPs have been used for many single-sensor approach applications in the field of sensing and biosensing. Their unique properties because of the selective of the tailored-made cavities within the polymer gained the attention of scientific community. MIPs, as recognition element, show comparable performance, in terms of affinity, to the biological counterparts such as enzymes, aptamers or antibodies. They demonstrate comparable selectivity is some cases, with the further addition of advantages such as better stability, cost-effectiveness process and tunability to a wide range of different chemical species and a high versatility in terms of operation conditions such as extreme temperatures or pH levels and organic solvents media.

Nevertheless, despite the potential demonstrated by MIPs in the field of sensors, those sensors may show cross-response and/or suffer from unwanted matrix effects. To surpass these issues, the more common approach is to improve the synthesised material, but more benefits can be obtained if we are to apply a chemometric method to the data obtained from the MIP sensor, an approach known as electronic tongue (ET).

An ET is a biomimetic system used to the analysis of liquid samples, which comprises an array of sensors plus a chemometric tool able to interpret and extract meaningful data from the dataset generated by the array [177,180]. In the case of BioETs (Bioelectronic tongues) one or more of the sensors in the array are biosensors.

It might be considered that the first ET published work was reported by Otto and Thomas in 1985. In this study was focused on the free metal ions determination by using an array of non-specific ISES. In this publication, it was also reported the advantages of using partial least squares regression (PLS) in comparison to ordinary least squares regression (OLS) [172]. In the same direction, a similar approach was used to improve biosensors performance, in what has been referred to as bioelectronic tongue (BioET) [177,178].

By using these strategies, the integration of imprinted polymers sensors into ET systems might be an interesting alternative, due to the already discussed advantages of the former, permitting to unleash new applications and opening the room for the evolution of what could be considered a new type of ETs based on its usage.

On one hand, the combination of MIP-based sensors into ETs permits to correct the loose of selectivity of the latter in a similar way that biosensors do. However, MIPs-based electrodes offer a cost-effective system with better stability and operability in a broader range of conditions, while permits to obtain an artificial suitable synthetic receptor towards almost any analyte that someone can imagine. On the other hand, the chemometric model present in the ETs allow to overcome possible interferences by shifting the complexity from the electrochemical field to the statistical field [177,180,181].

Although there is a growing use of MIPs in the scientific literature, the combination of employing these artificial, receptors with the application of chemometric tools such as electronic tongue system or similar ones has not yet been exploited, i.e., electronic noses or electronic eyes. Therefore, this is a field in incipient development and for which this Thesis is presented, although it is true that there is a lack of bibliographic studies on which to base our work [179].

One of those works is from Bueno et al. where different proteins (bovine haemoglobin, equine myoglobin, cytochrome C and bovine serum albumin) are detected by means of 4 modified GECs array with hydrogel-based MIPs. Following the same line, El- Sharif et al. demonstrated the potential of using haemoglobin MIPs for discriminating different meat species [182]. Another interesting work was reported by Chatterjee *et al.*, they developed a theaflavin polyacrylamide MIP sensor and correlated the electrochemical response with the theaflavin content; the study demonstrated showed a good predictive capabilities, despite the fact that extra validation might be necessary because of the reduced number of samples used [183].

It is the author opinion that this thesis compiles the first electronic tongue that comprising an array of MIP functionalized sensors.

Bibliography

[1] A. Agüera, M.J. Martínez Bueno, A.R. Fernández-Alba, New trends in the analytical determination of emerging contaminants and their transformation products in environmental waters, Environ. Sci. Pollut. Res. 20 (2013) 3496–3515. https://doi.org/10.1007/s11356-013-1586-0.

[2] J.M. Galindo-Miranda, C. Guízar-González, E.J. Becerril-Bravo, G. Moeller-Chávez, E. León-Becerril, R. Vallejo-Rodríguez, Occurrence of emerging contaminants in environmental surface waters and their analytical methodology - A review, Water Sci. Technol. Water Supply. 19 (2019) 1871–1884. https://doi.org/10.2166/ws.2019.087.

[3] R. Peltomaa, E. Benito-Peña, H.H. Gorris, M.C. Moreno-Bondi, Biosensing based on upconversion nanoparticles for food quality and safety applications, Analyst. 146 (2021) 13–32. https://doi.org/10.1039/d0an01883j.

[4] V. Mani, T. Beduk, W. Khushaim, A.E. Ceylan, S. Timur, O.S. Wolfbeis, K.N. Salama, Electrochemical sensors targeting salivary biomarkers: A comprehensive review, TrAC - Trends Anal. Chem. 135 (2021) 116164. https://doi.org/10.1016/j.trac.2020.116164.

[5] W. Lu, M. Xue, Z. Xu, X. Dong, F. Xue, F. Wang, Q. Wang, Z. Meng, Molecularly Imprinted Polymers for the Sensing of Explosives and Chemical Warfare Agents, Curr. Org. Chem. 19 (2015) 62–71. https://doi.org/10.2174/1385272819666141201215551.

[6] W. Lu, H. Li, Z. Meng, X. Liang, M. Xue, Q. Wang, X. Dong, Detection of nitrobenzene compounds in surface water by ion mobility spectrometry coupled with molecularly imprinted polymers, J. Hazard. Mater. 280 (2014) 588–594. https://doi.org/10.1016/j.jhazmat.2014.08.041.

[7] C. Cortada, L. Vidal, A. Canals, Determination of nitroaromatic explosives in water samples by direct ultrasound-assisted dispersive liquid-liquid microextraction followed by gas chromatography-mass spectrometry, Talanta. 85 (2011) 2546–2552. https://doi.org/10.1016/j.talanta.2011.08.011.

[8] F. Canfarotta, J. Czulak, A. Guerreiro, A.G. Cruz, S. Piletsky, G.E. Bergdahl, M. Hedström, B. Mattiasson, A novel capacitive sensor based on molecularly imprinted nanoparticles as recognition elements, Biosens. Bioelectron. 120 (2018) 108–114. https://doi.org/10.1016/j.bios.2018.07.070.

[9] A. Florea, T. Cowen, S. Piletsky, K. De Wael, Electrochemical sensing of cocaine in real

samples based on electrodeposited biomimetic affinity ligands, Analyst. 144 (2019) 4639–4646. https://doi.org/10.1039/C9AN00618D.

[10] R.A.S. Couto, S.S. Costa, B. Mounssef, J.G. Pacheco, E. Fernandes, F. Carvalho, C.M.P. Rodrigues, C. Delerue-Matos, A.A.C. Braga, L. Moreira Gonçalves, M.B. Quinaz, Electrochemical sensing of ecstasy with electropolymerized molecularly imprinted poly(o-phenylenediamine) polymer on the surface of disposable screen-printed carbon electrodes, Sensors Actuators, B Chem. 290 (2019) 378–386. https://doi.org/10.1016/j.snb.2019.03.138.

[11] A. Herrera-Chacón, X. Cetó, M. del Valle, Molecularly imprinted polymers - towards electrochemical sensors and electronic tongues, Anal. Bioanal. Chem. (2021). https://doi.org/10.1007/s00216-021-03313-8.

[12] C. Alexander, H.S. Andersson, L.I. Andersson, R.J. Ansell, N. Kirsch, I.A. Nicholls, J. O'Mahony, M.J. Whitcombe, Molecular imprinting science and technology: A survey of the literature for the years up to and including 2003, J. Mol. Recognit. 19 (2006) 106–180. https://doi.org/10.1002/jmr.760.

[13] M.V. Polyakov, Adsorption properties and structure of silica gel, Zhurnal Fizieskoj Khimii/Akad. 2 (1931) 799–805.

[14] I. Polyakov, M.V.; Kuleshina, L.; Neimark, On the dependence of silica gel adsorption properties on the character of its porosity, Zhurnal Fizieskoj Khimii/Akad. 10 (1937) 100–112.

[15] H.F. Breinl F, Chemical examinations on the precipitate from haemoglobin and anti-haemoglobin serum and comments on the nature of antibodies, Z.Physiol. Chem. 192 (1930) 45–57.

[16] L. Pauling, A Theory of the Structure and Process of Formation of Antibodies, J. Am. Chem. Soc. 62 (1940) 2643–2657. https://doi.org/10.1021/ja01867a018.

[17] F.H. Dickey, The preparation of specific adsorbents, Proc. Natl. Acad. Sci. USA. 35 (1949) 227–229.

[18] Martin AJP, In Nobel Lectures, Chemistry 1942–1962., Elsevier. (1952) 359–371.

[19] A. Wulff, G.; Sarhan, Use of polymers with enzyme-analogous structures for resolution of racemates, Angew. Chem. Int. Ed. 11 (1972) 341–344.

[20] T. Takagishi, I.M. Klotz, Macromolecule-small molecule interactions; introduction of additional binding sites in polyethyleneimine by disulfide cross–linkages,

Biopolymers. 11 (1972) 483–491. https://doi.org/10.1002/bip.1972.360110213.

[21] J. Sagiv, Organized Monolayers by Adsorption. III. Irreversible Adsorption and Memory Effects in Skeletonized Silane Monolayers, Isr. J. Chem. 18 (1979) 346–353. https://doi.org/10.1002/ijch.197900053.

[22] L. Andersson, B. Sellergren, K. Mosbach, Imprinting of amino acid derivatives in macroporous polymers, Tetrahedron Lett. 25 (1984) 5211–5214. https://doi.org/10.1016/S0040-4039(01)81566-5.

[23] M.J. Garcia-Soto, K. Haupt, C. Gonzato, Synthesis of molecularly imprinted polymers by photo-iniferter polymerization under visible light, Polym. Chem. 8 (2017) 4830–4834. https://doi.org/10.1039/c7py01113j.

[24] E. Fischer, Einfluss der Configuration auf die Wirkung der Enzyme, Berichte Der Dtsch. Chem. Gesellschaft. 27 (1894) 2985–2993. https://doi.org/10.1002/cber.18940270364.

[25] M.J. Whitcombe, N. Kirsch, I.A. Nicholls, Molecular imprinting science and technology: A survey of the literature for the years 2004-2011, 2014. https://doi.org/10.1002/jmr.2347.

[26] P.A.G. Cormack, A.Z. Elorza, Molecularly imprinted polymers: Synthesis and characterisation, J. Chromatogr. B Anal. Technol. Biomed. Life Sci. 804 (2004) 173–182. https://doi.org/10.1016/j.jchromb.2004.02.013.

[27] J. Wackerlig, P.A. Lieberzeit, Molecularly imprinted polymer nanoparticles in chemical sensing – Synthesis, characterisation and application, Sensors Actuators B Chem. 207 (2015) 144–157. https://doi.org/10.1016/j.snb.2014.09.094.

[28] F. Canfarotta, A. Cecchini, S. Piletsky, CHAPTER 1. Nano-sized Molecularly Imprinted Polymers as Artificial Antibodies, in: RSC Polym. Chem. Ser., The Royal Society of Chemistry, 2018: pp. 1–27. https://doi.org/10.1039/9781788010474-00001.

[29] K.J. Shea, E.A. Thompson, S.D. Pandey, P.S. Beauchamp, Template synthesis of macromolecules. Synthesis and chemistry of functionalized macroporous poly(divinylbenzene), J. Am. Chem. Soc. 102 (1980) 3149–3155. https://doi.org/10.1021/ja00529a044.

[30] K.J. Shea, E.A. Thompson, Template Synthesis of Macromolecules. Selective Functionalization of an Organic Polymer, J. Org. Chem. 43 (1978) 4253–4255.

https://doi.org/10.1021/jo00415a064.

[31] G. Wulff, A. Sarhan, K. Zabrocki, Enzyme-analogue built polymers and their use for the resolution of racemates, Tetrahedron Lett. 14 (1973) 4329–4332. https://doi.org/10.1016/S0040-4039(01)87213-0.

[32] K.J. Shea, G.J. Stoddard, D.M. Shavelle, F. Wakui, R.M. Choate, Synthesis and characterization of highly crosslinked poly(acrylamides) and poly(methacrylamides). A new class of macroporous polyamides, Macromolecules. 23 (1990) 4497–4507. https://doi.org/10.1021/ma00223a001.

[33] K.J. Shea, D.Y. Sasaki, G.J. Stoddard, Fluorescence probes for evaluating chain solvation in network polymers. An analysis of the solvatochromic shift of the dansyl probe in macroporous styrene-divinylbenzene and styrene-diisopropenylbenzene copolymers, Macromolecules. 22 (1989) 1722–1730. https://doi.org/10.1021/ma00194a037.

[34] G. Wulff, M. Lauer, H. Böhnke, Rapid Proton Transfer as Cause of an Unusually Large Neighboring Group Effect, Angew. Chemie Int. Ed. English. 23 (1984) 741–742. https://doi.org/10.1002/anie.198407411.

[35] Y. Tan, A study of a bio-mimetic recognition material for the BAW sensor by molecular imprinting and its application for the determination of paracetamol in the human serum and urine, Talanta. 55 (2001) 337–347. https://doi.org/10.1016/S0039-9140(01)00442-8.

[36] C. Baggiani, G. Giraudi, C. Giovannoli, A. Vanni, F. Trotta, A molecularly imprinted polymer for the pesticide bentazone, Anal. Commun. 36 (1999) 263–266. https://doi.org/10.1039/a902968k.

[37] O. Ramstroem, L.I. Andersson, K. Mosbach, Recognition sites incorporating both pyridinyl and carboxy functionalities prepared by molecular imprinting, J. Org. Chem. 58 (1993) 7562–7564. https://doi.org/10.1021/jo00078a041.

[38] L. Andersson, B. Ekberg, K. Mosbach, Synthesis of a new amino acid based cross-linker for preparation of substrate selective acrylic polymers, Tetrahedron Lett. 26 (1985) 3623–3624. https://doi.org/10.1016/S0040-4039(00)89207-2.

[39] B. Sellergren, B. Ekberg, K. Mosbach, Molecular imprinting of amino acid derivatives in macroporous polymers. Demonstration of substrate- and enantio-selectivity by chromatographic resolution of racemic mixtures of amino acid derivatives, J.

Chromatogr. A. 347 (1985) 1–10. https://doi.org/10.1016/S0021-9673(01)95464-0.

[40] H. Dong, A. Tong, L. Li, Syntheses of steroid-based molecularly imprinted polymers and their molecular recognition study with spectrometric detection, Spectrochim. Acta Part A Mol. Biomol. Spectrosc. 59 (2003) 279–284. https://doi.org/10.1016/S1386-1425(02)00179-8.

[41] M. Kempe, Oxytocin receptor mimetics prepared by molecular imprinting, Lett. Pept. Sci. 7 (2000) 27–33. https://doi.org/10.1023/A:1008919213207.

[42] D.A. Spivak, K.J. Shea, Binding of Nucleotide Bases by Imprinted Polymers, Macromolecules. 31 (1998) 2160–2165. https://doi.org/10.1021/ma971310d.

[43] L.I. Andersson, K. Mosbach, Enantiomeric resolution on molecularly imprinted polymers prepared with only non-covalent and non-ionic interactions, J. Chromatogr. A. 516 (1990) 313–322. https://doi.org/10.1016/S0021-9673(01)89273-6.

[44] A. Leonhardt, K. Mosbach, Enzyme-mimicking polymers exhibiting specific substrate binding and catalytic functions, React. Polym. Ion Exch. Sorbents. 6 (1987) 285–290. https://doi.org/10.1016/0167-6989(87)90099-7.

[45] O. Norrlöw, M. Glad, K. Mosbach, Acrylic polymer preparations containing recognition sites obtained by imprinting with substrates, J. Chromatogr. A. 299 (1984) 29–41. https://doi.org/10.1016/S0021-9673(01)97819-7.

[46] K. Haupt, K. Mosbach, Molecularly Imprinted Polymers and Their Use in Biomimetic Sensors, Chem. Rev. 100 (2000) 2495–2504. https://doi.org/10.1021/cr990099w.

[47] A. Beltran, R.M. Marcé, P.A.G. Cormack, F. Borrull, Synthetic approaches to parabens molecularly imprinted polymers and their applications to the solid-phase extraction of river water samples, Anal. Chim. Acta. 677 (2010) 72–78. https://doi.org/10.1016/j.aca.2010.07.021.

[48] P. Qi, J. Wang, L. Wang, Y. Li, J. Jin, F. Su, Y. Tian, J. Chen, Molecularly imprinted polymers synthesized via semi-covalent imprinting with sacrificial spacer for imprinting phenols, Polymer (Guildf). 51 (2010) 5417–5423. https://doi.org/10.1016/j.polymer.2010.09.037.

[49] Y. Tong, H. Guan, S. Wang, J. Xu, C. He, Syntheses of chitin-based imprinting polymers and their binding properties for cholesterol, Carbohydr. Res. 346 (2011) 495–500. https://doi.org/10.1016/j.carres.2010.12.013.

[50] X. Li, Y. Tong, L. Jia, H. Guan, Fabrication of molecularly cholesterol-imprinted polymer particles based on chitin and their adsorption ability, Monatshefte Für Chemie - Chem. Mon. 146 (2015) 423–430. https://doi.org/10.1007/s00706-014-1369-4.

[51] M.A. Khasawneh, P.T. Vallano, V.T. Remcho, Affinity screening by packed capillary high performance liquid chromatography using molecular imprinted sorbents, J. Chromatogr. A. 922 (2001) 87–97. https://doi.org/10.1016/S0021-9673(01)00932-3.

[52] A.L. Graham, C.A. Carlson, P.L. Edmiston, Development and Characterization of Molecularly Imprinted Sol−Gel Materials for the Selective Detection of DDT, Anal. Chem. 74 (2002) 458–467. https://doi.org/10.1021/ac0106142.

[53] M. Lübke, M.J. Whitcombe, E.N. Vulfson, A Novel Approach to the Molecular Imprinting of Polychlorinated Aromatic Compounds, J. Am. Chem. Soc. 120 (1998) 13342–13348. https://doi.org/10.1021/ja9818295.

[54] J.U. Klein, M.J. Whitcombe, F. Mulholland, E.N. Vulfson, Template-Mediated Synthesis of a Polymeric Receptor Specific to Amino Acid Sequences, Angew. Chemie Int. Ed. 38 (1999) 2057–2060. https://doi.org/10.1002/(SICI)1521-3773(19990712)38:13/14<2057::AID-ANIE2057>3.3.CO;2-7.

[55] N. Kirsch, C. Alexander, S. Davies, M.. Whitcombe, Sacrificial spacer and non-covalent routes toward the molecular imprinting of “poorly-functionalized” N-heterocycles, Anal. Chim. Acta. 504 (2004) 63–71. https://doi.org/10.1016/S0003-2670(03)00510-5.

[56] S. Tokonami, H. Shiigi, T. Nagaoka, Review: Micro- and nanosized molecularly imprinted polymers for high-throughput analytical applications, Anal. Chim. Acta. 641 (2009) 7–13. https://doi.org/10.1016/j.aca.2009.03.035.

[57] M. Soares da Silva, R. Viveiros, A. Aguiar-Ricardo, V.D.B. Bonifácio, T. Casimiro, Supercritical fluid technology as a new strategy for the development of semi-covalent molecularly imprinted materials, RSC Adv. 2 (2012) 5075. https://doi.org/10.1039/c2ra20426f.

[58] M.J. Whitcombe, M.E. Rodriguez, P. Villar, E.N. Vulfson, A New Method for the Introduction of Recognition Site Functionality into Polymers Prepared by Molecular Imprinting: Synthesis and Characterization of Polymeric Receptors for Cholesterol, J. Am. Chem. Soc. 117 (1995) 7105–7111. https://doi.org/10.1021/ja00132a010.

[59] Y. Fujii, K. Matsutani, K. Kikuchi, Formation of a specific co-ordination cavity for a

chiral amino acid by template synthesis of a polymer Schiff base cobalt(III) complex, J. Chem. Soc. Chem. Commun. 7 (1985) 415. https://doi.org/10.1039/c39850000415.

[60] S. Mallik, R.D. Johnson, F.H. Arnold, Synthetic Bis-Metal Ion Receptors for Bis-Imidazole "Protein Analogs," J. Am. Chem. Soc. 116 (1994) 8902–8911. https://doi.org/10.1021/ja00099a007.

[61] P.K. Dhal, F.H. Arnold, Metal-coordination interactions in the template-mediated synthesis of substrate-selective polymers: recognition of bis(imidazole) substrates by copper(II) iminodiacetate containing polymers, Macromolecules. 25 (1992) 7051–7059. https://doi.org/10.1021/ma00051a050.

[62] G. Chen, Z. Guan, C.-T. Chen, L. Fu, V. Sundaresan, F.H. Arnold, A glucose-sensing polymer, Nat. Biotechnol. 15 (1997) 354–357. https://doi.org/10.1038/nbt0497-354.

[63] S. Striegler, Selective discrimination of closely related monosaccharides at physiological pH by a polymeric receptor, Tetrahedron. 57 (2001) 2349–2354. https://doi.org/10.1016/S0040-4020(01)00117-X.

[64] S. Striegler, M. Dittel, A Sugar Discriminating Binuclear Copper(II) Complex, J. Am. Chem. Soc. 125 (2003) 11518–11524. https://doi.org/10.1021/ja035561f.

[65] S. Vidyasankar, M. Ru, F.H. Arnold, Molecularly imprinted ligand-exchange adsorbents for the chiral separation of underivatized amino acids, J. Chromatogr. A. 775 (1997) 51–63. https://doi.org/10.1016/S0021-9673(97)00280-X.

[66] H.S. Lee, J. Hong, Chiral and electrokinetic separation of amino acids using polypyrrole-coated adsorbents, J. Chromatogr. A. 868 (2000) 189–196. https://doi.org/10.1016/S0021-9673(99)01246-7.

[67] B.R. Hart, K.J. Shea, Synthetic peptide receptors: Molecularly imprinted polymers for the recognition of peptides using peptide-metal interactions [8], J. Am. Chem. Soc. 123 (2001) 2072–2073. https://doi.org/10.1021/ja005661a.

[68] M. Kempe, K. Mosbach, Separation of amino acids, peptides and proteins on molecularly imprinted stationary phases, J. Chromatogr. A. 691 (1995) 317–323. https://doi.org/10.1016/0021-9673(94)00820-Y.

[69] M. Kempe, M. Glad, K. Mosbach, An approach towards surface imprinting using the enzyme ribonuclease A, J. Mol. Recognit. 8 (1995) 35–39. https://doi.org/10.1002/jmr.300080106.

[70] P. Zahedi, M. Ziaee, M. Abdouss, A. Farazin, B. Mizaikoff, Biomacromolecule template-based molecularly imprinted polymers with an emphasis on their synthesis strategies: a review, Polym. Adv. Technol. 27 (2016) 1124–1142. https://doi.org/10.1002/pat.3754.

[71] C. Gonzato, P. Pasetto, F. Bedoui, P.-E.E. Mazeran, K. Haupt, On the effect of using RAFT and FRP for the bulk synthesis of acrylic and methacrylic molecularly imprinted polymers, Polym. Chem. 5 (2014) 1313–1322. https://doi.org/10.1039/c3py01246h.

[72] Z. Adali-Kaya, B. Tse Sum Bui, A. Falcimaigne-Cordin, K. Haupt, Molecularly Imprinted Polymer Nanomaterials and Nanocomposites: Atom-Transfer Radical Polymerization with Acidic Monomers, Angew. Chemie. 127 (2015) 5281–5284. https://doi.org/10.1002/ange.201412494.

[73] S. Gam-Derouich, M. Ngoc Nguyen, A. Madani, N. Maouche, P. Lang, C. Perruchot, M.M. Chehimi, Aryl diazonium salt surface chemistry and ATRP for the preparation of molecularly imprinted polymer grafts on gold substrates, Surf. Interface Anal. 42 (2010) 1050–1056. https://doi.org/10.1002/sia.3210.

[74] C. Wang, X. Hu, P. Guan, L. Qian, D. Wu, J. Li, Thymopentin Magnetic Molecularly Imprinted Polymers with Room Temperature Ionic Liquids as a Functional Monomer by Surface-Initiated ATRP, Int. J. Polym. Anal. Charact. 19 (2014) 70–82. https://doi.org/10.1080/1023666X.2014.864461.

[75] B. Zu, Y. Zhang, X. Guo, H. Zhang, Preparation of molecularly imprinted polymers via atom transfer radical â€œbulkâ€ polymerization, J. Polym. Sci. Part A Polym. Chem. 48 (2010) 532–541. https://doi.org/10.1002/pola.23750.

[76] S. Boonpangrak, M.J. Whitcombe, V. Prachayasittikul, K. Mosbach, L. Ye, Preparation of molecularly imprinted polymers using nitroxide-mediated living radical polymerization, Biosens. Bioelectron. 22 (2006) 349–354. https://doi.org/10.1016/j.bios.2006.04.014.

[77] K. Hattori, M. Hiwatari, C. Iiyama, Y. Yoshimi, F. Kohori, K. Sakai, S.A. Piletsky, Gate effect of theophylline-imprinted polymers grafted to the cellulose by living radical polymerization, J. Memb. Sci. 233 (2004) 169–173. https://doi.org/10.1016/j.memsci.2003.12.013.

[78] G.E. Southard, K.A. Van Houten, E.W. Ott, G.M. Murray, Luminescent sensing of organophosphates using europium(III) containing imprinted polymers prepared by

RAFT polymerization, Anal. Chim. Acta. 581 (2007) 202–207. https://doi.org/10.1016/j.aca.2006.08.027.

[79] F. Chen, J. Wang, H. Chen, R. Lu, X. Xie, Microwave-assisted RAFT polymerization of well-constructed magnetic surface molecularly imprinted polymers for specific recognition of benzimidazole residues, Appl. Surf. Sci. 435 (2018) 247–255. https://doi.org/10.1016/j.apsusc.2017.11.061.

[80] G. Pan, Y. Zhang, Y. Ma, C. Li, H. Zhang, Efficient One-Pot Synthesis of Water-Compatible Molecularly Imprinted Polymer Microspheres by Facile RAFT Precipitation Polymerization, Angew. Chemie Int. Ed. 50 (2011) 11731–11734. https://doi.org/10.1002/anie.201104751.

[81] T. Zhou, L. Jørgensen, M.A. Mattebjerg, I.S. Chronakis, L. Ye, Molecularly imprinted polymer beads for nicotine recognition prepared by RAFT precipitation polymerization: a step forward towards multi-functionalities, RSC Adv. 4 (2014) 30292–30299. https://doi.org/10.1039/C4RA04741A.

[82] C. Gonzato, M. Courty, P. Pasetto, K. Haupt, Magnetic molecularly imprinted polymer nanocomposites via surface-initiated RAFT polymerization, Adv. Funct. Mater. 21 (2011) 3947–3953. https://doi.org/10.1002/adfm.201100466.

[83] A. Herrera-Chacon, A. González-Calabuig, I. Campos, M. del Valle, Bioelectronic tongue using MIP sensors for the resolution of volatile phenolic compounds, Sensors Actuators B Chem. 258 (2018) 665–671. https://doi.org/10.1016/j.snb.2017.11.136.

[84] A. Herrera-Chacón, Ş. Dinç-Zor, M. del Valle, Integrating molecularly imprinted polymer beads in graphite-epoxy electrodes for the voltammetric biosensing of histamine in wines, Talanta. 208 (2020) 120348. https://doi.org/10.1016/j.talanta.2019.120348.

[85] A. Mujahid, P.A. Lieberzeit, F.L. Dickert, Chemical sensors based on molecularly imprinted sol-gel materials, Materials (Basel). 3 (2010) 2196–2217. https://doi.org/10.3390/ma3042196.

[86] B. Sellergren, K.J. Shea, Origin of peak asymmetry and the effect of temperature on solute retention in enantiomer separations on imprinted chiral stationary phases, J. Chromatogr. A. 690 (1995) 29–39. https://doi.org/10.1016/0021-9673(94)00905-O.

[87] P.T. Vallano, V.T. Remcho, Highly selective separations by capillary

electrochromatography: molecular imprint polymer sorbents, J. Chromatogr. A. 887 (2000) 125–135. https://doi.org/10.1016/S0021-9673(99)01199-1.

[88] S. Emara, Simultaneous determination of caffeine, theophylline and theobromine in human plasma by on-line solid-phase extraction coupled to reversed-phase chromatography, Biomed. Chromatogr. 18 (2004) 479–485. https://doi.org/10.1002/bmc.341.

[89] J. Yin, G. Yang, Y. Chen, Rapid and efficient chiral separation of nateglinide and its l-enantiomer on monolithic molecularly imprinted polymers, J. Chromatogr. A. 1090 (2005) 68–75. https://doi.org/10.1016/j.chroma.2005.06.078.

[90] H. Zeng, X. Yu, J. Wan, X. Cao, Rational design and synthesis of molecularly imprinted polymers (MIP) for purifying tylosin by seeded precipitation polymerization, Process Biochem. 94 (2020) 329–339. https://doi.org/10.1016/j.procbio.2020.03.025.

[91] O.I. Parisi, M. Ruffo, R. Malivindi, A.F. Vattimo, V. Pezzi, F. Puoci, Molecularly Imprinted Polymers (MIPs) as Theranostic Systems for Sunitinib Controlled Release and Self-Monitoring in Cancer Therapy, Pharmaceutics. 12 (2020) 41. https://doi.org/10.3390/pharmaceutics12010041.

[92] S.J. Torabi, A. Mohebali, M. Abdouss, M. Shakiba, H. Abdouss, S. Ramakrishna, Y.S. Teo, I. Jafari, E. Rezvani Ghomi, Synthesis and characterization of a novel molecularly imprinted polymer for the controlled release of rivastigmine tartrate, Mater. Sci. Eng. C. 128 (2021) 112273. https://doi.org/10.1016/j.msec.2021.112273.

[93] J. Wang, Y. Cheng, R. Peng, Q. Cui, Y. Luo, L. Li, Co-precipitation method to prepare molecularly imprinted fluorescent polymer nanoparticles for paracetamol sensing, Colloids Surfaces A Physicochem. Eng. Asp. 587 (2020) 124342. https://doi.org/10.1016/j.colsurfa.2019.124342.

[94] G. Zhao, J. Liu, M. Liu, X. Han, Y. Peng, X. Tian, J. Liu, S. Zhang, Synthesis of Molecularly Imprinted Polymer via Emulsion Polymerization for Application in Solanesol Separation, Appl. Sci. 10 (2020) 2868. https://doi.org/10.3390/app10082868.

[95] L. Díaz de León-Martínez, J. Meléndez-Marmolejo, K. Vargas-Berrones, R. Flores-Ramírez, Synthesis and Evaluation of Molecularly Imprinted Polymers for the Determination of Di(2-ethylhexyl) Phthalate (DEHP) in Water Samples, Bull. Environ. Contam. Toxicol. 105 (2020) 806–812. https://doi.org/10.1007/s00128-020-03023-4.

[96] N. Le Goff, I. Fomba, E. Prost, F. Merlier, K. Haupt, L. Duma, A. Fayeulle, A. Falcimaigne-Cordin, Renewable Plant Oil-Based Molecularly Imprinted Polymers as Biopesticide Delivery Systems, ACS Sustain. Chem. Eng. 8 (2020) 15927–15935. https://doi.org/10.1021/acssuschemeng.0c05145.

[97] X. Chen, F. Wu, J. Tang, K. Yang, Y. Ma, J. Pan, Anisotropic emulsion constructed boronate affinity imprinted Janus nanosheets for stir bar sorptive extraction of cis-diol-containing catechol, Chem. Eng. J. 395 (2020) 124995. https://doi.org/10.1016/j.cej.2020.124995.

[98] B. Hosseinzadeh, N. Nikfarjam, S.H. Kazemi, Hollow molecularly imprinted microspheres made by w/o/w double Pickering emulsion polymerization stabilized by graphene oxide quantum dots targeted for determination of l-cysteine concentration, Colloids Surfaces A Physicochem. Eng. Asp. 612 (2021) 125978. https://doi.org/10.1016/j.colsurfa.2020.125978.

[99] P. Yáñez-Sedeño, S. Campuzano, J.M. Pingarrón, Electrochemical sensors based on magnetic molecularly imprinted polymers: A review, Anal. Chim. Acta. 960 (2017) 1–17. https://doi.org/10.1016/j.aca.2017.01.003.

[100] J. Marfà, R.R. Pupin, M. Sotomayor, M.I. Pividori, Magnetic-molecularly imprinted polymers in electrochemical sensors and biosensors, Anal. Bioanal. Chem. (2021). https://doi.org/10.1007/s00216-021-03461-x.

[101] M. Marć, P.P. Wieczorek, The preparation and evaluation of core-shell magnetic dummy-template molecularly imprinted polymers for preliminary recognition of the low-mass polybrominated diphenyl ethers from aqueous solutions, Sci. Total Environ. 724 (2020) 138151. https://doi.org/10.1016/j.scitotenv.2020.138151.

[102] J. Giebułtowicz, N. Korytowska, M. Sobiech, S. Polak, B. Wiśniowska, R. Piotrowski, P. Kułakowski, P. Luliński, Magnetic Core–Shell Molecularly Imprinted Nano-Conjugates for Extraction of Antazoline and Hydroxyantazoline from Human Plasma—Material Characterization, Theoretical Analysis and Pharmacokinetics, Int. J. Mol. Sci. 22 (2021) 3665. https://doi.org/10.3390/ijms22073665.

[103] H. Karimi-Maleh, M.L. Yola, N. Atar, Y. Orooji, F. Karimi, P. Senthil Kumar, J. Rouhi, M. Baghayeri, A novel detection method for organophosphorus insecticide fenamiphos: Molecularly imprinted electrochemical sensor based on core-shell Co3O4@MOF-74

nanocomposite, J. Colloid Interface Sci. 592 (2021) 174–185. https://doi.org/10.1016/j.jcis.2021.02.066.

[104] G.A. Ruiz-Córdova, J.E.L. Villa, S. Khan, G. Picasso, M. Del Pilar Taboada Sotomayor, Surface molecularly imprinted core-shell nanoparticles and reflectance spectroscopy for direct determination of tartrazine in soft drinks, Anal. Chim. Acta. 1159 (2021) 338443. https://doi.org/10.1016/j.aca.2021.338443.

[105] P.X. Medina Rangel, S. Laclef, J. Xu, M. Panagiotopoulou, J. Kovensky, B. Tse Sum Bui, K. Haupt, Solid-phase synthesis of molecularly imprinted polymer nanolabels: Affinity tools for cellular bioimaging of glycans, Sci. Rep. 9 (2019) 3923. https://doi.org/10.1038/s41598-019-40348-5.

[106] P.X. Medina Rangel, E. Moroni, F. Merlier, L.A. Gheber, R. Vago, B. Tse Sum Bui, K. Haupt, Chemical Antibody Mimics Inhibit Cadherin-Mediated Cell–Cell Adhesion: A Promising Strategy for Cancer Therapy, Angew. Chemie Int. Ed. 59 (2020) 2816–2822. https://doi.org/10.1002/anie.201910373.

[107] C. Cáceres, E. Moczko, I. Basozabal, A. Guerreiro, S. Piletsky, Molecularly Imprinted Nanoparticles (NanoMIPs) Selective for Proteins: Optimization of a Protocol for Solid-Phase Synthesis Using Automatic Chemical Reactor, Polymers (Basel). 13 (2021) 314. https://doi.org/10.3390/polym13030314.

[108] K. Karim, F. Breton, R. Rouillon, E. V. Piletska, A. Guerreiro, I. Chianella, S.A. Piletsky, How to find effective functional monomers for effective molecularly imprinted polymers?, Adv. Drug Deliv. Rev. 57 (2005) 1795–1808. https://doi.org/10.1016/j.addr.2005.07.013.

[109] I.A. Nicholls, H.S. Andersson, C. Charlton, H. Henschel, B.C.G. Karlsson, J.G. Karlsson, J. O'Mahony, A.M. Rosengren, K.J. Rosengren, S. Wikman, Theoretical and computational strategies for rational molecularly imprinted polymer design, Biosens. Bioelectron. 25 (2009) 543–552. https://doi.org/10.1016/j.bios.2009.03.038.

[110] T. Cowen, K. Karim, S. Piletsky, Computational approaches in the design of synthetic receptors – A review, Anal. Chim. Acta. 936 (2016) 62–74. https://doi.org/10.1016/j.aca.2016.07.027.

[111] F. Bates, M. Busato, E. Piletska, M.J. Whitcombe, K. Karim, A. Guerreiro, M. del Valle, A. Giorgetti, S. Piletsky, Computational design of molecularly imprinted polymer for direct detection of melamine in milk, Sep. Sci. Technol. 52 (2017) 1441–1453.

https://doi.org/10.1080/01496395.2017.1287197.

[112] T.A. Sergeyeva, S.A. Piletsky, A.A. Brovko, E.A. Slinchenko, L.M. Sergeeva, A. V. El'skaya, Selective recognition of atrazine by molecularly imprinted polymer membranes. Development of conductometric sensor for herbicides detection, Anal. Chim. Acta. 392 (1999) 105–111. https://doi.org/10.1016/S0003-2670(99)00225-1.

[113] A.M. Rosengren, K. Golker, J.G. Karlsson, I.A. Nicholls, Dielectric constants are not enough: Principal component analysis of the influence of solvent properties on molecularly imprinted polymer-ligand rebinding, Biosens. Bioelectron. 25 (2009) 553–557. https://doi.org/10.1016/j.bios.2009.06.042.

[114] D. Xu, W. Zhu, Y. Jiang, X. Li, W. Li, J. Cui, J. Yin, G. Li, Rational design of molecularly imprinted photonic films assisted by chemometrics, J. Mater. Chem. 22 (2012) 16572–16581. https://doi.org/10.1039/c2jm32833j.

[115] B. Sellergren, L. Andersson, Molecular recognition in macroporous polymers prepared by a substrate analog imprinting strategy, J. Org. Chem. 55 (1990) 3381–3383. https://doi.org/10.1021/jo00297a074.

[116] N. Leibl, L. Duma, C. Gonzato, K. Haupt, Polydopamine-based molecularly imprinted thin films for electro-chemical sensing of nitro-explosives in aqueous solutions, Bioelectrochemistry. 135 (2020) 107541. https://doi.org/10.1016/j.bioelechem.2020.107541.

[117] Y.M. Yin, Y.P. Chen, X.F. Wang, Y. Liu, H.L. Liu, M.X. Xie, Dummy molecularly imprinted polymers on silica particles for selective solid-phase extraction of tetrabromobisphenol A from water samples, J. Chromatogr. A. 1220 (2012) 7–13. https://doi.org/10.1016/j.chroma.2011.11.065.

[118] A.R. Bagheri, M. Arabi, M. Ghaedi, A. Ostovan, X. Wang, J. Li, L. Chen, Dummy molecularly imprinted polymers based on a green synthesis strategy for magnetic solid-phase extraction of acrylamide in food samples, Talanta. 195 (2019) 390–400. https://doi.org/10.1016/j.talanta.2018.11.065.

[119] P. Gründler, Chemical Sensors, 1st ed., Springer Berlin Heidelberg, Berlin, Heidelberg, 2007. https://doi.org/10.1007/978-3-540-45743-5.

[120] N. Bhalla, P. Jolly, N. Formisano, P. Estrela, Introduction to biosensors, Essays Biochem. 60 (2016) 1–8. https://doi.org/10.1042/EBC20150001.

[121] W.S. Hughes, The potential difference between glass and electrolytes in contact with the glass, J. Am. Chem. Soc. 44 (1922) 2860–2867. https://doi.org/10.1021/ja01433a021.

[122] E.G. Griffin, J.M. Nelson, The influence of certain substances on the activity of invertase, J. Am. Chem. Soc. 38 (1916) 722–730. https://doi.org/10.1021/ja02260a027.

[123] W.R. Heineman, W.B. Jensen, Leland C. Clark Jr. (1918–2005), Biosens. Bioelectron. 21 (2006) 1403–1404. https://doi.org/10.1016/j.bios.2005.12.005.

[124] G.G. Guilbault, J.G. Montalvo, Urea-specific enzyme electrode, J. Am. Chem. Soc. 91 (1969) 2164–2165. https://doi.org/10.1021/ja01036a083.

[125] S.J. UPDIKE, G.P. HICKS, The Enzyme Electrode, Nature. 214 (1967) 986–988. https://doi.org/10.1038/214986a0.

[126] A. Hulanicki, S. Glab, F. Ingman, Chemical sensors: definitions and classification, Pure Appl. Chem. 63 (1991) 1247–1250. https://doi.org/10.1351/pac199163091247.

[127] O.S. Wolfbeis, Chemical sensors - survey and trends, Fresenius. J. Anal. Chem. 337 (1990) 522–527. https://doi.org/10.1007/BF00322857.

[128] V. Velusamy, K. Arshak, O. Korostynska, K. Oliwa, C. Adley, An overview of foodborne pathogen detection: In the perspective of biosensors, Biotechnol. Adv. 28 (2010) 232–254. https://doi.org/10.1016/j.biotechadv.2009.12.004.

[129] D.A. Skoog, D.M. West, F.J. Holler, S.R. Crouch, Fundamentals of analytical chemistry, 9th ed., Belmont (USA), 2014.

[130] A.J. Bard, L.R. Faulkner, Electrochemical methods fundamentals and applications, 2nd ed., New York, 2001. https://linkinghub.elsevier.com/retrieve/pii/B9780123813732000569.

[131] X. Luo, A. Morrin, A.J. Killard, M.R. Smyth, Application of nanoparticles in electrochemical sensors and biosensors, Electroanalysis. 18 (2006) 319–326. https://doi.org/10.1002/elan.200503415.

[132] A. Walcarius, S.D. Minteer, J. Wang, Y. Lin, A. Merkoçi, Nanomaterials for bio-functionalized electrodes: Recent trends, J. Mater. Chem. B. 1 (2013) 4878–4908. https://doi.org/10.1039/c3tb20881h.

[133] F. Arduini, L. Micheli, D. Moscone, G. Palleschi, S. Piermarini, F. Ricci, G. Volpe, Electrochemical biosensors based on nanomodified screen-printed electrodes: Recent

applications in clinical analysis, TrAC Trends Anal. Chem. 79 (2016) 114–126. https://doi.org/10.1016/j.trac.2016.01.032.

[134] A. Chen, S. Chatterjee, Nanomaterials based electrochemical sensors for biomedical applications, Chem. Soc. Rev. 42 (2013) 5425. https://doi.org/10.1039/c3cs35518g.

[135] G. Maduraiveeran, M. Sasidharan, V. Ganesan, Electrochemical sensor and biosensor platforms based on advanced nanomaterials for biological and biomedical applications, Biosens. Bioelectron. 103 (2018) 113–129. https://doi.org/10.1016/j.bios.2017.12.031.

[136] F. Bates, M. del Valle, Voltammetric sensor for theophylline using sol–gel immobilized molecularly imprinted polymer particles, Microchim. Acta. 182 (2015) 933–942. https://doi.org/10.1007/s00604-014-1413-4.

[137] J. Wang, M. Musameh, Y. Lin, Solubilization of carbon nanotubes by Nafion toward the preparation of amperometric biosensors, J. Am. Chem. Soc. 125 (2003) 2408–2409. https://doi.org/10.1021/ja028951v.

[138] J.D.R.M. Neto, W.D.J.R. Santos, P.R. Lima, S.M.C.N. Tanaka, A.A. Tanaka, L.T. Kubota, A hemin-based molecularly imprinted polymer (MIP) grafted onto a glassy carbon electrode as a selective sensor for 4-aminophenol amperometric, Sensors Actuators B Chem. 152 (2011) 220–225. https://doi.org/10.1016/j.snb.2010.12.010.

[139] T. Alizadeh, S. Amjadi, A tryptophan assay based on the glassy carbon electrode modified with a nano-sized tryptophan-imprinted polymer and multi-walled carbon nanotubes, New J. Chem. 41 (2017) 4493–4502. https://doi.org/10.1039/C6NJ04108F.

[140] M. Roushani, Z. Saedi, F. Hamdi, B.Z. Dizajdizi, Preparation an electrochemical sensor for detection of manganese (II) ions using glassy carbon electrode modified with multi walled carbon nanotube-chitosan-ionic liquid nanocomposite decorated with ion imprinted polymer, J. Electroanal. Chem. 804 (2017) 1–6. https://doi.org/10.1016/j.jelechem.2017.09.038.

[141] M. Matsuguchi, T. Uno, Molecular imprinting strategy for solvent molecules and its application for QCM-based VOC vapor sensing, Sensors Actuators, B Chem. 113 (2006) 94–99. https://doi.org/10.1016/j.snb.2005.02.028.

[142] M.B. Gholivand, M. Torkashvand, A novel high selective and sensitive metronidazole

voltammetric sensor based on a molecularly imprinted polymer-carbon paste electrode, Talanta. 84 (2011) 905–912. https://doi.org/https://doi.org/10.1016/j.talanta.2011.02.022.

[143] S.I. Khan, R.R. Chillawar, K.K. Tadi, R. V. Motghare, Molecular Imprinted Polymer Based Impedimetric Sensor for Trace Level Determination of Digoxin in Biological and Pharmaceutical Samples, Curr. Anal. Chem. 14 (2018) 474–482. https://doi.org/10.2174/1573411013666171117163609.

[144] R. Mourad, M. El badry Mohamed, E.Y.Z.Z. Frag, H.A. El-Boraey, S.S. EL-Sanafery, H.A. El-Boraey, S.S. EL-Sanafery, A Novel Molecularly Imprinted Potentiometric Sensor for the Fast Determination of Bisoprolol Fumarate in Biological Samples, Electroanalysis. 33 (2021) 66–74. https://doi.org/10.1002/elan.202060043.

[145] A. Garcia-Cruz, O.S. Ahmad, K. Alanazi, E. Piletska, S.A. Piletsky, Generic sensor platform based on electro-responsive molecularly imprinted polymer nanoparticles (e-NanoMIPs), Microsystems Nanoeng. 6 (2020) 83. https://doi.org/10.1038/s41378-020-00193-3.

[146] C. Malitesta, E. Mazzotta, R.A. Picca, A. Poma, I. Chianella, S.A. Piletsky, MIP sensors - The electrochemical approach, Anal. Bioanal. Chem. 402 (2012) 1827–1846. https://doi.org/10.1007/s00216-011-5405-5.

[147] D.J. Dyer, Photoinitiated Synthesis of Grafted Polymers, in: Surface-Initiated Polym. I, Springer-Verlag, Berlin/Heidelberg, 2006: pp. 47–65. https://doi.org/10.1007/12_064.

[148] A. Khlifi, S. Gam-Derouich, M. Jouini, R. Kalfat, M.M. Chehimi, Melamine-imprinted polymer grafts through surface photopolymerization initiated by aryl layers from diazonium salts, Food Control. 31 (2013) 379–386. https://doi.org/10.1016/j.foodcont.2012.10.013.

[149] A. Kidakova, J. Reut, R. Boroznjak, A. Öpik, V. Syritski, Advanced sensing materials based on molecularly imprinted polymers towards developing point-of-care diagnostics devices, Proc. Est. Acad. Sci. 68 (2019) 158–167. https://doi.org/10.3176/proc.2019.2.07.

[150] C. Malitesta, I. Losito, P.G. Zambonin, Molecularly imprinted electrosynthesized polymers: New materials for biomimetic sensors, Anal. Chem. 71 (1999) 1366–1370. https://doi.org/10.1021/ac980674g.

[151] L. Özcan, Y. Şahin, Determination of paracetamol based on electropolymerized-

molecularly imprinted polypyrrole modified pencil graphite electrode, Sensors Actuators B Chem. 127 (2007) 362–369. https://doi.org/https://doi.org/10.1016/j.snb.2007.04.034.

[152] R. Wang, L. Wang, J. Yan, D. Luan, Tao sun, J. Wu, X. Bian, Rapid, sensitive and label-free detection of pathogenic bacteria using a bacteria-imprinted conducting polymer film-based electrochemical sensor, Talanta. 226 (2021) 122135. https://doi.org/https://doi.org/10.1016/j.talanta.2021.122135.

[153] Y. Ma, X.L. Shen, Q. Zeng, L.S. Wang, A glassy carbon electrode modified with graphene nanoplatelets, gold nanoparticles and chitosan, and coated with a molecularly imprinted polymer for highly sensitive determination of prostate specific antigen, Microchim. Acta. 184 (2017) 4469–4476. https://doi.org/10.1007/s00604-017-2458-y.

[154] P. Ciosek, W. Wróblewski, Potentiometric Electronic Tongues for Foodstuff and Biosample Recognition—An Overview, Sensors. 11 (2011) 4688–4701. https://doi.org/10.3390/s110504688.

[155] M. Scampicchio, S. Benedetti, B. Brunetti, S. Mannino, Amperometric electronic tongue for the evaluation of the tea astringency, Electroanalysis. 18 (2006) 1643–1648. https://doi.org/10.1002/elan.200603586.

[156] G. Pioggia, F. Di Francesco, M. Ferro, F. Sorrentino, P. Salvo, A. Ahluwalia, Characterization of a carbon nanotube polymer composite sensor for an impedimetric electronic tongue, Microchim. Acta. 163 (2008) 57–62. https://doi.org/10.1007/s00604-008-0952-y.

[157] M. Cortina-Puig, X. Muñoz-Berbel, M.A. Alonso-Lomillo, F.J. Muñoz-Pascual, M. del Valle, EIS multianalyte sensing with an automated SIA system—An electronic tongue employing the impedimetric signal, Talanta. 72 (2007) 774–779.

[158] Á.A. Arrieta, M.L. Rodríguez-Méndez, J.A. de Saja, C.A. Blanco, D. Nimubona, Prediction of bitterness and alcoholic strength in beer using an electronic tongue, Food Chem. 123 (2010) 642–646. https://doi.org/10.1016/j.foodchem.2010.05.006.

[159] A. Cipri, C. Schulz, R. Ludwig, L. Gorton, M. del Valle, A novel bio-electronic tongue using different cellobiose dehydrogenases to resolve mixtures of various sugars and interfering analytes, Biosens. Bioelectron. 79 (2016) 515–521.

https://doi.org/10.1016/j.bios.2015.12.069.

[160] G. Faura, A. González-Calabuig, M. del Valle, Analysis of Amino Acid Mixtures by Voltammetric Electronic Tongues and Artificial Neural Networks, Electroanalysis. 28 (2016) 1894–1900. https://doi.org/10.1002/elan.201600055.

[161] A. Herrera-Chacon, A. Gonzalez-Calabuig, F. Bates, I. Campos, M. Del Valle, Novel voltammetric electronic tongue approach using polyelectrolyte modifiers to detect charged species, in: ISOEN 2017 - ISOCS/IEEE Int. Symp. Olfaction Electron. Nose, Proc., 2017: pp. 9–11. https://doi.org/10.1109/ISOEN.2017.7968927.

[162] C. Kalinke, P.R. Oliveira, M. Bonet San Emeterio, A. González-Calabuig, M. Valle, A. Salvio Mangrich, L. Humberto Marcolino Junior, M.F. Bergamini, Voltammetric Electronic Tongue Based on Carbon Paste Electrodes Modified with Biochar for Phenolic Compounds Stripping Detection, Electroanalysis. 31 (2019) 2238–2245. https://doi.org/10.1002/elan.201900072.

[163] D. Ortiz-Aguayo, M. Bonet-San-Emeterio, M. del Valle, Simultaneous Voltammetric Determination of Acetaminophen, Ascorbic Acid and Uric Acid by Use of Integrated Array of Screen-Printed Electrodes and Chemometric Tools, Sensors. 19 (2019) 3286. https://doi.org/10.3390/s19153286.

[164] A. Herrera-Chacón, F. Torabi, F. Faridbod, J.B. Ghasemi, A. González-Calabuig, M. del Valle, Voltammetric Electronic Tongue for the Simultaneous Determination of Three Benzodiazepines, Sensors. 19 (2019) 5002. https://doi.org/10.3390/s19225002.

[165] A. González-Calabuig, X. Cetó, M. Del Valle, A voltammetric electronic tongue for the resolution of ternary nitrophenol mixtures, Sensors (Switzerland). 18 (2018) 1–11. https://doi.org/10.3390/s18010216.

[166] Q. Wang, M. del Valle, Determination of Chemical Oxygen Demand (COD) Using Nanoparticle-Modified Voltammetric Sensors and Electronic Tongue Principles, Chemosensors. 9 (2021) 46. https://doi.org/10.3390/chemosensors9030046.

[167] A. González-Calabuig, M. del Valle, Voltammetric electronic tongue to identify Brett character in wines. On-site quantification of its ethylphenol metabolites, Talanta. 179 (2018) 70–74. https://doi.org/10.1016/j.talanta.2017.10.041.

[168] M. Sarma, N. Romero, X. Cetó, M. Del Valle, Optimization of Sensors to be Used in a Voltammetric Electronic Tongue Based on Clustering Metrics, Sensors. 20 (2020) 4798. https://doi.org/10.3390/s20174798.

[169] X. Cetó, A. González-Calabuig, N. Crespo, S. Pérez, J. Capdevila, A. Puig-Pujol, M. del Valle, Electronic tongues to assess wine sensory descriptors, Talanta. 162 (2017) 218–224. https://doi.org/10.1016/j.talanta.2016.09.055.

[170] A. González-Calabuig, X. Cetó, M. Del Valle, Electronic tongue for nitro and peroxide explosive sensing, Talanta. 153 (2016) 340–346. https://doi.org/10.1016/j.talanta.2016.03.009.

[171] X. Cetó, A. González-Calabuig, M. del Valle, Use of a Bioelectronic Tongue for the Monitoring of the Photodegradation of Phenolic Compounds, Electroanalysis. 27 (2015) 225–233. https://doi.org/10.1002/elan.201400394.

[172] M. Otto, J.D.R. Thomas, Model Studies on Multiple Channel Analysis of Free Magnesium, Calcium, Sodium, and Potassium at Physiological Concentration Levels with Ion-Selective Electrodes, Anal. Chem. 57 (1985) 2647–2651. https://doi.org/10.1021/ac00290a049.

[173] Y. Vlasov, A. Legin, Non-selective chemical sensors in analytical chemistry: From “electronic nose” to “electronic tongue,” Fresenius. J. Anal. Chem. 361 (1998) 255–260. https://doi.org/10.1007/s002160050875.

[174] K. Hayashi, M. Yamanaka, K. Toko, K. Yamafuji, Multichannel taste sensor using lipid membranes, Sensors Actuators B Chem. 2 (1990) 205–213. https://doi.org/10.1016/0925-4005(90)85006-K.

[175] F. Winquist, P. Wide, I. Lundström, An electronic tongue based on voltammetry, Anal. Chim. Acta. 357 (1997) 21–31. https://doi.org/10.1016/S0003-2670(97)00498-4.

[176] E. Tønning, S. Sapelnikova, J. Christensen, C. Carlsson, M. Winther-Nielsen, E. Dock, R. Solna, P. Skladal, L. Nørgaard, T. Ruzgas, J. Emnéus, Chemometric exploration of an amperometric biosensor array for fast determination of wastewater quality, Biosens. Bioelectron. 21 (2005) 608–617. https://doi.org/10.1016/j.bios.2004.12.023.

[177] X. Cetó, N.H. Voelcker, B. Prieto-Simón, Bioelectronic tongues: New trends and applications in water and food analysis, Biosens. Bioelectron. 79 (2016) 608–626. https://doi.org/https://doi.org/10.1016/j.bios.2015.12.075.

[178] M. del Valle, Bioelectronic Tongues Employing Electrochemical Biosensors, in: F.-M. Matysik (Ed.), Trends Bioelectroanal., Springer International Publishing, Cham, 2017: pp. 143–202. https://doi.org/10.1007/11663_2016_2.

[179] T.-P.P. Huynh, W. Kutner, Molecularly imprinted p olymers as recognition materials for electronic tongues, Biosens. Bioelectron. 74 (2015) 856–864. https://doi.org/10.1016/j.bios.2015.07.054.

[180] M. del Valle, Electronic Tongues Employing Electrochemical Sensors, Electroanalysis. 22 (2010) 1539–1555. https://doi.org/10.1002/elan.201000013.

[181] Y. Ni, S. Kokot, Does chemometrics enhance the performance of electroanalysis?, Anal. Chim. Acta. 626 (2008) 130–146. https://doi.org/10.1016/j.aca.2008.08.009.

[182] H.F. El-Sharif, D. Stevenson, S.M. Reddy, MIP-based protein profiling: A method for interspecies discrimination, Sensors Actuators, B Chem. 241 (2017) 33–39. https://doi.org/10.1016/j.snb.2016.10.050.

[183] T. Nandy Chatterjee, R. Banerjee Roy, B. Tudu, P. Pramanik, H. Deka, P. Tamuly, R. Bandyopadhyay, Detection of theaflavins in black tea using a molecular imprinted polyacrylamide-graphite nanocomposite electrode, Sensors Actuators, B Chem. 246 (2017) 840–847. https://doi.org/10.1016/j.snb.2017.02.139.

2. Objectives

2. OBJECTIVES

In the presented manuscript an assortment of voltammetric MIP based sensors were manufactured to develop an array of biomimetic sensors for different applications. The field of interest were food and beverage industry, homeland security, explosive detection and environmental monitoring. The electrochemical data obtained was processed employing chemometrics, and essentially using, principal component analysis, artificial neural networks and the electronic tongue approach. While the former is employed to develop qualitative studies, the other ones are applied to obtain quantitative purposes.

The specific objectives of this thesis were divided into three sections, related to the use of the application of interest:

1. In the beverage production field:

    1.1. To design and synthesise molecularly imprinted polymers (MIPs) using as a template: 4-ethylphenol and 4-ethylguaiacol, separately.

    1.2. To study the applicability of these polymers, as artificial receptors, which are able to be used in voltammetric sensors by an appropriate transduction mechanism.

    1.3. To develop, for the very first time, a voltammetric MIP based sensor array able to be employed in the electronic tongue approach for discrimination of a mixture of 4-ethylphenols responsible of the Brett character in wine.

2. In the beverage preservation field:

    2.1. To implement and test the synthesis of MIPs using histamine as a template.

    2.2. To study the advantage of MIP polymer in contrast with the non-imprinted polymer by confocal microscopy and differential pulse voltammetry techniques.

    2.3. To determine and quantify histamine employing MIP based voltammetric sensors, as well as to optimise their electrochemical performance.

    2.4. To compare the feasibility of the presented voltammetric method with the industry gold standard one (an official fluorimetric method).

3. In the security and environmental field:

    3.1. To synthesise a dummy molecularly imprinted polymer against 2,4,6-trinitrotoluene (TNT), using its chemically and structurally analogue 2,4-dinitrophenol.

    3.2. To develop a voltammetric sensor, that uses a dummy MIP as an artificial receptor, to quantify TNT and DNP.

    3.3. To study the sensor discrimination capabilities in water samples, as a persistent and emerging contaminant, among their related nitroaromatic compounds.

3. Experimental

3. EXPERIMENTAL

In this part of the manuscript, materials, instrumentation, apparatus and the main protocols that had been performed for the experimental part of this thesis will be presented. The same structure as in the introduction will be maintained starting with MIP design and synthesis, followed by GEC sensor construction for posterior polymer immobilisation and finally the modelling and calculations necessary for the application in each case.

All the experimental details are related to the following articles compiled in this thesis:

- Article 1 - Herrera-Chacon, A., González-Calabuig, A., Campos, I., & del Valle, M. (2018). Bioelectronic tongue using MIP sensors for the resolution of volatile phenolic compounds. Sensors and Actuators B: Chemical, 258, 665-671.
- Article 2 - Herrera-Chacón, A., Dinç-Zor, Ş., & del Valle, M. (2020). Integrating molecularly imprinted polymer beads in graphite-epoxy electrodes for the voltammetric biosensing of histamine in wines. Talanta, 208, 120348.
- Article 3 - Herrera-Chacon, A., González-Calabuig, A., & del Valle, M. (2021). Dummy Molecularly Imprinted Polymers Using DNP as a Template Molecule for Explosive Sensing and Nitroaromatic Compound Discrimination. Chemosensors, 9(9), 255.

3.1. MIP synthesis

Materials and instrumentation

In article 1, 4-ethylphenol (4-EP) and 4-ethylguaiacol (4-EG) were employed as templates, separately for each synthesis. Divinylbenzene (DVB) was used as a functional monomer. All of these materials were purchased from Merck (Darmstadt, Germany). Ethylene glycol dimethacrylate (EGDMA) was acting as a crosslinker and it was acquired from Acros Organic (Geel, Belgium). Ethanol (EtOH) (96% v/v, Multisolvent® for HPLC ACS UV-VIS) was employed as a solvent; a mixture of methanol (MeOH) and acetic acid in ratio 9:1 was used, all of them were purchased from Scharlab (Barcelona, Spain). 2.2'-azobis(2,4-dimethylvaleronitrile) (AIVN), the initiator, was acquired from Wako chemicals (Neuss, Germany).

In article 2, histamine dihydrochloride was used as a template and it was acquired from Acros Organic. In the same line in article 3, 2,4-dinitrophenol (DNP) was the chosen template and it was purchased from Merck. In both articles, methacrylic acid (MAA) from Acros Organic was used as a monomer. The crosslinker, radical initator, solvent and template extraction reagents were the same products as article 1.

For the synthesis of MIP and NIP, a water bath controlled with a Huber CC1 thermoregulating pump (Huber GmbH, Offenburg, Germany) was used, equipped with 250 mL round bottom flask. For the template extraction cleaning process, a Soxhlet extractor was employed and the polymer was emplaced into a filter package paper. All the glassware was purchased from Scharlab.

Protocols and procedures

The same procedure was used in all articles following a non-covalent approach and precipitation polymerisation by FRP. For all the polymers, at least three synthesis batches were prepared for MIP and NIP, using the same conditions.
In a 250 mL round bottom flask, 40 mL of solvent were transferred dissolving 0.5 mmol of template and 2.05 mmol of monomer, that were stirred during at least 30 minutes with magnetic agitation, after sealing the round bottom flask. Meanwhile, EGDMA was treated with alumina in order to remove the remaining stabiliser. A glass pipette was filled with a little portion of cotton (in the bottom and the top part) and Al_2O_3 placed in the middle. Then, EGDMA was filtered by using this pipette. The filtered EGDMA was maintained in the fridge while it was not in used. The radical initiator was weighted and dissolved in an Eppendorf® tube where 1 mL of solvent was added. Once, the pre-polymerisation complex between the monomer and the template was formed, the crosslinker and the

initiator were gently transferred into the flask. Immediately after, the round bottom flask was placed into a gel bath and purged under nitrogen gas for at least 5 minutes to remove all the oxygen (see Figure 3.1.A). This step is critical to obtain an oxygen free atmosphere to proceed with the polymerisation in the optimal conditions and let the initiator start the reaction. The flask was then placed in a water bath at 60°C for 10 hours, sealing them with a nitrogen balloon (see Figure 3.1.B). MIPs and NIPs were dried at room temperature and transferred in a package of filter paper. As can be seen in Figure 3.1., this package was placed into the Soxhlet system in order to remove the template (in MIP case) and unreacted reagents (for both polymers) [1].

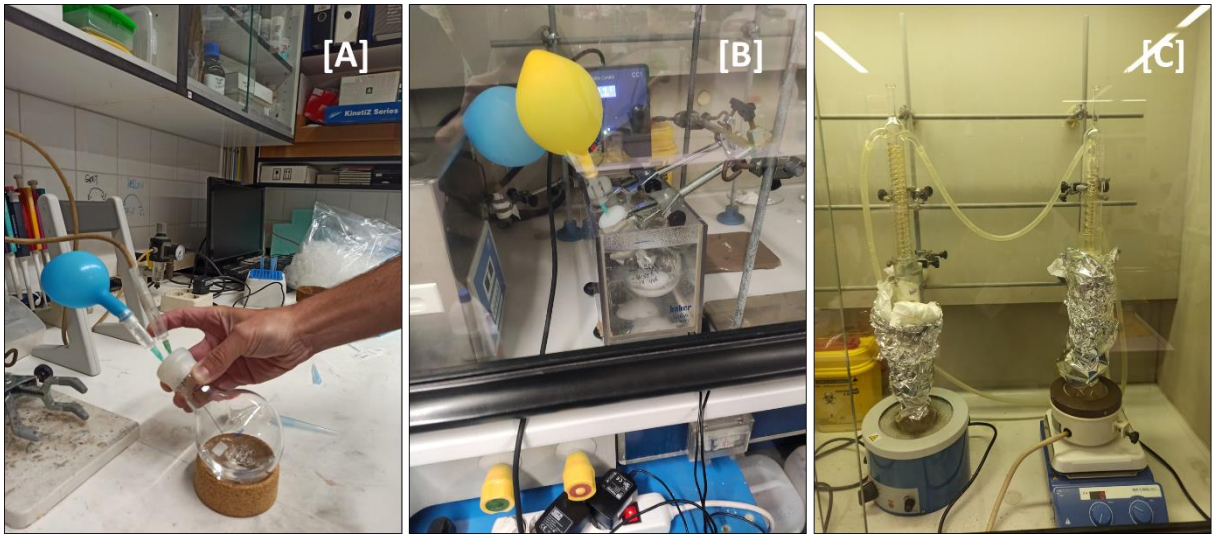

Figure 3.1. [A] Degassing process when radical initiator and crosslinker were added into the pre-polymerisation complex solution. [B] Polymer synthesis was carried out in the water bath. [C] Soxhlet extraction for both polymers.

3.2. Sensors construction

Materials and instrumentation

In all articles, graphite epoxy composites (GECs) electrodes were built employing the same materials. Copper foils and grade polish sandpapers of different roughness were purchased from Maranges (Cerdanyola, Spain). 20 mm inner

diameter PVC tube was obtained from Servei Estació (Barcelona, Spain). All the electrochemical connectors and cables employed to fabricate the electrodes, as well as, the connector cables were purchased from Onda Radio (Sant Joan Despí, Barcelona). Graphite powder (particle size <50 µm) was received from BDH (BDH Laboratory Supplies, Poole, UK) and Resineco Epoxy Kit resin was supplied from Resinecogreen composites (Barcelona, Spain).

Protocols and procedures

For the GECs electrodes construction, a 5 mm diameter copper disc was properly cut and cleaned in HCl 0.1 M over 30 minutes. Then, an electrical connector was soldered on top of the copper disc. Then, a 6 mm PVC tube was cut and polished in order to place the modified connector inside. Thereafter, the graphite epoxy resin was prepared *in situ* and used to fill the PVC tube, from the top down, this constitutes the transducer surface. Finally, the electrodes are cured in the oven for at least 48h at 40°C, then polished with different roughness grades of sandpaper to obtain a smooth, polished and clean transducer surface of the GEC electrode.

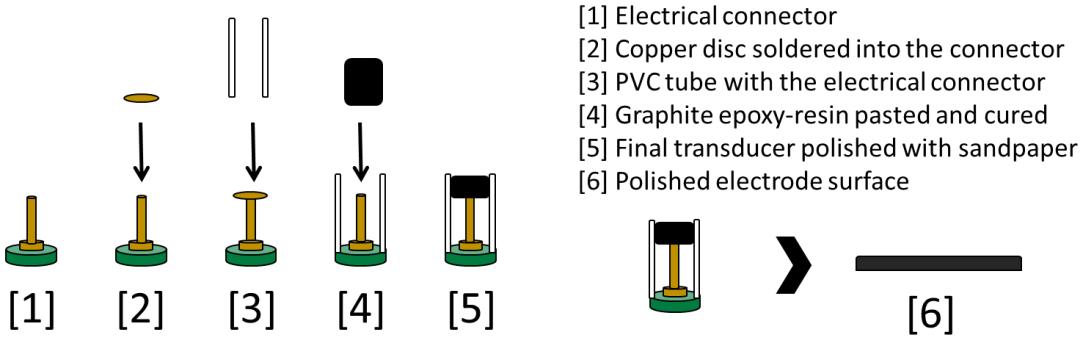

Figure 3.2. Graphite epoxy composite transducer fabrication.

It is needed to be mentioned, that this procedure is a commonly employed in the GSB group to build GEC sensors [2,3] and several studies were published with modifications of this sensor [4–7].

3.3. Microscopy and Fourier transform infrared spectroscopy (FT-IR) characterisation

Materials and instrumentation

All polymers included in this manuscript were characterised by scanning electron microscopy (SEM) in the Microscopy Service of *Universitat Autònoma de Barcelona*. Polymer powders were placed onto different aluminum stubs coated with carbon tape. Then, they were metallised by a K850 Critical Point Dryer Emitech (Ashford, UK).

Electrode surfaces were examined by SEM using MERLIN FE-SEM (Zeiss GmbH, Jena, Germany) without any kind of metallisation. The only special treatment with electrode surfaces was to put carbon tape surrounding the region of interest to avoid the charging effect, specially in the case of insulating polymers. The resulting microscopy images were treated with Fiji package software and Image J software [8].

In article 2, a confocal study using optical microscopy was done in order to characterise the differences between MIPs and NIPs complexing abilities by using o-phthalaldehyde (OPA) reagent purchased from Merck.

In article 3, FT-IR spectroscopy was performed (Fourier transform-infrared spectroscopy) employing an IR Spectrophotometer Tensor 27, Bruker, respectively. The chemical composition of the methacrylic molecular-printed polymer was difficult to characterise with other techniques as it is a non-soluble high cross-linked polymer. Therefore, an FT-IR was performed to observe the main chemical bonds.

Protocols and procedures

To prepare the samples for SEM first, a small amount of dried polymer was sprinkled in an aluminim stub that had a carbon tape attached to it. Then, nitrogen gas was blowed to remove the sample excess. Polymer stubs were placed into the metalliser holder tilted 45º over 4 minutes to each side to obtain an appropriate surface. On the other hand, the array of sensors were placed in metallic holder and carbon tape was used to cover the surroundings of the sensors to avoid PVC charging effect during imaging.

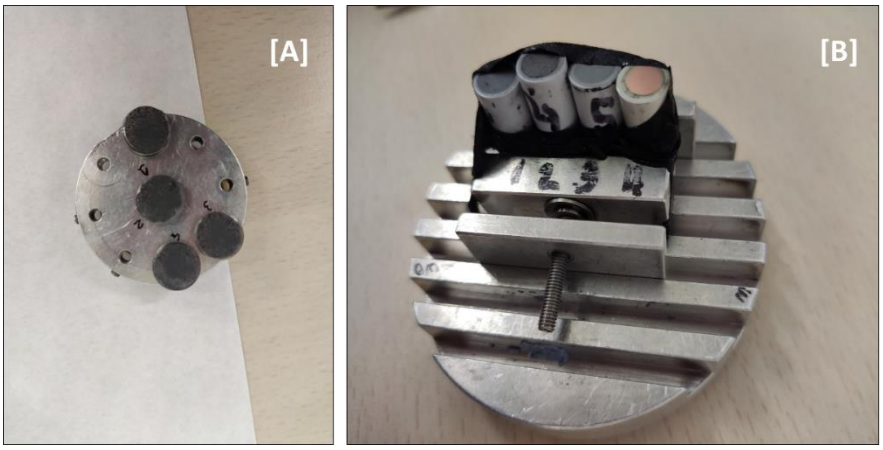

Figure 3.3. [A] Metallised polymers onto the stubs. [B] Sensor preparation holder.

In article 2, OPA reagent was used to form a fluorescence complex with histamine that can be studied by confocal microscopy. This complex was equilibrated with the dried powder polymer to compare the binding capacities between MIP and NIP. First, the dying reaction needed to be prepared before adding the polymer. Then, the dried polymer beads were equilibrated with OPA-histamine complex at the concentration of 5 µg mL^{-1} (in 0.1M HCl media). In order to check this study and obtain a real background, a negative control was also examined without histamine. Next the reagent generating the fluorescent complex was added, as the developer of the interaction, see Figure 3.4.

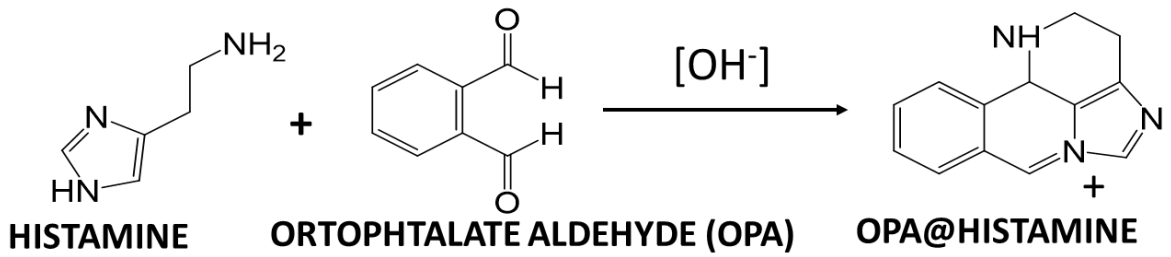

Figure 3.4. Histamine and OPA complex reaction used in confocal studies.

In article 3, the chemical composition of the methacrylic molecular-printed polymer was characterised by triplicate for both NIP's and MIP's samples using FT-IR spectroscopy technique. A tip of spatula of polymer powder, for each polymer, was placed directly onto the apparatus and scanned in order to acquire the spectra.

3.4. Polymer integration onto sensor surface

Materials and instrumentation

For the integration of these polymers in GEC electrodes, tetramethyl orthosilicate (TEOS) and hydrochloric acid were acquired from Merck. The EtOH used was the same grade and purity that the one used in the synthesis step and Milli-Q water was collected from Milli-Q System (Millipore, Billerica, MA, USA). The apparatus to agitate and break polymers aggregates employed were: IKA® VORTEX 3 (vortex shaker, 230V, 1/cs) purchased in Merck and ultrasonic cleaning machine J.P Selecta (Barcelona, Spain) and Thermo Scientific™ Tube Revolver Rotator rotisserie (tube revolver) (Madrid, Spain).

Protocols and procedures

First of all, a polymer suspension was prepared mixing 15 mg of polymer in 1 mL of EtOH and let it resting for at least 72h in the tube protected from light, in order to control the polymer size. After that, the suspension was homogenized in the tube rotisserie. For the sol-gel immobilisation, 500 µL de EtOH, 500 µL of

TEOS, 250 µL of Milli-Q water and 25 µL of HCl 0.1 M were transferred in a 2 mL tube. Then, they were mixed using IKA vortex for 45 minutes with mild agitation followed by 35 minutes of still incubation at room temperature (but resting the tube without agitation) to acquire a synergic stage. Afterwards, 200 µL of this mixture were transferred in a tube containing 7 mg of graphite powder, and were sonicated over 5 minutes. When the suspension is disrupted, 40 µL of polymer suspension were extremely caution pipetted and placed into the graphite mixture [1].

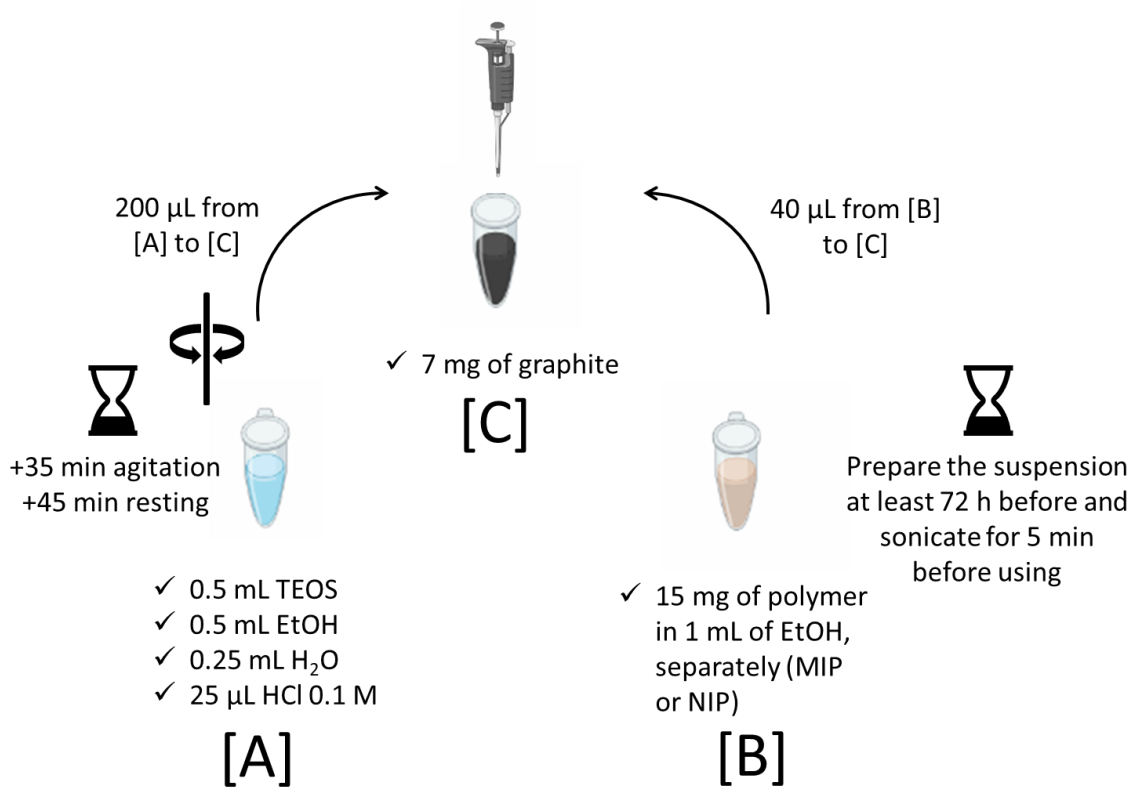

Figure 3.5. Polymer sol-gel suspension procedure.

Then, this sol-gel matrix suspension was agitated using IKA vortex over 10 minutes. Finally, 10 µL of the suspension were added onto the GEC surface by drop-casting and immediately spin-coated.

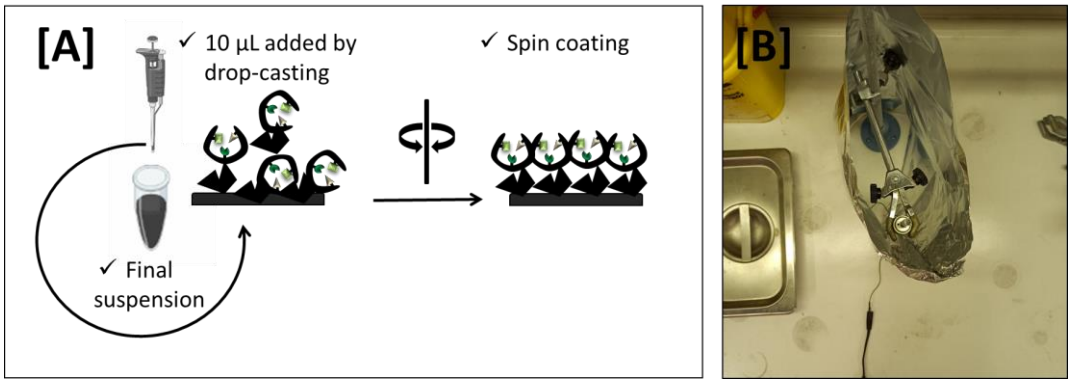

Figure 3.6. [A] Immobilisation via sol gel and drop-casting. [B] Home-made spin coater.

3.5. Electrochemical measurements

Materials and instrumentation

The following reagents were employed in the electrochemical measurements. In article 1, gallic acid, 4-ethylguaiacol and quercetin were acquired from Merck. In article 2, tyramine, gallic acid and coumaric acid were also purchased from Merck. In article 3, 1,3-dinitrobenzene (DNB), 2-nitrotoluene (NT), 2,4-dinitritoluene (DNT), 2,6-dinitrotoluene and 2,4-dinitrophenol (DNP), acetaminophen (AP), serotonin (SER) and tryptamine (TRYPT) were purchased from Merck. 1-nitrobenzene (NB) and 4-nitrotoluene (NT) were supplied by Acros Organics. 2,4,6-trinitrotoluene (TNT) was obtained from LGC standards (Teddington, Middlesex, UK).

Table 3.1. Table of buffers employed in the electrochemical measurements.

Buffer	Composition	Ph	Article
Potassium hydrogen phthalate	50 mM HP^-/P^{2-} +100 mM KCl	5	[9]
Phosphate	50 mM H_2PO4^-/ HPO_4^{2-} + 100 mM KCl	6	
Phosphate	50 mM H_2PO4^-/ HPO_4^{2-} + 100 mM KCl	7	[9,10]
Tris-hydroxymethyl-aminomethane	50 mM Tris + 100 mM NaCl	8	[9]
Acetate	100 mM CH_3COOH/ CH_3COO^- + 100 mM KCl	4.5	[11]
Phosphate	100 mM H_2PO4^-/ HPO_4^{2-} + 100 mM KCl	6	
Phosphate	100 mM H_2PO4^-/ HPO_4^{2-} + 100 mM KCl	7	
Tris-hydroxymethyl-aminomethane	100 mM Tris + 150 mM NaCl	8	
Tris-hydroxymethyl-aminomethane	100 mM Tris + 150 mM NaCl	9	

In order to perform the electrochemical measurements, in Article 1 and 3 was employed an electrochemical cell consisting in a commercial 52–61 combined Ag/AgCl reference and counter platinum electrode (Crison Instruments, Barcelona Spain) and was connected to an AUTOLAB PGSTAT30 (Metrohm AG, Herisau, Switzerland) controlled with GPES Multichannel 4.7 software package.

In the same line, in Article 2 the same cell was used but the electrochemical measurements were performed with MultiEmStat multichannel potentiostat controlled by Multitrace 4.2. software (both from Palm Instruments BV, Houten, The Netherlands).

Protocols and procedures

For the electrochemical measurements, specific conditions and cleaning steps were optimised and applied.

In article 1, Differential Pulse Voltammetry (DPV) measurements were recorded by scanning potential from 0 V to 0.9 V vs. Ag/AgCl at a scan rate of 100 mV/s, with a step potential of 5 mV and a pulse amplitude of 50 mV, at room temperature without stirring. After each measurement, the electrodes were cleaned by repeating the DPV measurement in pH 7 phosphate buffer solution (PBS, the same used in the DPV measurements, see the table below).

In article 2, DPV technique was used to scan the potential between 0 to 1.5 V at a scan rate of 100 mV/s, with a step potential of 5 mV and a pulse amplitude of 50 mV, at room temperature without stirring. All electrodes were regenerated after each measurement by electrochemical cleaning, applying 1.5 V for 45 s in a pH 7.0 PBS.

In article 3, DPV technique was used with a potential window between 0 V to -1.2 V with a scan rate of 100 mV/s, a step potential of 5 mV and a pulse amplitude of 50 mV, at room temperature without stirring. A cleaning step was performed between measurements, applying a potential of 1.4 V for 45 s in 0.1 M NaOH solution.

3.6. Application in real samples (Article 2)

Materials and instrumentation

Real white wine samples were purchased at random at local supermarket in Sabadell, Barcelona. An extraction funnel was used for histamine transfer into different solvents, the funnel was purchased at Scharlab.

Protocols and procedures

The developed electrochemical method was compared with the OPA fluorimetric reference method using white wine samples, for comparison purposes. Histamine reacts with OPA generating a fluorescent complex that allows its quantification at the ng·mL^{-1} level. This complex absorbs at a wavelength of 350 nm and emits at 444 nm, being stable during 2 hours after stopping the reaction with phosphoric acid after 4 min of placing them in contact; after 2 hours the complex degrades and fluorescence decays. Histamine was extracted from wine samples in order to minimise the sample matrix effect. 25 mL of white wine aliquot was gently extracted from the wine bottle and its pH was basified up to pH=11. Next, this solution was transferred to an extraction funnel, where 10 mL of n-butanol were added. Then, it was necessary to extract histamine to the organic phase, reason why the funnel was vigorously shacked over 5 min. Then, the aqueous phase was removed and 10 mL of HCl 0.1M were added to the organic phase; the funnel was then vigorously shaken during 5 min, due to the exchange phase. The organic phase was removed and the fluorimetric reaction was produced in the remaining aqueous phase, where the histamine was transferred [12]. It is important to mention that a calibration with aqueous standards was performed but without any extraction pre-treatment, in order to calculate the concentration in the wine sample [13].

3.7. Data analysis, chemometrics and ET

Software

For all the articles presented in this manuscript, the Design of Experiments (DOE) was performed using Modde® 8.0 software. Qualitative studies or PCA routines and quantitative experiments or ANNs were programmed by the authors using MATLAB 2016b (MathWorks, Natick, MA). Graphical representation and analysis of the results were performed with Sigmaplot or Origin 8.0.

Protocols and procedures

Principal component analysis was implemented with scripted routines written by other members of GSB group and was employed to evaluate the capabilities of the different sensor or sensor arrays to produce an electrochemical response different enough to at plain sight separate the different analytes or samples considered. PCA was explained in more detail in section 1.3.2. The different experiments involving PCA have been done with 3 or 5 replicates of each sample to be studied in order to provide an adequate cluster of samples.

In article 1, a full factorial sample design was used to be able to build an appropriate model, with 4 levels and 2 factors. The data set employed to evaluate the performance of the model, (*i.e.*, test subset), is randomly generated within the limits of the training subset. Figure 3.7. illustrates the data space depicting the training and testing data sample sets. A set of 16 samples was used as training, while an external set of 9 samples was prepared for validation purpose, in a range of 3 to 20 µg mL^{-1} of 4-EP and 4-EG analytes.

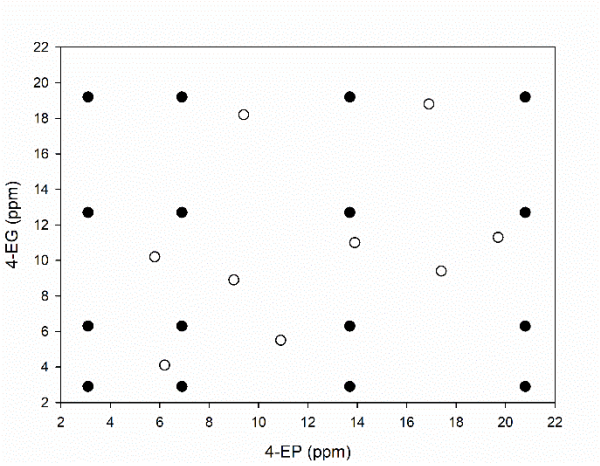

Figure 3.7. Train and test data set distribution model training (●, solid line) and testing subsets (○, dashed line).

In order to build the ANNs models a two different sample sets are required, the training subset which usually comprises around the 75% of the total samples and the testing subset which contains the remaining 25% of samples. The training and testing subset are independent and will be used, for different purposes according to their name.

The electronic tongue approach employed in article 1 was carried out with ANNs as the chemometric tool of choice. ANNs modelling was implemented with scripts written by other members of GSB.

Due to the nature of ANNs the method to obtain the final model is by trial-and-error. Several models were evaluated and optimized, the best among them is chosen. Among the several parameters that we can vary in a ANNs model for the models presented in the articles of this thesis only the following were evaluated: data pre-treatment and compression, number of hidden layer neurons and transfer functions. See introduction for a detailed explanation of ANNs and its particularities.

Bibliography

[1] F. Bates, M. del Valle, Voltammetric sensor for theophylline using sol–gel immobilized molecularly imprinted polymer particles, Microchim. Acta. 182 (2015) 933–942. https://doi.org/10.1007/s00604-014-1413-4.

[2] S. Alegret, J. Alonso, J. Bartrolí, F. Céspedes, E. Martínez-Fàbregas, M.D. Valle, Amperometric biosensors based on bulk-modified epoxy graphite biocomposites, Sensors Mater. 8 (1996) 147–153.

[3] R. Olivé-Monllau, M. Baeza, J. Bartrolí, F. Céspedes, Novel amperometric sensor based on rigid near-percolation composite, Electroanalysis. 21 (2009) 931–938. https://doi.org/10.1002/elan.200804494.

[4] C. Ocaña, M. Del Valle, Signal amplification for thrombin impedimetric aptasensor: Sandwich protocol and use of gold-streptavidin nanoparticles, Biosens. Bioelectron. 54 (2014) 408–414. https://doi.org/10.1016/j.bios.2013.10.068.

[5] A. González-Calabuig, D. Guerrero, N. Serrano, M. del Valle, Simultaneous Voltammetric Determination of Heavy Metals by Use of Crown Ether-modified Electrodes and Chemometrics, Electroanalysis. 28 (2016) 663–670. https://doi.org/10.1002/elan.201500512.

[6] Y. Aceta, M. del Valle, Graphene electrode platform for impedimetric aptasensing, Electrochim. Acta. 229 (2017) 458–466. https://doi.org/10.1016/j.electacta.2017.01.113.

[7] X. Cetó, A. González-Calabuig, N. Crespo, S. Pérez, J. Capdevila, A. Puig-Pujol, M. del Valle, Electronic tongues to assess wine sensory descriptors, Talanta. 162 (2017) 218–224. https://doi.org/10.1016/j.talanta.2016.09.055.

[8] J. Schindelin, I. Arganda-carreras, E. Frise, V. Kaynig, M. Longair, T. Pietzsch, S. Preibisch, C. Rueden, S. Saalfeld, B. Schmid, J. Tinevez, D.J. White, V. Hartenstein, K. Eliceiri, P. Tomancak, A. Cardona, Fiji : an open-source platform for biological-image analysis, Nat. Methods. 9 (2019) 676–682. https://doi.org/10.1038/nmeth.2019.

[9] A. Herrera-Chacon, A. Gonzalez-Calabuig, M. del Valle, Dummy Molecularly Imprinted Polymers Using DNP as a Template Molecule for Explosive Sensing and Nitroaromatic Compound Discrimination, Chemosensors. 9 (2021) 255. https://doi.org/10.3390/chemosensors9090255.

[10] A. Herrera-Chacon, A. González-Calabuig, I. Campos, M. del Valle, Bioelectronic tongue using MIP sensors for the resolution of volatile phenolic compounds, Sensors Actuators B Chem. 258 (2018) 665–671. https://doi.org/10.1016/j.snb.2017.11.136.

[11] A. Herrera-Chacón, Ş. Dinç-Zor, M. del Valle, Integrating molecularly imprinted polymer beads in graphite-epoxy electrodes for the voltammetric biosensing of histamine in wines, Talanta. 208 (2020) 120348. https://doi.org/10.1016/j.talanta.2019.120348.

[12] S. Gorinstein, M. Zemser, F. Vargas-Albores, J.L. Ochoa, O. Paredes-Lopez, C. Scheler, J. Salnikow, O. Martin-Belloso, S. Trakhtenberg, Proteins and amino acids in beers, their contents and relationships with other analytical data, Food Chem. 67 (1999) 71–78. https://doi.org/10.1016/S0308-8146(99)00071-0.

[13] AOAC Official Method 997.13. Histamine in Seafood<http://www.aoac.org/aoac_ prod_imis/AOAC_Docs/OMA/977_13aoacmethod.pdf.>(accessed 21 october2018).

4. Results and Discussion

4. RESULTS AND DISCUSSION

The purpose of this work has been the continuation of the group's line research to integrate MIPs onto the sensors and to develop the electronic tongue approach for different applications. In addition, the aim was also the study of MIPs as recognition element to improve the performance of sensors and to obtain useful analytical information through the use of chemometric tools, in comparison with unmodified sensors. Also, the development of versatile and simple protocols to be used in the laboratory for future works, from synthesis to the final application. An ET system, as already described in the introduction of this thesis (see section 1.4.), is in a simplified form an array of sensors that show a cross-response, i.e. low selectivity, and therefore, with

specific data handling, allow the resolution of multiple analytes. The imprinting technology allows us to obtain polymers, MIPs and NIPs, to be used as recognition elements on the surface of the electrodes.

By following these steps, it has been possible to publish three papers devoted to: (1) apply the electronic tongue approach to solve a mixture of 4-EP and 4-EG; (2) identify and quantify histamine in wine samples comparing a feasible electrochemical method with a gold standard method; and (3) detect and quantify TNT with a dummy molecularly strategy and discriminate among different nitroaromatic species that are considered emerging contaminants in water.

This chapter will be divided in article sections, explaining separately and for each case the results obtained.

- Article 1 - Herrera-Chacon, A., González-Calabuig, A., Campos, I., & del Valle, M. (2018). Bioelectronic tongue using MIP sensors for the resolution of volatile phenolic compounds. Sensors and Actuators B: Chemical, 258, 665-671.
- Article 2 - Herrera-Chacón, A., Dinç-Zor, Ş., & del Valle, M. (2020). Integrating molecularly imprinted polymer beads in graphite-epoxy electrodes for the voltammetric biosensing of histamine in wines. Talanta, 208, 120348.
- Article 3 - Herrera-Chacon, A., Gonzalez-Calabuig, A., & del Valle, M. (2021). Dummy Molecularly Imprinted Polymers Using DNP as a Template Molecule for Explosive Sensing and Nitroaromatic Compound Discrimination. Chemosensors, 9(9), 255.

Article 1

Bioelectronic tongue using MIP sensors for the resolution of volatile phenolic compounds

Herrera-Chacon, A., González-Calabuig, A., Campos, I., & del Valle, M.

Sensors and Actuators B: Chemical, 2018, 258, 665-671.

4.1. Article 1, Bioelectronic tongue using MIP sensors for the resolution of volatile phenolic compounds

This article reports the combination of biomimetic sensors modified with MIPs and the modelling capabilities of ANNs to develop for the very first time a BioET. Tailored-made polymers towards 4-EP, 4-EG, and their control polymer non-imprinted were integrated onto the bare sensor surface in order to improve sensor performance and its response. Receptor elements, polymers, were incorporated onto the GEC bare sensor via sol-gel and drop-casting technique. Polymers and modified sensor surfaces were characterised by SEM. Modified MIP sensors were employed to arrange an array of different biomimetic sensors to quantify by means of ANNs.

4.1.1. Microscopy studies

Once the polymers were synthetised towards 4-EP, 4-EG and their respective NIP, the polymers and their posterior integration onto the sensor surface were characterised by SEM. Polymer images show that similar polymeric materials with non-regular spherical particles were obtained (see Figure 4.1). From the obtained images, the particle size distribution was analysed for each polymer, counting at least 300 particles from 5 different images.

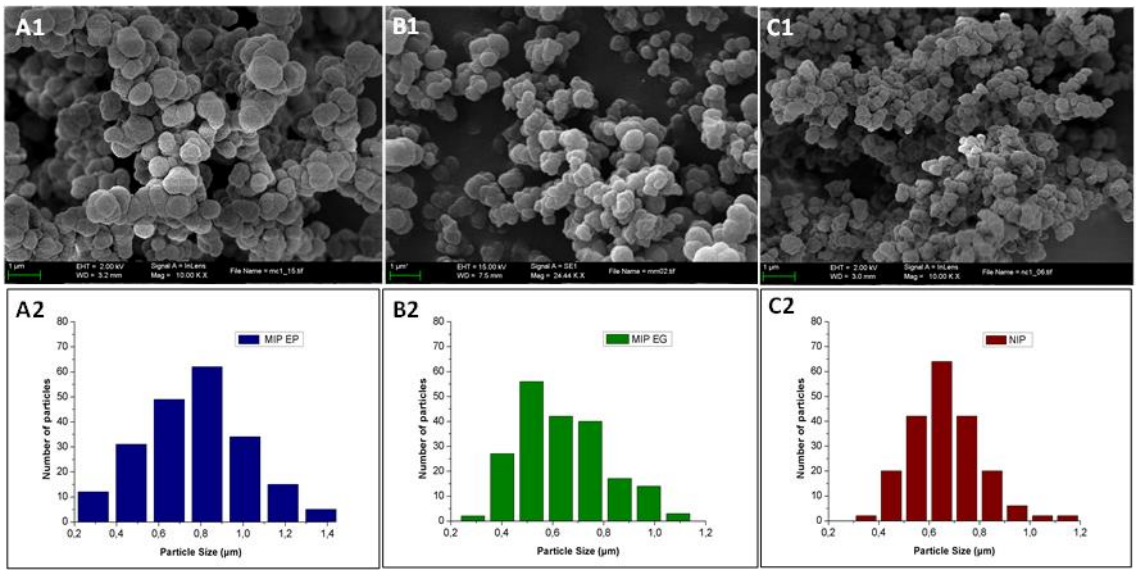

Figure 4.1. (A1/B1/C1) SEM of the obtained 4-EP MIP (left), 4-EG MIP (middle) and NIP (right). (A2/B2/C3) Particle size distribution of the 4-EP MIP (left), 4-EG MIP (centre) and NIP (right).

The average diameters and their standard deviations of 4-EP MIP, 4-EG MIP and NIP were 0.76 ± 0.034 µm, 0.64 ± 0.17 µm and 0.67 ± 0.14 µm, respectively. According to the results observed, it might be considered that all polymers obtained have a similar particle size and distribution, showing a high degree of crosslinking as can be interfered from the images.

To evaluate the immobilisation of the polymers onto the sensor surface, SEM images for the 5 different sensors were acquired, see Figure 4.2. SEM images were performed to manifest, on one hand, the polymer and the sol-gel presence; and on the other hand, to check the distribution and differences among the sensor arrays.

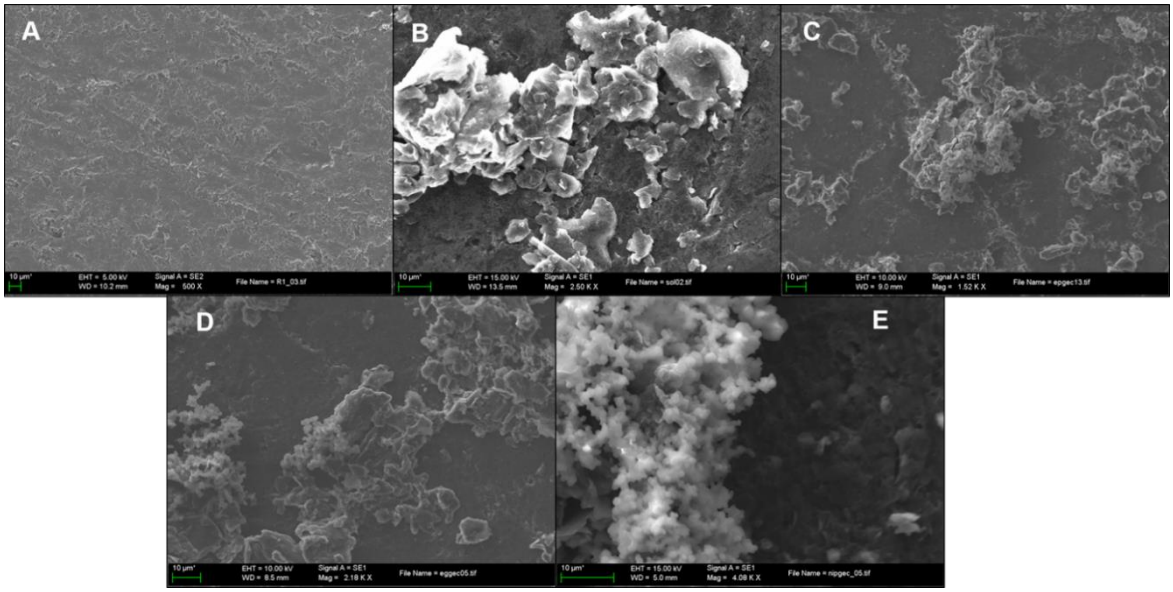

Figure 4.2. SEM of the different electrode surfaces (A) GEC, (B) Sol-gel, (C) 4-EP MIP, (D) 4-EG MIP and (E) NIP sensors.

Figure 4.2.A shows the SEM image from the GEC surface while the rest of the images display the modified sensors with (B) sol-gel, (C) 4-EP MIP, (D) 4-EG MIP and (E) NIP. From the presented images, it can be concluded that there are not significative differences among the polymer modified sensors. It can be perfectly seen the presence of the polymer and the sol-gel without any different from the MIP-EP, MIP-EG and NIP polymer sensor surfaces. Besides, GEC surface is totally smooth and sol-gel modified surface is widely rough, both of them are free of polymer.

4.1.2. Individual electrochemical response

In order to use the sensor array for the ET application, the electrochemical performance and the different behaviour of each sensor were evaluated, specifically towards the two analytes of interest 4-EP and 4-EG. Two main studies were developed: an adsorption kinetics, and a cross-calibration for each sensor towards the analyte of interest separately.

The adsorption kinetics of each sensor *versus* the analytes of interest was studied, see Figure 4.3. It was necessary to determine the time when the specific adsorption processes are predominant over to the unspecific ones, counter-balancing the time used to measure and a good electrochemical response. 4-EP MIP and 4-EG MIP sensors were studied with 7 μg mL^{-1} solution of their corresponding analyte and compared with the control non-imprinted polymer and the sol-gel sensors.

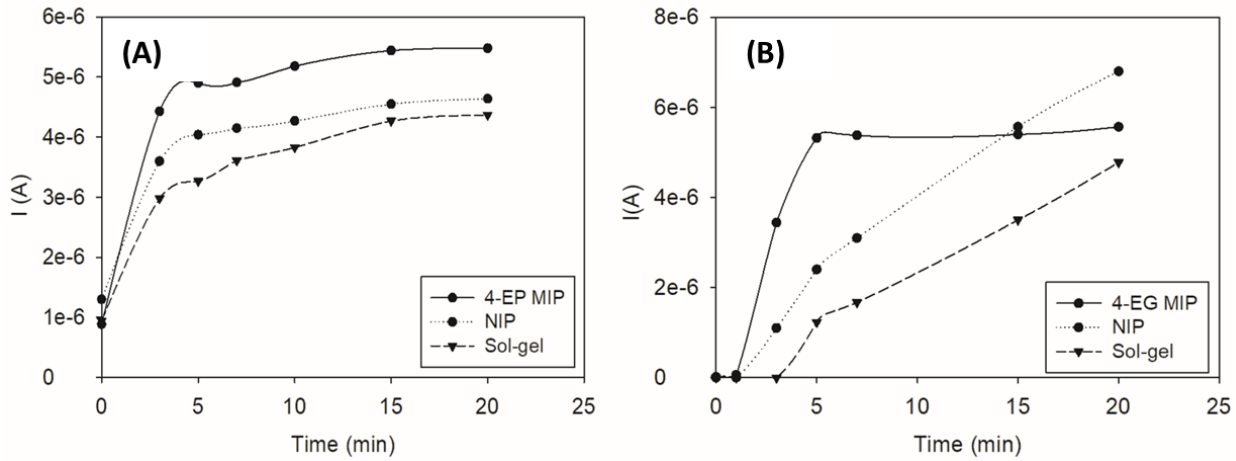

Figure 4.3. Adsorption kinetics of the MIP, NIP and sol-gel sensors towards 4-EP (A) and for 4-EG (B).

Figure 4.3.A and 4.3.B show the array of sensor kinetic response towards 4-EP and 4-EG, employing the 4-EP MIP, 4-EG MIP, NIP and sol-gel sensors. From the above figure, it can be seen that the template adsorption processes are fast reactions when using the MIP-based sensors. It can be noticed, that the maximum saturation value is reached in a temporal range from 3 to 5 minutes.

However, the adsorption values for the control polymers (NIP and sol-gel) are slower than MIP sensors. Also, the NIP and sol-gel sensors show slower adsorption values than the MIP-based sensors. Moreover, it is in the 3 to 5 minutes region that the greatest difference in intensity response regarding the

MIP-sensors and the rest of the them is reached. Consequently, since the reaction time is fast and in order to maximise the differences between the sensors' intensity response, the optimal stripping time was determined to be 3 minutes.

Nevertheless, if we look at the 4-EG graph (Figure 4.3B), we can see how the non-specific interactions are pre-accumulating in the sensor and finally the NIP surpasses the MIP-sensor in terms of intensity values. This phenomenon is due to the fact that in this pre-accumulation study no cleaning steps have been performed in order to avoid unspecific reactions. This test is the only one in which no cleaning steps were performed. Furthermore, it can be also inferred from the same figure that we should avoid long pre-concentration times in order to maximise the difference between the sensors. In general, the longer the measuring time, the higher the measuring intensity. However, it requires a higher voltage during the cleaning procedure, which could damage the sensor surface. Thus, once again, it is needed to counter-balance the gain in the signal towards the sensor exposure, which may change in its durability or the measurement stability. From these studies, the more efficient stripping time was determined to be between 3 minutes.

Another important factor to control before attempting the ET was to study the cross-calibration response, due to it is an application constrain by ET definition. This condition was expected in this study because the similar chemical structure of both targets. As presented in table 4.1., 4 types of electrodes (4-EP MIP, 4-EG-MIP, NIP and sol-gel modified sensors) were fabricated and their response to 4-EP and 4-EG compounds were studied. This test was done to evaluate that both MIPs show a higher response by their respective sensors and also than the

control sensors (NIP and sol-gel). This can be seen due to the major sensitivity in comparison with the other sensors, using the same experimental conditions. In Table 4.1. the main linear fitting parameters are presented to corroborate this behaviour. The fitting parameters were obtained by performing four calibration curves with MIP, NIP and sol-gel sensors towards the template compounds.

Table 4.1. Cross-calibration slope (µA/µgmL-1) and correlation values for MIP, NIP and sol-gel in the presence of 4-EP and 4-EG.

Sensor	Sensitivity towards 4-EP ($\mu A \cdot \mu g^{-1} mL^{-1}$)	Correlation value 4-EP	Sensitivity towards 4-EG ($\mu A \cdot \mu g^{-1} mL^{-1}$)	Correlation value 4-EG
4-EP MIP	0.270	0.976	0.217	0.981
4-EG MIP	0.245	0.970	0.401	0.989
NIP	0.094	0.906	0.069	0.994
Sol-gel	0.231	0.989	0.299	0.990

In the above table, it can be seen that the 4-EP MIP sensor response towards 4-EP presents a higher value than the same sensor *versus* 4-EG, being slope values of 0.270 ± 0.015 and 0.217 ± 0.011 µA $\mu g^{-1} mL^{-1}$, respectively. An equivalent sensor response was obtained when the 4-EG MIP sensor was evaluated towards 4-EP and 4-EG, obtaining values of 0.245 ± 0.015 and 0.401 ± 0.014 µA $\mu g^{-1} mL^{-1}$, respectively. Furthermore, the correlation parameters were closer to 1 when each analyte was measured using their corresponding MIP-based sensors. It corroborates the goodness of the linear fitting. Additionally, the correlation parameters were closer to 1 when each analyte was measured using its corresponding MIP sensors, corroborating the goodness of the linear fitting. As it was expected, the obtained slope values of the NIP-sensor were negligible comparing with the MIP ones. On the other hand, the slope values obtained by

using sol-gel sensors exhibited similar values to the MIP sensor response. However, it is needed to be mentioned that the advantage in the use of MIPs sensors is the improvement in the selectivity instead of the sensitivity. As can be seen below in Figure 4.5.A, when MIPs are used, the interferents compounds are not able to reach the sensor surface, improving the selectivity of the system.

4.1.3. Calibration curves and reproducibility of the sensors

Calibration curves were performed in order to evaluate each polymer sensor towards their corresponding template by DPV technique (Figure 4.4.).

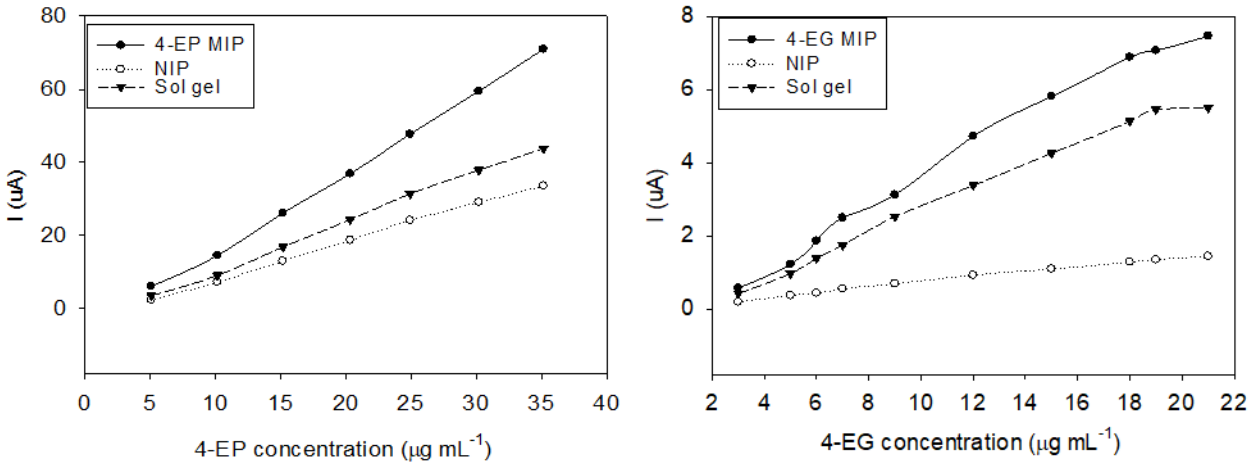

Figure 4.4. Calibration curves of 4-EP MIP, NIP and sol-gel sensors towards 4-EP (left) and 4-EG MIP, NIP and sol-gel sensors towards 4-EG (right).

Focusing on the 4-EP substance study, the calibration curve was performed from 5 to 35 µg mL^{-1} concentration range (See Figure 4.4. left) and the slope values were 2.19 ± 0.04 µA $µg^{-1}mL^{-1}$ for the 4-EP MIP sensors, 1.06 ± 0.02 µA $µg^{-1}mL^{-1}$ for the NIP and 1.38 ± 0.03 µA $µg^{-1}mL^{-1}$ for the sol-gel. The corresponding LODs were 1.33, 1.28 and 1.52 µg mL^{-1} of 4-EP, respectively. The slope value of the MIP sensor was twice that of the NIP and sol-gel, indicating that the affinity for the analyte is higher than in the other cases when the same experimental conditions were used. It is related to the polymer binding cavities or the polymer

imprinting activity. In the same line, this study was also performed for the 4-EG MIP sensor (See Figure 4.4. right) from 3 to 21 µg mL^{-1} linear range concentrations. The values obtained derived from this test presented the slope values of 0.401 ± 0.014, 0.069 ± 0.002 and 0.299 ± 0.015 µA $\mu g^{-1}mL^{-1}$ for 4-EG MIP, NIP and sol-gel sensors, respectively. The LODs values were 1.55, 1.22 and 1.51 µg mL^{-1} towards 4-EG compound, respectively. With the objective to estimate the reproducibility of this sensors, 2 calibration curves were performed using 4-EP MIP sensor towards 4-EP in consecutive days. In order to evaluate this work, in the second curve the standards were introduced at random. The slope values for this study were 0.797 ± 0.043 and 0.703 ± 0.021 µA $\mu g^{-1}mL^{-1}$ for the first and the second day with correlation values of 0.979 and 0.993, respectively. A comparison between the values of each calibration curve shows, on one hand, a negligible reduction in the slope value and; on the other hand, a non-significant increase in the regression coefficient. From these results, it can be concluded that the sensors can be used, demonstrating a good reproducibility for at least 20 measurements. Another important aspect is that this study also confirms the protocol performed, in terms of measurements and cleaning steps and operation error. Finally, it can be concluded that (1) the sensors are suitable for use in a BioET, and (2) a similar cleaning process can be performed during the BioET.

4.1.4. Qualitative studies

PCA was performed to evaluate the array capabilities to separate the different samples. Gallic acid, quercetin, 4-ethylphenol and 4-ethylguaiacol were the analytes used to be evaluated. The use of this compounds is justified because gallic acid and quercetin are wine phenolic compounds; and 4-EP and 4-EG are volatile phenols responsible of the Brett character, see Figure 4.5.

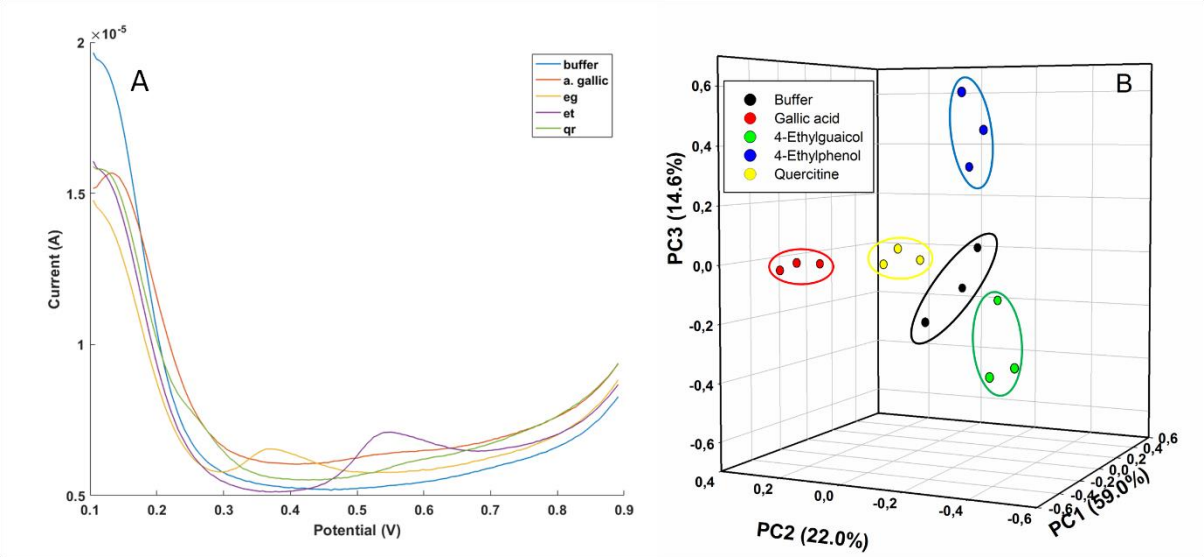

Figure 4.5. (A) DPV signals obtained for the considered compounds with MIP (solid line). (B) PCA for the analytes 4-EP, 4-EG, quercetin, gallic acid and buffer.

In this study, all the samples were diluted, prepared and measured in a pH=7 PBS by triplicate. The concentrations of the different substances used were: 25 µg mL^{-1} for gallic acid and quercetin and 3 µg mL^{-1} for 4-EP and 4-EG.

In Figure 4.5.A, the voltammetric response is shown for the aforementioned compounds. The DPV signals of the sensor array were subjected to PCA to visualize better the differences among the samples (Figure 4.5.B). Figure 4.5.B shows different sample clusters, each compound forming its own separated cluster with no overlapping. In this case, only the scores of the three first PCs are shown which represent the 95.6% of the accumulated explained variance.

4.1.5. Quantification studies

PLS and ANNs studies were applied to quantify 4-EP and 4-EG mixtures using the modified MIP array of sensors. The designed sensor array was employed to train a quantification model constructed on a full factorial experimental design with 4 levels and 2 factors, resulting in 16 samples, see Figure 4.6.

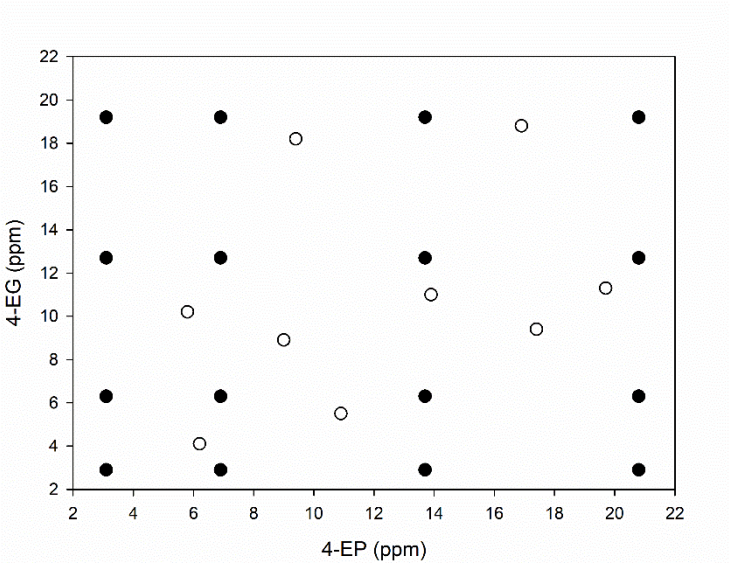

Figure 4.6. Full factorial experimental design with 4 levels and 2 factors for training (●, solid line) and testing subsets (○, dashed line).

These 16 samples were used to train the model and its concentration ranged from 3 to 20 µg mL^{-1}. Furthermore, 9 additional samples were prepared for testing purposes, the concentration of these samples was randomly generated within the 3 to 20 µg mL^{-1} limits.

A huge amount of voltammetric data was generated for each sample with the 6-sensor array; however, this amount of data results in a problem when chosen model is an ANNs. This huge amount of data needs to be reduced to improve model performance and avoid exponentially long training times. The original signals were reduced by applying a compression by means of Discrete Wavelet Transform: each voltammogram was compressed using the mother function *Daubechies* 3 and a 3rd decomposition level. In this particular case, the data set was reduced from 986 (6 sensors x 164 x sample) to 144 points, achieving a compression ratio of 85.4%.

The resulting neural network model had 144 neurons in the input layer (the number of wavelet coefficients obtained in the compression step), 3 neurons and the *tansig* transfer function in the hidden layer and 2 neurons and the *purelin* transfer function in the in the output layer (corresponding to the concentrations of 4-EP and 4-EG). The modelled sample predictions are shown in Figure 4.7.

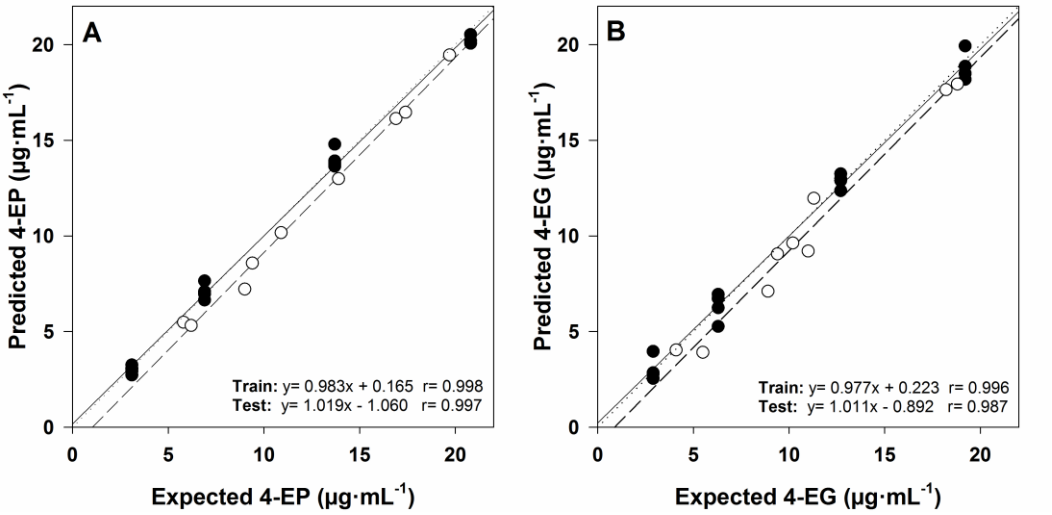

Figure 4.7. ANN fittings of predicted vs. expected concentrations for (A) 4-EP and (B) 4-EG, both for training (●, solid line) and testing subsets (○, dashed line). Dotted lines correspond to ideal behaviour (diagonal line).

From figure 4.7. we can see that the model shows a linear trend for 4-EP and 4-EG for train and test samples. Moreover, it can be seen that predictions for the training samples are more accurate. This is an expected fact since these samples have been used to build the model. Nevertheless, the test subset, which is an independent set of samples that has not intervened during the construction of the model, also shows a linear trend. Complete regression parameters for train and test samples are disclosed in Table 4.2.

Table 4.2. Detailed fitting results for obtained vs. expected values for the training and testing sets for 4-EG and 4-EP (intervals calculated at 95% confidence level).

Sensor	Correlation	Slope	Intercept (μg mL^{-1})	RMSE (μg mL^{-1})	NRMSE	Total RMSE (μg mL^{-1})	Total NRMSE
Train Subset							
4-EP	0.998	0.983±0.075	0.162±0.893	0.454	0.023	0.764	0.038
4-EG	0.996	0.977±0.106	0.223±1.274	0.614	0.031		
Test Subset							
4-EP	0.997	1.019±0.152	-1.060±1.978	0.980	0.049	1.527	0.076
4-EG	0.987	1.010±0.299	-0.892±3.537	1.171	0.059		

As aforementioned, a good linear trend is obtained for 4-EP and 4-EG. The fitting obtained for the test subset had intersections close to the ideal value of 0, slopes and correlations near 1 (ideal value 1) and a NRMSE as low as of 0.049 and 0.059 for 4-EP and 4-EG, respectively. The constructed model predicted the concentration values of the 9 mixtures of phenols with a total NRMSE of 0.076.

As a benchmark model, PLS was employed which is the most common tool on the chemometric field. PLS linear fittings are shown in Figure 4.8.

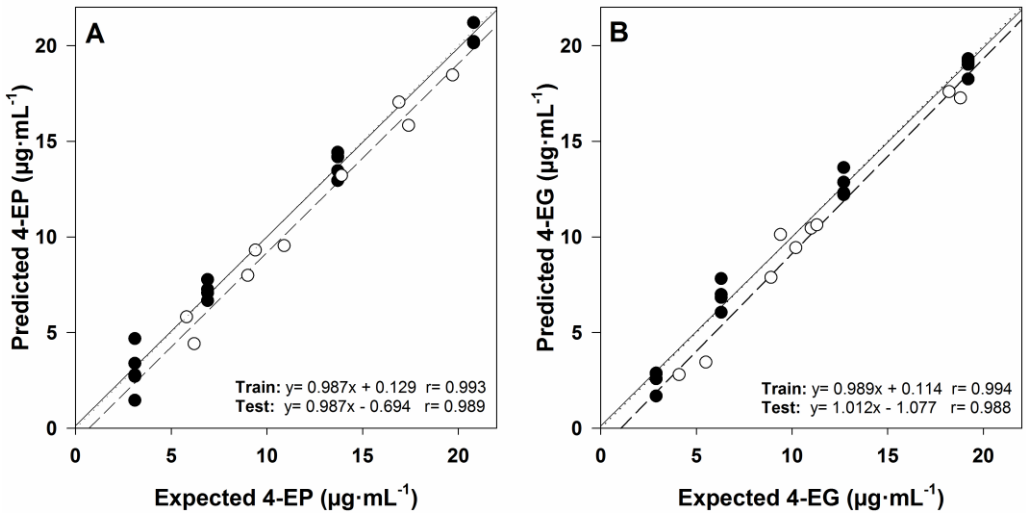

Figure 4.8. PLS fittings of predicted vs. expected concentrations for (A) 4-EP and (B) 4-EG, both for training (●, solid line) and testing subsets (○, dashed line). Dotted lines correspond to ideal behaviour (diagonal line).

From the comparison of the results of both models it can be seen that the ANN model and PLS model have similar performance in regard to slopes and correlation coefficients. However, the ANN model has a slightly better performance, with slopes closer to 1.0 and correlation coefficients near to 1.0. The obtained NRMSE values for train and test for the PLS model were 0.051 and 0.083, respectively. Again, if it is compared the ANN to PLS model, the ANN model performs slightly better than PLS model. To the best of the authors knowledge, the improvement in the predictive performance is probably caused by some degree of non-linear response which ANN models are able to predict to certain degree.

In conclusion, the first BioET was successfully applied for the very first time in the literature using a MIP-based sensor array. Furthermore, this ANN model was also compared with common PLS and presenting slightly better results.

Article 2

Integrating molecularly imprinted polymer beads in graphite-epoxy electrodes for the voltammetric biosensing of histamine in wines

Herrera-Chacón, A., Dinç-Zor, Ş., & del Valle, M.

Talanta, 2020, 208, 120348.

4.2. Article 2, Integrating molecularly imprinted polymer beads in graphite-epoxy electrodes for the voltammetric biosensing of histamine in wines

In this work a new voltammetric biomimetic MIP-based sensor is presented to quantify histamine in wine. This method was benchmarked against the fluorimetric reference method. Once MIP and NIP were synthesised by standard precipitation polymerisation approach, polymers were immobilised onto the sensor surface through sol-gel immobilisation and drop-casting technique. Scanning and confocal microscopy images allowed to characterise the materials and the sensor surfaces. Adsorptive stripping voltammetry in differential mode was employed for the histamine detection, an enrichment time of 5 min was selected. Calibration curves were performed to obtain the concentration linear range and the respective LODs for the different MIP-based sensors. PCA was employed to demonstrate that the prepared modified MIP-based sensors were able to discriminate between biogenic amines and potential interfering compounds.

4.2.1. Microscopy characterisation

In this article, SEM and CM techniques were employed to characterise: (1) the different polymers morphology; (2) the sensor surface modification; and (3) the polymer powder affinity towards the template (histamine) for MIP and NIP. Furthermore, the imprinting was evaluated by comparing the affinities obtained by optical and electrochemical methods.

4.2.1.1. Polymer examination

Once Histamine-MIP and its respective non-imprinted polymer were synthesised, the obtained polymer structures were inspected using SEM microscopy in order to characterise the material. This study was done before their immobilisation onto the sensor surface. From these SEM images a particle size study was performed in order to obtain morphological information about MIP and NIP, see Figure 4.9.

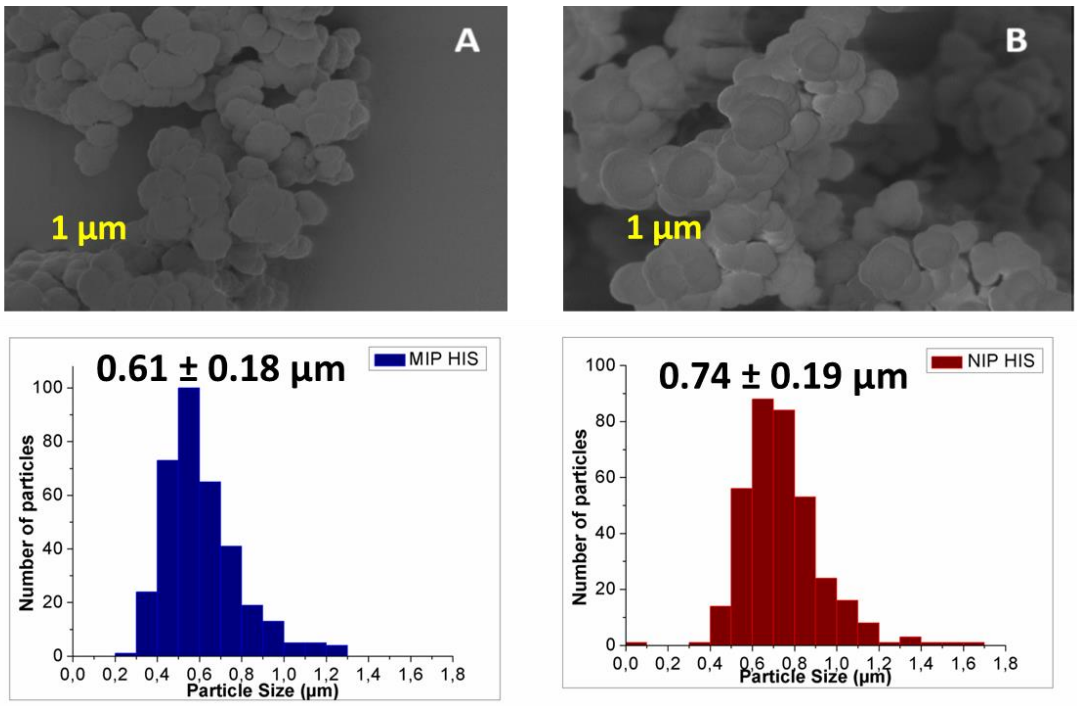

Figure 4.9. SEM images of (A) histamine-MIP, (B) NIP and their respective histograms below.

As it is depicted in Figure 4.9., polymer particles exhibited a non-homogeneous and highly crosslinked atactic structure for MIP and NIP. Their average diameters and their standard deviations were 0.61 ± 0.18 µm in the case of the MIP and 0.74 ± 0.19 µm NIP.

As it can be observed from the abovementioned figure, both types of polymer particles had a similar size distribution which made the authors think that the obtained NIPs particles were suitable to be employed as the control polymer.

4.2.1.2. Sensor surface modification

Additionally, Figure 4.10. shows the obtained SEM images for the sensors constructed in this work. A Histamine-MIP sensor in A, a NIP sensor in B and a non-modified GEC sensor in C, the last one was employed as an additional control.

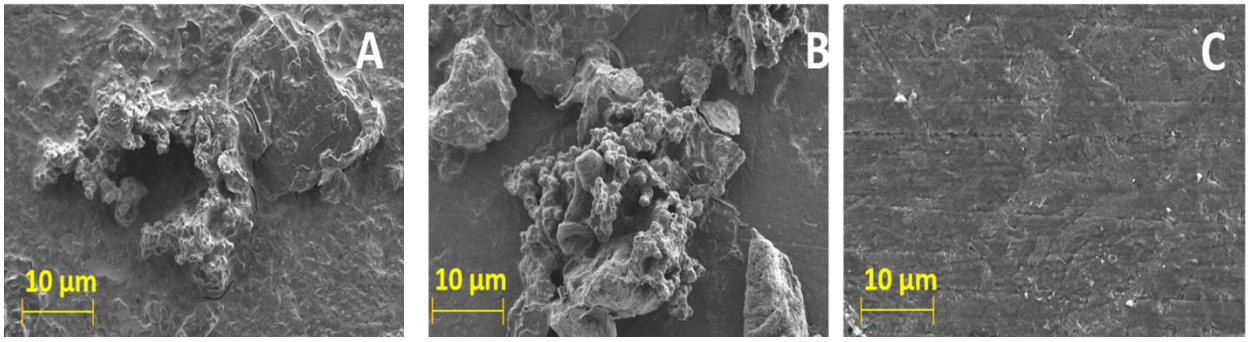

Figure 4.10. SEM images for the functionalised sensors with Histamine-MIP (A), NIP (B) and unmodified GEC sensor (C).

Histamine-MIP and NIP were deposited via sol-gel and drop-casting technique onto the clean GEC surface displaying an uneven surface where the particles and graphite fragments are clearly seen. In contrast, and as expected, the GEC surface shows a relatively flat surface.

As it can be appreciated the incorporation of the polymer, imprinted or not, results in a rough surface while showing no apparent difference between MIP and NIP functionalised sensors; therefore, any difference in the electrochemical response can be attributed to the presence of histamine imprinted sites.

4.2.1.3. Confocal study

The use of CM allowed us to characterise the complexing capabilities of Histamine-MIP and NIP polymers in almost real time as the fluorimetric OPA-histamine complex was created in situ, just before to start the experiment.

To accomplish this objective, MIP and NIP polymer powder were contacted with histamine solutions, in a 5 µg mL^{-1} concentration in 0.1 M HCl media, until the equilibrium was reached. A negative control, with absence of histamine, was also prepared. Then, the solution comprising an excess of OPA was added, resulting in the formation of the fluorescent OPA-histamine complex. CM results are shown in Figure 4.11.

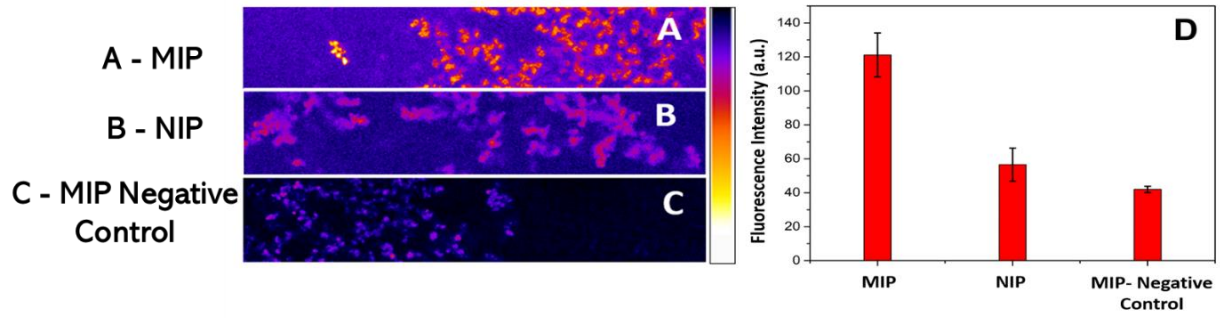

Figure 4.11. CM images for Histamine-MIP (A) and NIP (B). Background fluorescence of MIPs without the fluorescence complex as the control (C). (D) Fluorescence Intensity (a.u.).

Histamine-MIP, NIP and the negative control presented different fluorescence caused by the bonded OPA-histamine complex. In all cases, this complex that is formed between histamine and the OPA reagent interacts with the polymer penetrating into the cavities due to the imprinting activity of the polymers. As shown in Figure 4.11A and B, Histamine-MIP exhibits a much higher intensity than NIP. It is interesting to remark that the negative control, Figure 4.11C, exhibits some degree of autofluorescence, which was used as background.

The direct calculation of obtained confocal data established that Histamine-MIP presented 2.15 times more fluorescence intensity than the NIPs. This difference in intensity, and the sites where it is generated, point us towards the presence of histamine imprinted sites.

4.2.2. Electrochemical measurements

Some parameters were studied in order to obtain an optimised electrochemical response such as: (1) the buffer solution type employed and its pH; (2) the preconcentration time (the adsorptive time); (3) the repeatability and reproducibility; (4) the calibration curves; (5) a qualitative study; and finally (6) the real sample application.

4.2.2.1. Influence and optimisation of pH

Histamine is a strong base with a side chain nitrogen of pKa 9.4 and an imidazole nitrogen group of pKa 5.8. However, the compound contains three nitrogen atoms, it is a diacidic base because of resonance in the imidazole nucleus. The DPV used to study the electrochemical response of the modified electrodes in the oxidation of 5 µg mL^{-1} histamine solution was investigated in several buffer solutions at different pH values. The medias employed were: (1) 0.1 M acetate buffer at pH 4.5, (2) 0.05 M PBS at pH 6.0, (3) 0.05 M PBS at pH 7.0, and (4) 0.1 M Tris-HCl buffer solutions at pH 8.0 and (4) 0.1 M Tris-HCl buffer solutions at pH 9.0. The obtained performances are shown in Figure 4.11.

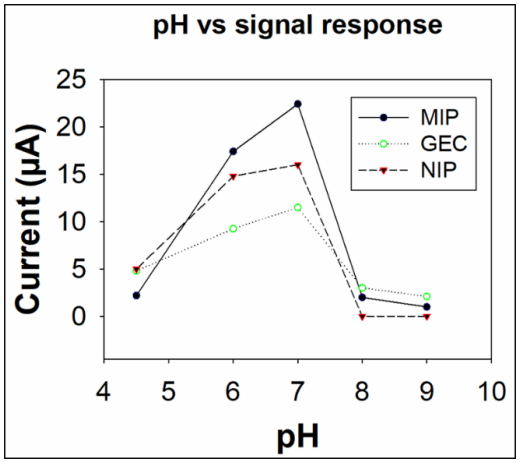

Figure 4.12. Optimisation of the DPV response of the developed Histamine-MIP according to pH.

As it would be expected, the role of pH can affect the oxidation of histamine. In acidic media, the NH_2^- group of the analyte will be protonated to NH_3^+ and, consequently, the adsorption mechanisms may be altered, modifying the current signal for histamine peaks in acid.

The highest current signal was found when measuring at pH=7.0. For this reason, it can be concluded that this buffer was used for the following electrochemical measurements and this study was done in order to optimise the DPV conditions.

It is worth mentioning, that under these conditions, histamine exists as a positively charged species at pH 7, but MIP particles are negatively charged due to deprotonated MAA residues (pKa = 6-7). Consequently, these interactions could help to generate electrostatic interactions favourable for our objective, the detection of histamine via the polymer binding cavities. The electrochemical signal used in other calibration curves was a single oxidation peak at +1.10 to 1.15 V against Ag/AgCl.

4.2.2.2. Contact time optimisation

In order to optimise the electrochemical conditions, contact time is an important parameter to consider during adsorptive stripping measurements. This is the reason why, the different sensors were submerged into histamine solutions of 5 µg mL^{-1} for several times without any polarisation neither cleaning steps; a voltammetric study was done to determine the intensity of the histamine oxidation peak to determine the counter-balanced contact time, see Figure 4.13.

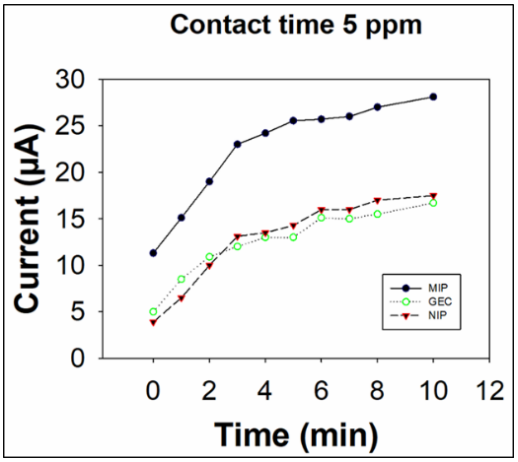

Figure 4.13. Optimisation of the contact time previous to the voltammetric determination of histamine using the different modified sensors.

As shown in Figure 4.13., as expected, the increase in contact time leads to an increase in the histamine peak current of until about 5 min. After 5 min a slower

uptake of histamine can be seen. An enrichment time of 5 min was chosen for further DPV experiments based on these results. This obtained time agrees with shorter times needed to evaluate the template and MIP-modified sensors responses. The same behaviour was observed when this experiment was repeated at lower concentrations, i.e., 1 µg mL^{-1} histamine. Thus, by increasing the enrichment time it was able to attain an increase in the intensity peak, potentially achieving the detection at lower concentrations.

4.2.2.3. Repeatability and reproducibility

To check the intra-day repeatability of current peak magnitude was determined by repeating measurements (n=12) of a 5 µg mL^{-1} histamine in PBS. Following all the optimisations parameters above presented, see Figure 4.14.

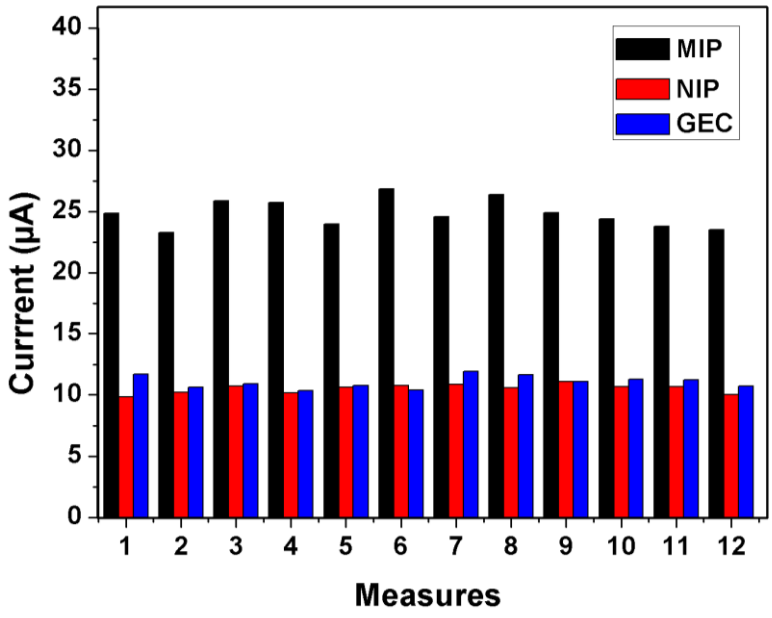

Figure 4.14. Repeatability measurements (n=12) of Histamine-MIP, NIP and GEC sensors.

The obtained relative standard deviation (RSD) for the Histamine-MIP sensor was 4.62%, indicating an excellent repeatability.

To study the daily reproducibility of the imprinted sensor, the linear fitting parameters of three calibration curves were evaluated, measuring each

calibration on different days, see the linear fitting parameter in Table 4.3. The reproducibility of these measurements provided a RSD value of 2.61 %, which was extracted from the variation of the slopes of the different calibrations. As can be inferred from the values in the table, the reproducibility of the sensors presents acceptable values.

Table 4.3. Day-to-day reproducibility of a given Histamine-MIP sensor.

	Slopes (μA/ mg.L^{-1})	Intercept (mg/ L^{-1})	Correlation Coefficient
Day 1	4.919	0.065	0.9989
Day 2	4.675	0.184	0.9997
Day 3	4.816	0.166	0.9989

4.2.2.4. Calibration study

Calibration curves were constructed by DPV technique using the optimised conditions studied in previous sections. They are depicted for the different modified polymer-based sensors versus the bare electrode (GEC) in Figure 4.15.

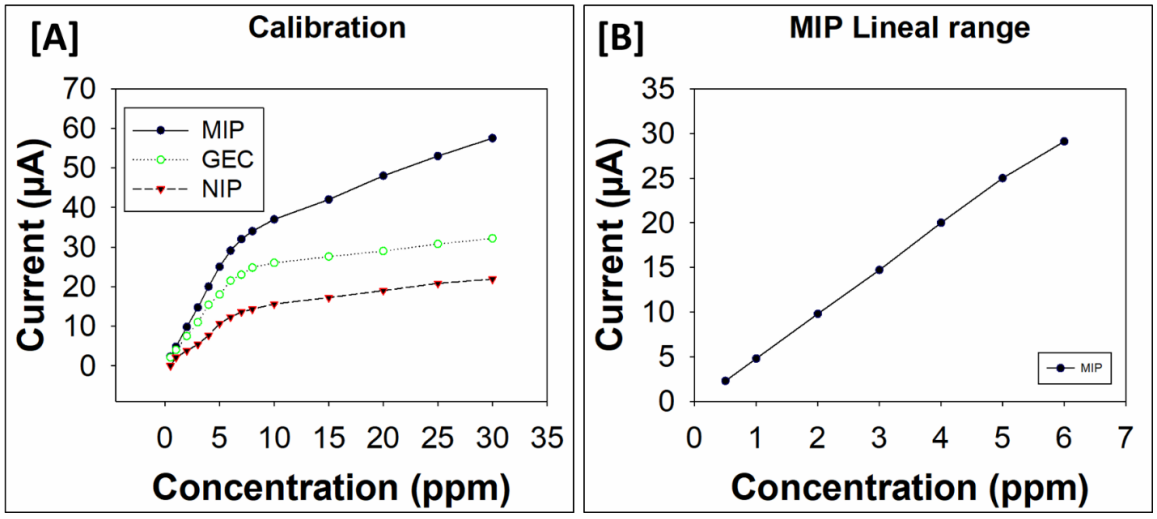

Figure 4.15. [A] DPV response of the modified polymer-based sensors versus the bare electrode (GEC). [B] MIP lineal range.

As it can be seen in Figure 4.15A, there are two linear segments that are due to sensors saturation. This process happens due to the filling of the available

cavities in the polymer. Focusing on the lower linear range of the first linear segment, we can determine a range of concentrations from 0.5 µg mL^{-1} to 6.0 µg mL^{-1} (or 2.7-32.4 µM). The equation derived from the linear fitting yielded an equation: Y=4.9416 C - 0.0779 (R^2=0.9992). The limit of detection (LOD) and limit of quantification (LOQ) were calculated using the equation of 3S/m and 10S/m, respectively, where S is the standard deviation of the regression and m is the sensitivity of the calibration. LOD and LOQ values were calculated to give values of 0.19 µg mL^{-1} (1.0 µM) and 0.62 µg mL^{-1} (3.4 µM), respectively.

Comparing the sensitivities (slope value) for the Histamine-MIP and NIP (in the low concentration range), the slope ratio was found to be 2.27, a value that again can be considered the imprinting factor, and which is consistent with the previous figure obtained by CM (section 4.2.1.3.).

Comparing the obtained calibration curve voltammograms for histamine *versus* the Histamine-MIP and the NIP sensors, it can be seen, that the Histamine-MIP sensor displays higher currents than the NIP, showing better sensitivity, see Figure 4.16.

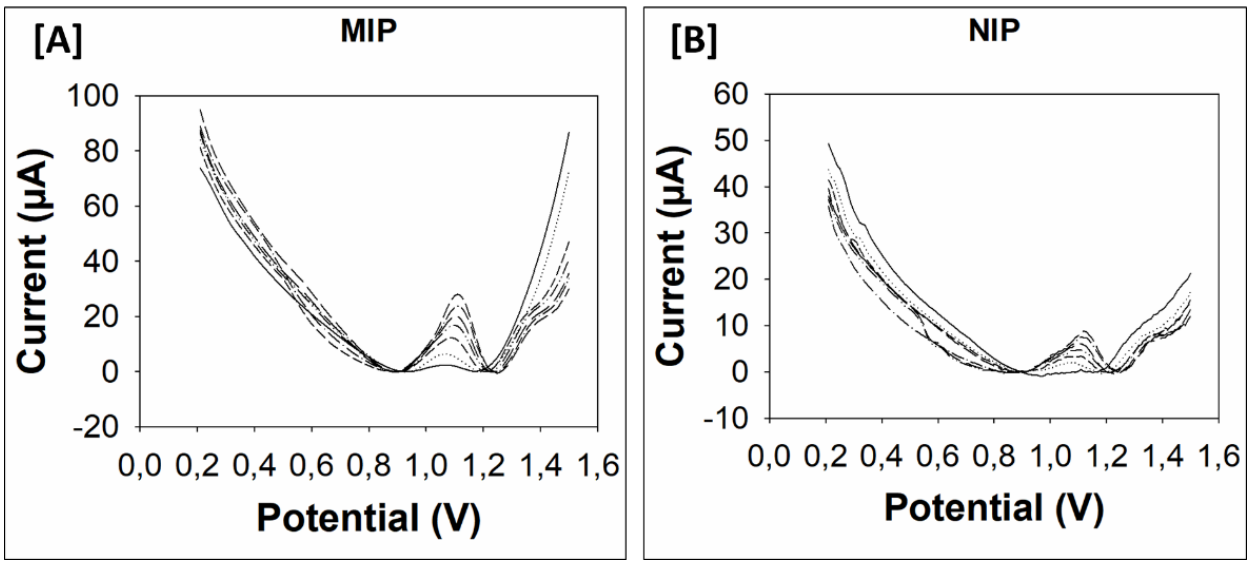

Figure 4.16. DPV measurements for the [A] Histamine-MIP and [B] NIP sensors.

4.2.2.5. Interferents

PCA was performed to evaluate the capabilities of the developed functionalised electrode towards possible interferents in wine matrix. The interferent were selected from biogenic amines and polyphenolic compounds which are present in wine. In particular the following compounds were chosen: tyramine, coumaric acid and gallic acid. Calibration curves were performed for the abovementioned compounds and its voltammetric responses were treated with PCA, see Figure 4.17.

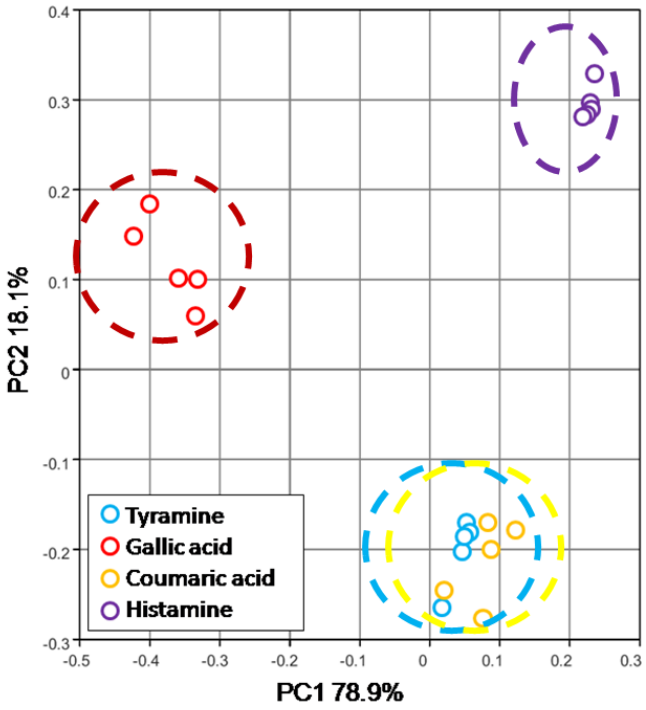

Figure 4.17. Scores of the 2 first PCs for histamine, gallic acid, p-coumaric acid and tyramine.

From the previous figure, it can be seen that histamine and gallic acid are clustered in its own groups, this fact shows that those compounds present a particular voltammetric fingerprint. Nevertheless, coumaric acid and tyramine samples are grouped together. The PCA demonstrate that the array response is clearly distinct for histamine versus the three possible interferents.

4.2.2.6. Application to real sample analysis

The feasibility of the proposed Histamine-MIP was evaluated employing wine samples. Those sample were analysed with the developed electrochemical method and compared with a fluorimetric reference method in accordance with international standards. The electrochemical approach was done using histamine concentrations from 2 to 12 µg mL^{-1} in PBS at pH 7.0. Comparison results between the two methods are shown in Table 4.4.

Table 4.4. Results obtained for two wine samples using the developed Histamine-MIP sensor and the reference fluorimetric method.

	FLUORIMETRIC		VOLTAMMETRIC	
	Wine1 ($mg.L^{-1}$)	**Wine2 ($mg.L^{-1}$)**	**Wine1($mg.L^{-1}$)**	**Wine2 ($mg.L^{-1}$)**
Replicate 1	0.033	0.273	0.048	0.254
Replicate 2	0.037	0.280	0.036	0.245
Replicate 3	0.039	0.294	0.043	0.223
Replicate 4	0.038	0.299	-	-
Mean (ppm)	0.037	0.287	0.042	0.241
s (ppm)	0.002	0.012	0.006	0.016

Focusing on the values of Table 4.4., it can be concluded that the new electrochemical MIP-based method is comparable with the fluorimetric method, using real white wine samples. When comparing the standard deviation values, slight differences can be observed, as higher values were obtained with the electrochemical approach. These differences might happen because in the case of the fluorimetric approach, the original wine matrix is removed by means of a histamine extraction pre-treatment and also due to the incorporation of an additional sample measurement. Focusing on the electrochemical one, the use of the white wine can be interfered by the well-known matrix effect of wine.

To conclude, the developed method showed comparable results with the possibility of on-site sample measurements without the requirement of an extraction pre-treatment.

Article 3

Dummy Molecularly Imprinted Polymers Using DNP as a Template Molecule for Explosive Sensing and Nitroaromatic Compound Discrimination

Herrera-Chacon, A., Gonzalez-Calabuig, A., & del Valle, M.

Chemosensors, 2021, 9(9), 255.

4.3. Article 3, Dummy Molecularly Imprinted Polymers Using DNP as a Template Molecule for Explosive Sensing and Nitroaromatic Compound Discrimination

In this article, a fast, easy and cost-effective voltammetric sensor is presented based on molecularly imprinted technology. This strategy is based on a dummy MIP that uses DNP as a template for the quantification of TNT and DNP. Moreover, the identification and discrimination of the modified polymer-based sensors and its bare electrode (GEC) is also studied and evaluated to nitro aromatic substances. The polymer was synthesised by common methacrylic thermal precipitation polymerisation. Afterwards, the synthesised polymer was deposited onto a GEC bare electrode using sol-gel and casting immobilisation. The polymer was characterised by means of SEM and FT-IR. Electrochemical performance *versus* DNP and TNT were analysed for the different modified polymer-based sensors, as well as some optimisations in order to obtain an improved response. PCA study was performed to demonstrate the suitability of the dummy MIP based electrodes for nitroaromatic compounds discrimination.

4.3.1. MIP physical characterisation

The methacrylic MIP synthesis produced the artificial receptor material in crosslinked beads form. After this procedure, the template used was removed in order to free the tailored cavities, providing the polymer specific imprinting activity towards the template. SEM was performed to check: on one hand, the morphology of the polymers (MIP and NIP); and on the other hand, the sensor surface after the deposition of the sol-gel polymer matrix. Figure 4.18. shows SEM images for MIP and NIP and their size distribution, respectively.

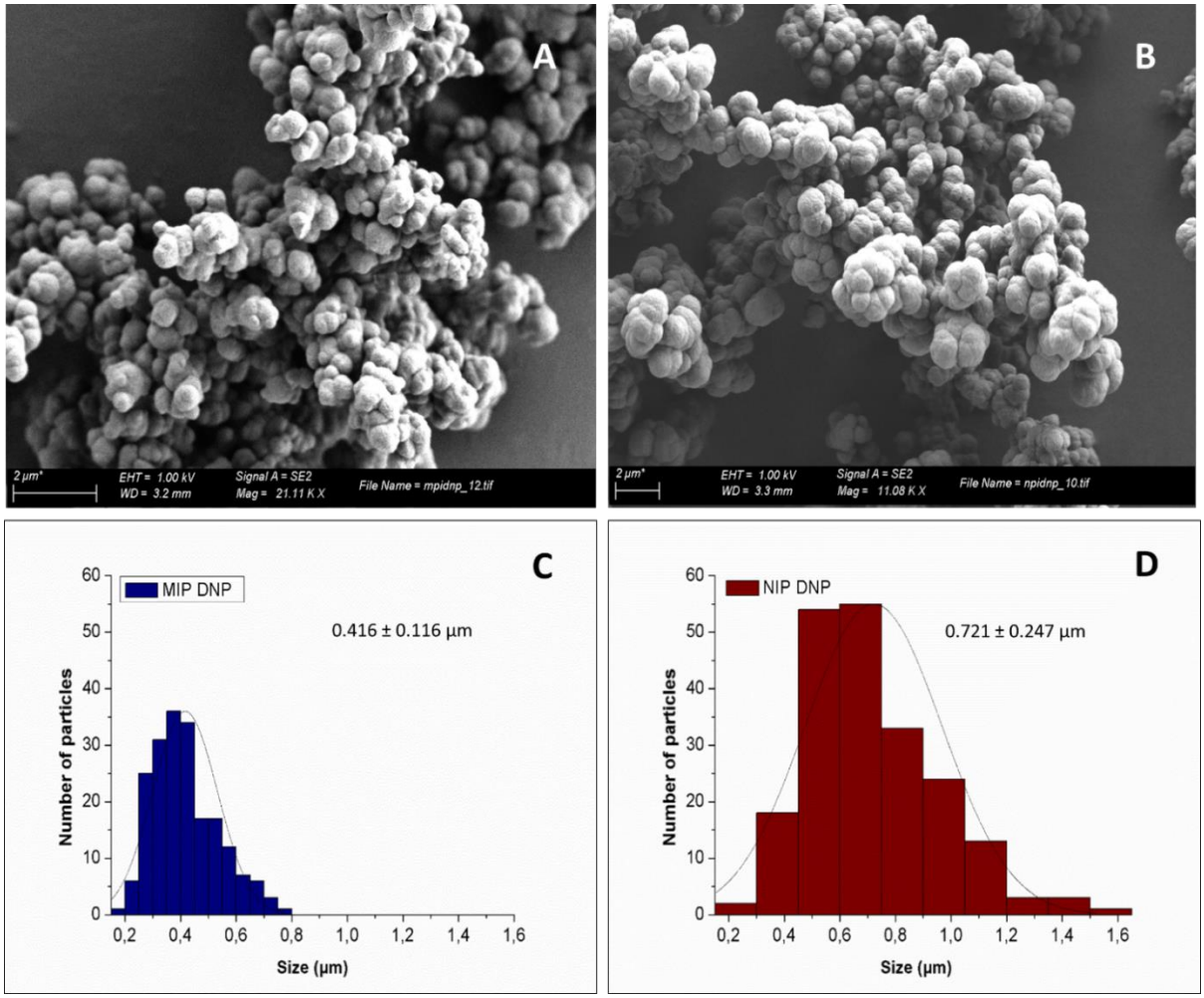

Figure 4.18. Characterisation of the polymers for MIP (A,C) and NIP (B,D). SEM (A,B) and size distribution of the particles (C,D).

From Figure 4.18, it could be observed the spherical, non-regular and highly crosslinking disordered structure of the polymer beads from MIPs and NIPs. The respective average sizes and standard deviations of diameter particle for MIPs and NIPs were calculated giving values of 0.416 ± 0.116 µm and 0.721 ± 0.247 µm, respectively.

In this case, MIPs particle size study reveal a slightly small polymer particle size diameter, when compared to NIPs. This could be explained because of an increased reactivity during the synthesis, which could happen due to the template addition, favouring the imprinting process.

Figure 4.19. shows the different electrode surface after the deposition of the sol-gel polymer matrix, a key step of the immobilisation via sol-gel and drop-casting technique.

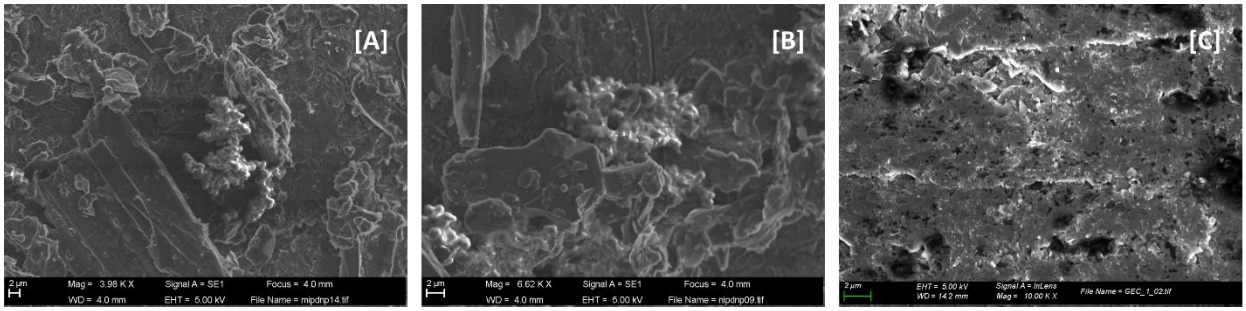

Figure 4.19. SEM images for [A] MIP-sensor, [B] NIP-sensor and [C] GEC electrode.

Polymers were added onto the surface electrode via sol-gel and drop-casting immobilisation for MIP and NIP sensors, while the GEC bare electrode remains unmodified for control purposes. The three electrodes presented homogeneous surfaces. In the case of [A] MIP and [B] NIP sensor surfaces (Figure 4.19A, 4.19B), the polymer and the graphite (coming from the sol-gel matrix) can easily be seen. On the other hand, the [C] GEC electrode surface is smooth and regular without any presence of the polymer neither the graphite (Figure 4.19C). The surface modification is self-evident when comparing the modified sensors with the unmodified one.

In order to obtain more characterisation information about the polymers, FT-IR technique was incorporated into this study revealing the main chemical bonds, when compared with a database. FT-IR was repeated three-times for each polymer case, MIPs and NIPs powder. Figure 4.20. shows no significant differences between both polymers as observed by its almost identical FT-IR spectra. Moreover, the same conclusion can be extracted by the triplicate samples. For that reason, it can be concluded that there is an absence of

template into the polymer structure so the synthesis as well as the template extraction were successfully done.

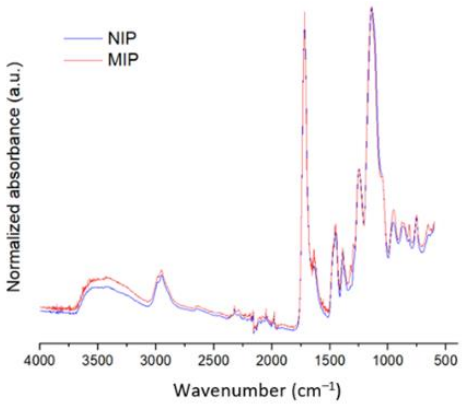

Figure 4.20. Comparison between the synthesised MIP (red) and NIP (blue) FT-IR spectra.

From the spectra, it was detected: (1) the broad band of hydroxyl groups around 3430 cm^{-1} that can be attributed from the MMA units; (2) around 2950-2980 cm^{-1} and 1450-1470 cm^{-1} the stretching and bending bands of methyl groups from the MMA and the EGDMA were respectively detected; (3) it was also found the carbonyl stretching at 1720 cm^{-1}; (4) the double C–O–C stretching at 1145 and 1250 cm^{-1}; (5) the rocking of the C–H stretching at 750 cm^{-1}; in the same line, at 1636 cm^{-1}, this peak can be associated with the double C=C bonding, which might indicate an incompletely monomer polymerisation or an unreactive portion of EGDMA that was not totally crosslinked.

If DNP was retained, especially in MIP synthesis or due to the incompletely removal during the Soxhlet extraction, the nitro groups showed a strong band around 1550 and 1350 cm^{-1} corresponding to asymmetric and symmetric stretching, respectively. Because of the absence of bands at 1150 cm^{-1}, it can be inferred that there is no presence of template in the polymer, neither in the NIP (due to an unprovable contamination). When focusing on 1390 cm^{-1} band, it

could be explained as the asymmetric bending of the –OH groups present on the carboxylic acid of the MMA units.

The chemical bonding values obtained from the FT-IR agreed with the expected polymer produced from FRP. The minimal value discrepancies in the wavenumber and peak intensity might be related to the chemical structure and space distribution due to synthesis replicates.

4.3.2. Electrochemical response

In this article, several studies were performed to elucidate the optimal conditions for electrochemical measurements. These included: (1) the establishment of an enrichment time well-balanced to differentiate MIP and NIP specific entrapment onto the electrode surface *versus* a feasible time measurement that might include cleaning processes; (2) a buffer and pH optimisation test; (3) a repeatability and reproducibility study; and (4) a specificity test to verify the imprinting process with MIP-based sensors in different ratio of interferents species that could affect the pre-concentration process of TNT. Finally, (5) calibrations curves against DNP and TNT were added and (6) a PCA qualitative study was performed with several nitro aromatic compounds to check the response of the dummy MIP sensor, its respective NIP sensor and the GEC used as a bare sensor.

4.3.2.1. Enrichment time

To check the enrichment time in order to optimise the experimental conditions to perform DPV measures, stock solutions of 10 µmol L^{-1} for TNT and DNP were measured. Without a cleaning step, the aforementioned solutions were incubated and measured with a contact time range from 0 to 100 minutes. From this experiment the resultant plots and non-linear fittings are shown in Figure 4.21.

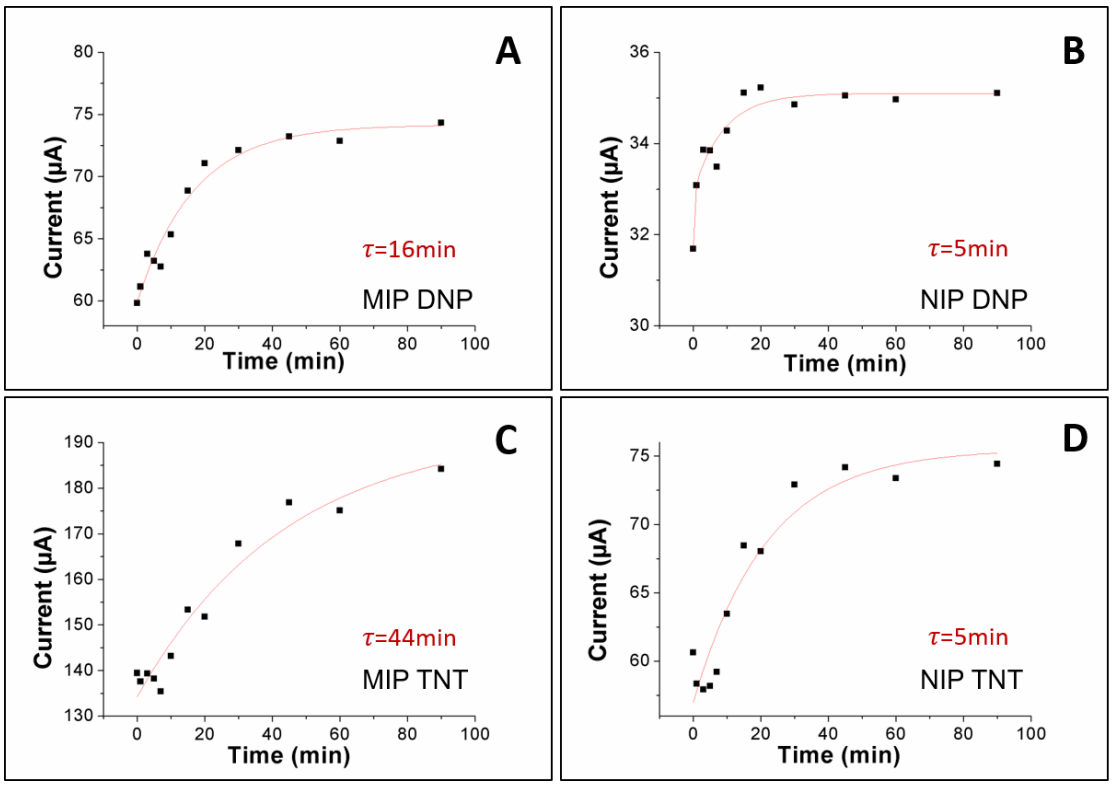

Figure 4.21. Enrichment time fitted curves for MIPs-sensors (A,C) and NIPs-sensors (B,D) from 0 to 100 minutes when measuring a stock solution of 15 µmol L-1 for DNP and TNT.

To achieve optimal experimental conditions, the measurement time (including cleaning steps) must be counter-balanced to obtain a good electrochemical signal in terms of current intensity, and excessive scanning speeds must be avoided. For this reason, a time of 5 minutes was chosen to obtain more than two thirds of the final response with a reduced analysis time.

4.3.2.2. pH and buffer optimisation

In order to optimise the conditions to achieve the highest peak value, the pH range was studied. The pH range was evaluated between values ranging from 5 to 8, see Figure 4.22.

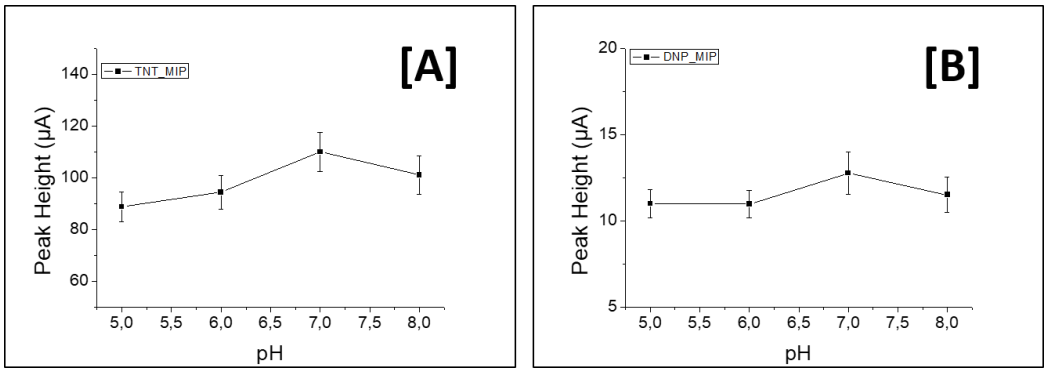

Figure 4.22. pH responses using 3 MIP sensors towards [A] TNT and [B] DNP at different buffer conditions.

Finally, the concluded maximum peak height value were obtained with PBS pH 7 due to TNT and DNP presenting better signals than other buffers.

4.3.2.3. Repeatability and reproducibility study

A repeatability test was performed in order check for sensor capabilities. Three MIP and 3 NIP modified sensors were used to measure, 10 µmol L^{-1} samples of TNT and DNP, in separated solutions for 15 times on the same day, taking the precaution to clean the surface electrode before each measurement.

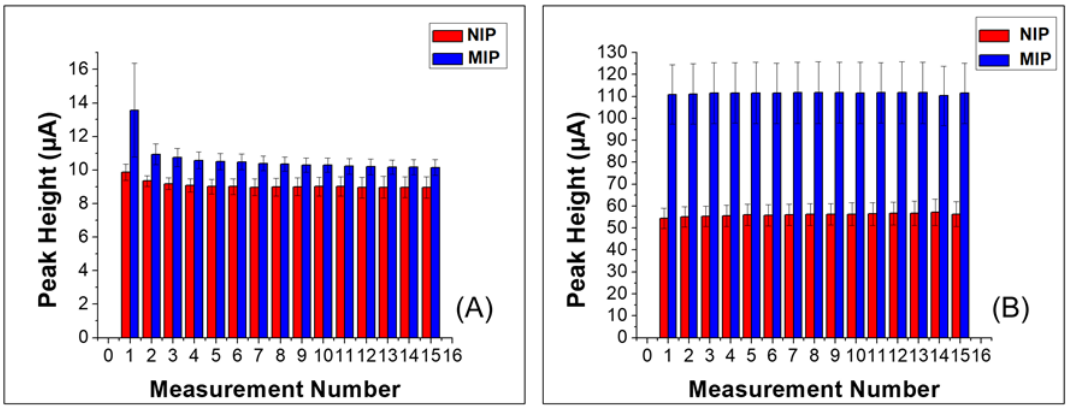

Figure 4.23. Repeatability measurements of MIP and NIP for (A) DNP and (B) TNT (n = 3).

As it shown in the figure above, repeatability values were obtained for 3 DNP-MIPs and 3 DNP-NIPS sensors towards TNT and DNP. For TNT measures, the values were 3.97% and 4.61%, respectively for MIP and NIP sensor. For DNP, repeatability values were of 9.14% and 7.34%, respectively. The reproducibility was studied five times for three DNP-MIP sensors with a concentration of 10 µmol L^{-1} samples. Both TNT and DNP samples were measured five times, obtaining values of 6.5% for TNT and 5.5% for DNP. DNP-MIP sensors' repeatability values against DNP showed slightly better results than TNT, which is explained by the dummy imprinting performed for DNP, as can be seen in the abovementioned figure.

4.3.2.4. Specificity study

Ten µmol L^{-1} TNT samples were measured in presence of various analytes (acetaminophen, serotonin and tryptamine) to observe any interferent effects for 3 different MIP sensors. These three substances could be considered emergent contaminants, e.g., paracetamol is a common drug and tryptamine is an amine. Serotonin was chosen because its different structures and functionality cavities purpose, see Figure 4.24.

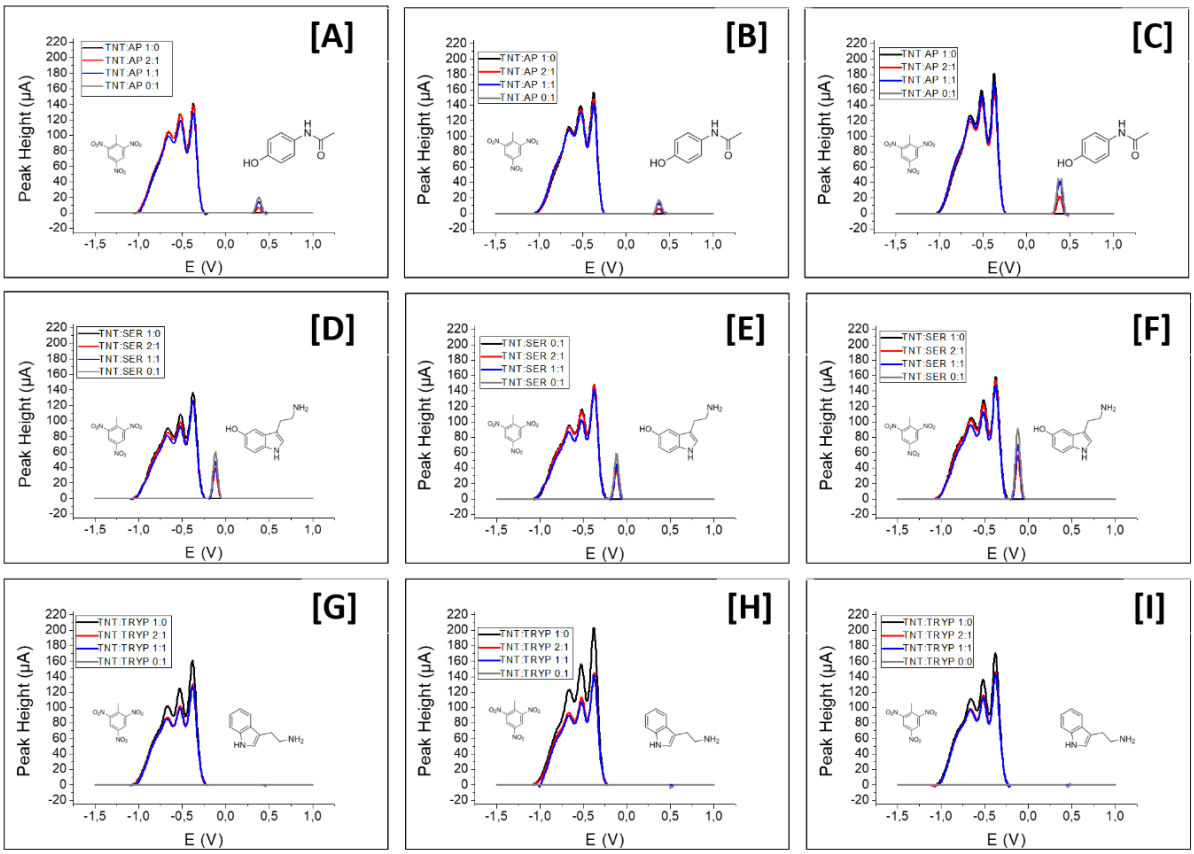

Figure 4.24. Interferent study at different ratios of TNT versus acetaminophen [A,B,C], serotonin [D,E,F] and tryptamine [G,H,I]. Each row corresponds to different MIP-sensors (n=3).

As can be seen in the figures above there is no decrease of TNT reduction peaks in presence of the different substances. In fact, this experiment was also performed to validate the reproducibility of the different MIP-sensor construction. If the figures' rows are examined, it can be observed that there are no significant differences among the different sensors' response. This behavior is due to the cavities being keyed to DNP or TNT, the more dissimilar the structure of the compounds is, the lower is the adsorption in such cavities, thus, lower is the signal. The size of the molecule, as well as steric hindrance may play a big role in the adsorption of the different molecules in the cavities. TNT signal remains the same intensity with the addition of these substances. This can indicate that the polymers have specificity (as the TNT imprinting is not

affected), and also there is another specificity due to the electrochemical technique (because of the different potential signal).

4.3.2.5. Calibration curves

Raw data of the DPV voltammetric signals towards DNP and TNT are depicted in Figure 4.25, for the different type of sensors *versus* DNP and TNT.

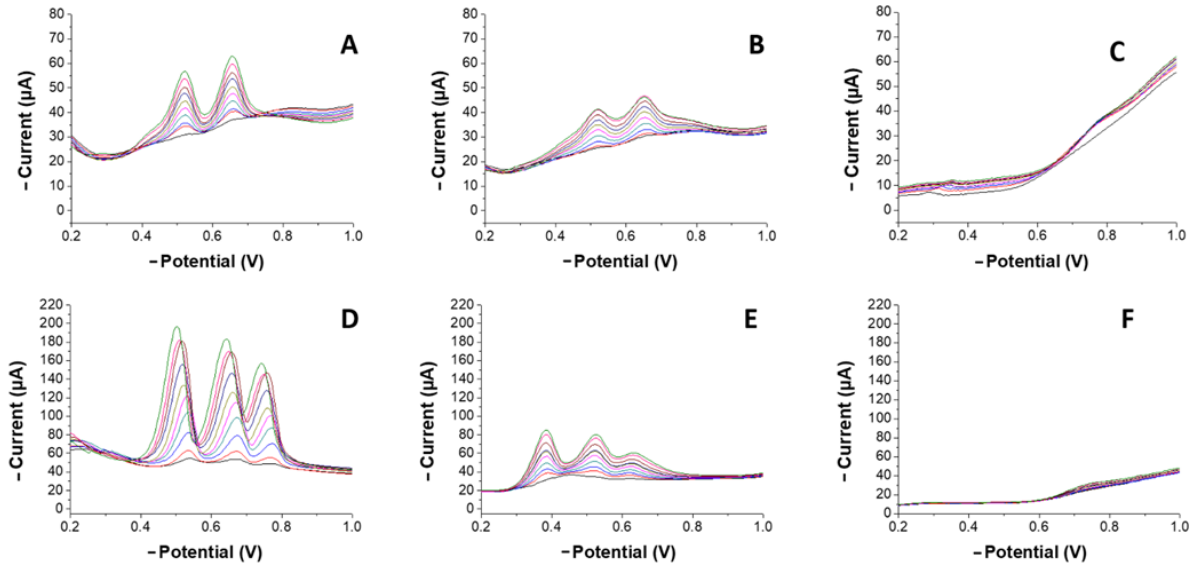

Figure 4.25. Voltammetric responses from 0.55 to 19 µmol L^{-1} of DNP and from 0.45 to 15 µmol L^{-1} TNT for the prepared sensors. (A) MIP sensor versus DNP. (B) NIP sensor versus DNP. (C) GEC sensor versus DNP. (D) MIP sensor versus TNT. (E) NIP sensor versus TNT. (F) GEC sensor versus TNT.

The electrochemical signals of nitroaromatic compounds is quite characteristic. In the case of DNP, it has a double reduction peak between -0.4 V and -0.6 V, whereas TNT has three reduction peaks in the same region. The number of peaks correspond to the number of nitro groups. The first nitro group reduction is produced around -0.5 V, and usually has a sharp and defined peak; the second nitro group is reduced around -0.65 V; the last nitro group is around -0.75 V. It seems that the reduction that takes place in the MIP electrode surface shifted these reduction peaks to more negative potentials when compared with the NIP electrode, which presented peaks at -0.35 V, -0.55 V and -0.65 V. For DNP, the

two nitro reduction peaks appeared at -0.52 V and -0.68 V for MIP and NIP. DNP did not present any difference in the reduction potential, i.e., no peak shift was observed.

The concentrations ranges studied for both compounds were as follows: 0.55 to 15 µmol L^{-1} for DNP and 0.45 to 10 µmol L^{-1} for TNT. Then, calibration curves were constructed for DNP and TNT for each of the different electrodes, i.e., MIP sensor, NIP sensor and GEC electrode, as shown in Figure 4.26.

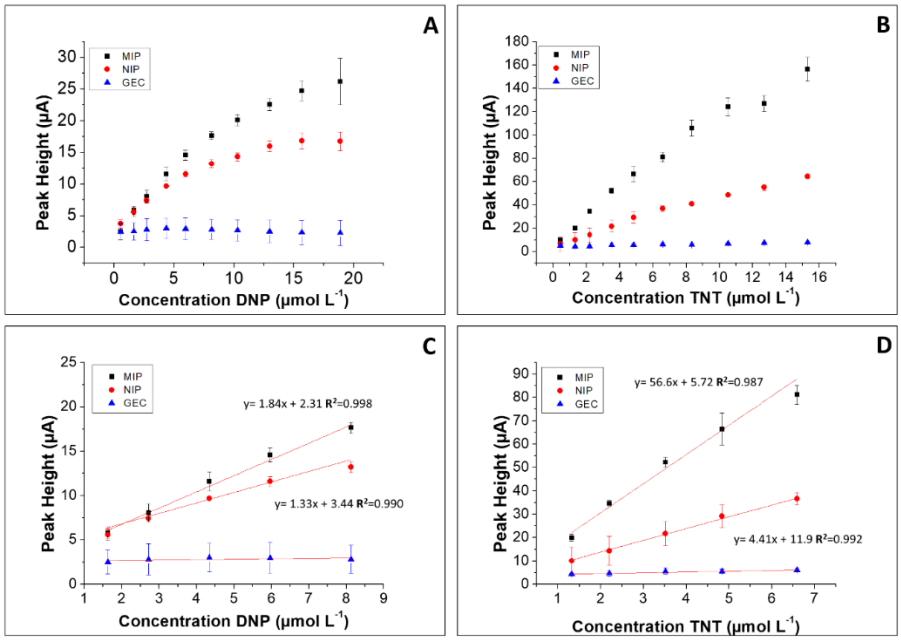

Figure 4.26. Calibration curves from 0.55 to 19 µmol L^{-1} for DNP (A) and from 0.45 to 15 µmol L^{-1} for TNT (B) for the three different sensor types used in this study. Linear ranges from 1.6 to 8.0 µmol L^{-1} for DNP and from 1.3 to 6.5 µmol L^{-1} for TNT are added in (C,D).

The samples for the calibration curves were measured per triplicate, each triplicate in a different day. The baseline of the obtained voltammograms was corrected and the first peak height was chosen to build the calibration curves. Figure 4.27 shows the voltammograms for each specie and sensor incorporating the baseline correction.

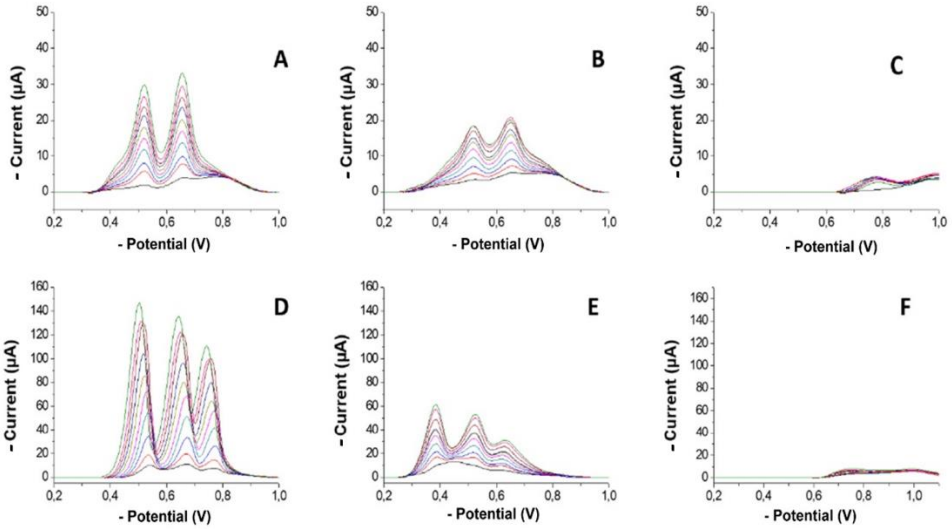

Figure 4.27. Voltammetric with baseline correction responses from 0.55 to 19 µmol L^{-1} of DNP and from 0.45 to 15 µmol L^{-1} TNT for the prepared sensors. (A) MIP sensor *versus* DNP. (B) NIP sensor *versus* DNP. (C) GEC sensor *versus* DNP. (D) MIP sensor *versus* TNT. (E) NIP sensor *versus* TNT. (F) GEC sensor *versus* TNT.

LOD values (S/N = 3) were calculated form the calibration curves. The regression lines were fitted with the first five concentration points, that is from 1.6 to 8.0 mol L^{-1} for DNP and 1.3 to 6.5 mol L^{-1} for TNT. Fitting parameters for the calibration curves are shown in Table 4.5.

Table 4.5. Summary of calibration results in the linear concentration region from 1.6 to 8.0 µmol L^{-1} towards DNP and from 1.3 to 6.5 µmol L^{-1} for TNT.

	MIP		NIP	
	DNP	**TNT**	**DNP**	**TNT**
Sensitivity (µA μmol^{-1} L^{-1})	1.84	56.6	1.33	4.41
Intercept (µA)	2.31	5.72	3.44	11.9
R^2	0.99	0.98	0.99	0.99
LOD (μmol^{-1} L)	0.59	0.29	1.38	0.95
LOQ (μmol^{-1} L)	1.79	0.88	4.18	2.87

According to the results obtained, the MIP electrode's affinity is higher towards TNT than towards DNP, the original template molecule. This behaviour may be explained when considering the electrostatic interactions between the nitro groups of the target molecule and the tailor-made binding sites, that is TNT has three groups whereas DNP only has two. Thus, affinity is higher for TNT.

Additionally, the specificity was evaluated. The interference effect in mixtures with TNT was studied, in this case the chosen compounds where acetaminophen, tryptamine and serotonin. The objective was to determine if the presence of these compounds in a sample containing TNT had any impact in the uptake of TNT by the sensor.

For all the studied compounds (Figure 4.24), the TNT signals did not present any substantial change; thus, the selectivity of the constructed MIP electrode was demonstrated.

4.3.3. Specificity versus other nitroaromatic compounds

PCA was performed to evaluate the array capabilities to separate the different samples. For that reason, mono-nitro and di-nitro aromatic species accessible in the laboratory were measured per quintuplet at the same experimental conditions including the same concentration in order to evaluate the specificity of the imprinted sensor. This evaluated compounds, in extension to DNP and TNT, were 2,4-DNT, 2,6-DNT, 2-NT, 1,3-DNB, 4-NT and 1-NB. Because of that, a fix concentration of 10 mol L^{-1} of the corresponding analytes were used to evaluate the differences in specificity response, see Figure 4.28.

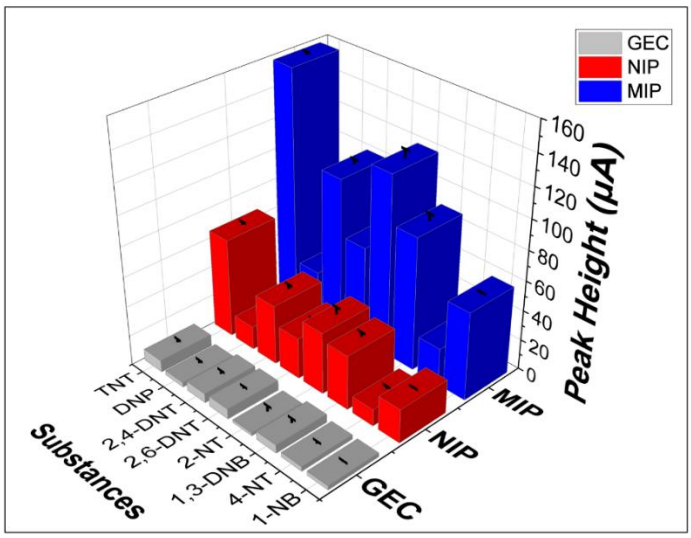

Figure 4.28. Comparison of voltammetric response of 10 µmol L^{-1} nitroaromatic compounds for each sensor and different nitroaromatic species.

As can be seen in Figure 4.28, in the case of the MIP sensors the current intensities are significantly higher compared to the NIP and GEC sensors for the entire set of compounds group. This higher current intensity can be attributed to the higher enrichment of electroactive species at the surface electrode due to the active and specific imprinted sites able in the polymer. This study was done with 3 replicates sensors of each sensor type.

However, when focusing on the specificity derived from this study, it seems clear that TNT has a higher current than the rest of the species. In fact, TNT presents a higher current followed by the group formed by 2-NT, 2,4-DNT, 1,3-DNB and 2,6-DNT, and finally, in the last group, we observe 4-NT, 1-NB and DNP. These sub-groups can be explained by the nitro groups present in the molecule, but also, the higher number of nitro groups helps to a higher concentration on the surface of the polymer and consequently an increase of the signal intensity.

From this previous study, it can be seen that these sensors are able to discriminate the different nitroaromatic compounds. Depending on the type of

sensor the signal could be higher or lower in terms of peak height value. This happened due to the MIP-polymer presence and their imprinting capabilities.

In order to identify the presence of specific compounds, their fingerprint signal may be extracted from the complete DPV measurement, a task that can be done using PCA. An example of application was done with a set of mono-, di- and tri-nitro compounds to check abilities for identification and quantification. For this purpose, five samples of each considered substance at 10 µmol L^{-1} concentration level were measured using the MIP, NIP and GEC sensors. Results can be observed in Figure 4.29.

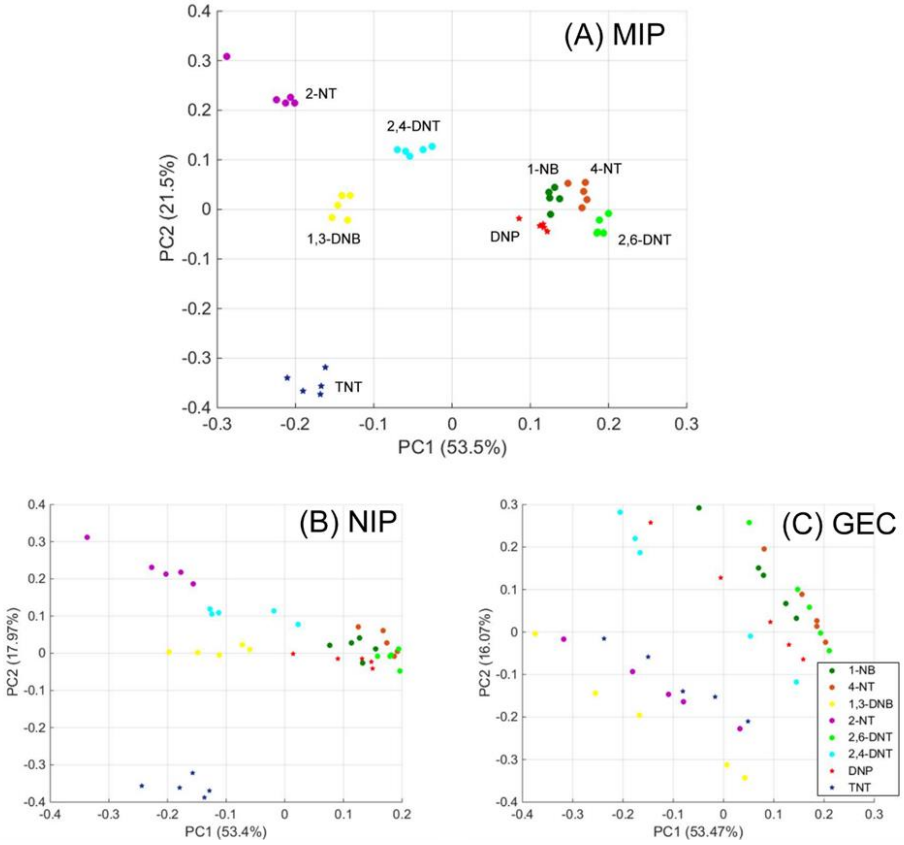

Figure 4.29. Score plots for each nitroaromatic compound performed with the voltammetric signals of (A) MIP, (B) NIP and (C) GEC sensors for five replicates of each nitroaromatic compound at 10 µmol L^{-1} after principal component analysis.

As can be seen in Figure 4.29., identification is really facilitated when employing the MIP sensor (Figure 4.29A), given each substance is clearly grouped in its own cluster. Focusing on NIP and GEC sensors (Figure 4.29B and Figure 4.29C, respectively) also a certain grouping is observed, but the clustering degree is lower. In fact, in case of GEC sensors the degree of clustering is almost inexistent. As a distinctive feature, it is to be mention that the main compounds in this work, DNP and TNT appear in different clusters. This means a clear difference in the obtained voltammograms, both for DNP and TNT is showed in the respective fingerprints. The other substances in the study, the mono-nitro and di-nitro compounds demonstrate their similarity by resulting placed in neighbour positions, allowing their identification. The PCA scores plot for the MIP sensor showed a better performance visualising better separation between each nitroaromatic tested. To conclude, these results demonstrate the generic ability of using MIP recognition elements combined with voltammetric sensors, being as a generic starting point for a certain group of substances, allowing for advanced identification applications "*a le carte*".

5.Conclusions

5. CONCLUSIONS

In the presented doctoral thesis an assortment of voltammetric MIP based sensors were manufactured to develop an array of biomimetic sensors for different applications, making them a versatile and affordable option in comparison with their biological counterparts. MIP sensors were used to improve the electrochemical response and performance using these polymers as artificial receptors, in comparison with classical non-modified sensors, *i.e.,* NIP or GEC. The analytical parameters such as linear range, sensibilities and limits of detection or quantification are improved with its use, especially in the case of large preconcentration times. Several applications of MIP sensors were explored in different fields such as food and beverage industry, homeland

security, explosive detection and environmental monitoring. In comparison with the conventional methods of analysis, sensing and biosensing field has better capabilities in terms of time, power consumption, pre-treatment and portability.

The main conclusions are presented and divided in three sections according to the representative work presented in this manuscript:

1. In the beverage production field:

    1.1. MIP polymers were successfully synthesised and tested for two different templates: 4-ethylphenol and 4-ethylguaiacol. To prove the imprinting selectivity of those MIPs, a blank control namely the respective non-imprinted polymer was synthesised and used for both templates indistinctively.

    1.2. Polymer based sensors were constructed by adding MIP or NIP polymers, respectively, onto the bare electrode surface by via drop-casting and spin coating immobilisation. MIP based sensor modification improved the electrochemical response and its performance with an appropriate transducer mechanism, in comparison with the NIP sensor or the bare electrode (called GEC).

    1.3. Once polymer sensors were constructed a sensory MIP array was developed to use the electronic tongue approach for the very first time. This electronic tongue was successfully applied for the identification, quantification and discrimination of a mixture of 4-ethylphenols responsible of the *Brett* character.

2. In the beverage preservation field:

2.1. MIP polymer was successfully synthesised and tested using histamine as a molecular template. Similarly, to the previous study (see section 1.1.) the respective non-imprinted polymer was synthesised.

2.2. Polymer and their corresponding sensors were strongly characterised by microscopy techniques including: morphological polymer studies and surface sensor examination using SEM and optical microscopy with confocal technique, that was used to verify the imprinting effect.

2.3. Histamine MIP sensors were developed and optimised in order to obtain a better electrochemical performance and improving the analytical parameters of interest.

2.4. Similarly, to the first article, the comparison among MIP, NIP and bare sensor was carried out in detail. The results show a clear improvement from MIP sensor respect the other ones.

2.5. The feasibility of the presented MIP voltammetric sensor was compared with the industry gold standard. An agreement was found, with non-significative differences, between the fluorimetric reference method and the proposed electrochemical approach.

3. In the security and environmental field:

3.1. The strategy of a dummy MIP was favourably applied, synthesising a dummy molecularly imprinted polymer against 2,4,6-trinitrotoluene (TNT), using the chemical and structurally analogue 2,4-dinitrophenol.

3.2. Imprinted polymers were used in order to improve non-modified sensor capabilities to quantify TNT and DNP. Better limits of detection were obtained in the case of MIP sensors for both compounds, as well as obtaining good results in repeatability, reproducibility and specificity studies.

3.3. Discrimination sensor ability was presented in all sensors for a myriad of nitroaromatic compounds. Which are catalogued as emerging contaminants derives from TNT use.

Future perspectives

The present compendium presented three articles that use imprinting technology to improve the voltammetric sensor response. MIPs can be combined with the electrochemical techniques, and these articles proved that the methodology enhanced the performance of the voltammetric sensors in the ET approach. Furthermore, the research work compiled in this thesis have used to gain experience and acquire the necessary know-how to elaborate, design and validate the use of MIPs in electrochemical sensors. In fact, the introduction of MIPs in the GSB laboratory, combined with the experience in advanced chemometric calculations, allowed the improvement of the ET approach in food and beverage, homeland security and environmental applications.

For that reason, the incorporation of computational approaches for the design of MIPs might be an option to improve the synthetic pathway. This allows the choice of better synthesis reagents, favouring the interactions among them in the different stages of the synthesis to finally obtain an improved imprinting effect.

In the same direction, the use of different methods and types of polymerisation might improve the homogeneity of the polymer. Including different methods of synthesis might offer smaller particles that might allow the development of new protocols for their subsequent incorporation into sensing platforms, especially in the case of emulsion approach. On the other hand, focusing on the type of polymerisation, the implementation of controlled radical polymerisation, (*i.e.*, ATRP, NMP or RAFT), might provide a better growth of the branched chains which would give the option to obtain a more homogeneous polymer.

In-situ polymerisation using conductive polymers opens up a new direct polymerisation route using electrochemical techniques in one step synthesis, by which it would be possible to obtain a better response and an immobilisation onto the electrode surface by layers.

Also, novel techniques such as ink printing might be used to incorporate these polymers onto sensor platforms in a more controlled and systematic procedure. Paper based platforms might also be a good platform to develop a new branch for cost-effective and versatile sensors.

These new approaches might open new MIP-based sensors to miniaturise future devices for a portable, easy to operate and unequivocal response.

6. Publications

Article 1

Bioelectronic tongue using MIP sensors for the resolution of volatile phenolic compounds

Herrera-Chacon, A., González-Calabuig, A., Campos, I., & del Valle, M.

Sensors and Actuators B: Chemical, 2018, 258, 665-671

DOI: 10.1016/j.snb.2017.11.136

Sensors and Actuators B 258 (2018) 665–671

Contents lists available at ScienceDirect

Sensors and Actuators B: Chemical

journal homepage: www.elsevier.com/locate/snb

Bioelectronic tongue using MIP sensors for the resolution of volatile phenolic compounds

Anna Herrera-Chacon, Andreu González-Calabuig, Inmaculada Campos, Manel del Valle*

Sensors and Biosensors Group, Department of Chemistry, Universitat Autònoma de Barcelona, Edifici Cn, 08193 Bellaterra, Barcelona, Spain

ARTICLE INFO

Article history:
Received 27 July 2017
Received in revised form 8 November 2017
Accepted 22 November 2017
Available online 23 November 2017

Keywords:
Molecularly imprinted polymer
Electronic tongue
Artificial neural networks
Differential pulse voltammetry
Volatile phenols

ABSTRACT

The proposed approach reports the combined advantages of biosensors made of molecularly imprinted polymers (MIPs) and the modelling capabilities of Artificial Neural Networks (ANN) in a bio-electronic tongue (BioET) analysis system for the very first time. Molecularly imprinted polymers taylor-made for 4-ethylphenol (4-EP) and 4-ethylguaiacol (4-EG) and their control polymers, non-imprinted polymers (NIPs), were succesfully synthesized with similar morphologies and integrated onto an electrochemical sensor surface, as the recognition element, via sol-gel immobilization. The resulting MIP-functionalized electrodes were employed to arrange an array of different biosensor electrodes to quantify by means of ANN the binary mixtures of 4-EP and 4-EG yielding an obtained vs. expected correlation coefficient >0.98 and a normalized root mean square error (NRMSE) <0.076 (external test subset).

1. Introduction

Since the first electronic tongue (ET) analysis system was proposed in 1998 by Vlasov [1], a vast number of publications and applications of these devices have been described in the literature. This approach is based on the use of several sensors displaying cross-response for the elements in a sample, with the combination of advanced mathematical data treatment in order to analyse complex situations e.g. when the traditional sensors present undesirable matrix effect. Although employing wide scope sensors is the norm in ET research, the use of highly-selective sensing materials may help in the final specificity of the analytical system, where a sought goal might be the resolution of a mixture of similar compounds, e.g. sugars or phenols.

Nowadays, there is an increasing interest in the improvement of the ET performance, and thus in the generation of new application fields which has ended in the development of a second generation of ET named BioET [2,3]. The BioET follows the same approach of the ET, but introducing one or more sensors modified with a specific bio-recognition element into the array. In the literature there are examples that have already integrated different bio-recognition elements such as antibodies or enzymes [4]. For instance, laccase and tyrosinase have been widely integrated in the electronic tongue and applied for the detection of phenolic compounds in wines [5], another interesting example is the use of different types of native or recombinant acetylcholinesterases (AChE) for pesticide detection in water taking profit of the different inhibition pattern [6].

Besides, examples using another biomolecular recognition system that can be applied in the development of the BioET is that of the Molecularly Imprinted Polymers (MIPs). MIPs are plastic materials able to recognize biological and chemical species, which are synthesized using host-guest principles [7]. In these, chemicals targets are firstly used as templates during the polymerization to generate molecular motifs, for example tailored made supramolecular cavities allowing for the selective capture of the desired molecules. MIPs present advantages towards other biorecognition elements due to the possibility to work: in a wider pH range, using higher temperatures or pressures, having physical robustness and the feasibility of mimicking biological specificity reactions in a non-physiological media. They also show high selectivity and affinity towards the target molecule and they have low synthesis costs and higher mechanical and chemical stability [8]. They can be, in principle, synthetized 'à la carte' for almost any given substance and there have been described MIPs for metal ions, organic molecules, macromolecules, proteins, even microorganisms. Different types of synthesis are used in molecularly imprinted technology such as bulk [9], co-precipitation [10], nanoimprinting [11]. This field maintains active research such in areas like: solid phase extraction (SPE) [12], high liquid performance chromatography (HLPC) [13], drug delivery [14], environmental monitoring [15] sensing [16,17] and electrochemical sensors [10,18]. Although the interest in MIPs as recognition elements has increased in the last few years, their integration in BioET system still to be developed. Examples

* Corresponding author at: Sensors and Biosensors Group, Universitat Autonoma de Barcelona, Campus UAB, Edifici Cn, 08193 Bellaterra, Spain.
E-mail address: manel.delvalle@uab.cat (M. del Valle).

https://doi.org/10.1016/j.snb.2017.11.136
0925-4005/

using fluorescence electronic tongue have been developed for the discrimination of several nucleobases by using docecanethiol MIP films and PCA [19]; in the discrimination of different aryl amine environmental toxins [20] or the classification of six health risk compound including atrazine or chlorphyrifos among them [21].

An important limitation in the development of BioET with electrochemical transduction and using MIPs is the complexity in the MIP integration onto the electrode surface [10–22]. The major problem with MIP polymers is that they usually produce insulating layers, making difficult their integration in the electrochemical sensors; this is due to the impossibility of electron transfer between the analyte captured by the MIP and the electrode. To this aim, different approaches have been proposed in the literature such as MIP entrapment onto gels followed by its deposition onto the electrode surface [10,23], the electropolymerization within a conducting polymer enviroment [24,25], or the direct synthesis as a thin layer MIP onto a surface.

The case selected for application was the analysis of volatile phenols, as defects during wine production. The presence of *Brettanomyces* yeast during the wine fermentation stages causes losses, running into millions, in the beverage sector industry. Due to the use of oak barrels and the natural presence of the yeast in the grape fruit [26], the proliferation of *Brettanomyces* yeast produces volatile phenolic compounds such as 4-ethylphenol (4-EP), 4-ethylguaiacol (4-EG) and 4-ethylcatechol (4-EC) among others [27], their presence in wine can modify the beverage properties providing a sort of uncontrolled flavours and aromas that highly modify the wine sensory perception [28]. Traditional analytical methods for their detection are expensive, time-consuming, require qualified technicians and high-cost equipments, making the development of rapid and low-cost analysis method a real need in the wine industry to avoid major losses [29]. The human threshold is approximately 0.5 $\mu g\,mL^{-1}$ for 4-ethylphenol [26], making the detection of this compound in early fermentation stages a challenging demand on the analytical chemistry sector, which needs on-site and label free real time measurements.

Following the interest in ET of our group, in this work we propose a new BioET approach based on the use of MIPs as recognition element integrated in the multielectrode array and utilizing differential pulse voltammetry (DPV) for the 4-EP and 4-EG detection. MIP particles were integrated in the electrode using sol-gel technique in the presence of graphite as conducting material. 4-EP and 4-EG MIP were synthetized using co-polymerization standard protocols and immobilized onto the surface via a sol-gel membrane [10]. The voltammetric data from the MIP modified electrodes was analysed using chemometrics tools, such as principal component analysis (PCA) for identification and Artificial Neural Networks (ANN) for quantitative analysis. Our results demonstrate that MIPs, obtained for the two selected templates, were successfully integrated by a sol-gel immobilization onto each electrode surface providing an electrode array which forms the first BioET using MIPs as recognition element. Interferent studies showed that typical polyphenol present in wine did not interfere in the detection of 4-EP and 4-EG. Moreover, a classification study carried out using the BioET and PCA demonstrated a good discrimination performance among the 4-EP, 4-EG and the rest of the interferents. The developed BioET was finally applied for the determination of 4-EP and 4-EG mixtures, in a concentration range of 3–20 $\mu g\,mL^{-1}$.

2. Experimental

2.1. Chemicals and reagents

Reagents used were analytical reagent grade and all solutions were made up using MilliQ water from MilliQ System (Millipore, Billerica, MA, USA). Divinylbenzene (DVB), 4-ethylphenol (4-EP), 4-ethylguaiacol (4-EG), tetramethyl orthosilicate (TEOS) and hydrochlohic acid (HCl) were purchased from Sigma-Aldrich (St. Louis, Mo, USA). Ethylene dimethacrylate (EGDMA) was purchased from Fischer Scientific. Methanol (MeOH) and Ethanol (EtOH) were purchased from Scharlau (Barcelona, Spain) and 2,2′-azobis(2,4-dmethylvaleronitrile) (AIVN) was purchased from Wako Chemicals GmbH (Neuss, Germany). Graphite powder (particle size <50 μm) was received from BDH (BDH Laboratory Supplies, Poole, UK) and Resineco Epoxy Kit resin was supplied from Resineco green composites (Barcelona, Spain).

2.2. MIP synthesis

In a round bottomed flask, it was added 40 mL of EtOH, 0.5 mmol of template (4-EP or 4-EG) and 2.05 mmol of DVB. The mixture was then stirred gently at low temperature for 15 min. Afterwards 9.81 mmol of EGDMA and 0.08 mmol of AIVN were added and then all the mixture was purged with nitrogen for 2 min. Synthesis of MIP was done in a water bath thermally controlled at 60 °C during 16 h with magnetic stirring (See Figure SP1, supplementary data). Then the polymer was extracted and dried for an overnight at room temperature. The material was packaged in a cartridge and the template extraction was performed with a Soxhlet using MeOH:HAC (9:1) during 72 h. Control non-imprinted polymers (NIP) were also synthesized for comparison purposes under the same conditions that the MIP, but in the absence of the template molecule. All the synthesized polymers were characterized by scanning electron microscopy (SEM) by using a scanning electron microscope EVO® MA10 operated at 30 kV. The resulting microscopy images were treated with Fiji package software and Image J software (Zeiss GmbH, Jena, Germany) and Origin 8.0.

2.3. Integration of the MIP onto the sensor surface

Each final biosensor was prepared by the immobilization of the MIP polymers in micro beads form onto the surface of a graphite epoxy composite (GEC) electrode previously developed elsewhere [30], using a sol-gel technique [10]. For preparation of the sol-gel 0.5 mL of TEOS, 0.5 mL of EtOH, 0.25 mL of H_2O and 25 μL of HCl 0.1 M were vigorously mixed for 45 min and then rested for approximately 35 min to arrive at the syneresis stage. Then 0.2 mL of the rested solution were added to a 7 mg of graphite and 40 μL of a 15 $mg\,mL^{-1}$ polymer (4-EP MIP, 4-EG MIP or NIP) suspension in EtOH. This mixture was then spin-coated by depositing 10 μL of the solution onto the surface of the electrode and spinned using a spin-coater made from a 12V DC motor. Polymerization was finished drying the electrodes overnight at 4 °C. An additional electrode was produced adding only 40 μL of EtOH without any MIP or NIP polymer; this was employed as control electrode, modified uniquely with the sol-gel layer.

2.4. Sample preparation

All samples were prepared in phosphate buffer (100 mM KCl, 42 mM $K_2HPO_4{\cdot}2H_2O$, 8 mM KH_2PO_4, pH 7.0). For the electrochemical sensor characterization 4-EP and 4-EG samples were prepared in 20 mL of phosphate buffer in a concentration range of 5–35 $\mu g\,mL^{-1}$. Moreover, for the adsorption kinetics onto the electrode surface, the reproducibility and classification studies, a unique sample of 7 $\mu g\,mL^{-1}$ was prepared and measured for both analytes. Furthermore, for classification studies, 3 samples of 25 $\mu g\,mL^{-1}$ for gallic acid and quercitine in the presence of 3 $\mu g\,mL^{-1}$ of 4-EP and 4-EG were prepared. For quantification studies a total of 33 samples were prepared by mixing both 4-EP and 4-EG in 4 concentrations levels in the range of 3–20 $\mu g\,mL^{-1}$ and

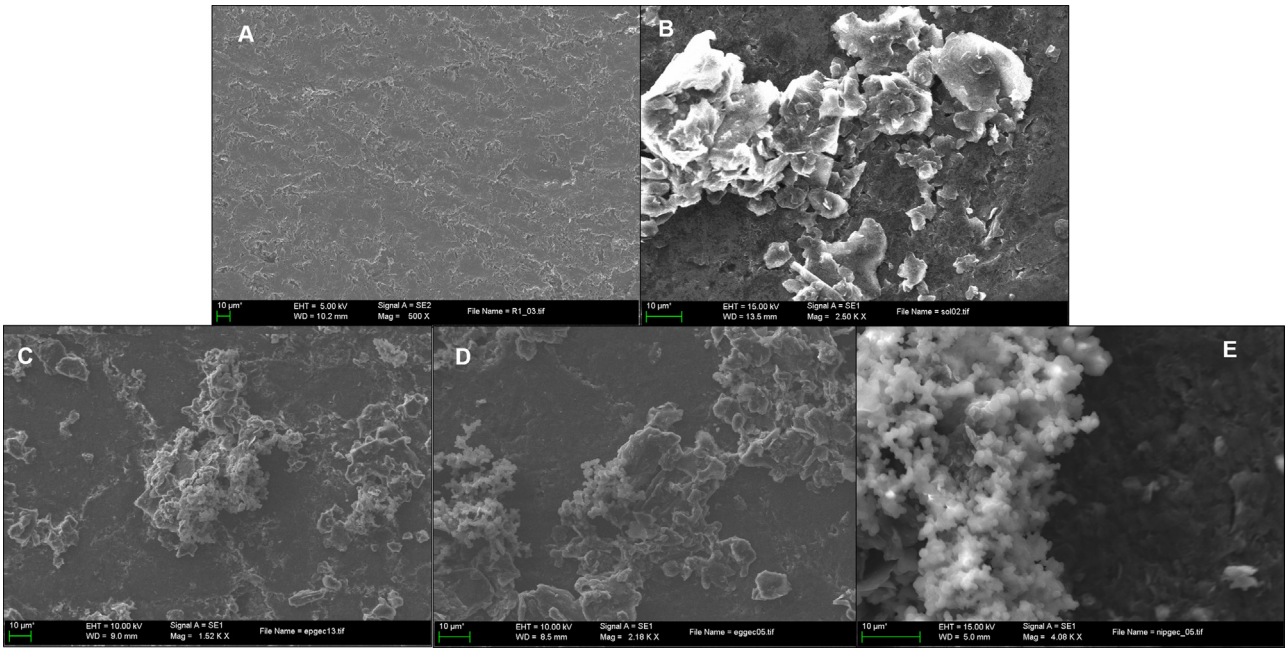

Fig. 1. SEM images of the GEC surface (A), and GEC after sol-gel immobilization (B). SEM images for the modified electrodes using: 4-EP MIP (C), 4-EG MIP (D) and NIP (E).

subdivided in two sets (16 samples for the training set and 9 samples for validation set) by the use of an experimental design.

2.5. Electrochemical measurement

All the electrochemical measurements were performed using AUTOLAB PGSTAT30 (Ecochemie, Netherlands) controlled with GPES Multichannel 4.7 software package. The used voltammetric cell consisted of a Ag/AgCl electrode as a reference electrode and a platinum electrode as counter electrode. Graphite epoxy composite electrodes (GECs) modified with MIPs, NIP and sol-gel were used as working electrodes [32]. Differential Pulse Voltammetry (DPV) measurements were recorded by scanning potential from 0 V and 0.9 V vs. Ag/AgCl with a step potential of 5 mV and a pulse amplitude of 50 mV at room temperature without stirring. After each measurement the electrodes were cleaned by repeating the DPV measurement in pH 7 phosphate buffer solution.

2.6. Data processing

All the preprocessing and artificial neural networks routines were built by the authors using MATLAB 2016b (MathWorks, Natick, MA) programming environment and its Wavelet, Neural Network and Statistical Toolboxes; while the graphical representation and analysis of the results was performed with Sigmaplot (Systat Software Inc., San Jose, CA).

3. Result and discussions

3.1. SEM microscopy

The polymers and their integration onto the surface were characterized by SEM technique. Images from the polymers before their immobilization onto the electrodes show that similar polymeric materials (see Figure SP2, supplementary data) with non-regular spherical particles were obtained. The average size and standard deviation of 4-EP MIP, 4-EG MIP and NIP was $0.76 \pm 0.034\,\mu m$, $0.64 \pm 0.17\,\mu m$ and $0.67 \pm 0.14\,\mu m$ respectively, where it can be assumed that all the materials have a similar particle size and distribution and they are also highly cross-linked. Additionally, these equivalence make them especially suitable for comparison experiments.

Fig. 1 displays the SEM images for the 5 different electrode biosensors prepared in this work. The images were taken in order to corroborate the presence of the polymers onto the electrode surface and also to confirm that the polymer morphology was preserved after the sol-gel deposition. The Fig. 1 A shows the SEM image from the GEC surface while the rest of the images display the modified electrodes with sol-gel (B), 4-EP MIP (C), 4-EG MIP (D) and NIP (E). Due to the similar size of the polymers the only conclusion that can be extracted from the comparison of the images is that the sol-gel is immobilized onto the electrode surface, increasing the roughness of it, but it was not possible to differentiate among the synthesized polymers. In other words, equivalent surfaces were obtained, independently of the MIP/NIP polymers used.

3.2. Individual electrochemical response

Prior to use the sensor as a BioET, the electrochemical behaviour of each MIP biosensor was evaluated by studying the response of each kind of electrode towards the two analytes of interest. By the study of the adsorption kinetics of each electrode, the stripping time was also established. A total of 4 types of electrodes were prepared and their response against 4-EP and 4-EG evaluated with the aim to demonstrate that both MIPs present higher response than the control electrodes (NIP and sol-gel) but also to show their cross-selectivity to each analyte, a pre-requisite for developing an ET.

3.2.1. Adsorption kinetics

Since one of the characteristics to take into account in the use of MIPs is the adsorption kinetics of the materials, the optimal time where the specific adsorption processes are predominant to the unspecific ones was investigated. This is a main feature to be optimized in adsorptive stripping voltammetry (ASV). For this reason, the 4-EP MIP and 4-EG MIP electrodes were evaluated in the presence of $7\,\mu g\,mL^{-1}$ of their corresponding template analyte and compared with the control NIP electrode and the sol-gel electrode.

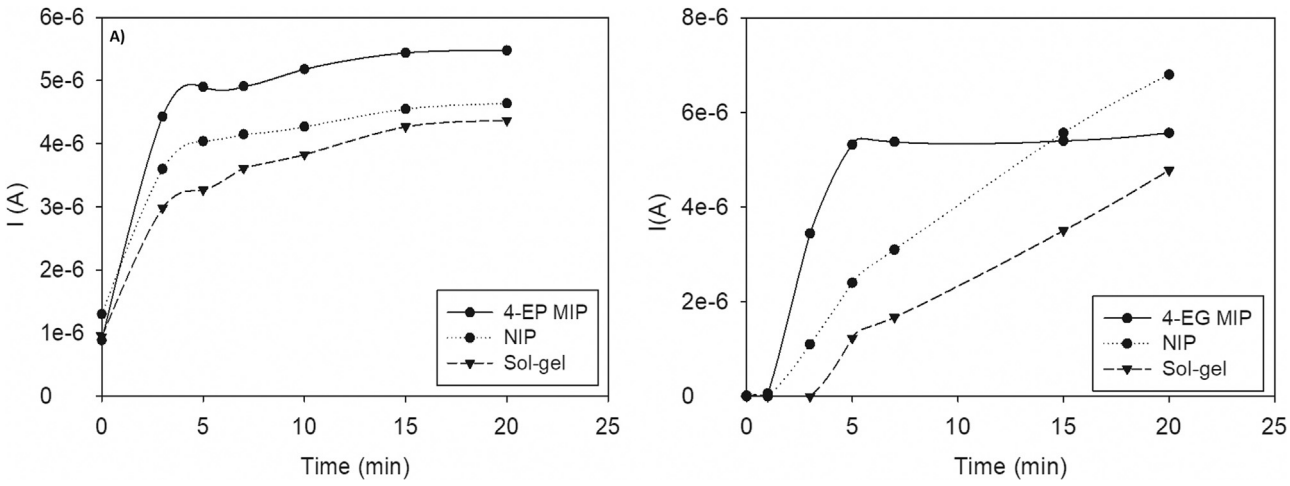

Fig. 2. Adsorption kinetics of the electrodes modified with MIP, NIP and sol-gel for the analytes 4-EP (left) and 4-EG (right).

The Fig. 2A displays the 4-EP kinetics obtained for the 4-EP MIP electrode while Fig. 2B shows the results obtained for the 4-EG MIP electrode in the presence of 4-EG. In both cases the adsorption processes of their respective templates present faster adsorption processes, reaching the saturation value between 3 and 5 min, while the adsorption values for the control polymers (NIP and sol-gel) are slower than the MIP. This region of the isotherm also showed the maximum differences in the adsorption capabilities among the MIP, NIP and sol-gel, indicating that the optimal stripping time to perform the measurements was 3 min. However, in the case of 4-EG, when the time increases, the control polymer displays a similar signal to the MIP. This phenomenon can be attributed to the fact that the unspecific adsorption processes acquire a major importance in the final adsorption signal, providing another reason to avoid long-time stripping conditions.

3.2.2. Calibration curves and reproducibility of the electrodes

The biosensor performance of each MIP electrode was evaluated towards their corresponding template. In all cases, the response of MIP, NIP and sol-gel electrode was evaluated by DPV. In the case of 4-EP, the calibration curve was measured in a concentration range between 5 and 35 $\mu g\,mL^{-1}$ (See Figure SP3 (left)) and the slope values were $2.19 \pm 0.04\,\mu A\,\mu g^{-1}\,mL^{-1}$ for the 4-EP MIP electrode, $1.06 \pm 0.02\,\mu A\,\mu g^{-1}\,mL^{-1}$ for the NIP and $1.38 \pm 0.03\,\mu A\,\mu g^{-1}\,mL^{-1}$ for the sol-gel; the corresponding LODs were 1.33, 1.28 and 1.52 $\mu g\,mL^{-1}$ of 4-EP, respectively. The slope value of the MIP was double than the NIP and the sol-gel, indicating that the affinity for the analyte is better than in the rest of the cases due to the presence of the tailored-made cavities. The same experiment was carried out for the 4-EG MIP electrode (Figure SP3 (right)) with a concentration range of 3–21 $\mu g\,mL^{-1}$. In this case the slope values were 0.401 ± 0.014, 0.069 ± 0.002 and $0.299 \pm 0.015\,\mu A\,\mu g^{-1}\,mL^{-1}$ for 4-EG MIP, NIP and sol-gel electrodes, respectively and the LODs were 1.55, 1.22 and 1.51 $\mu g\,mL^{-1}$ of 4-EG, respectively [31].

In order to evaluate the day-to day reproducibility of the sensors, two different calibration using 4-EP MIP electrode towards 4-EP were carried out using the same electrodes in two different days. Moreover, in the second curve, the standards were introduced at random. Slope values achieved were 0.797 ± 0.043 and $0.703 \pm 0.021\,\mu A\,\mu g^{-1}\,mL^{-1}$ for the first and the second day respectively, with correlation values of 0.979 and 0.993, respectively [31]. Comparing both results, a negligible reduction in the slope value and a minimal increase in the regression coefficient was observed, indicating that the electrodes can be used at least for 20 measurements with good reproducibility; furthermore, it demonstrates the electrodes are suited to be used in a BioET.

Table 1
Cross-calibration slope ($\mu A/\mu g\,mL^{-1}$) and correlation value for MIP, NIP and sol-gel in the presence of 4-EP and 4-EG.

	Modification			
	4-EP MIP	4-EG MIP	NIP	Sol-gel
Sensitivity ($\mu A/mg\,mL^{-1}$) towards 4-EP	0.270	0.245	0.094	0.231
Correlation value 4-EP	0.976	0.970	0.961	0.989
Sensitivity ($\mu A/mg\,mL^{-1}$) towards 4-EG	0.217	0.401	0.069	0.299
Correlation value 4-EG	0.981	0.989	0.994	0.990

3.2.3. Cross-selectivity

As it is well known, the cross-selectivity towards all components in the sample is a mandatory feature which have to be present in the BioET electrode array, condition that was expected in this study due to the similarity in the chemical structure of both targets. For this reason, the response of each MIP-electrode was evaluated towards 4-EP and 4-EG. To corroborate this behaviour, 4 calibration curves were carried out, which linear fitting parameters are shown in Table 1. As it was expected, the response of the 4-EP MIP electrode towards the 4-EP was significantly higher than the response for 4-EG, giving slope values of 0.270 ± 0.015 and $0.217 \pm 0.011\,\mu A\,\mu g^{-1}\,mL^{-1}$, respectively. Equivalent behaviour was found when the 4-EG MIP response was evaluated, obtaining values of 0.245 ± 0.015 and $0.401 \pm 0.014\,\mu A\,\mu g^{-1}\,mL^{-1}$ for 4-EP and 4-EG, respectively. In addition, the correlation parameters were closer to 1 when each analyte was measured using their corresponding MIP electrode.

Furthermore, the response of the NIP and sol-gel electrodes was also evaluated. Although for the NIP electrode the obtained slope values were negligible comparing with the MIP electrodes, in the case of the sol-gel the slope values were comparable to the MIP electrode response. However, the advantage in the use of MIPs is the improvement in the selectivity instead of the sensitivity. As can be seen below (Fig. 3), when MIPs are used, the interferents cannot reach the electrode surface increasing the selectivity of the system.

3.3. Classification studies

In the qualitative approach, the following pure compounds were evaluated: gallic acid, quercitine, 4-ethylphenol and 4-ethylguaiacol. The first two as typical phenolic compounds present in wine, the other two as volatile phenols responsible of the Brett

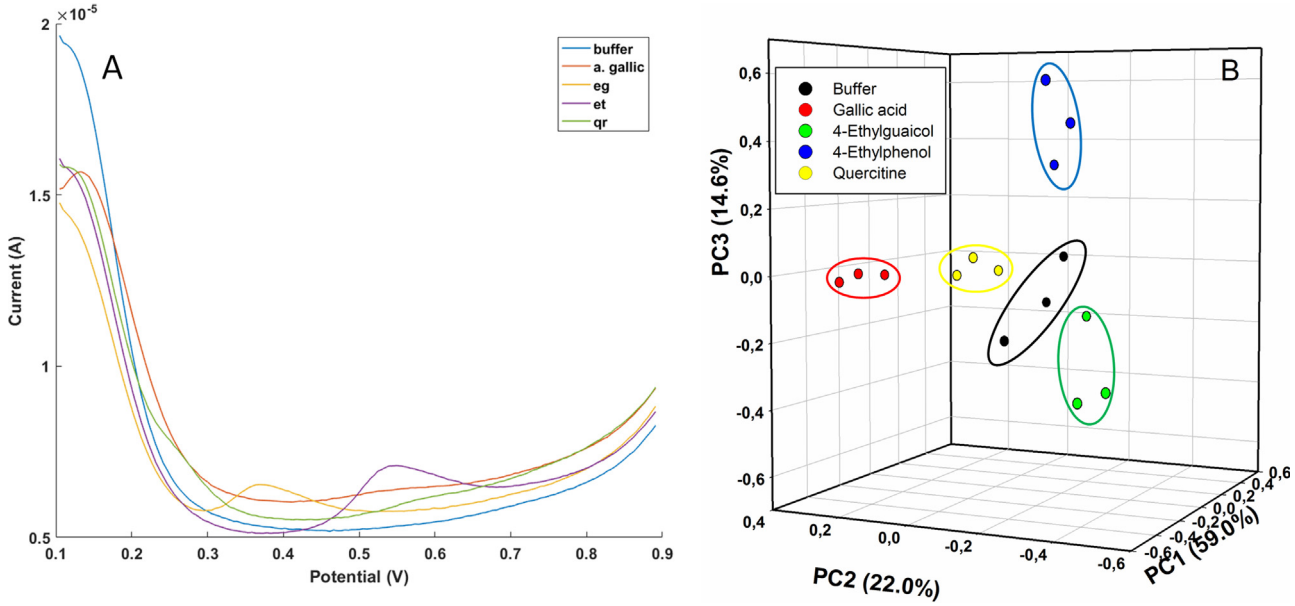

Fig. 3. (**A**) Differential pulse voltammetry signals obtained for the considered compounds with the MIP (solid line) and GEC (dashed line) sensor and (**B**) Scores plot for the three first principal components for the analytes 4-EP, 4-EG, and two polyphenols present in wine, Quercitine and Gallic acid.

character. All the samples were prepared in phosphate buffer solution and the polyphenol concentrations were 25 $\mu g\,mL^{-1}$ for gallic acid and quercitine and 3 $\mu g\,mL^{-1}$ for 4-EP and 4-EG. The solutions were prepared and measured by triplicate and the resulting voltammetric responses (See Fig. 3A as example) were processed employing Principal Component Analysis (PCA) for cluster visualization. Data used for the processing, for each sample, included the unfolded DPV voltammograms of the four biosensors forming the array: the 4-EP and 4-EG MIPs, the NIP and the sol-gel.

As can be seen in Fig. 3B, which depicts the scores of the three first principal components and represents the 95.6% of the accumulated explained variance, each cluster corresponds to a specific compound, with a clear separation between them.

3.4. Quantification study

Using the above biosensor array, the quantification model was built based on a full factorial experimental design with 4 levels and 2 factors: a set of 16 samples in the range of 3–20 $\mu g\,mL^{-1}$ were used for training the model and an external set of 9 samples was prepared for validation purpose. The sample concentrations in the test subset were randomly distributed inside the concentration range of the experimental domain.

The voltammetric data obtained with the 6-sensor array for each sample is very rich but unfortunately this richness results in complex highly dimensional data that difficults its processing using ANNs. This data complexity has to be reduced, as it may hinder the model performance and increase the training time exponentially. The reduction of the complexity of the input signal (6 sensors x 164 current values at different potentials) is a necessary step that compresses the highly dimensional data of the original signals while it preserves the relevant information; by applying a compression step the generated model will perform better and will have a better generalization ability [32].

The compression of the voltammetric data was achieved in this case by means of Discrete Wavelet Transform [33]: each voltammogram was compressed using the mother function *Daubechies 3* and a 3rd decomposition level. In this manner, the 986 inputs per sample were reduced down to 144 coefficients [34], achieving a compression ratio of 85.4%.

After the compression step, the architecture of the neural network was systematically evaluated: the final DWT-ANN model had 144 neurons in the input layer (the number of wavelet coefficients obtained in the compression step), 3 neurons and *tansig* transfer function in the hidden layer and 2 neurons and the *purelin* transfer function in the in the output layer (corresponding to the concentrations of 4-EP and 4-EG).

The performance of the obtained DWT-ANN model is shown in Fig. 4. Therefore, it can be seen that the model shows a linear trend for both subsets. Nevertheless, the training subset is showing better results but this fact is expected as it has been used to build the prediction model; the test subset, a totally independent set of samples, is used to evaluate the performance of the obtained model and as it is shown a linear trend is obtained.

The detailed regression parameters are shown in Table 2. A satisfactory linear trend is obtained for both cases considered, as commented previously with better results for the training subsets; with intersections close to 0, slopes and correlations near 1 and a normalized root mean square error (NRMSE) of 0.049 and 0.059 for 4-EP and 4-EG respectively. The model was able to predict the concentration of the binary test samples with a total NRMSE of 0.076.

In order to provide some contrast to the approach, results obtained with the ANN model were compared with a PLS model, one of the most widely employed chemometric methods. The linear fittings and selection of variables are shown in Fig. SP4 and SP5, as it can be seen the ANN model has a slightly better performance with slopes closer to 1.0 and correlation coefficients near 1.0. The train and test NRMSE values for the PLS model are 0.051 and 0.083 respectively, slightly larger than those obtained for the ANN model. This small improvement in the overall predictive capabilities is probably caused by some degree of non-linear response which results in a better ANN model performance.

4. Conclusions

This work presents the combination of MIPs as recognitions elements and chemometrics tools such as ANN in a bio-electronic tongue approach for the very first time. Molecularly imprinted polymers for 4-EP and 4-EG and control polymer were synthesized

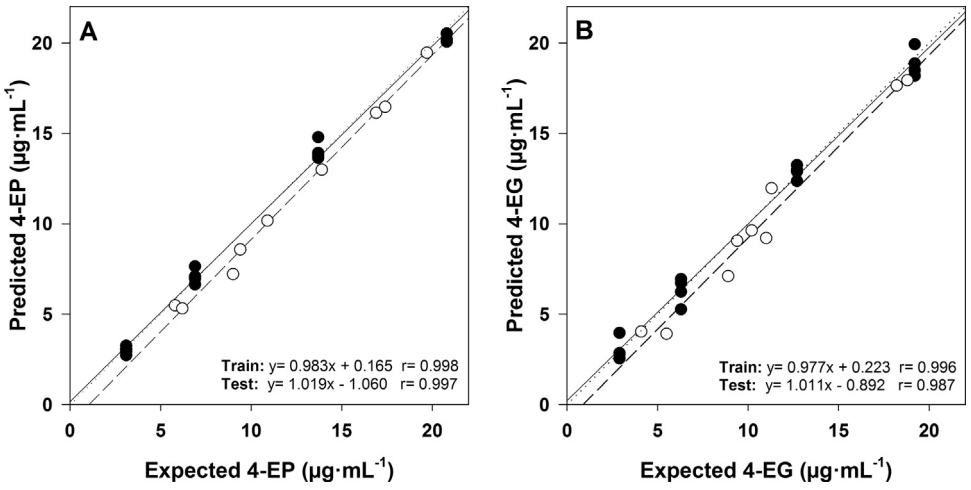

Fig. 4. Fittings of predicted vs. expected concentrations for (A) 4-EP and (B) 4-EG, both for training (●, solid line) and testing subsets (○, dashed line). Dotted line corresponds to ideal behaviour (diagonal line).

Table 2
Results of the fitted regression lines for the comparison between obtained vs. expected values, both for the training and testing sets for the considered species (intervals calculated at 95% confidence level).

	Compound	Correlation	Slope	Intercept ($\mu g\,mL^{-1}$)	RMSE ($\mu g\,mL^{-1}$)	NRMSE	Total RMSE ($\mu g\,mL^{-1}$)	Total NRMSE
Train subset	4-EP	0.998	0.983 ± 0.075	0.162 ± 0.893	0.454	0.023	0.764	0.038
	4-EG	0.996	0.977 ± 0.106	0.223 ± 1.274	0.614	0.031		
Test subset	4-EP	0.997	1.019 ± 0.152	-1.060 ± 1.978	0.980	0.049	1.527	0.076
	4-EG	0.987	1.010 ± 0.299	-0.892 ± 3.537	1.171	0.059		

RMSE: root mean square error; NRMSE: normalized root mean square error.

and characterized successfully with similar morphologies. The synthesized polymers were successfully integrated onto the sensor surface, as a recognition element, via sol-gel immobilization.

The resulting MIP-functionalized electrodes were employed to arrange an array of electrodes able to identify 4-EP and 4-EG from some of the different polyphenolic compounds present in wine, such as gallic acid or quercitine, even though their analogue chemical structure.

The ANN model built has demonstrated a good performance for the quantification of the binary mixtures of 4EP and 4EP with a correlation coefficient >0.98 and a NRMSE <0.076.

4-EP and 4-EG can be discriminated with an estimated detection limit of 1.3 $\mu g\,mL^{-1}$ for 4-EP and 2.4 $\mu g\,mL^{-1}$ for 4-EG, a slightly worse value for the latter, originated in the fact that calibrations here are with the two compounds simultaneously present.

Reported principles is of generic use, utilizable for a wide variety of examples where the conditions is that differentiated MIPs can be synthetized and template compounds are electroactive, a necessary condition to obtain the voltammetric transduction.

Obviously this opens up an immense scope of possibilities where advantages of one technology fits the other: the lack of selectivity of MIPs is solved by ET principles and the lack of sensors for a certain application is provided by molecular imprinting.

Acknowledgments

Financial support for this work was provided by the Spanish Ministry of Economy and Innovation, MINECO (Madrid) through projects CTQ2013-41577-P and CTQ2016-80170-P. Anna Herrera-Chacon and Andreu González-Calabuig thank Universtitat Autònoma de Barcelona (UAB) for the PIF fellowship. Inmaculada Campos thanks the Spanish Ministry of Science for the Juan de la Cierva fellowship. Manel del Valle thanks the support from program ICREA Academia.

Appendix A. Supplementary data

Supplementary data associated with this article can be found, in the online version, at https://doi.org/10.1016/j.snb.2017.11.136.

References

[1] Y. Vlasov, A. Legin, A. Rudnitskaya, C. Di Natale, A. D'Amico, Nonspecific sensor arrays (electronic tongue) for chemical analysis of liquids (IUPAC Technical Report), Pure Appl. Chem. 77 (2005) 1965–1983.
[2] A. Gutés, F. Céspedes, S. Alegret, M. del Valle, Determination of phenolic compounds by a polyphenol oxidase amperometric biosensor and artificial neural network analysis, Biosens. Bioelectron. 20 (2005) 1668–1673.
[3] X. Cetó, N.H. Voelcker, B. Prieto-Simón, Bioelectronic tongues: new trends and applications in water and food analysis, Biosens. Bioelectron. 79 (2016) 608–626.
[4] M. del Valle, Bioelectronic tongues employing electrochemical biosensors, Bioanal. Rev. 6 (2017) 143–202.
[5] X. Cetó, F. Céspedes, M.I. Pividori, J.M. Gutiérrez, M. del Valle, Resolution of phenolic antioxidant mixtures employing a voltammetric bio-electronic tongue, Analyst 137 (2012) 349–356.
[6] G. Valdés-Ramírez, M. Gutiérrez, M. del Valle, M.T. Ramírez-Silva, D. Fournier, J.L. Marty, Automated resolution of dichlorvos and methylparaoxon pesticide mixtures employing a Flow Injection system with an inhibition electronic tongue, Biosens. Bioelectron. 24 (2009) 1103–1108.
[7] L. Ye, K. Haupt, Molecularly imprinted polymers as antibody and receptor mimics for assays, sensors and drug discovery, Anal. Bioanal. Chem. 378 (2004) 1887–1897.
[8] G. Wulff, Enzyme-like catalysis by molecularly imprinted polymers, Chem. Rev. 102 (2002) 1–27.
[9] R.H. Schmidt, A.-S. Belmont, K. Haupt, Porogen formulations for obtaining molecularly imprinted polymers with optimized binding properties, Anal. Chim. Acta. 542 (2005) 118–124.
[10] F. Bates, M. del Valle, Voltammetric sensor for theophylline using sol-gel immobilized molecularly imprinted polymer particles, Microchim. Acta 182 (2015) 933–942.
[11] C.A. Barrios, C. Zhenhe, F. Navarro-Villoslada, D. López-Romero, M.C. Moreno-Bondi, Molecularly imprinted polymer diffraction grating as label-free optical bio (mimetic) sensor, Biosens. Bioelectron. 26 (2011) 2801–2804.
[12] S.N.N.S. Hashim, L.J. Schwarz, R.I. Boysen, Y. Yang, B. Danylec, M.T.W. Hearn, Rapid solid-phase extraction and analysis of resveratrol and other polyphenols in red wine, J. Chromatogr. A 1313 (2013) 284–290.

[13] C. Giovannoli, C. Passini, F. Di Nardo, L. Anfossi, C. Baggiani, Determination of ochratoxin a in italian red wines by molecularly imprinted solid phase extraction and HPLC analysis, J. Agric. Food Chem. 62 (2014) 5220–5225.
[14] C. Alvarez-Lorenzo, A. Concheiro, Molecularly imprinted polymers for drug delivery, J. Chromatogr. B 804 (2004) 231–245.
[15] S. Rodriguez-Mozaz, M.J.L. de Alda, M.-P. Marco, D. Barceló, Biosensors for environmental monitoring: a global perspective, Talanta 65 (2005) 291–297.
[16] A. Merkoçi, S. Alegret, New materials for electrochemical sensing IV. Molecular imprinted polymers, TrAC Trends Anal. Chem. 21 (2002) 717–725.
[17] A. Ben Aissa, A. Herrera-Chacon, R.R. Pupin, M. Sotomayor, M.I. Pividori, Magnetic molecularly imprinted polymer for the isolation and detection of biotin and biotinylated biomolecules, Biosens. Bioelectron. 88 (2017) 101–108.
[18] M.C. Blanco-López, M.J. Lobo-Castañón, A.J. Miranda-Ordieres, P. Tuñón-Blanco, Electrochemical sensors based on molecularly imprinted polymers, TrAC Trends Anal. Chem. 23 (2004) 36–48.
[19] T. Hirsch, H. Kettenberger, O.S. Wolfbeis, V.M. Mirsky, A simple strategy for preparation of sensor arrays: molecularly structured monolayers as recognition elements, Chem. Commun. 43 (2003) 432–433.
[20] N.T. Greene, S.L. Morgan, K.D. Shimizu, Molecularly imprinted polymer sensor arrays, Chem. Commun. 117 (2004) 1172–1173.
[21] D. Xu, W. Zhu, C. Wang, T. Tian, J. Cui, J. Li, H. Wang, G. Li, Molecularly imprinted photonic polymers as sensing elements for the creation of cross-reactive sensor arrays, Chem. –A Eur. J. 20 (2014) 16620–16625.
[22] T.P. Huynh, W. Kutner, Molecularly imprinted polymers as recognition materials for electronic tongues, Biosens. Bioelectron. 74 (2015) 856–864.
[23] C. Malitesta, E. Mazzotta, R.A. Picca, A. Poma, I. Chianella, S.A. Piletsky, MIP sensors–the electrochemical approach, Anal. Bioanal. Chem. 402 (2012) 1827–1846.
[24] E. Mazzotta, R.A. Picca, C. Malitesta, S.A. Piletsky, E.V. Piletska, Development of a sensor prepared by entrapment of MIP particles in electrosynthesised polymer films for electrochemical detection of ephedrine, Biosens. Bioelectron. 23 (2008) 1152–1156.
[25] E. Mazzotta, R.A. Picca, C. Malitesta, S.A. Piletsky, E.V. Piletska, Development of a sensor prepared by entrapment of MIP particles in electrosynthesised polymer films for electrochemical detection of ephedrine, Biosens. Bioelectron. 23 (2008) 1152–1156.
[26] P. Chatonnet, D. Dubourdie, J. Boidron, M. Pons, The origin of ethylphenols in wines, J. Sci. Food Agric. 60 (1992) 165–178.
[27] H. Maarse, Volatile Compounds in Foods and Beverages, CRC press, 1991.
[28] J. Licker, T. Henick-Kling, T. Acree, Impact of brettanomyces yeast on wine flavor: sensory description of wines with different 'Brett' aroma character, in: E. Lemperle (Ed.), Proceedings of the 12th International Enology Symposium, New York Wine Industry Workshop Proceedings (2000) 218–240.
[29] R. Larcher, G. Nicolini, C. Puecher, D. Bertoldi, S. Moser, G. Favaro, Determination of volatile phenols in wine using high-performance liquid chromatography with a coulometric array detector, Anal. Chim. Acta 582 (2007) 55–60.
[30] S. Alegret, J. Alonso, J. Bartrolí, F. Céspedes, E. Martinez-Fabregas, M. del Valle, Amperometric biosensors based on bulk modified epoxy graphite biocomposites, Sensors Mater. 8 (1996) 147–153.
[31] J.N. Miller, J.C. Miller, Statistics and Chemometrics for Analytical Chemistry, 6th ed., Pearson Harlow, 2010 (Chapter 5).
[32] J.M. Gutierrez, L. Moreno-Baron, M.I. Pividori, S. Alegret, M. del Valle, A voltammetric electronic tongue made of modified epoxy-graphite electrodes for the qualitative analysis of wine, Microchim. Acta 169 (2010) 261–268.
[33] L. Moreno-Barón, R. Cartas, A. Merkoçi, S. Alegret, J.M. Gutiérrez, L. Leija, P.R. Hernandez, R. Munoz, M. del Valle, Data compression for a voltammetric electronic tongue modelled with artificial neural networks, Anal. Lett. 38 (2005) 2189–2206.
[34] X. Cetó, F. Céspedes, M. del Valle, Comparison of methods for the processing of voltammetric electronic tongues data, Microchim. Acta 180 (2013) 319–330.

Biographies

Anna Herrera-Chacon completed her M.Sc. degree in Chemistry in 2015 at the Universitat Autònoma de Barcelona, where she is enrolled in the PhD program since 2016 in its Analytical Chemistry laboratories. Her main research topic is the development of molecularly imprinted polymers and its applicability in the development of electrochemical sensors and bioelectronics tongues.

Andreu González-Calabuig received his M.Sc. degree in Chemistry in 2013 from the Universitat Autònoma de Barcelona, where he is presently completing his Ph.D. in Analytical Chemistry. His main research topics deal with the development and application of Electronic Tongues as a tool for security and food safety analysis

Inmaculada Campos completed her M.Sc. degree in chemistry in 2007 at University of Valencia and received her PhD in chemistry in 2013 at Polytechnic University of Valencia. At present, she is a postdoctoral researcher at Sensor and Biosensor Group at Universitat Autònoma de Barcelona. Her main research topics deal with the development of new voltammetric (bio)sensors and the application of electronic tongues and chemometric tools for data analysis.

Manel del Valle received his Ph.D. in Chemistry in 1992 from the Universitat Autònoma de Barcelona, where he got a position of associate professor in Analytical Chemistry. He is a member of the Sensors & Biosensors Group where he is a specialist for instrumentation and electrochemical (bio)sensors. He has initiated there the research lines of sensor arrays and electronic tongues. Other interests of his work are the use of impedance measurements for sensor development, biosensors and the design of automated flow systems.

Bioelectronic tongue using MIP sensors for the determination of volatile phenolic compounds

Anna Herrera-Chacon, Andreu Gonzalez-Calabuig, Inmaculada Campos and Manel del Valle[1*]

Sensors and Biosensors Group, Department of Chemistry, Universitat Autònoma de Barcelona, Edifici Cn, 08193 Bellaterra, Barcelona, Spain

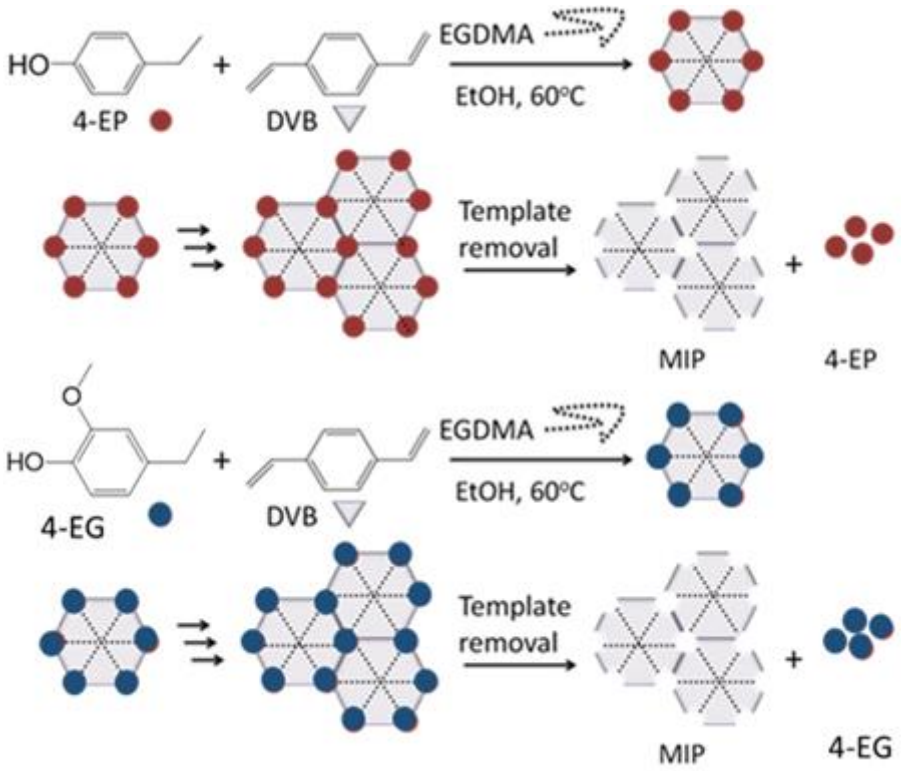

Figure SP1. Schematic representation of MIP synthesis towards both 4-EP and 4-EG.

* E-mail: manel.delvalle@uab.cat; tel: +34 93 5813235; fax: +34 93 5812379

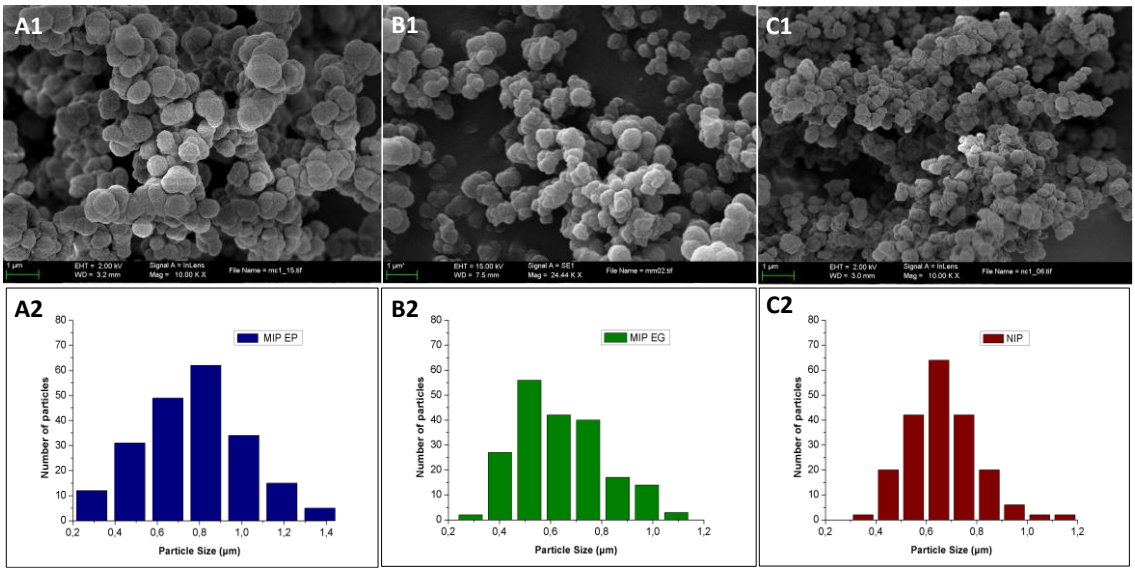

Figure SP2.(A1/B1/C1) Scanning electron microscopy of the obtained 4-EP MIP (left), 4-EG MIP (midle) and NIP (right). (A2/B2/C3) Histograms of the 4-EP MIP (letf), 4-EG MIP (center) and NIP (right).

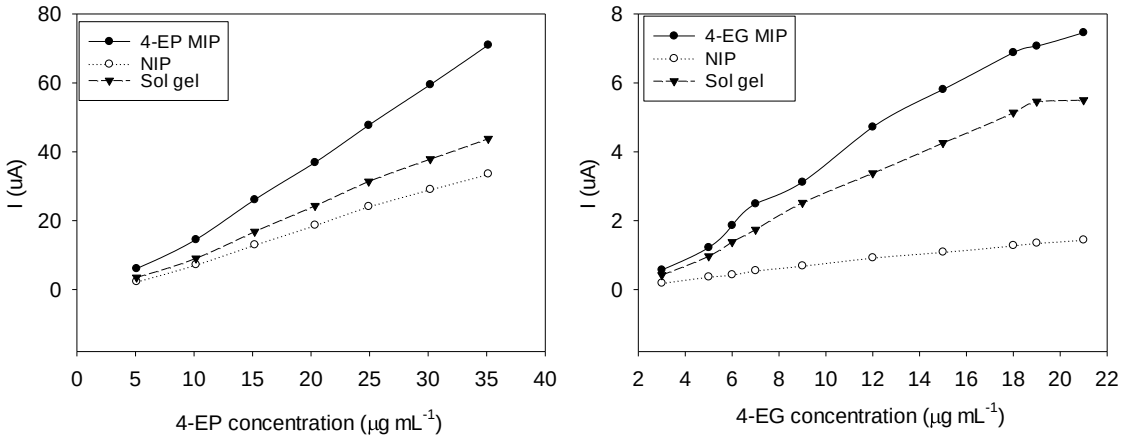

Figure SP3. Calibration curves of 4-EP MIP, NIP and sol-gel for 4-EP (left) and 4-EG MIP, NIP and sol-gel for 4-EG (right).

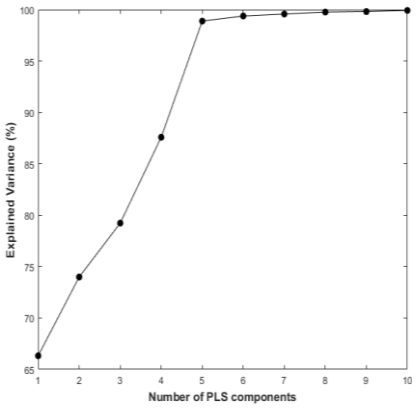

Figure SP4. Plot of the explained variance vs. number of PLS components.

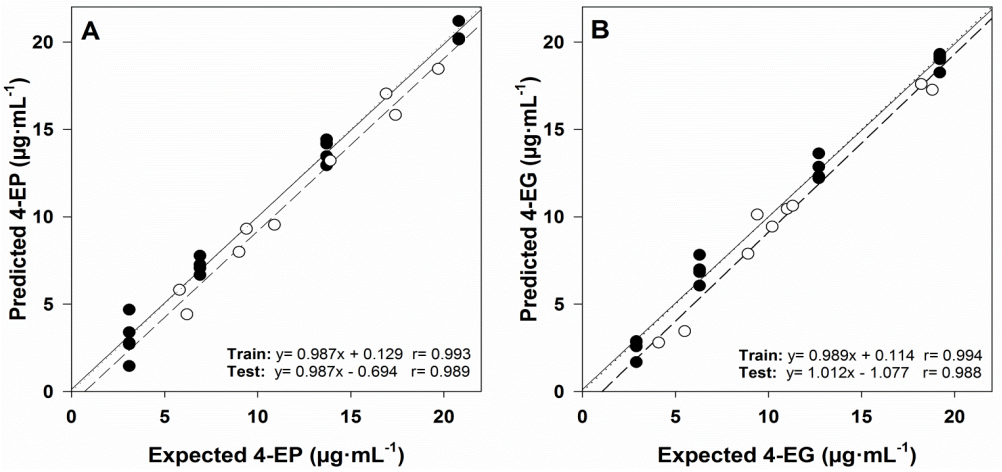

Figure SP5. PLS-2 fittings of predicted vs. expected concentrations for (A) 4-EP and (B) 4-EG, both for training (●, solid line) and testing subsets (○, dashed line). Dotted line corresponds to theoretical diagonal line.

Article 2

Integrating molecularly imprinted polymer beads in graphite-epoxy electrodes for the voltammetric biosensing of histamine in wines

Herrera-Chacón, A., Dinç-Zor, Ş., & del Valle, M.

Talanta, 2020, 208, 120348

DOI: 10.1016/j.talanta.2019.120348

Talanta 208 (2020) 120348

Contents lists available at ScienceDirect

Talanta

journal homepage: www.elsevier.com/locate/talanta

Integrating molecularly imprinted polymer beads in graphite-epoxy electrodes for the voltammetric biosensing of histamine in wines

Anna Herrera-Chacón[a], Şule Dinç-Zor[b], Manel del Valle[a,*]

[a] Sensors and Biosensors Group, Department of Chemistry, Universitat Autònoma de Barcelona, Edifici Cn, 08193, Bellaterra, Barcelona, Spain
[b] Department of Chemistry, Yildiz Technical University, Istanbul, Turkey

ARTICLE INFO

Keywords:
Molecularly imprinted polymer
Sensors
Biogenic amines
Histamine
Voltammetry

ABSTRACT

This manuscript presents a voltammetric biosensing study with use of molecularly imprinted polymers to detect histamine in wine. Polymer beads were synthesized by standard precipitation polymerization method and implemented on the electrode surface via sol-gel immobilization. Scanning and confocal microscopy examinations permitted characterizing the material. Adsorptive stripping voltammetry in differential mode was the technique chosen for final application, selecting an enrichment time of 5 min. These conditions permitted a limit of detection of 0.19 μg mL^{-1} (1.0 μM), with a linear response range from 0.5 to 6.0 μg mL^{-1} (2.71–32.4 μM). The repeatability of the measurements was 4.6% relative standard deviation (n = 12). Principal component analysis showed the ability of the prepared receptor for discriminating other biogenic amines and potential interfering species. A final application, illustrating the determination of histamine, was completed to show agreement of results between the fluorimetric reference method and the proposed electrochemical approach.

1. Introduction

Biogenic amines (BAs) can be found in different foods and beverages associated to their microbiological degradation; they involve several chemical species such as histamine, tyramine, cadaverine and putrescine, among others. Normally, these compounds originate from the decarboxylation of amino acids. BAs are considered as a hazard from a biological and a chemical point of view as they are indicators of improper or poor food preservation. Therefore, they can be used as control parameter indicating storage, monitoring and hygienic condition of several types of food and beverages. From a physiological point of view, BAs may cause disorders and health problems that can include several clinical profiles related with toxicological issues [1], gastric or/and intestinal problems, or allergic responses [2]; other type of symptomatic effects can be headaches, nausea and asthma [3]. An uncontrolled ingestion of histamine in the stomach, could cause a decrease of pH level due to HCl release, inducing gastric ulceration [4]. Despite of the awareness that BAs may become toxic, it is difficult to establish an individual level of toxicity because of their chemical variety, their presence in different types of food and beverages and the difficulty to associate the symptomatology with their ingestion. Among BAs, histamine is the most common one, with abundant presence in fermentation and degradation processes, especially in fish, meat, egg, cheese, beer or wine; in these, histamine is generated through the decarboxylation of free histidine by histidine decarboxylase enzyme [5]. It is reported that *Leuconostoc mesenteroides* bacteria have a high potential to produce histamine and tyramine in wine [6]. In the beverage field, it can be considered that the latter can be present at concentration levels of 5–50 mg dm^{-3} [7]. Despite individual BAs have been analyzed with help of separation methods such as HPLC [8] and GC [9], nowadays they are also determined by immunoassay [10], sensors [11] and biosensors [12]. Recent criticisms to chromatographic methods are that they are expensive, time consuming, of low efficiency and with requirements of qualified personnel to perform sample pre-treatment, analysis and determination. For these reasons, (bio)sensors can be a good option to minimize cost and optimize the determination of BAs [13].

Molecularly imprinted polymers (MIPs) are artificial receptors based on host-guest principles with the aim of creating cavities in a polymeric matrix which are specific for a molecule or molecule moiety [14]. Moreover, they are highly crosslinked and contain recognition sites mimicking antibody function [15,16]. The synthetic nature of MIPs provides this material with interesting properties such as versatility, robustness, cost effectiveness and the possibility to work out of physiological conditions in terms of pH, temperature and ionic strength among others [17]. Specially, performance of these new materials is to be emphasized because of their non-denaturing and reusable features. Notwithstanding these noticeable benefits, there are important

* Corresponding author.
E-mail address: manel.delvalle@uab.cat (M. del Valle).

https://doi.org/10.1016/j.talanta.2019.120348
Received 15 April 2019; Received in revised form 9 September 2019; Accepted 11 September 2019
Available online 12 September 2019
0039-9140/

difficulties in integrating this material on sensors and biosensors, a challenging field that attracts the interest of the scientific community worldwide [18,19].

Synthesis of MIPs needs a monomer capable of interacting through labile bonds with the analyte template. With this idea in mind, methacrylic acid (MAA) imprinted polymers are widely used to maximise the interaction with amino and carboxylic groups, present in the template and the monomer, respectively [20]. Recent literature contains specific studies using MAA based-MIP selective histamine and its analogues, as first scheme capable to detect and quantify this BA [21,22]. In an approach to devise MIPs with improved performance, computational methods can be employed as tools to predict the better affinity among functional monomer, crosslinker and template. This type of calculations can be of great interest to avoid useless synthesis and to maximise experimental efforts [23–25].

Several alternatives have been described employing biosensors using MIPs for BAs detection, e.g. the use of a quartz crystal microbalance [26], the use of a colorimetric sensor array [10], fluorescence detection using graphene and quantum dots [27], electrochemical MIP beads integrated in a carbon paste electrode [28], solid-phase imprinted nanoparticles as recognition elements in polymeric matrix ion selective electrodes [29] or sol-gel SiO_2 layer presenting absorbance transduction for BAs [30].

Concerning MIPs and histamine, it is convenient to highlight two interesting works that appeared in the recent literature. The first reports a magnetic-bead functionalized with MIPs employed for preconcentration of the samples, improving the yield in the washing steps and minimizing the matrix effect [31]; the other one features an assay equivalent to an immunoassay with specific MIP and fluorescence detection in a fish matrix [32]. Specific MIPs for BAs have been also employed to perform solid phase extraction from wine matrix [33].

The main objective of this report is to develop an electrochemical sensor based on the use of MIPs as recognition elements for histamine detection, with use of the differential pulse voltammetry technique and with application to wine analysis. In the present trend of increasing selectivity and sensitivity of analytical procedures, molecular imprinting technique is one of the most effective, cheap and simple methods used in molecular recognition. In this context, MIP bead particles were synthesized and integrated onto graphite epoxy composite (GEC) electrodes using a sol-gel immobilization matrix. Then, their responses towards histamine were investigated and compared to those of non-imprinted polymer and bare GEC electrodes. This characterization is completed with a study of the specificity of this MIP sensor with another BAs and analogue compounds that also can be found in the wine. Final determination in wine matrix and comparison against the reference method concluded the study. The developed protocol is generalizable to any target molecule, with the only condition that the latter must possess electroactive behaviour and must have potential imprinting capabilities; the procedure is also versatile as can be used with beads of different MIP types.

2. Materials and methods

2.1. Chemicals and reagents

Reagents used were of analytical reagent grade and all solutions were made up using MilliQ water from MilliQ System (Millipore, Billerica, MA, USA). Tetramethyl orthosilicate (TEOS), hydrochloric acid, sodium hydroxide, gallic acid, *p*-coumaric acid, and *o*-phthaldialdehyde (OPA) were purchased from Sigma-Aldrich (Madrid, Spain). Ethylene dimethacrylate (EGDMA) was purchased from Fisher Scientific (Madrid, Spain). Methacrylic acid (MAA), phosphoric acid, histamine dihydrochloride and tyramine hydrochloride were purchased from Acros Organics (Geel, Belgium). Methanol (MeOH), Ethanol (EtOH) and Acetic acid (HAc) were purchased from Scharlab (Barcelona, Spain) and 2,2′-azobis(2,4-dimethylvaleronitrile) (AIVN) was purchased from Wako Chemicals GmbH (Neuss, Germany). Graphite powder (particle size $< 50\,\mu m$) was received from BDH (BDH Laboratory Supplies, Poole, UK) and Resineco Epoxy Kit resin was supplied from Resineco green composites (Barcelona, Spain). Measured samples were prepared in phosphate buffer (100 mM KCl, 42 mM $K_2HPO_4{\cdot}2H_2O$, 8 mM KH_2PO_4, pH 7.0).

2.2. Instrumentation

All polymerizations were done in a water bath controlled with a Huber CC1 thermoregulating pump (Huber GmbH, Offenburg, Germany). The electrochemical measurements were performed with a PalmSensTM four-channel multipotentiostat (Palm Instruments BV, Houten, The Netherlands), and using a commercial 52–61 combination electrode Ag/AgCl reference and platinum counter electrode (Crison Instruments, Barcelona, Spain).

Fluorimetric measurements were recorded on a Fluorolog 1 Modular spectrofluoriometer (Horiba Jobin Yvon, Longjumeau, France).

All the synthesized polymers were characterized by scanning electron microscopy (SEM) by using a scanning electron microscope EVO®MA10 operated at 30 kV. The sensors were examined with MERLIN-FE-SEM microscopy operated at 15 kV. Confocal Microscopy inspections were performed with a TCP- SP5 Leica microscope.

2.3. Software and data processing

The electrochemical measurements were done employing the Multitrace 4.2. software (Palm Instruments BV, Houten, The Netherlands). The resulting microscopy images were treated with Fiji package software and Image J software (Zeiss GmbH, Jena, Germany). Principal Component Analysis (PCA) routines were programmed by the authors using MATLAB 2016b (MathWorks, Natick, MA); while the graphical representation and analysis of the results was performed with Sigmaplot (Systat Software, San Jose, CA).

2.4. Polymer synthesis

An amount of 0.5 mmol of histamine dihydrochloride was weighted and transferred to into a 250 mL round bottomed flask and dissolved with 40 mL of ethanol. Subsequently, 2.05 mmol of MAA were added into the flask and the mixture was stirred gently for 15 min. An amount of 10.2 mmol of EGDMA and 0.10 mmol of AIVN were then added and the mixture was purged with a flow of dry nitrogen for 10 min. Polymerization was initiated in a water bath at 60 °C for 17 h with magnetic stirring. After completing the reaction, the obtained polymer beads were dried for an overnight at room temperature; next, they were repeatedly extracted with methanol: acetic acid mixture (9:1 v/v) using a Soxhlet system for 72 h to completely remove the template molecule. Non-imprinted polymers (NIPs) for comparison purpose were synthesized in the same manner described above, but without the addition of the template histamine.

2.5. MIPs integration onto sensor via sol-gel immobilization

Biosensors were prepared by sol-gel immobilization of the polymer beads onto the carbon electrodes; this consists essentially on creating an appropriate conductive gel which incorporates the insulating polymer beads. Once prepared, it can be deposited onto the sensor surface of a graphite epoxy composite (GEC) [34] to obtain the final biosensor. For the sol-gel preparation, 0.5 mL of TEOS, 0.5 mL of EtOH, 0.25 mL of H_2O and 25 µL of HCl 0.1 M were vigorously mixed for 45 min and then rested 35 min in order to achieve the optimal polymerization conditions Then 0.2 mL of the previous solution were mixed with 7 mg of graphite and 40 µL of a 15 mg mL^{-1} MIP polymer suspension in EtOH. In a parallel set up, 40 µL of EtOH were added to obtain a sol-gel modified electrode without beads, which was taken as a control. The mixture was

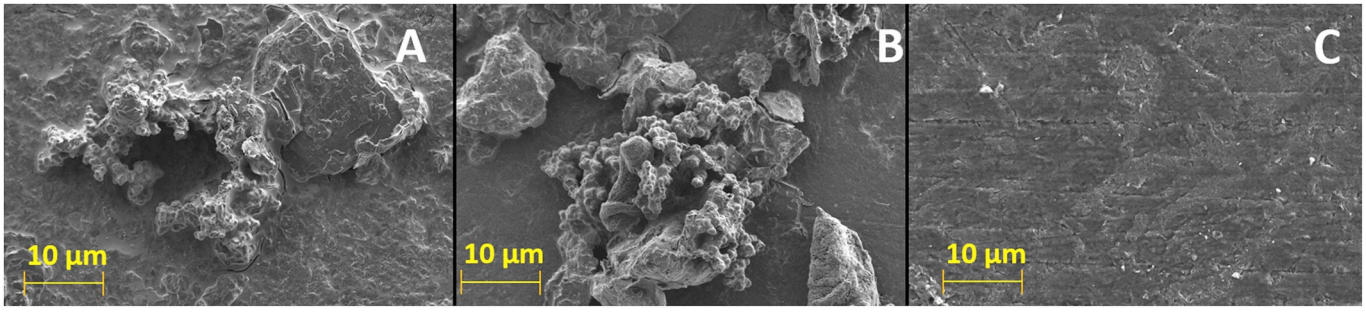

Fig. 1. SEM images of the MIP beads (A) and NIP beads (B) immobilized via sol-gel and bare graphite-epoxy composite (GEC) electrode (C).

stirred for 10 min at 1400 rpm. The membrane was then spin-coated by depositing 10 µL of the solution onto the electrode surface and spun using a home-made spin-coater (1 min at 11 × *g*). An equivalent control sensor was prepared using 40 µL of a 15 mg mL^{-1} NIP beads suspension for comparison purpose. Preparation of the biosensors was finished drying the electrodes overnight at 4 °C [35] (Figure SP1, supplementary material).

2.6. Electrochemical measurements

A first enrichment step was performed without any polarization of the sensor. Next, the stripping was conducted using the differential pulse voltammetric technique. For this purpose, potential was scanned between 0 and 1.5 V at a scan rate of 100 mV/s, with a step potential of 5 mV and a pulse amplitude of 50 mV, without stirring. Different buffer solutions made of acetate (0.1 M CH_3COOH–CH_3COONa, pH 4.5), phosphate (0.05 M KH_2PO_4·K_2HPO_4, pH 6.0–7.0), and tris-hydroxymethyl-aminomethane buffer solution (0.1 M tris-HCl, pH 8.0–9.0) were prepared for pH optimization of the electrochemical measurements. All these solutions incorporated an additional 0.1 M KCl saline background for better electrochemical response. Calibrations were obtained by the addition of aliquots of the histamine standard solutions (1000 µg mL^{-1}) into the measurement cell containing 20.0 mL of the pH 7.0 phosphate buffer solution. All electrodes were regenerated after each measurement by electrochemical cleaning, applying 1.5 V for 45 s in phosphate buffer pH 7.0 (the working solution). The cleaning is a key step to regenerate the polymers capacity of response, avoiding the unspecific interaction responses that may affect their capacity binding.

2.7. Application to wine samples

White wine samples were analysed in parallel with the developed sensor and with the OPA fluorimetric reference method, for comparison purposes. Histamine generates a highly fluorescent complex with *o*-phtaldialdehyde (OPA) that permits its determination at the ng·mL^{-1} level. The complex absorbs at a wavelength of 350 nm and emits at 444 nm. It is important to mention that the reaction is stopped by phosphoric acid after 4 min of placing them in contact, being the complex stable for 2 h; afterwards, it is degraded and the fluorescence decays. To minimize sample matrix effects a previous extraction procedure is done. A wine aliquot of 25 mL was taken and its pH adjusted at pH = 11 using NaOH 1M. Next, this alkaline solution was transferred to an extraction funnel and 10 mL of *n*-butanol were added, shaking for 5 min. The aqueous phase was removed from the funnel and 10 mL of HCl 0.1M were added; the funnel was then vigorously shaken during 5 min. The organic phase was removed and the fluorimetric reaction was produced in the aqueous phase, where the histamine is transferred [36]. A calibration with aqueous standards was performed but without any extraction, in order to calculate the concentration in the wine sample [37].

3. Results and discussions

3.1. Microscopy characterization

Once the MIP and NIP synthesis was completed, the obtained beads particles were inspected using SEM microscopy, before their immobilization onto the sensor surface. Aluminium stubs were used as supports. A conductive carbon-tape or a conductive aluminium-tape was added to the aluminium surface. A small amount of sample of MIPs and NIPs was sprinkled into this. Then the conductive carbon-tapes were metalized by an Au–Pd alloy (80:20) during 4 min adding a 15–20 nm layer on the sample, which permitted to visualize the synthesized polymer beads with a good contrast. The polymer beads showed a non-regular, spherical shape (see Figure SP2, supplementary material). Their average size and standard deviation were 0.61 ± 0.18 µm and 0.74 ± 0.19 µm for MIPs and NIPs, respectively (see Figure SP3, supplementary material). As can be observed there, both types of particles presented a similar size and visual aspect, which made the NIPs suitable to act as control.

On the other hand, Fig. 1 displays SEM images of the biosensors constructed during this study, just after their preparation: MIP-modified, NIP-modified and graphite-epoxy composite (GEC), used as electrode contrast. MIPs and NIPs, immobilized via sol-gel onto the GEC surface resembled in their aspect, while GEC showed a totally different surface. Apparently, there is a clear alteration in the surface roughness after the deposition of sol-gel while there are no clear differences between MIPs and NIPs; any difference of response is to be due by the imprinted sites towards histamine.

Confocal microscopy gave us a unique opportunity to characterize the differences between MIPs and NIPs complexing ability, if the fluorimetric OPA-histamine complex was created in situ. For this purpose, MIP and NIP beads were equilibrated with histamine at the same concentration of 5 µg mL^{-1} (in 0.1M HCl media) and a negative control was also performed without histamine, that is, in absence of the complex. Next the reagent generating the fluorescent complex was added, as the developer of the interaction. As it is shown in Fig. 2, MIPs, NIPs and the control presented different fluorescence caused by the developed OPA-histamine complex. In Fig. 2A MIPs exhibit a much higher intensity than NIPs (Fig. 2B), a proof of the specific capture through the imprinted sites generated. It is interesting to remark that the negative control (Fig. 2C) exhibits some degree of autofluorescence. Direct calculation of obtained confocal data permitted establishing that the MIP beads presented 2.15 times more fluorescence intensity than the NIPs, a value that can be assigned to the imprinting factor.

3.2. Electrochemical measurements

3.2.1. Influence and optimization of pH

Histamine is a strong base with two basic centres of pKa 9.4 for the side chain nitrogen, and of pKa 5.8 for the imidazole nitrogen group. Although the compound contains three nitrogen atoms, it is a di-acidic base because of resonance in the imidazole nucleus. Electroanalytical

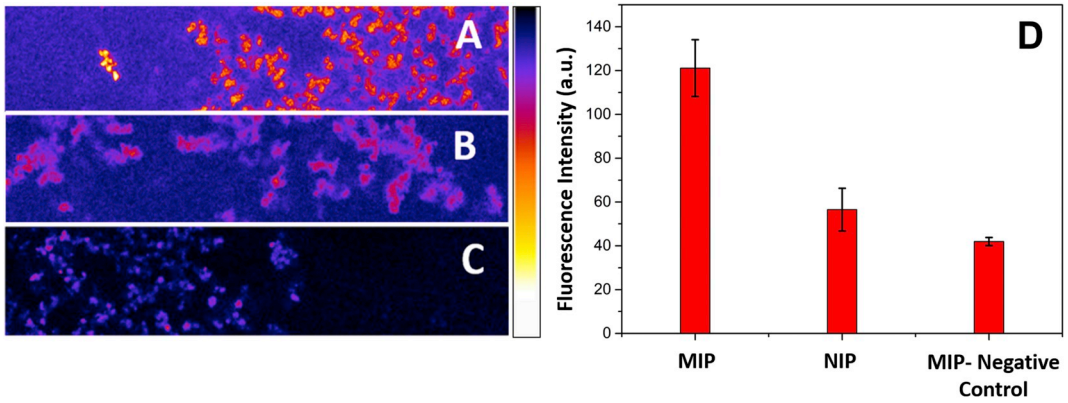

Fig. 2. Confocal microscopy of MIP beads (A) and NIP beads (B) after contact with a 5 μg mL^{-1} histamine-OPA complex. (C) Background fluorescence of MIPs as a negative control. (D) Fluorescence Intensity (a.u.).

performance of the modified electrodes in the oxidation of histamine solution (5 μg mL^{-1}) was investigated in various supporting electrolytes at different pH values by differential pulse voltammetry. The different media 0.1 M acetate buffer at pH 4.5, 0.05 M phosphate buffer at pH 6.0 and 7.0, and 0.1 M Tris-HCl buffer solutions at pH 8.0 and 9.0 were tested for this purpose. The pH of the supporting electrolyte has a significant influence on the electrooxidation of histamine at the modified electrode (see Figure SP4, supplementary material). For example, in acidic media, the NH_2– group of the analyte will protonate to NH_3^+– and consequently the adsorptive mechanisms will change, resulting in a decreasing current for the histamine peaks in acidic solution (pH 4.5). Since the maximum peak current for histamine was recorded at pH 7.0, further experiments were performed at phosphate solution buffered at this pH. Furthermore, while histamine exists as positively charged at pH 7, the MIP microparticles are negatively charged due to the deprotonated MAA (pKa = 6–7) moieties; thus, electrostatic interactions can also occur, providing proper conditions for enrichment in the adsorptive procedure explained next. The final utilizable signal was a single oxidation peak, centred at +1.10, +1.15 V vs. Ag/AgCl.

3.2.2. Contact time optimization

Contact time was another important parameter that was examined and optimized for the adsorptive stripping procedure. For this aim, the prepared electrodes were inserted into 5 μg mL^{-1} histamine solutions for various times, without any explicit polarization, and next, voltammetric determination was performed, observing oxidation of adsorbed analyte (see Figure SP5, supplementary material). According to this figure, increasing contact time leads to a marked increase in the observed peak current of histamine until about 5 min, when a turning point is perceptible. From this experience, an enrichment time of 5 min was chosen for further DPV experiments. The same behaviour was observed when this experiment was repeated at 1 μg mL^{-1} histamine concentration. Therefore, response characteristics can be modulated, if needed, by increasing the enrichment time to attain a lower concentration range (or the contrary for a larger one).

3.2.3. Repeatability and reproducibility

The intra-day repeatability of the peak current magnitude was determined by successive measurements (n = 12) of a 5 μg mL^{-1} histamine standard in phosphate buffer under the optimized experimental conditions. The relative standard deviation (RSD) was calculated as 4.62% (Fig. 3), indicating a good repeatability of the MIP sensor. These satisfactory results confirm a proper choice in running an electrochemical cleaning step between samples, which minimized cross-talk in analysis.

In order to evaluate the day-to-day reproducibility of the imprinted sensor, three different calibration curves were carried out in three different days, as detailed in Table 1. Reproducibility of these

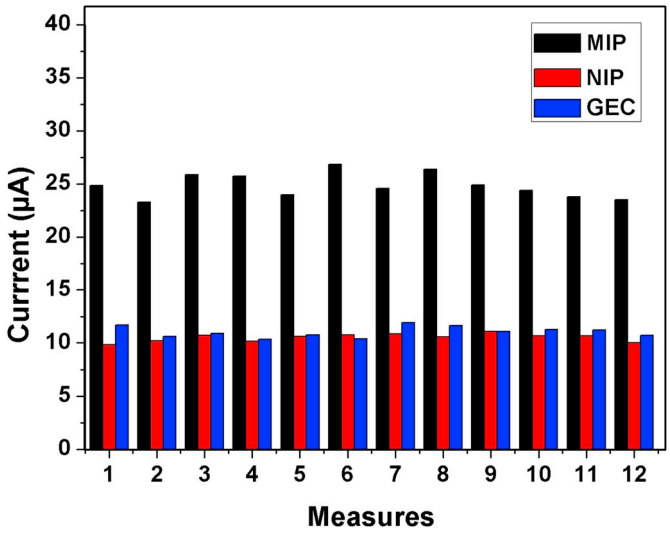

Fig. 3. Repeatability measurements (n = 12) of biosensors prepared from MIP beads, NIP beads and comparison against the bare graphite-epoxy composite (GEC) electrode.

Table 1
Day-to-day reproducibility of calibration of a given histamine MIP biosensor.

	Slope (μA mg^{-1}·L)	Intercept (mg·L^{-1})	Correlation Coefficient
Day 1	4.919	0.065	0.9989
Day 2	4.675	0.184	0.9997
Day 3	4.816	0.166	0.9989

measurements was calculated as 2.61% RSD, extracted from the variation of the slopes. These results showed that the sensor had a remarkable reproducibility, again thanks to the proper definition of the measuring protocol.

3.2.4. Calibration study

The calibration plot was constructed from the DPV response, and is illustrated in Fig. 4; this clearly shows two linear segments, probably caused by the saturation of the amount of available recognition sites in the MIP beads. The MIP sensor presented thus a good linear relationship in the lower range, starting from 0.5 μg mL^{-1} to 6.0 μg mL^{-1} (or 2.7–32.4 μM). The linear regression equation was determined as follows: Y = 4.9416 C – 0.0779 (R^2 = 0.9992). The limit of detection (LOD) and limit of quantification (LOQ) were calculated as 3S/m and 10S/m respectively, where S represents the standard deviation of the regression and m is the sensitivity of the calibration. The LOD and LOQ

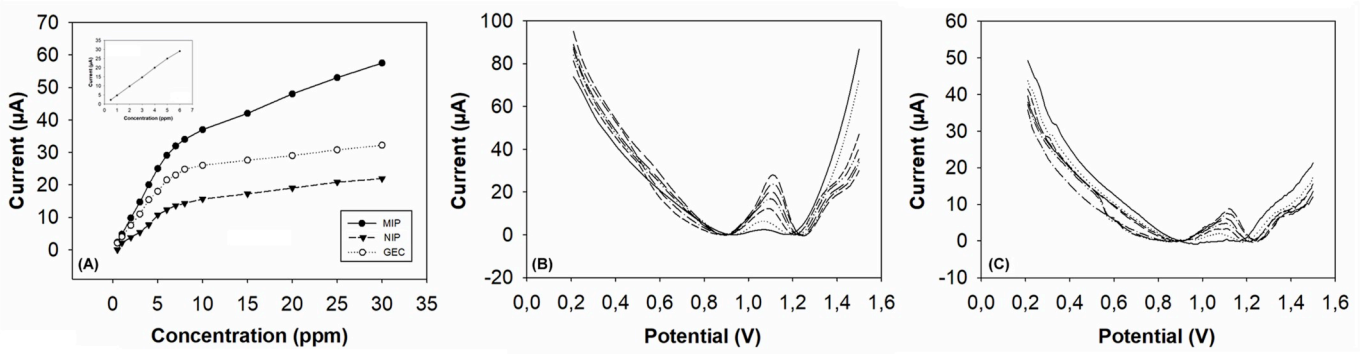

Fig. 4. Adsorptive DPV response of the developed sensors against histamine (phosphate buffer pH = 7.0).(A) Generic calibration range examined with the inset of the low concentration linear range; (B) Obtained voltammograms for the MIP sensors; (C) Obtained voltammograms for the NIP sensors.

values were calculated as 0.19 μg mL^{-1} (1.0 μM) and 0.62 μg mL^{-1} (3.4 μM), respectively. When comparing the slopes obtained for MIP and NIP beads (at the lower concentration range), the ratio of slopes resulted 2.27, a value that again can be considered the imprinting factor, and which is consistent with the previous figure obtained by confocal microscopy (Section 3.1).

3.2.5. Interferents

In order to evaluate the response of the MIP sensor in wine matrix, different potentially interfering compounds were evaluated. In addition to histamine the compounds chosen were tyramine, as a second, related compound, biogenic amine and coumaric acid and gallic acid, as potential polyphenolic interfering species, in the wine matrix.

The tool employed to inspect the different voltammetric responses was principal component analysis (PCA). Calibration curves were performed for tyramine, coumaric acid and gallic acid and its voltammetric responses were processed using PCA. As can be seen in Fig. 5 histamine forms a very distinct cluster indicating a differentiated voltammetric response, and only coumaric acid and tyramine are confounded by the prepared sensor, an insignificant fact, as their detection is not the desired purpose.

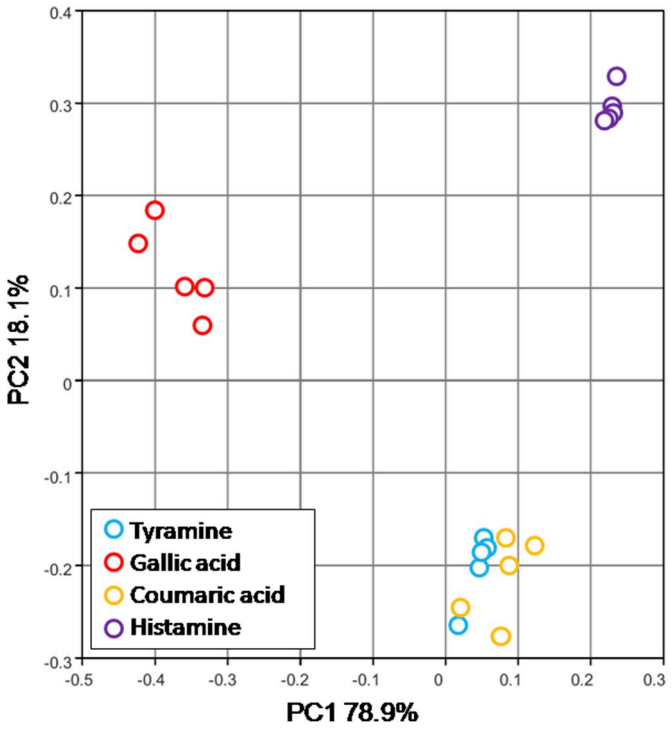

Fig. 5. Multivariate transformation using principal component analysis (PCA) of the voltammetric responses of the selectivity features of the MIP-modified sensors; discrimination of histamine, gallic acid, *p*-coumaric acid and tyramine.

3.3. Application to real sample analysis

In order to evaluate the feasibility of the proposed MIP biosensor, wine samples were analysed by electrochemical method and compared with the fluorimetric reference procedure, in accordance with standard international recommendation [37]. Previously, the histamine peak could not be seen in beer samples at +1.10 V, suggesting an extremely low level which forced us to consider only wines. The electrochemical method was performed with histamine ranging from 2 to 12 μg mL^{-1} in phosphate buffer at pH 7. The comparison results of the two methods are summarised in Table 2. In this, it can be observed that the electrochemical results obtained from wine samples were comparable to the gold standard fluorimetric method. The standard deviation for fluorimetric procedure was slightly better than the electrochemical one, probably due to the matrix effect of the wine samples in the electrochemical method, while the fluorimetric one included its removal. Also, it used one extra replicate, that probably could also improve this feature.

4. Conclusions

This research has provided a biosensor based on molecularly imprinted polymers used as recognition elements for histamine detection and integrated in a voltammetric transducer. MIP and NIP beads were successfully synthesized and presented a similar, high porosity morphology that made them comparable. Confocal microscopy showed an increasing binding capacity for OPA-histamine complex in the MIPs when compared with the control. The integration of the polymers onto GECs surface via sol-gel immobilization provided a homogeneous layer that allowed a satisfactory preconcentration of histamine in wine. The biosensor presented a linear range from 0.5 μg mL^{-1} to 6.0 μg mL^{-1} and a LOD of 0.19 μg mL^{-1} for histamine, values that could be

Table 2
Results obtained for two wine samples using the developed MIP biosensor, in comparison with the reference fluorimetric method.

	FLUORIMETRIC		VOLTAMMETRIC	
	Wine1 (mg·L^{-1})	Wine2 (mg·L^{-1})	Wine1 (mg·L^{-1})	·Wine2 (mg L^{-1})
Replicate 1	0.033	0.273	0.048	0.254
Replicate 2	0.037	0.280	0.036	0.245
Replicate 3	0.039	0.294	0.043	0.223
Replicate 4	0.038	0.299	–	–
Mean (ppm)	0.037	0.287	0.042	0.241
s (ppm)	0.002	0.012	0.006	0.016

diminished if longer enrichment times were used. The study of interferents demonstrated a good capability for histamine discrimination as the voltammetric signals from interfering substances were clearly distinct from the histamine signal. The method disclosed herein is compared with the reference fluorimetric method for histamine detection in white wine samples; the results obtained with the presented electrochemical method show comparable performance with the reference method. The alternative presented, that combines molecular imprinting technology and electrochemical sensing, provides a fast, robust, on-site and cost-effective method that is comparable with the official method. Finally, it has to be remarked the effectiveness and simplicity of the concepts applied in this work, which in addition can represent a generic universal approach that may be custom-adapted to any given analyte with the only condition that it may allow the imprinting. In addition, it does not require any specific polymer chemistry, whereas any MIP attainable in bead form might be integrated in this biosensor.

Acknowledgments

Financial support for this work was provided by Spanish Ministry of Economy and Innovation, MINECO (Madrid) through project CTQ2016-80170-P. M. del Valle thanks the support from program ICREA Academia.

Appendix A. Supplementary data

Supplementary data to this article can be found online at https://doi.org/10.1016/j.talanta.2019.120348.

References

[1] V. Ladero, M. Calles-Enriquez, M. Fernandez, M.A. Alvarez, Toxicological effects of dietary biogenic amines, Curr. Nutr. Food Sci. 6 (2010) 145–156, https://doi.org/10.2174/157340110791233256.
[2] A.R. Shalaby, Significance of biogenic amines to food safety and human health, Food Res. Int. 29 (1996) 675–690, https://doi.org/10.1016/S0963-9969(96)00066-X.
[3] S.L. Taylor, R.R. Eitenmiller, Histamine food poisoning: toxicology and clinical aspects, CRC Crit. Rev. Toxicol. 17 (1986) 91–128, https://doi.org/10.3109/10408448609023767.
[4] H.P. Toroudi, M. Rahgozar, A. Bakhtiarian, B. Djahanguiri, Potassium channel modulators and indomethacin-induced gastric ulceration in rats, Scand. J. Gastroenterol. 34 (1999) 962–966, https://doi.org/10.1080/003655299750025048.
[5] L. Beneduce, A. Romano, V. Capozzi, P. Lucas, L. Barnavon, B. Bach, P. Vuchot, F. Grieco, G. Spano, Biogenic amines in wines, Ann. Microbiol. 60 (2010) 573–578, https://doi.org/10.1007/s13213-010-0094-4.
[6] F. Aflaki, V. Ghoulipour, N. Saemian, M. Salahinejad, A simple method for benzoyl chloride derivatization of biogenic amines for high performance liquid chromatography, Analytical Methods 6 (2014) 1482–1487, https://doi.org/10.1039/c3ay41830h.
[7] M. Papageorgiou, D. Lambropoulou, C. Morrison, E. Kłodzińska, J. Namieśnik, J. Płotka-Wasylka, Literature update of analytical methods for biogenic amines determination in food and beverages, Trac. Trends Anal. Chem. 98 (2018) 128–142, https://doi.org/10.1016/j.trac.2017.11.001.
[8] A.C. Manetta, L. Di Giuseppe, R. Tofalo, M. Martuscelli, M. Schirone, M. Giammarco, G. Suzzi, Evaluation of biogenic amines in wine: determination by an improved HPLC-PDA method, Food Control 62 (2016) 351–356, https://doi.org/10.1016/j.foodcont.2015.11.009.
[9] M. Papageorgiou, D. Lambropoulou, C. Morrison, J. Namieśnik, J. Płotka-Wasylka, Direct solid phase microextraction combined with gas chromatography – mass spectrometry for the determination of biogenic amines in wine, Talanta 183 (2018) 276–282, https://doi.org/10.1016/j.talanta.2018.02.006.
[10] D.M. Linares, B. Del Rio, B. Redruello, V. Ladero, M.C. Martin, M. Fernandez, P. Ruas-Madiedo, M.A. Alvarez, Comparative analysis of the in vitro cytotoxicity of the dietary biogenic amines tyramine and histamine, Food Chem. 197 (2016) 658–663, https://doi.org/10.1016/j.foodchem.2015.11.013.
[11] X. Zhong, D. Huo, H. Fa, X. Luo, Y. Wang, Y. Zhao, C. Hou, Rapid and ultrasensitive detection of biogenic amines with colorimetric sensor array, Sens. Actuators B Chem. 274 (2018) 464–471, https://doi.org/10.1016/j.snb.2018.07.129.
[12] W. Henao-Escobar, L. Del Torno-De Román, O. Domínguez-Renedo, M.A. Alonso-Lomillo, M.J. Arcos-Martínez, Dual enzymatic biosensor for simultaneous amperometric determination of histamine and putrescine, Food Chem. 190 (2016) 818–823, https://doi.org/10.1016/j.foodchem.2015.06.035.
[13] K. Kivirand, T. Rinken, Biosensors for biogenic amines: the present state of art mini-review, Anal. Lett. 44 (2011) 2821–2833, https://doi.org/10.1080/00032719.2011.565445.
[14] G. Wulff, Enzyme-like catalysis by molecularly imprinted polymers, Chem. Rev. 102 (2002) 1–28, https://doi.org/10.1021/cr980039a.
[15] R.H. Schmidt, A.-S. Belmont, K. Haupt, Porogen formulations for obtaining molecularly imprinted polymers with optimized binding properties, Anal. Chim. Acta 542 (2005) 118–124, https://doi.org/10.1016/j.aca.2005.03.064.
[16] L. Ye, K. Haupt, Molecularly imprinted polymers as antibody and receptor mimics for assays, sensors and drug discovery, Anal. Bioanal. Chem. 378 (2004) 1887–1897, https://doi.org/10.1007/s00216-003-2450-8.
[17] A. Merkoçi, S. Alegret, New materials for electrochemical sensing IV . Molecular imprinted polymers, Trac. Trends Anal. Chem. 21 (11) (2002) 717–725, https://doi.org/10.1016/S0165-9936(02)01119-6.
[18] M.C. Blanco-Lopez, M.J. Lobo-Castañon, A.J. Miranda-Ordieres, P. Tuñon-Blanco, Electrochemical sensors based on molecularly imprinted polymers, Trac. Trends Anal. Chem. 23 (2004) 36–48, https://doi.org/10.1016/S0165-9936(04)00102-5.
[19] F. Bates, M. del Valle, Voltammetric sensor for theophylline using sol–gel immobilized molecularly imprinted polymer particles, Microchimica Acta 182 (2015) 933–942, https://doi.org/10.1007/s00604-014-1413-4.
[20] A. Sahebnasagh, G. Karimi, S.A. Mohajeri, Preparation and evaluation of histamine imprinted polymer as a selective sorbent in molecularly imprinted solid-phase extraction coupled with high performance liquid chromatography analysis in canned fish, Food Analytical Methods 7 (2014) 1, https://doi.org/10.1007/s12161-013-9579-7.
[21] F. Horemans, J. Alenus, E. Bongaers, A. Weustenraed, R. Thoelen, J. Duchateau, L. Lutsen, D. Vanderzande, P. Wagner, T.J. Cleij, MIP-based sensor platforms for the detection of histamine in the nano- and micromolar range in aqueous media, Sens. Actuators B Chem. 148 (2010) 392–398, https://doi.org/10.1016/j.snb.2010.05.003.
[22] A. Tong, H. Dong, L. Li, Molecular imprinting-based fluorescent chemosensor for histamine using zinc(II)-protoporphyrin as a functional monomer, Anal. Chim. Acta 466 (2002) 31–37, https://doi.org/10.1016/S0003-2670(02)00471-3.
[23] F. Bates, M. Busato, E. Piletska, M.J. Whitcombe, K. Karim, A. Guerreiro, M. del Valle, A. Giorgetti, S. Piletsky, Computational design of molecularly imprinted polymer for direct detection of melamine in milk, Separ. Sci. Technol. 52 (2017) 1441–1453, https://doi.org/10.1080/01496395.2017.1287197.
[24] F. Ahmadi, H. Rezaei, R. Tahvilian, Computational-aided design of molecularly imprinted polymer for selective extraction of methadone from plasma and saliva and determination by gas chromatography, J. Chromatogr. A 1270 (2012) 9–19, https://doi.org/10.1016/j.chroma.2012.10.038.
[25] F. Ahmadi, E. Yawari, M. Nikbakht, Computational design of an enantioselective molecular imprinted polymer for the solid phase extraction of S-warfarin from plasma, J. Chromatogr. A 1338 (2014) 9–16, https://doi.org/10.1016/j.chroma.2014.02.055.
[26] J. Dai, Y. Zhang, M. Pan, L. Kong, S. Wang, Development and application of quartz crystal microbalance sensor based on novel molecularly imprinted sol-gel polymer for rapid detection of histamine in foods, J. Agric. Food Chem. 62 (2014) 5269–5274, https://doi.org/10.1021/jf501092u.
[27] Q. Wang, D. Zhang, A Novel Fluorescence Sensing Method Based on Quantum Dot-Graphene and a Molecular Imprinting Technique for the Detection of Tyramine in Rice Wine, (2018), https://doi.org/10.1039/c8ay01117f.
[28] M. Akhoundian, A. Rüter, S. Shinde, Ultratrace detection of histamine using a molecularly-imprinted polymer-based voltammetric sensor, Sensors (2017) 17, https://doi.org/10.3390/s17030645.
[29] I. Basozabal, A. Guerreiro, A. Gomez-Caballero, M. Aranzazu Goicolea, R.J. Barrio, Direct potentiometric quantification of histamine using solid-phase imprinted nanoparticles as recognition elements, Biosens. Bioelectron. 58 (2014) 138–144, https://doi.org/10.1016/j.bios.2014.02.054.
[30] P. Nedeljko, M. Turel, A. Lobnik, Hybrid sol-gel based sensor layers for optical determination of biogenic amines, Sens. Actuators B Chem. 246 (2017) 1066–1073, https://doi.org/10.1016/j.snb.2017.02.011.
[31] A.H.A. Hassan, L. Sappia, S.L. Moura, F.H.M. Ali, W.A. Moselhy, M. del, P.T. Sotomayor, M.I. Pividori, Biomimetic magnetic sensor for electrochemical determination of scombrotoxin in fish, Talanta 194 (2019) 997–1004, https://doi.org/10.1016/j.talanta.2018.10.066.
[32] L. Mattsson, J. Xu, C. Preininger, B. Tse Sum Bui, K. Haupt, Competitive fluorescent pseudo-immunoassay exploiting molecularly imprinted polymers for the detection of biogenic amines in fish matrix, Talanta 181 (2018) 190–196, https://doi.org/10.1016/j.talanta.2018.01.010.
[33] I. Basozabal, A. Gomez-Caballero, G. Diaz-Diaz, A. Guerreiro, S. Gilby, M.A. Goicolea, R.J. Barrio, Rational design and chromatographic evaluation of histamine imprinted polymers optimised for solid-phase extraction of wine samples, J. Chromatogr. A 1308 (2013) 45–51, https://doi.org/10.1016/j.chroma.2013.08.002.
[34] S. Alegret, J. Alonso, J. Bartrolí, F. Céspedes, E. Martínez-Fàbregas, M. del Valle, Amperometric biosensors based on bulk-modified epoxy graphite biocomposites, Sens. Mater. 8 (1996) 147–153.
[35] A. Herrera-Chacon, A. González-Calabuig, I. Campos, M. del Valle, Bioelectronic tongue using MIP sensors for the resolution of volatile phenolic compounds, Sens. Actuators B Chem. 258 (2018) 665–671, https://doi.org/10.1016/j.snb.2017.11.136.
[36] S. Gorinstein, M. Zemser, F. Vargas-Albores, J.L. Ochoa, O. Paredes-Lopez, C. Scheler, J. Salnikow, O. Martin-Belloso, S. Trakhtenberg, Proteins and amino acids in beers, their contents and relationships with other analytical data, Food Chem. 67 (1999) 71–78, https://doi.org/10.1016/S0308-8146(99)00071-0.
[37] AOAC Official Method 997.13. Histamine in Seafood < http://www.aoac.org/aoac_prod_imis/AOAC_Docs/OMA/977_13aoacmethod.pdf. > (accessed 21 october 2018).

Integrating Molecularly Imprinted Polymer beads in Graphite-Epoxy electrodes for the voltammetric biosensing of histamine in wines

Anna Herrera-Chacón[a], Sule Dinc Zor[b], Manel del Valle[a,*]

[a] Sensors and Biosensors Group, Department of Chemistry, Universitat Autònoma de Barcelona, Edifici Cn, 08193 Bellaterra, Barcelona, Spain

[b] Department of Chemistry, Yildiz Technical University, Istanbul, Turkey

Supplementary Material

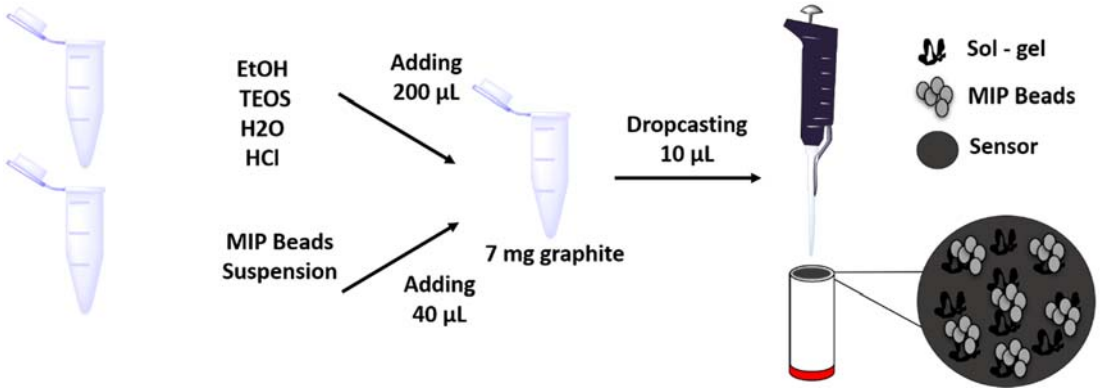

Figure S1. Process followed for the MIP beads integration onto the sensor surface via sol-gel immobilization.

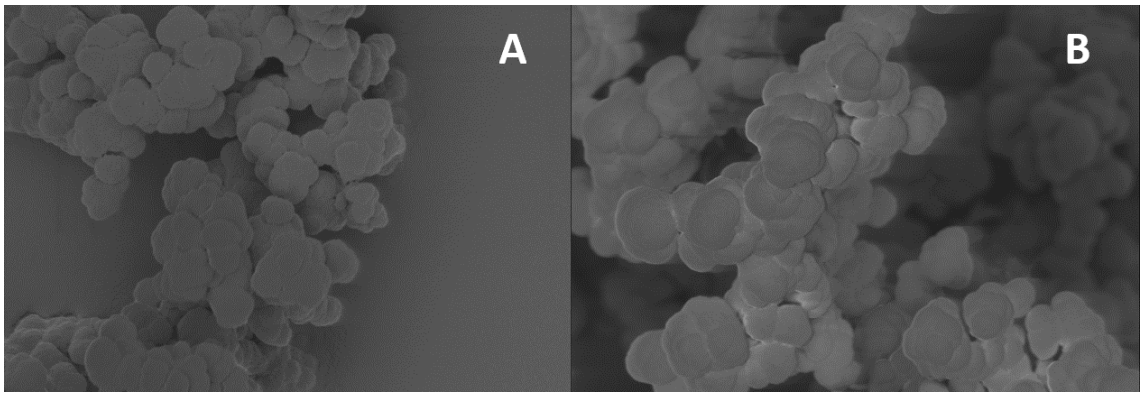

Figure S2. Scanning electron microscopy (SEM) images of (A) histamine imprinted polymer (MIP) beads, and (B) the non-imprinted polymer (NIP) beads.

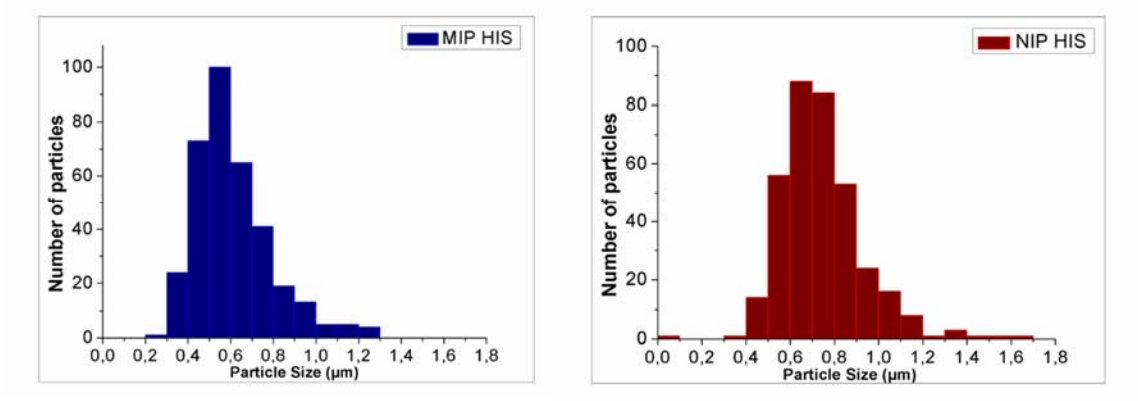

Figure S3. Histograms corresponding to the measured bead size of synthesized MIPs (left) and NIPs (right).

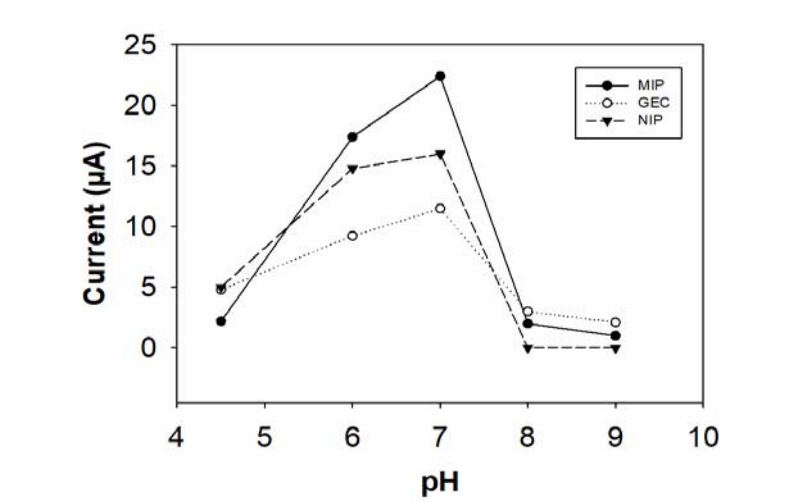

Figure S4. Optimization of the voltammetric response of the developed MIP biosensors according to pH.

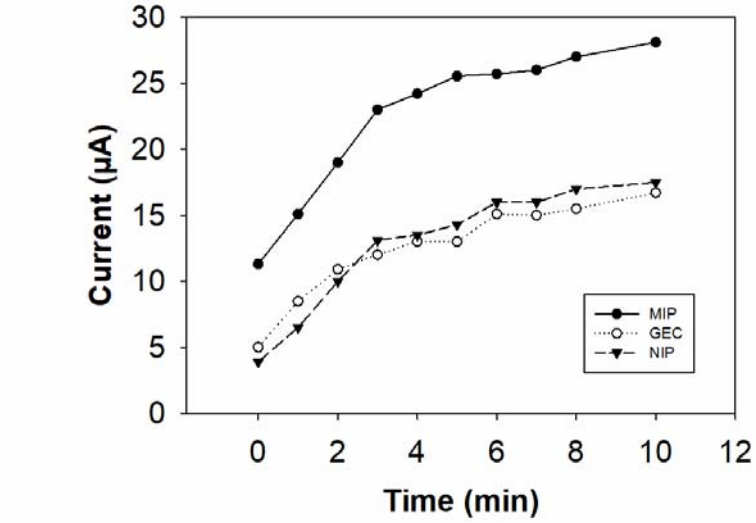

Figure S5. Optimization of the enrichment time previous to the voltammetric determination of histamine using the MIP developed biosensor.

Article 3

Dummy Molecularly Imprinted Polymers Using DNP as a Template Molecule for Explosive Sensing and Nitroaromatic Compound Discrimination

Herrera-Chacon, A., Gonzalez-Calabuig, A., & del Valle, M.

Chemosensors, 2021, 9(9), 255

DOI: 10.3390/chemosensors9090255

chemosensors

MDPI

Article

Dummy Molecularly Imprinted Polymers Using DNP as a Template Molecule for Explosive Sensing and Nitroaromatic Compound Discrimination

Anna Herrera-Chacon, Andreu Gonzalez-Calabuig and Manel del Valle *

Sensors and Biosensors Group, Department of Chemistry, Universitat Autònoma de Barcelona, Edifici Cn, Bellaterra, 08193 Barcelona, Spain; anna.herrera@uab.cat (A.H.-C.); andreugc27@gmail.com (A.G.-C.)
* Correspondence: manel.delvalle@uab.cat

Abstract: This work reports a rapid, simple and low-cost voltammetric sensor based on a dummy molecularly imprinted polymer (MIP) that uses 2,4-dinitrophenol (DNP) as a template for the quantification of 2,4,6-trinitrotoluene (TNT) and DNP, and the identification of related substances. Once the polymer was synthesised by thermal precipitation polymerisation, it was integrated onto a graphite epoxy composite (GEC) electrode via sol–gel immobilisation. Scanning electron microscopy (SEM) was performed in order to characterise the polymer and the sensor surface. Responses towards DNP and TNT were evaluated, displaying a linear response range of 1.5 to 8.0 μmol L^{-1} for DNP and 1.3 to 6.5 μmol L^{-1} for TNT; the estimated limits of detection were 0.59 μmol L^{-1} and 0.29 μmol L^{-1}, for DNP and TNT, respectively. Chemometric tools, in particular principal component analysis (PCA), demonstrated the possibilities of the MIP-modified electrodes in nitroaromatic and potential interfering species discrimination with multiple potential applications in the environmental field.

Keywords: molecularly imprinted polymers; dummy template; voltammetric detection; 2,4,6-trinitrotoluene; nitroaromatic compounds

Citation: Herrera-Chacon, A.; Gonzalez-Calabuig, A.; del Valle, M. Dummy Molecularly Imprinted Polymers Using DNP as a Template Molecule for Explosive Sensing and Nitroaromatic Compound Discrimination. *Chemosensors* **2021**, *9*, 255. https://doi.org/10.3390/chemosensors9090255

Academic Editor: Pi-Guey Su

Received: 4 August 2021
Accepted: 6 September 2021
Published: 8 September 2021

1. Introduction

There is an increasing interest in analytical methods for determining, quantifying and discriminating pollutant compounds in different matrices. Desirably, the analytical response should be fast, portable, reliable, cost-effective, with low-power consumption, easy to manipulate, and able to be used in indoor and outdoor spaces for on-site measurements. The field of sensors and biosensors tackles this challenging demand, improving sensing abilities year by year. A key element in the performance of sensing devices is its recognition capability. Molecularly imprinted polymers (MIPs) can be introduced in biosensing as the necessary recognition element, in this case derived from a synthetic approach. As a result, the sensor field can improve response features in a simple and inexpensive manner by incorporating these new recognition elements, which may constitute an alternative to antibodies, for example.

MIPs acting as artificial receptors have demonstrated their applicability in several fields; among these, we can note the food industry [1,2], environmental monitoring [3,4], clinical diagnosis [5,6] and forensic field [7]. MIPs are perfect candidates to improve the performance of current analytical methods due to their versatility, functionality, and ability to sample pre-concentration [8], separation [9] and/or purification [10]; alternatively, they may be used as a recognition element for the development of different biosensing strategies [11,12] and also in drug delivery [13].

Recently, the use of dummy MIPs has been described, i.e., when MIPs are synthesised towards an analogue molecule of the target analyte, which cannot be used as a template during the synthesis of the polymer. This happens when the analyte is (1) expensive, (2) has a poor solubility or by-products are generated that hinder the imprinting, or (3) is

considered a hazard. For example, the use of dummy MIPs has been reported for detecting fluoroquinolones in fish samples [14], for detecting bisphenol A in river water samples [15], and for providing an alternative to acrylamide removal in foodstuffs [16].

Precisely, the use of dummy MIPs is a choice of interest when aiming for the detection of explosive compounds [17], such as nitroaromatic species [18]. A habitual task in forensic laboratories is to detect or confirm the presence of explosives [19] or explosive residues [20]. There is also a need to quantify explosives at trace level after a detonation [21,22], or in contaminated underground water reservoirs [23].

Nitroaromatic species are excellent candidates for electrochemical sensing due to inherent electroactivity, given their characteristic electron-transfer reduction reactions and their electron-acceptor properties [24,25]. For all the above reasons, their electrochemical sensing ability has become a promising alternative to address the growing security needs of society. Specifically, TNT, a common nitroaromatic explosive, complies with the above-mentioned characteristics, making it a candidate to employ the dummy MIP strategy [26]. The following Table 1 presents a survey of recently published methods for determining TNT and related substances, focusing on sensor based procedures.

Table 1. Summary of recent studies dedicated to the detection of TNT, detailing the strategy and technique employed, linear range and limit of detection.

Sensing Platform	Interferents	Technique	Linear Range (mol L^{-1})	LOD (mol L^{-1})	Reference
Molecularly imprinted polydopamine films onto gold electrodes	Trimesic acid, isopthalic acid and 4-nitrophenol	Cyclic Voltammetry	0.1×10^{-9}–10.0×10^{-9}	50.0×10^{-12}	[27]
Carbon paste electrodes modified with MIP particles	Phenol, Aniline, para-Nitrophenol, Benzoic acid and Nitrobenzene	Square-Wave Voltammetry	5.0×10^{-9}–1.0×10^{-6}	1.5×10^{-9}	[28]
Gold nanoparticles/poly (carbazole-aniline) film-modified glassy carbon electrode	Paracetamol-caffeine-based analgesic drug, acetylsalicylic acid (aspirin), sweetener, and sugar	Square-Wave Voltammetry	4.4×10^{-7}–4.4×10^{-6}	1.1×10^{-7}	[29]
Alkanethiols self-assembled on AuNPs modified glassy carbon	Trinitrobenzene, dinitrotoluene and dinitrobenzene	Differential Pulse Voltammetry	4.0×10^{-8}–3.2×10^{-6}	1.3×10^{-8}	[30]
Dummy molecularly imprinted polymers with capped CdTe quantum dots	2,4-dinitrophenol, 4-nitrophenol, phenol, and dinitrotoluene	Fluorescence	0.8×10^{-6}–30.0×10^{-6}	0.28×10^{-6}	[18]
Naphthalene based fluorescent probe	Nitrobenzene, p-Nitrotoluene, Dinitrotoluene, Trinitrophenol, cyclotrimethylenetrinitramine, cyclotetra-methylenetetranitramine and Hexanitrohexaazaisowurtzi-tane	UV–Vis spectroscopy	5×10^{-9}–1×10^{-6}	1.5×10^{-9}	[31]
Amine functionalised nanoparticles	Nitrobenzene, dinitrotoluene and trinitrophenol	Fluorescence	4.4×10^{-11}–4.0×10^{-8}	4.3×10^{-11}	[32]
Fluorescent paper	Nitrobenzene, dinitrotoluene and trinitrophenol	Fluorescence	2.2×10^{-10}–3.1×10^{-8}	1.4×10^{-10}	[33]
MIP functionalised carbon graphite epoxy composite electrodes	Paracetamol, serotonin, tryptamine	Differential pulse voltammetry	1.5×10^{-6}–8×10^{-6}	0.29×10^{-6}	The present work

The presence of TNT and its degradation products in bodies of water has been considered by environmental agencies as a major concern. For example, monitoring, clean-up and adsorption experimental methods are needed, especially in the case of explosive-related compounds, where the legally tolerated levels in ground waters are in the microgram per litre range [34]. Apart from facilities dedicated to the manufacturing, processing and

storage of munitions, TNT can be released into the environment through spills, weapon firing, leaching from inadequately sealed impoundments, or zone demilitarization. TNT has been classified as a probable human carcinogen by the United States Environmental Protection Agency (USEPA) [35]. According to USEPA, TNT in drinking water poses a considerable risk of inducing cancer at concentrations above 0.44 μmol L^{-1} [36]. Thus, there is a need to develop affordable and reliable methods to determine TNT levels, which can be deployed on-field, especially in countries where the access to more sophisticated techniques, e.g., high-performance liquid chromatography (HPLC) or solid-phase extraction and gas chromatography/mass spectrometry (GC/MS), may not be accessible. In the same direction, the electrochemical sensor and polymer synthesis proposed here is easy to conduct in non-specialist laboratories and undemanding to reproduce, due to the cheap and readily available reagents and laboratory apparatus, which is an advantage in cases of resource-limited facilities.

Electrochemical sensors for the detection of nitroaromatic compounds, such as TNT, have been described in the literature in studies that use screen-printed sensors [37,38]; additionally, voltammetric sensors modified with cobalt phtalocyanine [39], carbon fibres [28], carbon nanotubes [40], mesoporous carbon [41] and gold nanoparticles and poly(carbazole-aniline) have been specially electropolymerized to imprint nitroaromatics and nitramines [29]. These electrochemical sensors have special advantages, including their ability to be miniaturised which enables them to be used in portable equipment, making on-field detection in difficult scenarios possible. In the same line, these electrochemical sensors may be also involved in the detection of analytes in water samples without the need for sample pre-treatment, which translates to faster measurements due to the absence of extractions with organic solvents or demanding procedures to clean up and pre-treat the samples.

Although several approaches have been recently reported, see Table 1, with extensive linear ranges and low limits of detection, we think that there has been a persistent, urgent need for a simple, cheap, and robust sensor which is able to detect and quantify TNT and DNP and to identify related substances in a fast and reliable manner in on-field situations.

In this study, the abovementioned purpose was accomplished by a molecularly imprinted polymer for TNT using the TNT analogue 2,4-dinitrophenol (DNP) as a dummy template. Obtained polymers in the form of microbeads were next integrated into graphite epoxy composite (GEC) electrodes in a fast, simple and versatile process, converting insulating polymers in a biomimetic recognition element able to be employed as a reusable voltammetric sensor. Responses of these developed sensors towards TNT and DNP were studied, and the selectivity was evaluated with respect to additional nitroaromatic species which could be interferents in real samples, such as: 1-nitrobenzene (1-NB), 4-nitrotoluene (4-NT), 1,3-dinitrobenzene (1-DNB), 2-nitrotoluene (NT), 2,4-dinitrotoluene (2,4-DNT), and 2,6-dinitrotoluene (2-DNT). At the same time, many of these mono-nitro and dinitroaromatic compounds may be degradation products of energetic materials, which envisages their use in environmental applications [42–44].

The schematic plot of the imprinting process is depicted in Figure 1. The dummy molecularly imprinting approach is shown by replacing the DNP imprinting motif by the TNT as the final analyte.

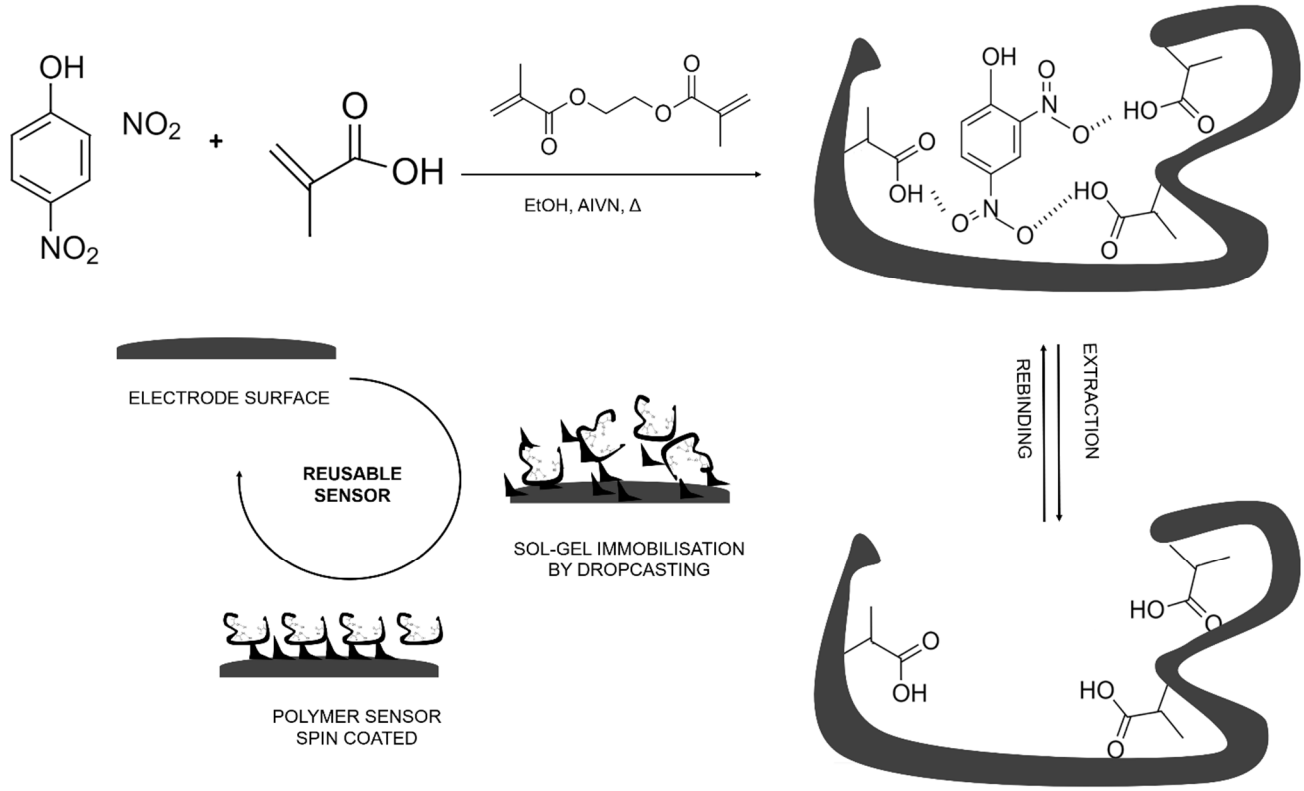

Figure 1. Schematic procedure of polymer imprinting synthesis process employing 2,4-dinitrophenol (DNP) and its immobilization onto the surface sensor.

2. Materials and Methods

2.1. Chemicals and Reagents

Tetramethyl orthosilicate (TEOS), hydrochloric acid, sodium hydroxide, 1,3-dinitrobenzene (DNB), 2-nitrotoluene (NT), 2,4-dinitritoluene (DNT), 2,6-dinitrotoluene and 2,4-dinitrophenol (DNP) were purchased from Merck (Darmstadt, Germany). Ethylene dimethacrylate (EGDMA), methacrylic acid (MAA), 1-nitrobenzene (NB) and 4-nitrotoluene (NT) were supplied by Acros Organics (Geel, Belgium). 2,4,6-trinitrotoluene (TNT) was obtained from LGC standards (Teddington, Middlesex, UK). Methanol (MeOH), ethanol (EtOH) and acetic acid (HAc) were acquired from Scharlab (Barcelona, Spain) and 2,2-azobis(2,4-dimethylvaleronitrile) (AIVN) was purchased from Wako Chemicals GmbH (Neuss, Germany). Graphite powder (particle size < 50 µm) was received from BDH (BDH Laboratory Supplies, Poole, UK) and Resineco Epoxy Kit resin was supplied by Resineco Green Composites (Barcelona, Spain). All reagents used were of analytical reagent grade, and all solutions were made up using MilliQ water from MilliQ System (Millipore, Billerica, MA, USA). The final experimental samples were prepared in phosphate buffer (100 mmol L^{-1} KCl, 50 mmol L^{-1} $K_2HPO_4 \cdot 2H_2O$, 50 mmol L^{-1} KH_2PO_4, pH 7.0).

2.2. Equipment and Software

Imprinted polymers were synthesized in a water bath controlled with a Huber CC1 thermoregulation pump (Huber GmbH, Offenburg, Germany). Polymer beads and polymer-modified electrodes were characterized by scanning electron microscopy (SEM) and FT-IR, employing a MERLIN FE-SEM and an IR Spectrophotometer Tensor 27, Bruker, respectively. The resulting microscopy images were treated with Fiji package software and Image J software [45] (Zeiss GmbH, Jena, Germany). The electrochemical cell for voltammetric measurements employed a commercial 52–61 combined Ag/AgCl reference and counter platinum electrode (Crison Instruments, Barcelona, Spain) and was connected

to an AUTOLAB PGSTAT30 (Ecochemie, Utrecht, The Netherlands) controlled with the GPES Multichannel 4.7 software package. Electrochemical data were plotted using Origin 8.0, whereas PCAs were calculated by the authors using techniques in MATLAB 2016b (MathWorks, Natick, MA, USA).

2.3. Polymer Synthesis

Quantities of 0.5 mmol of DNP and 1.05 mmol of MAA were transferred into a 250 mL round-bottomed flask and dissolved with 40 mL of EtOH. The solution was gently stirred in an ice bath for 30 min. Afterwards, 10.2 mmol of EGDMA and 0.10 mmol of AIVN were added to the solution and the obtained mixture was purged with a flow of dry nitrogen for 15 min. Polymerisation, in bead forms, was initiated in a water bath at 60 °C with magnetic stirring; the obtained polymer was collected after an overnight reaction. After this, the MIP was dried overnight at room temperature, the polymer was transferred into a Soxhlet system, and the template was extracted using a mixture of methanol:acetic acid (9:1) over 72 h. Non-imprinted polymers (NIPs) were prepared following the same methodology, but without the addition of the template molecule.

2.4. Sensor Preparation

The so-called graphite epoxy composite (GEC) electrode was prepared by soldering a 5 mm diameter copper disc into an electrical connector. Then, the connector was placed into a 6 mm inner diameter PVC tube. Afterwards, a mixture of epoxy resin and graphite was prepared in order to allocate the conductive graphite particles into a robust matrix. Once the epoxy graphite resin was added, the sensor was cured for 48 h in an oven at 65 °C. The resulting sensors had a sturdy surface which could be regenerated after a light polishing with sandpaper [46,47] and easily functionalised with several recognition elements [48,49]. Once the bare sensor was prepared, the MIPs were incorporated into the sensor. Once discarded, GEC sensors could be regenerated and reused by repeating the polishing procedure.

2.5. MIP Modification of Electrodes by Sol–Gel Entrapment

The polymers employed herein had an insulator nature; therefore, the proposed strategy was to create a conductive paste which incorporated insulating polymer beads and graphite particles. The polymer beads were allocated into the surface electrode by drop-casting via sol–gel immobilisation. The employed sol–gel was prepared with 0.5 mL of TEOS, 0.5 mL of EtOH, 0.25 mL of H_2O and 25 µL of HCl 0.1 mol L^{-1} which were vigorously stirred for 45 min and then rested for 35 min in order to achieve the optimal polymerisation conditions. Subsequently, 0.2 mL of the rested solution and 7 mg of graphite were added to 40 µL of a 15 mg mL^{-1} polymer (MIP or NIP) suspension in EtOH. This mixture was stirred for 10 min at 1400 rpm. Then, the surface was prepared by spin-coating 10 µL of the polymer solution using a homemade spin-coater. Polymerisation was ended with overnight drying of the electrodes at 4 °C [46,47].

2.6. Characterisation by Scanning Electron Microscopy

In order to prepare the sample for SEM studies, MIP and NIP beads were sprinkled into different aluminium stubs that contained carbon-tape on the surface. Then, the conductive carbon-tapes were metallised, employing a Au–Pd alloy (80:20) for 4 min, which added a 15–20 nm layer onto the sample, which enabled visualisation of the synthesised polymer beads with an adequate contrast. Five SEM images were developed for each kind of polymer (MIPs and NIPs) in order to count at least 500 particles in order to obtain a histogram of both polymers (Figures 2 and S1). Microscopy studies for the electrodes were performed by placing them on the stage and fixing them with carbon tape without employing any kind of metallisation.

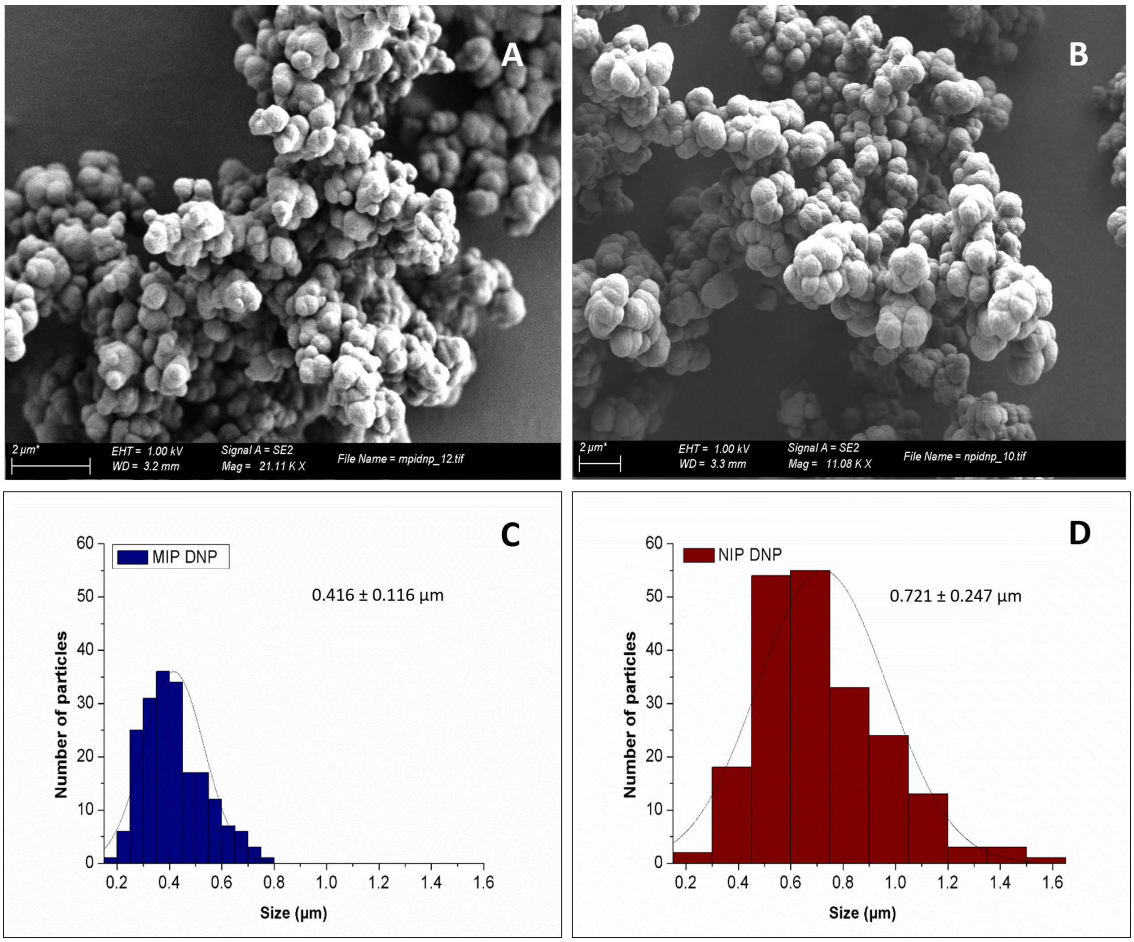

Figure 2. Characterisation of the polymers for MIP (**A**,**C**) and NIP (**B**,**D**): scanning electron microscopy (SEM) with secondary electron (**A**,**B**) and size distribution of the particles (**C**,**D**).

2.7. Electrochemical Measurements

All the electrochemical measurements were performed using the differential pulse voltammetry (DPV) technique. The potential scan window was performed between 0 V and −1.2 V with a scan rate of 100 mV/s, a step potential of 5 mV and a modulation amplitude of 50 mV. No stirring was employed during the measurements. A cleaning step was performed between measurements, applying a potential of +1.4 V for 45 s in NaOH 0.1 mol L^{-1}. According to previous studies in our laboratories, immersion of the electrode into the solution for at least 5 min is desirable to preconcentrate the analyte and to obtain a perceptible signal [2,50]. All stock standard solutions were prepared at 5000 mg L^{-1} in acetonitrile (ACN). All the electrochemical measurements were treated with baseline correction (Figure S5, supplementary data) and all the analytical response calculations were performed for the first peak reduction, around −0.45 V, as suggested in the literature for TNT [25]. The first peak was considered for quantification of all the aforementioned nitro-derived species.

3. Results and Discussion

3.1. MIP Physical Characterisation

Standard acrylic MIP synthesis was adopted in order to obtain the recognition material in beads form. Once the polymers were synthesised and the template was removed, SEM was performed in order to check the morphology of the abovementioned polymers before electrode immobilisation. Obtained MIPs beads showed a non-regular, highly cross-linked material with a spherical shape. Their average size and standard deviation were diameters of 0.416 ± 0.116 µm and 0.721 ± 0.247 µm for MIPs and NIPs, respectively, (Figure 2).

As can be observed, the MIPs presented a slightly smaller particle size in comparison with NIPs. This might suggest that during the synthesis there was more reactivity due to the imprinting, which might be due the template presence.

One of the key steps of the presented protocol is the immobilisation onto the electrode, as can be seen in Figure 3. Materials were deposited by a drop-casting, spin-coating technique via sol–gel immobilisation, as mentioned below, presenting a homogeneous dispersion on the whole surface of the sensors. On the other hand, Figure 3 also shows that the surface of the bare electrode was totally different from the polymer-modified sensors. As can be seen, the surface modification is self-evident; the roughness after sol–gel deposition is very noticeable when comparing unmodified sensors (Figure 3C) with modified sensors (Figure 3A,B). There are no clear differences between MIPs and NIPs: both present a modified surface where the immobilized polymer beads can be seen alongside the sol–gel and graphite.

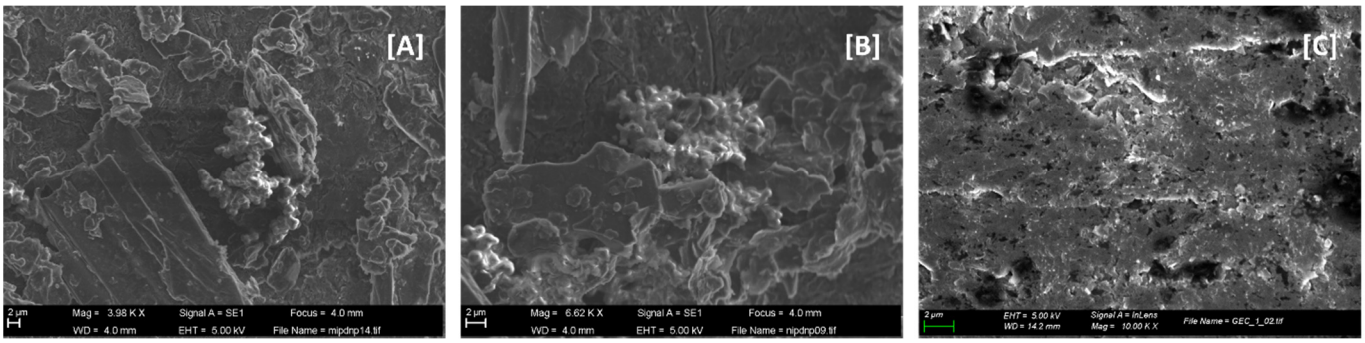

Figure 3. Scanning electron microscopy (SEM) images with secondary electron detector for the MIP-sensor (**A**) and NIP-sensor (**B**) and GEC electrode (**C**).

An FT-IR assay was performed to observe the main chemical bonds. The FT-IR was performed in triplicates of MIP and NIP samples. MIP and NIP polymers showed very similar FT-IR spectra with little or no significant differences (Figure S2). Thus, no differences in the chemical bonds were observed between the different synthesis methodologies. The main bands observed are the broad band of hydroxyl groups around 3430 cm^{-1} from the MMA units; the stretching and bending of methyl groups from the MMA and the EGDMA at the band around 2950–2980 cm^{-1} and 1450–1470 cm^{-1}; the carbonyl stretching at 1720 cm^{-1}; the C–O–C stretching at 1145 and 1250 cm^{-1}; and the rocking of the C–H stretching at 750 cm^{-1}. The peak at 1636 cm^{-1} is associated with C=C bonds, which indicates an incompletely polymerized monomer. Probably, EGDMA was not totally crosslinked.

In the case of MIPs, in which DNP could be retained during the synthesis, the nitro groups showed a strong band around 1550 and 1350 cm^{-1}, corresponding to asymmetric and symmetric stretching, respectively. The absence of a band at 1550 cm^{-1} confirmed the absence of DNP from the polymer. The band at 1390 cm^{-1} could be related to the asymmetric bending of the –OH groups of the carboxylic acid of the MMA units.

The obtained chemical bonding agreed with the expected polymer produced from free radical polymerisation. The slight differences in the wavenumber and peak intensity could be associated with the chemical structure and space distribution due to differences in the synthesis.

3.2. Electrochemical Response

Prior to the evaluation of the electrochemical response, the pH and enrichment times between template sample and sensor were studied and optimised. Stock solutions of 10 µmol L^{-1} for TNT and DNP were employed. The samples were measured with a contact time from 0 to 100 min, and the resultant plots and fittings are shown in Figure S3, in the supplementary information. The evaluated pH ranged from 5 to 8 (Figure S4). pH 7

was chosen because TNT and DNP presented maximum peak intensities at this neutral value. In order to achieve a balance between the increase in signal and speed, plus for simplicity of the method, a contact time of 5 min was chosen, which enabled reaching more than two-thirds of the final response with a reduced analysis time.

In order to study the repeatability of the manufactured sensors, 10 µmol L^{-1} samples of TNT and DNP were measured 15 times with three DNP-MIP-sensors and three DNP-NIP-sensors on the same day. The obtained repeatability values for DNP-MIPs and DNP-NIPS sensors when measuring TNT were 3.97% and 4.61%, respectively. For DNP, the DNP-MIP and DNP-NIP sensors had repeatability values of 9.14% and 7.34%, respectively.

The reproducibility was studied for three DNP-MIP sensors: 10 µmol L^{-1} samples of TNT and DNP were measured five times, obtaining values of 6.5% for TNT and 5.5% for DNP. DNP-MIP sensors' repeatability values against DNP showed slightly better results than TNT, which is explained by the dummy imprinting performed for DNP, as can be seen in Figure 4.

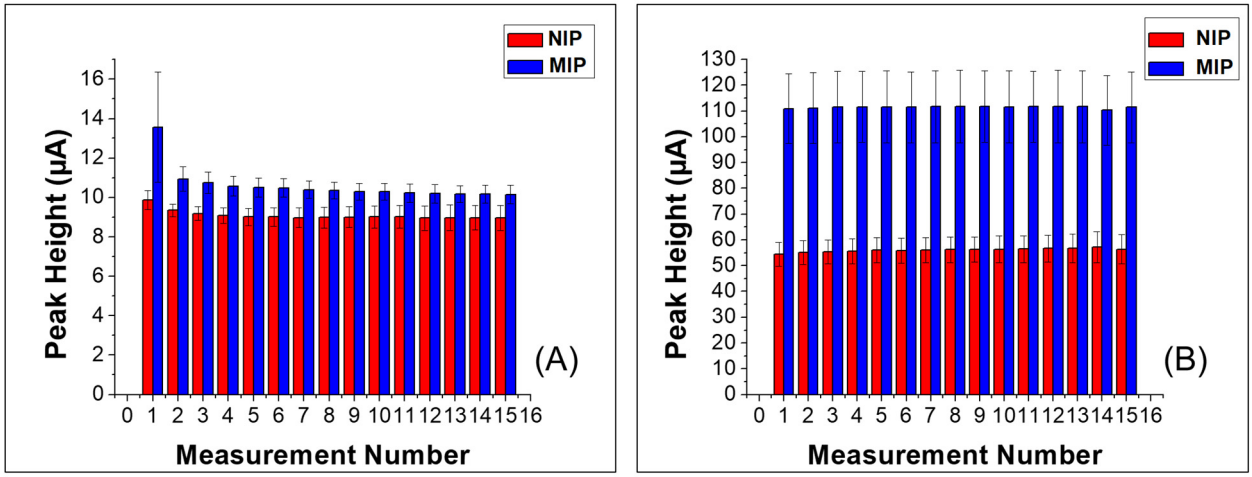

Figure 4. Repeatability measurements of MIP and NIP for (**A**) DNP and (**B**) TNT (n = 3).

The obtained voltammograms for DNP and TNT are presented in Figure 5. DNP has a double reduction peak between −0.4 V and −0.6 V, whereas TNT exhibits three reduction peaks in the same region. The three peaks that TNT presents are due the reduction in the three nitro groups. The first nitro reduction is produced around −0.5 V, and usually presents a sharper and more defined peak; the second nitro group is reduced around −0.65 V; and the last nitro group is around −0.75 V when measured with MIP-functionalised electrodes. It appears that the MIP electrode shifted these reduction peaks to more negative potentials when compared with the NIP electrode, which presented peaks at −0.35 V, −0.55 V and −0.65 V. In the case of DNP, the two nitro reduction peaks appeared at around −0.52 V and −0.68 V for MIP and NIP, respectively, with no apparent shift in potential.

These substances were studied in a concentration range of 0.55 to 19 µmol L^{-1} for DNP and from 0.45 to 10 µmol L^{-1} for TNT.

3.3. Calibration Curves

An MIP sensor, NIP sensor and bare electrode (GEC) were used to compare the voltammetric responses for DNP and TNT in detail, as depicted in Figure 6. Three sensors of each type were used to build the calibration curves on different days. The obtained voltammograms were treated with baseline correction and the first peak was chosen to determine the peak height. To illustrate the processing, the baseline-corrected voltammograms are plotted in Figure S5, in the supplementary information.

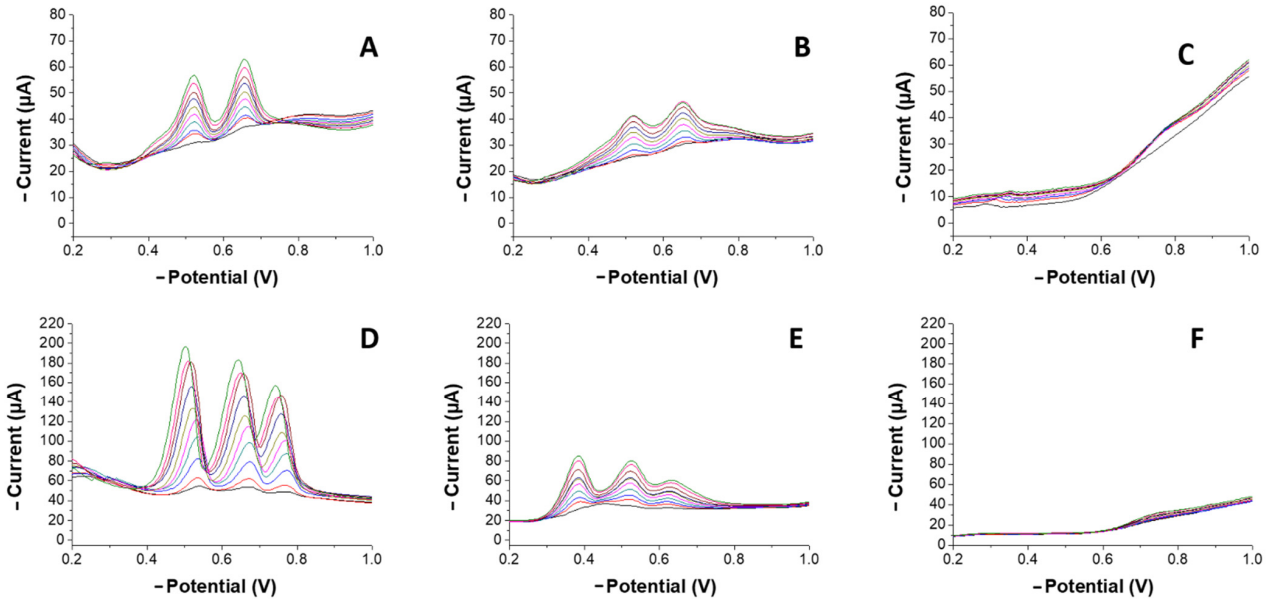

Figure 5. Voltammetric responses from 0.55 to 19 µmol L^{-1} of DNP and from 0.45 to 15 µmol L^{-1} TNT for the prepared sensors (each colour represents an increasing concentration of the corresponding compound). (**A**) Voltammetric response vs. DNP measured with the MIP sensor. (**B**) Voltammetric response vs. DNP measured with the NIP sensor. (**C**) Voltammetric response of DNP measured with the GEC sensor. (**D**) Voltammetric response vs. TNT measured with the MIP sensor. (**E**) Voltammetric response of TNT measured with the NIP sensor. (**F**) Voltammetric response vs. TNT measured with the GEC sensor.

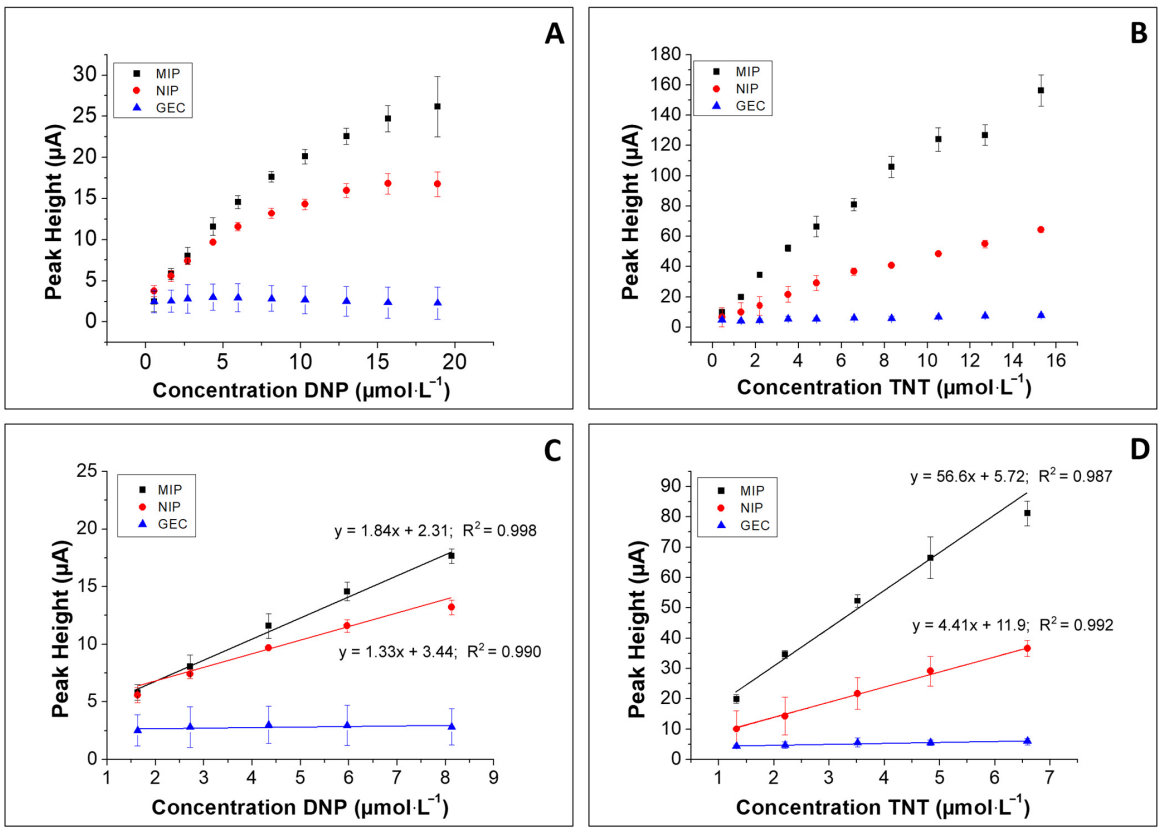

Figure 6. Calibration curves from 0.55 to 19 µmol L^{-1} for DNP (**A**) and from 0.45 to 15 µmol L^{-1} for TNT (**B**) for the three different sensor types used in this study. Linear ranges from 1.6 to 8.0 µmol L^{-1} for DNP and from 1.3 to 6.5 µmol L^{-1} for TNT are added in (**C**,**D**).

In order to obtain LOD values (S/N = 3), the regression lines were fitted with the first five concentration values of the calibration curves, from 1.6 to 8.0 μmol L^{-1} for DNP and 1.3 to 6.5 μmol L^{-1} for TNT, and the linear portions of the calibration curve were used for the calculation. Detailed parameters of the calibration curves are shown in Table 2.

Table 2. Summary of calibration results in the linear concentration region from 1.6 to 8.0 μmol L^{-1} towards DNP and from 1.3 to 6.5 μmol L^{-1} for TNT.

	MIP		**NIP**	
	DNP	TNT	DNP	TNT
Sensitivity (μA μmol^{-1} L)	1.84	56.6	1.33	4.41
Intercept (μA)	2.31	5.72	3.44	11.9
R^2	0.99	0.98	0.99	0.99
LOD (μmol^{-1} L)	0.59	0.29	1.38	0.95
LOQ (μmol^{-1} L)	1.79	0.88	4.18	2.87

As per the results obtained, it may seem that the affinity of the MIP is better for TNT than for DNP. These results may be explained in view of the electrostatic attraction between a bulk polymer and the number of nitro groups borne by each compound: TNT has three groups whereas DNP only has two.

A quick assessment of specificity was performed, verifying the interference effect of three related phenolic compounds, acetaminophen, tryptamine and serotonin, in mixtures with TNT, to check any significant alteration of the voltammetric signals and/or the adsorption abilities of the MIP materials. In all assayed cases (Figure S6, supplementary info), the TNT signals were only minimally affected, demonstrating the accomplished selectivity with the MIP modified devices.

3.4. Specificity versus Other Nitroaromatic Compounds

Other mono-nitro and di-nitro aromatic compounds available in the laboratory were measured five times at the same concentration in order to evaluate the specificity of the imprinted sensor. Examined compounds, in addition to DNP and TNT, were 2,4-dinitrotoluene (2,4-DNT), 2,6-dinitrotoluene (2,6-DNT), 2-nitrotoluene (2-NT), 1,3-dinitrobenzene (1,3-DNB), 4-nitrotoluene (4-NT) and 1-nitrobezene (1-NB). Fixed concentrations of 10 μmol L^{-1} of the corresponding compounds were employed to evaluate the differences in specificity.

As can be seen in Figure 7, current intensities are clearly higher for the MIP sensor when compared with the NIP and GEC sensors for all the evaluated compounds. This higher current may be attributed to the enrichment of electroactive species on the surface electrode due to the imprinted sites.

However, when we examined the specificity, it was evident that TNT exhibited the highest current, followed by the group formed by 2-NT, 2,4-DNT, 1,3-DNB and 2,6-DNT, and finally, in the last group, we observed 4-NT, 1-NB and DNP. These different groups can be explained again by the number of nitro groups present in the molecule. It may seem that a larger number of nitro groups allows a higher concentration on the polymer surface and an increase in the signal intensity.

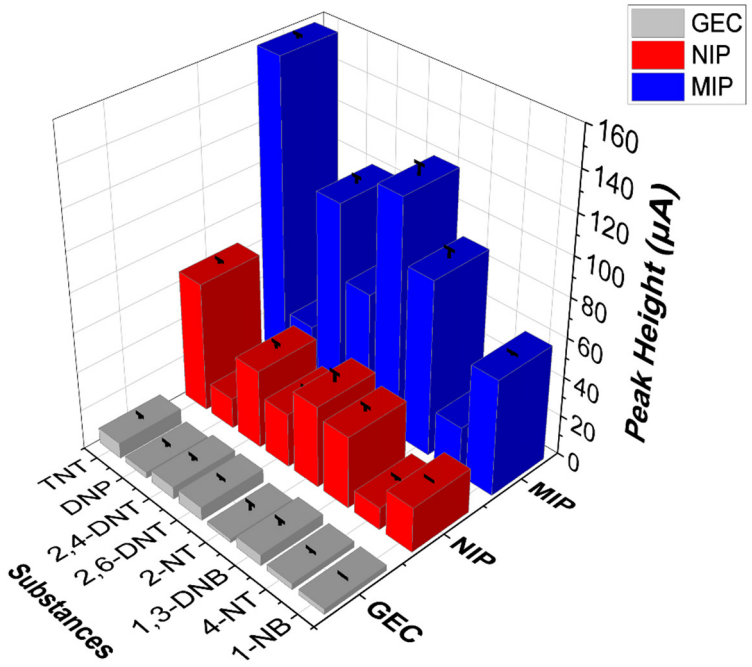

Figure 7. Comparison of voltammetric response of 10 μmol L^{-1} nitroaromatic compounds for each sensor and different nitroaromatic species.

As an additional feature that may be derived from these assays, we foresee possible uses in discriminating the different nitroaromatic compounds in a type of intelligent sensor, for which an exploratory application was attempted. Multivariate analysis of the complete voltammogram employing a principal component analysis (PCA) was performed in order to evaluate whether the voltammetric signals obtained were promising for future studies involving classification and/or quantification of the substances. Five samples for each compound at 10 μmol L^{-1} were measured with the MIP, NIP and GEC sensors (see characteristic voltammogram profiles in the supplementary information, Figure S8). In Figure 8, the scores obtained after the PCA transformation are plotted, and as can be seen, each different compound formed its own cluster in the case of MIP [A], whereas in the case of the NIP sensor [B] and GEC sensor [C], the samples were grouped clearly but with a lower degree of clustering, or did not group at all in the case of the GEC sensor. It is significative that the intended compounds in this study, i.e., DNP and TNT, exhibited distinct clusters, meaning that there is a clear difference in the response obtained from the template (DNP) and the intended analyte (TNT). The remaining compounds considered as possible interferents appeared in clusters more or less together; however, a separation could be seen inside the main "nitroaromatic cluster", and each mono-nitro and di-nitro compound tested enabled its identification. The differences in the PCA results for the compared sensors show that the MIP sensor enabled a better discrimination among the tested nitroaromatic compounds (as can be seen in Figure 8). These results shown by this PCA treatment are a promising starting point to apply a combination of electrochemistry and chemometrics, which is commonly known as Electronic Tongue [51], to identify nitrated compounds in the environmental field.

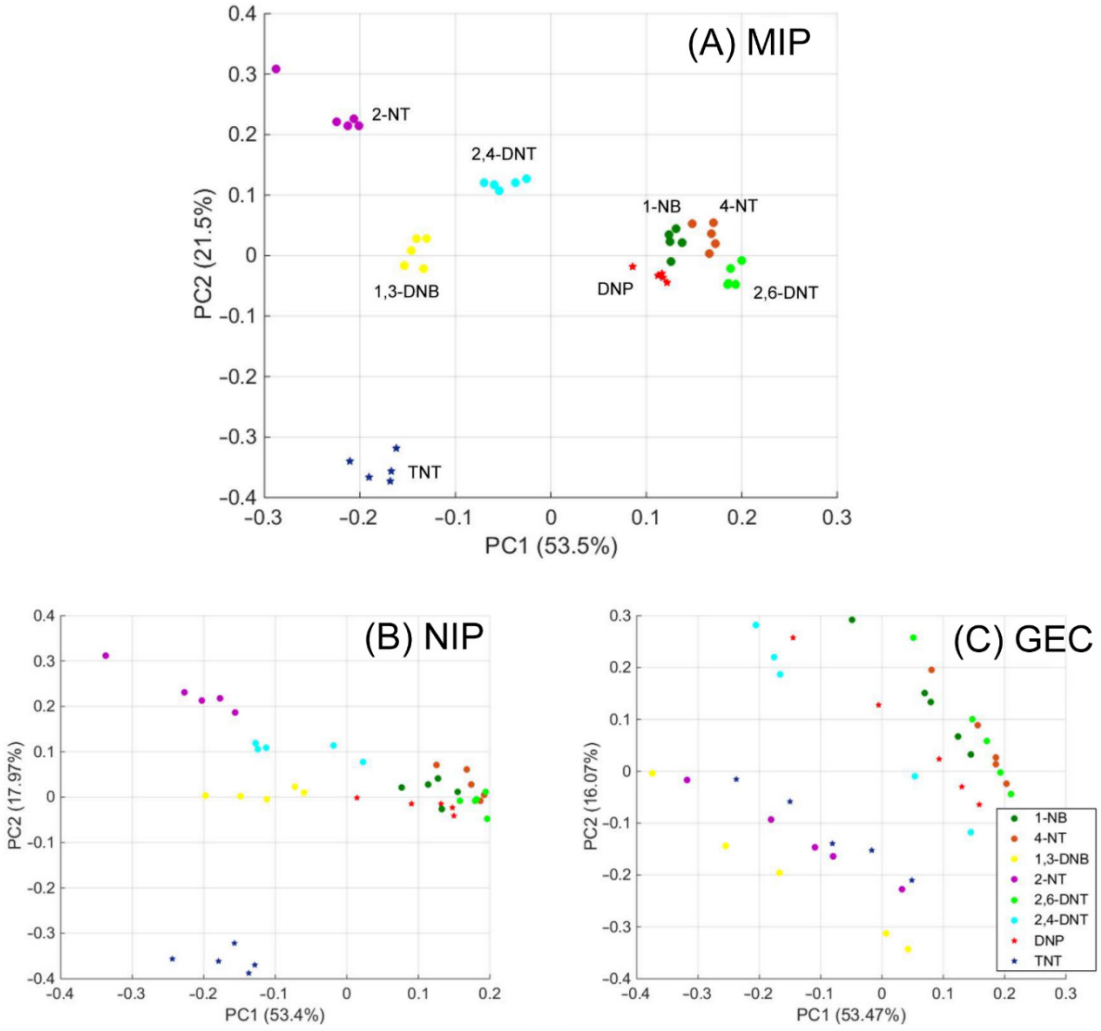

Figure 8. Score plots for each nitroaromatic compound performed with the voltammetric signals of (**A**) MIP, (**B**) NIP and (**C**) GEC sensors for five replicates of each nitroaromatic compound at 10 μmol L^{-1} after principal component analysis.

4. Conclusions

The use of DNP as a dummy template in a biomimetic MIP-based sensor for the determination and discrimination of TNT has been proven to offer a suitable electrochemical response for identification and quantification of the latter. Electron microscopy showed how the spatial distribution of the synthesized MIP was homogeneous within the electrodes modified by spin-coating. The optimisation of the electroanalytical system resulted in a linear response range from 1.6 to 8.0 μmol L^{-1} for DNP and from 1.3 to 6.5 μmol L^{-1} for TNT. Furthermore, a specificity study was carried out in order to discriminate TNT from other nitroaromatic species. The constructed sensory platform was sensitive to TNT, capable of detecting TNT below the concentrations where it is considered a risk, i.e., 0.44 μmol L^{-1}, among other mono, di and tri-nitro compounds that can be found and discriminated as derivate species in polluted surface or underground waters. However, more work is still needed to improve the sensitivity of MIP-GEC sensors while retaining a high selectivity; this is needed as well as choosing the simplest way of increasing the enrichment time by one or more orders of magnitude.

In future studies, the authors intend to apply this approach to build a sensor array with different imprinted polymers and use chemometrics to extract the maximum amount of information from the obtained electrochemical data in the electronic tongue approach [52]. Obtaining such an electronic tongue will hopefully enable the simultaneous quantification and identification of different nitrobenzene species in complex mixtures with enhanced

sensitivity and selectivity features, with remarkable interest specifically in environmental applications.

Supplementary Materials: The following are available online at https://www.mdpi.com/article/10.3390/chemosensors9090255/s1, Figure S1: Representative SEM images employed to determine the polymers' particle sizes for [A] MIP and [B] NIP. Figure S2: Comparison between MIP (red) and NIP (blue) FT-IR spectra. Figure S3: Adsorptive kinetics fitted curves for the different sensor types. Figure S4: [A] pH study for TNT at different pH values; [B] pH study for DNP at different pH vales for the three MIP sensors (n = 3). Figure S5: Voltammetric results with baseline correction responses for the calibration curves. Figure S6: Interferent study at different ratios for TNT versus acetaminophen, serotonin and tryptamine. Figure S7: Schematic representation of different species used into the discrimination study. Figure S8. Differential pulse voltammograms for 10 mol L^{-1} of [A] NB, [B] NT, [C] 1,3-DNB, [D] 2-NT, [E] 2,6-DNT, [F] 2,4-DNT, [G] 2,4-DNP, and [H] TNT employed in the principal component Analysis.

Author Contributions: Conceptualization, M.d.V.; Methodology, M.d.V.; Investigation, A.H.-C., A.G.-C.; A.H.-C. performed the design and synthesis of polymers and the experimental measurements. A.G.-C. performed the calculations for the qualitative modelling. M.d.V.; supervision, M.d.V.; funding acquisition. All authors contributed to the writing, reviewing and editing of the manuscript. All authors have read and agreed to the published version of the manuscript.

Funding: Financial support for this work was provided by the Spanish Ministry of Economy and Innovation, MINECO (Madrid) through project PID2019-107102RB-C21. Manel del Valle thanks the support from program ICREA Academia from Generalitat de Catalunya.

Institutional Review Board Statement: Not applicable.

Informed Consent Statement: Not applicable.

Data Availability Statement: Not applicable.

Acknowledgments: Anna Herrera-Chacon and Andreu González-Calabuig thank Universitat Autònoma de Barcelona (UAB) for the PIF fellowship.

Conflicts of Interest: The authors declare no conflict of interest.

References

1. Liang, C.; Ristic, R.; Jiranek, V.; Jeffery, D.W. Chemical and Sensory Evaluation of Magnetic Polymers as a Remedial Treatment for Elevated Concentrations of 3-Isobutyl-2-methoxypyrazine in Cabernet Sauvignon Grape Must and Wine. *J. Agric. Food Chem.* **2018**, *66*, 7121–7130. [CrossRef]
2. Herrera-Chacon, A.; González-Calabuig, A.; Campos, I.; del Valle, M. Bioelectronic tongue using MIP sensors for the resolution of volatile phenolic compounds. *Sens. Actuators B Chem.* **2018**, *258*, 665–671. [CrossRef]
3. Yola, M.L.; Atar, N. Electrochemical Detection of Atrazine by Platinum Nanoparticles/Carbon Nitride Nanotubes with Molecularly Imprinted Polymer. *Ind. Eng. Chem. Res.* **2017**, *56*, 7631–7639. [CrossRef]
4. Nabavi, S.A.; Vladisavljević, G.T.; Zhu, Y.; Manović, V. Synthesis of Size-Tunable CO2-Philic Imprinted Polymeric Particles (MIPs) for Low-Pressure CO_2 Capture Using Oil-in-Oil Suspension Polymerization. *Environ. Sci. Technol.* **2017**, *51*, 11476–11483. [CrossRef] [PubMed]
5. Jiang, W.; Liu, L.; Chen, Y. Simultaneous Detection of Human C-Terminal p53 Isoforms by Single Template Molecularly Imprinted Polymers (MIPs) Coupled with Liquid Chromatography-Tandem Mass Spectrometry (LC-MS/MS)-Based Targeted Proteomics. *Anal. Chem.* **2018**, *90*, 3058–3066. [CrossRef] [PubMed]
6. Chunta, S.; Suedee, R.; Lieberzeit, P.A. Low-Density Lipoprotein Sensor Based on Molecularly Imprinted Polymer. *Anal. Chem.* **2016**, *88*, 1419–1425. [CrossRef] [PubMed]
7. Turner, A.P.F.; Piletsky, S. Biosensors and Biomimetic Sensors for the Detection of Drugs, Toxins and Biological Agents. In *Defense against Bioterror. NATO Security through Science Series*; Morrison, D., Milanovich, F., Ivnitski, D., Austin, T.R., Eds.; Springer: Dordrecht, The Nerthlands, 2005; pp. 261–272.
8. Huang, Y.; Pan, J.; Liu, Y.; Wang, M.; Deng, S.; Xia, Z. A SPE method with two MIPs in two steps for improving the selectivity of MIPs. *Anal. Chem.* **2019**, *91*, 8436–8442. [CrossRef] [PubMed]
9. Chen, L.; Huang, X. Sensitive Monitoring of Fluoroquinolones in Milk and Honey Using Multiple Monolithic Fiber Solid-Phase Microextraction Coupled to Liquid Chromatography Tandem Mass Spectrometry. *J. Agric. Food Chem.* **2016**, *64*, 8684–8693. [CrossRef]
10. Gómez-Arribas, L.N.; Urraca, J.L.; Benito-Penìa, E.; Moreno-Bondi, M.C. Tag-specific affinity purification of recombinant proteins by using molecularly imprinted polymers. *Anal. Chem.* **2019**, *91*, 4100–4106. [CrossRef]

11. Ben Aissa, A.; Herrera-Chacon, A.; Pupin, R.R.; Sotomayor, M.D.P.T.; Pividori, M.I. Magnetic molecularly imprinted polymer for the isolation and detection of biotin and biotinylated biomolecules. *Biosens. Bioelectron.* **2017**, *88*, 101–108. [CrossRef]
12. Klimuntowski, M.; Alam, M.M.; Singh, G.; Howlader, M.M.R. Electrochemical Sensing of Cannabinoids in Biofluids: A Noninvasive Tool for Drug Detection. *ACS Sens.* **2020**, *5*, 620–636. [CrossRef]
13. Wackerlig, J.; Schirhagl, R. Applications of Molecularly Imprinted Polymer Nanoparticles and Their Advances toward Industrial Use: A Review. *Anal. Chem.* **2016**, *88*, 250–261. [CrossRef] [PubMed]
14. Sun, X.; Wang, J.; Li, Y.; Yang, J.; Jin, J.; Shah, S.M.; Chen, J. Novel dummy molecularly imprinted polymers for matrix solid-phase dispersion extraction of eight fluoroquinolones from fish samples. *J. Chromatogr. A* **2014**, *1359*, 1–7. [CrossRef] [PubMed]
15. Yin, Y.M.; Chen, Y.P.; Wang, X.F.; Liu, Y.; Liu, H.L.; Xie, M.X. Dummy molecularly imprinted polymers on silica particles for selective solid-phase extraction of tetrabromobisphenol A from water samples. *J. Chromatogr. A* **2012**, *1220*, 7–13. [CrossRef] [PubMed]
16. Bagheri, A.R.; Arabi, M.; Ghaedi, M.; Ostovan, A.; Wang, X.; Li, J.; Chen, L. Dummy molecularly imprinted polymers based on a green synthesis strategy for magnetic solid-phase extraction of acrylamide in food samples. *Talanta* **2019**, *195*, 390–400. [CrossRef]
17. McCluskey, A.; Holdsworth, C.I.; Bowyer, M.C. Molecularly imprinted polymers (MIPs): Sensing, an explosive new opportunity? *Org. Biomol. Chem.* **2007**, *5*, 3233–3244. [CrossRef] [PubMed]
18. Xu, S.; Lu, H.; Li, J.; Song, X.; Wang, A.; Chen, L.; Han, S. Dummy molecularly imprinted polymers-capped CdTe quantum dots for the fluorescent sensing of 2,4,6-trinitrotoluene. *ACS Appl. Mater. Interfaces* **2013**, *5*, 8146–8154. [CrossRef]
19. Yılmaz, E.; Garipcan, B.; Patra, H.K.; Uzun, L. Molecular imprinting applications in forensic science. *Sensors* **2017**, *17*, 691. [CrossRef]
20. Zhu, H.; Zhang, H.; Xia, Y. Planar Is Better: Monodisperse Three-Layered MoS2 Quantum Dots as Fluorescent Reporters for 2,4,6-Trinitrotoluene Sensing in Environmental Water and Luggage Cases. *Anal. Chem.* **2018**, *90*, 3942–3949. [CrossRef]
21. Lu, W.; Xue, M.; Xu, Z.; Dong, X.; Xue, F.; Wang, F.; Wang, Q.; Meng, Z. Molecularly Imprinted Polymers for the Sensing of Explosives and Chemical Warfare Agents. *Curr. Org. Chem.* **2015**, *19*, 62–71. [CrossRef]
22. Lu, W.; Li, H.; Meng, Z.; Liang, X.; Xue, M.; Wang, Q.; Dong, X. Detection of nitrobenzene compounds in surface water by ion mobility spectrometry coupled with molecularly imprinted polymers. *J. Hazard. Mater.* **2014**, *280*, 588–594. [CrossRef]
23. Cortada, C.; Vidal, L.; Canals, A. Determination of nitroaromatic explosives in water samples by direct ultrasound-assisted dispersive liquid-liquid microextraction followed by gas chromatography-mass spectrometry. *Talanta* **2011**, *85*, 2546–2552. [CrossRef]
24. Shi, L.; Hou, A.G.; Chen, L.Y.; Wang, Z.F. Electrochemical sensor prepared from molecularly imprinted polymer for recognition of TNT. *Polym. Compos.* **2015**, *36*, 1280–1285. [CrossRef]
25. Wang, J. Electrochemical sensing of explosives. *Electroanalysis* **2007**, *19*, 415–423. [CrossRef]
26. Pesavento, M.; D'Agostino, G.; Alberti, G.; Biesuz, R.; Merli, D. Voltammetric platform for detection of 2,4,6-trinitrotoluene based on a molecularly imprinted polymer. *Anal. Bioanal. Chem.* **2013**, *405*, 3559–3570. [CrossRef] [PubMed]
27. Leibl, N.; Duma, L.; Gonzato, C.; Haupt, K. Polydopamine-based molecularly imprinted thin films for electro-chemical sensing of nitro-explosives in aqueous solutions. *Bioelectrochemistry* **2020**, *135*, 107541. [CrossRef] [PubMed]
28. Alizadeh, T.; Zare, M.; Ganjali, M.R.; Norouzi, P.; Tavana, B. A new molecularly imprinted polymer (MIP)-based electrochemical sensor for monitoring 2,4,6-trinitrotoluene (TNT) in natural waters and soil samples. *Biosens. Bioelectron.* **2010**, *25*, 1166–1172. [CrossRef]
29. Sağlam, Ş.; Üzer, A.; Erçağ, E.; Apak, R. Electrochemical Determination of TNT, DNT, RDX, and HMX with Gold Nanoparticles/Poly(Carbazole-Aniline) Film–Modified Glassy Carbon Sensor Electrodes Imprinted for Molecular Recognition of Nitroaromatics and Nitramines. *Anal. Chem.* **2018**, *90*, 7364–7370. [CrossRef]
30. Nie, D.; Jiang, D.; Zhang, D.; Liang, Y.; Xue, Y.; Zhou, T.; Jin, L.; Shi, G. Two-dimensional molecular imprinting approach for the electrochemical detection of trinitrotoluene. *Sens. Actuators B Chem.* **2011**, *156*, 43–49. [CrossRef]
31. Zhang, Z.; Chen, S.; Shi, R.; Ji, J.; Wang, D.; Jin, S.; Han, T.; Zhou, C.; Shu, Q. A single molecular fluorescent probe for selective and sensitive detection of nitroaromatic explosives: A new strategy for the mask-free discrimination of TNT and TNP within same sample. *Talanta* **2017**, *166*, 228–233. [CrossRef] [PubMed]
32. Ma, Y.; Wang, L. Upconversion luminescence nanosensor for TNT selective and label-free quantification in the mixture of nitroaromatic explosives. *Talanta* **2014**, *120*, 100–105. [CrossRef]
33. Ma, Y.; Li, H.; Peng, S.; Wang, L. Highly Selective and Sensitive Fluorescent Paper Sensor for Nitroaromatic Explosive Detection. *Anal. Chem.* **2012**, *84*, 8415–8421. [CrossRef] [PubMed]
34. Zimmermann, Y.; Broekaert, J.A.C. Determination of TNT and its metabolites in water samples by voltammetric techniques. *Anal. Bioanal. Chem.* **2005**, *383*, 998–1002. [CrossRef] [PubMed]
35. *Drinking Water Standards and Health Advisories*; EPA 822-S-12-001; United States Environmental Protection Agency: Washington, DC, USA, 2012; pp. 1–20.
36. *Technical Fact Sheet—2,4,6-Trinitrotoluene (TNT)*; United States Environmental Protection Agency: Washington, DC, USA, 2014; pp. 1–8.
37. Wang, J.; Lu, F.; MacDonald, D.; Lu, J.; Ozsoz, M.E.S.; Rogers, K.R. Screen-printed voltammetric sensor for TNT. *Talanta* **1998**, *46*, 1405–1412. [CrossRef]

38. Caygill, J.S.; Collyer, S.D.; Holmes, J.L.; Davis, F.; Higson, S.P.J. Disposable screen-printed sensors for the electrochemical detection of TNT and DNT. *Analyst* **2013**, *138*, 346–352. [CrossRef] [PubMed]
39. Caygill, J.S.; Collyer, S.D.; Holmes, J.L.; Davis, F.; Higson, S.P.J. Electrochemical Detection of TNT at Cobalt Phthalocyanine Mediated Screen-Printed Electrodes and Application to Detection of Airborne Vapours. *Electroanalysis* **2013**, *25*, 2445–2452. [CrossRef]
40. Wang, J.; Hocevar, S.B.; Ogorevc, B. Carbon nanotube-modified glassy carbon electrode for adsorptive stripping voltammetric detection of ultratrace levels of 2,4,6-trinitrotoluene. *Electrochem. Commun.* **2004**, *6*, 176–179. [CrossRef]
41. Zang, J.; Guo, C.X.; Hu, F.; Yu, L.; Li, C.M. Electrochemical detection of ultratrace nitroaromatic explosives using ordered mesoporous carbon. *Anal. Chim. Acta* **2011**, *683*, 187–191. [CrossRef] [PubMed]
42. Yu, J.; Wang, X.; Kang, Q.; Li, J.; Shen, D.; Chen, L. One-pot synthesis of a quantum dot-based molecular imprinting nanosensor for highly selective and sensitive fluorescence detection of 4-nitrophenol in environmental waters. *Environ. Sci. Nano* **2017**, *4*, 493–502. [CrossRef]
43. Saloni, J.; Walker, K.; Hill, G. Theoretical investigation on monomer and solvent selection for molecular imprinting of nitrocompounds. *J. Phys. Chem. A* **2013**, *117*, 1531–1534. [CrossRef] [PubMed]
44. Lopez-Nogueroles, M.; Lordel-Madeleine, S.; Chisvert, A.; Salvador, A.; Pichon, V. Development of a selective solid phase extraction method for nitro musk compounds in environmental waters using a molecularly imprinted sorbent. *Talanta* **2013**, *110*, 128–134. [CrossRef] [PubMed]
45. Schindelin, J.; Arganda-Carreras, I.; Frise, E.; Kaynig, V.; Longair, M.; Pietzsch, T.; Preibisch, S.; Rueden, C.; Saalfeld, S.; Schmid, B.; et al. Fiji: An open-source platform for biological-image analysis. *Nat. Methods* **2019**, *9*, 676–682. [CrossRef] [PubMed]
46. Olivé-Monllau, R.; Baeza, M.; Bartrolí, J.; Céspedes, F. Novel amperometric sensor based on rigid near-percolation composite. *Electroanalysis* **2009**, *21*, 931–938. [CrossRef]
47. Alegret, S.; Alonso, J.; Bartrolí, J.; Céspedes, F.; Martínez-Fàbregas, E.; del Valle, M. Amperometric biosensors based on bulk-modified epoxy graphite biocomposites. *Sens. Mater.* **1996**, *8*, 147–153.
48. Aceta, Y.; del Valle, M. Graphene electrode platform for impedimetric aptasensing. *Electrochim. Acta* **2017**, *229*, 458–466. [CrossRef]
49. Ocaña, C.; del Valle, M. Signal amplification for thrombin impedimetric aptasensor: Sandwich protocol and use of gold-streptavidin nanoparticles. *Biosens. Bioelectron.* **2014**, *54*, 408–414. [CrossRef]
50. Herrera-Chacón, A.; Dinç-Zor, Ş.; del Valle, M. Integrating molecularly imprinted polymer beads in graphite-epoxy electrodes for the voltammetric biosensing of histamine in wines. *Talanta* **2020**, *208*, 120348. [CrossRef]
51. Ciosek, P.; Wróblewski, W. Sensor arrays for liquid sensing—Electronic tongue systems. *Analyst* **2007**, *132*, 963–978. [CrossRef]
52. Del Valle, M. Electronic Tongues Employing Electrochemical Sensors. *Electroanalysis* **2010**, *22*, 1539–1555. [CrossRef]

Dummy Molecularly Imprinted Polymers Using DNP as a Template Molecule for Explosive Sensing and Nitroaromatic Compound Discrimination

Anna Herrera-Chacon, Andreu Gonzalez-Calabuig and Manel del Valle *

Sensors and Biosensors Group, Department of Chemistry, Universitat Autònoma de Barcelona, Edifici Cn, Bellaterra, 08193 Barcelona, Spain; anna.herrera@uab.cat (A.H.-C.); andreugc27@gmail.com (A.G.-C.)
* Correspondence: manel.delvalle@uab.cat

Supplementary Information

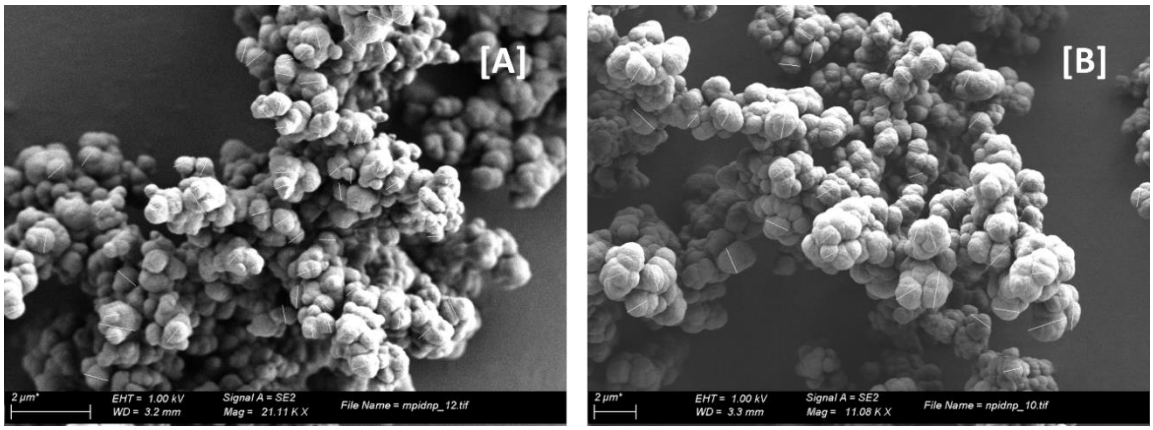

Figure S1. Representative SEM images employed to determine the polymers particle size for [**A**] MIP and [**B**] NIP. As can be seen in the figures each counted particles has a measurement line (light grey) that the employed software will process in order to obtain the histograms.

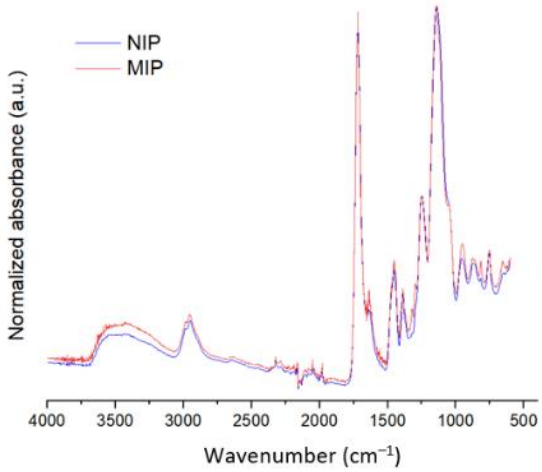

Figure S2. Comparison between the synthetised MIP (red) and NIP (blue) FT-IR spectra.

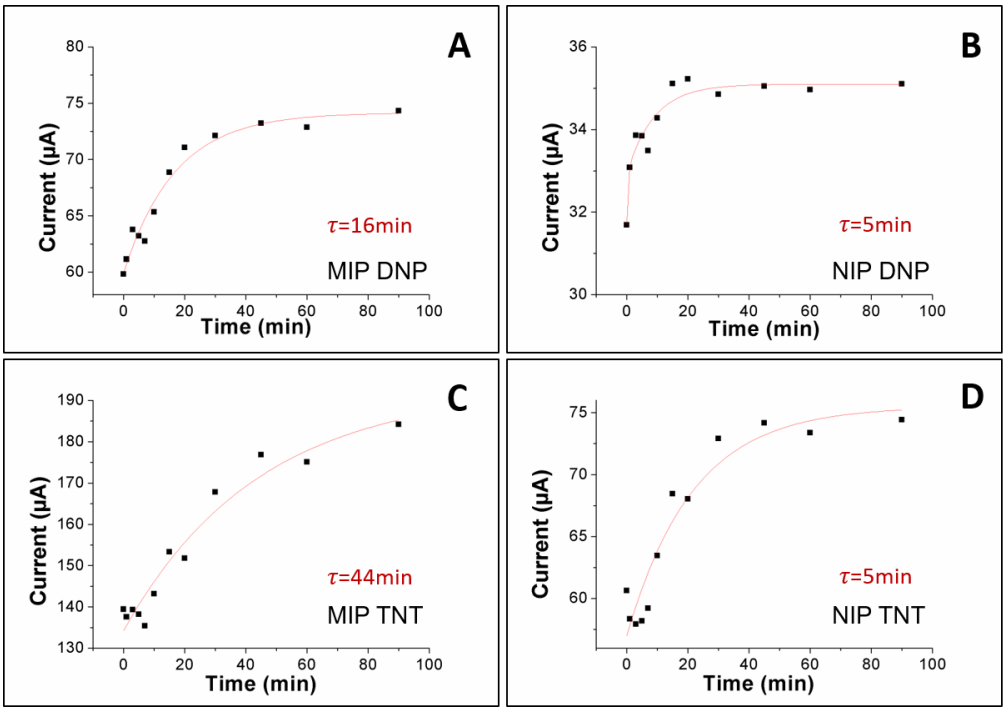

Figure S3. Adsorptive kinetics fitted curves for MIPs-sensors (**A**,**C**) and NIPs-sensors (**B**,**D**) from 0 to 100 min when measuring a stock solution of 15 μmol L^{-1} for DNP and TNT.

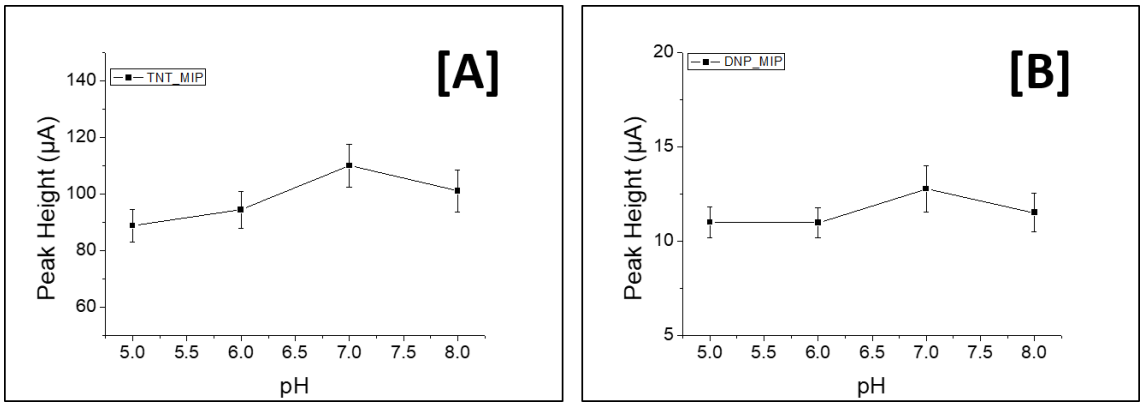

Figure S4. [**A**] pH study for TNT at different pH [**B**] pH study for DNP at different pH for three MIP sensors (n=3).

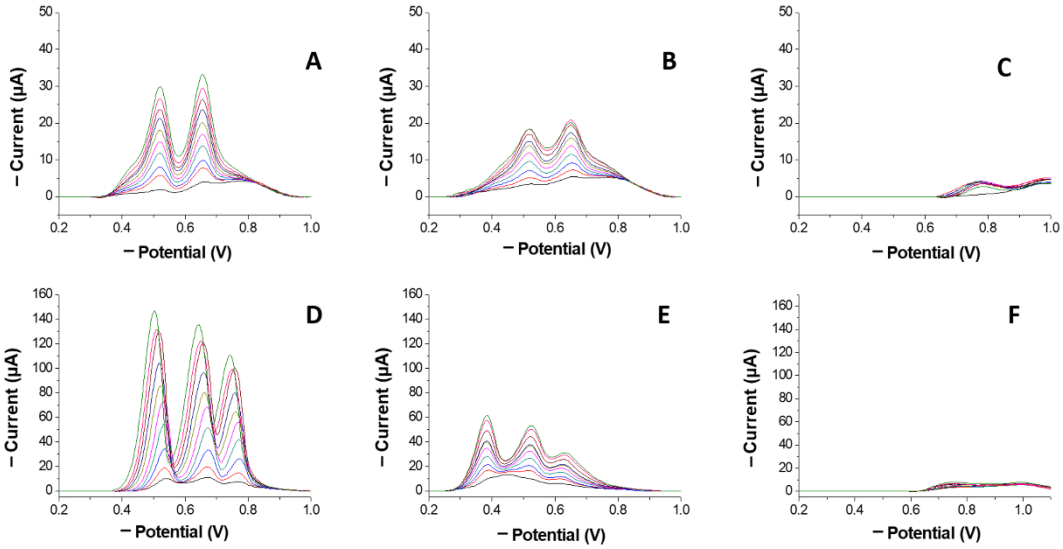

Figure S5. Voltammetric with baseline correction responses from 0.55 to 19 µmol L^{-1} of DNP and from 0.45 Table 15. µmol L^{-1} TNT for the different sensors (each color represents an increasing concentration of the corresponding compound). **A)** Voltammetric response *vs.* DNP measured with the MIP sensor. **B)** Voltammetric response *vs.*DNP measured with the NIP sensor. **C)** Voltammetric response *vs.*DNP measured with GEC sensor. **D)** Voltammetric response *vs.*TNT measured with the MIP sensor. **E)** Voltametric response *vs.*TNT measured with the NIP sensor. **F)** Voltammetric response *vs.*TNT measured with the GEC sensor.

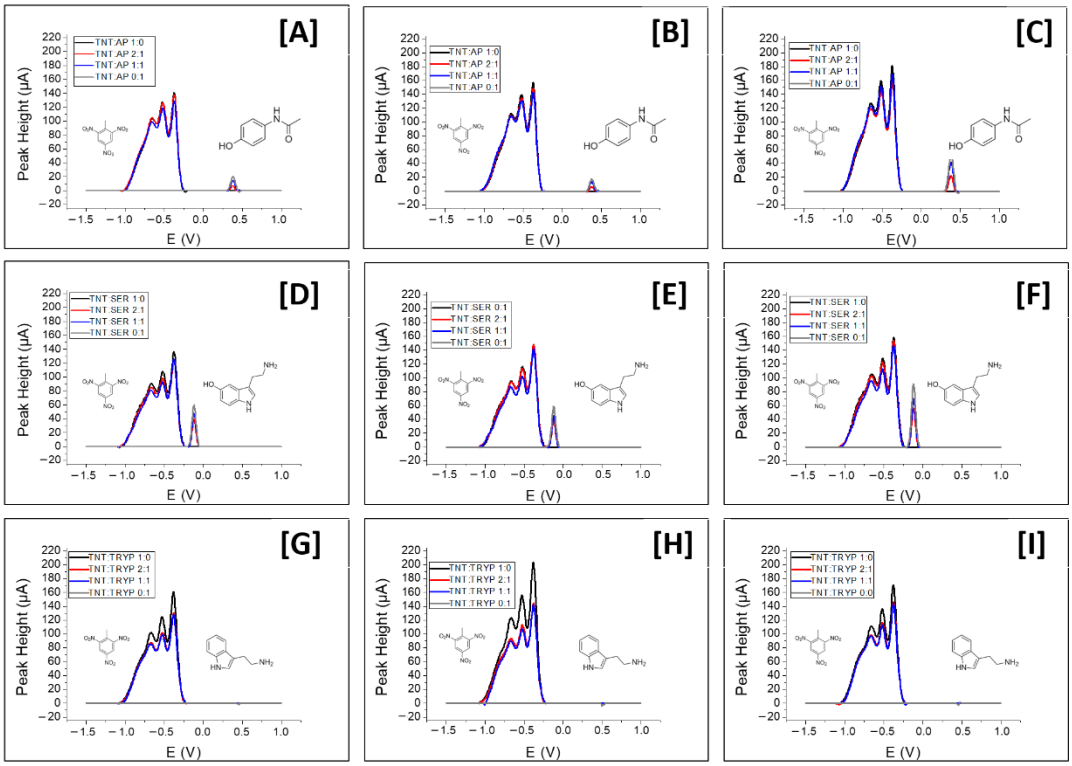

Figure S6. Interferent study at different ratios for TNT versus acetaminophen, serotonin and tryptamine. Table 1. [**A**], sensor 2 [**B**] and sensor 3[**C**]. TNT and serotonin are showed in the first row for sensor 1 [**D**], sensor 2 [**E**] and sensor 3[**F**]. TNT and tryptamine are showed in the first row for sensor 1 [**G**], sensor 2 [**H**] and sensor 3[**I**].

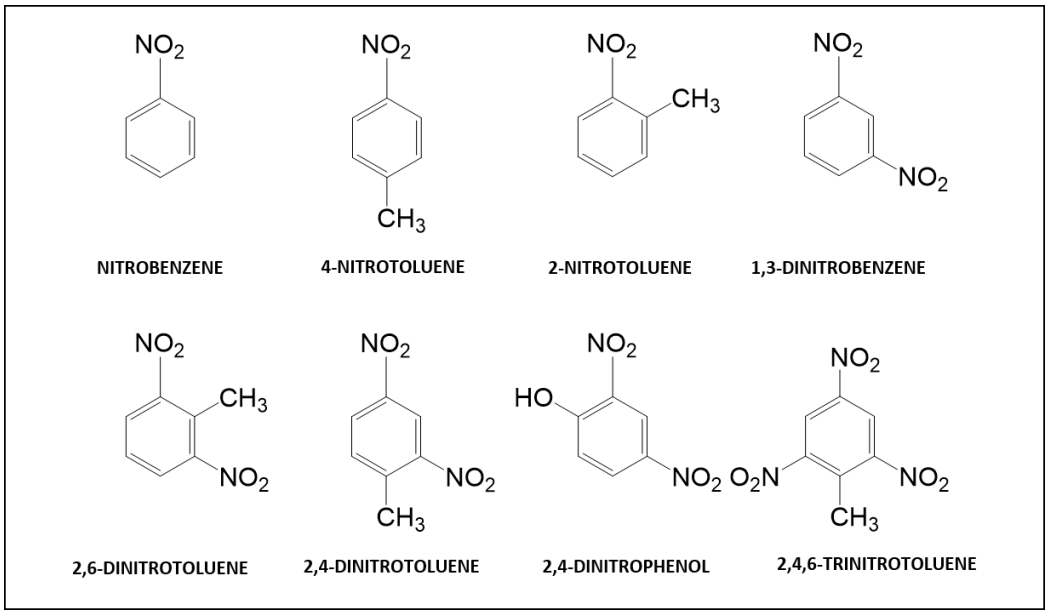

Figure S7. Schematic representation of different species used into the discrimination study.

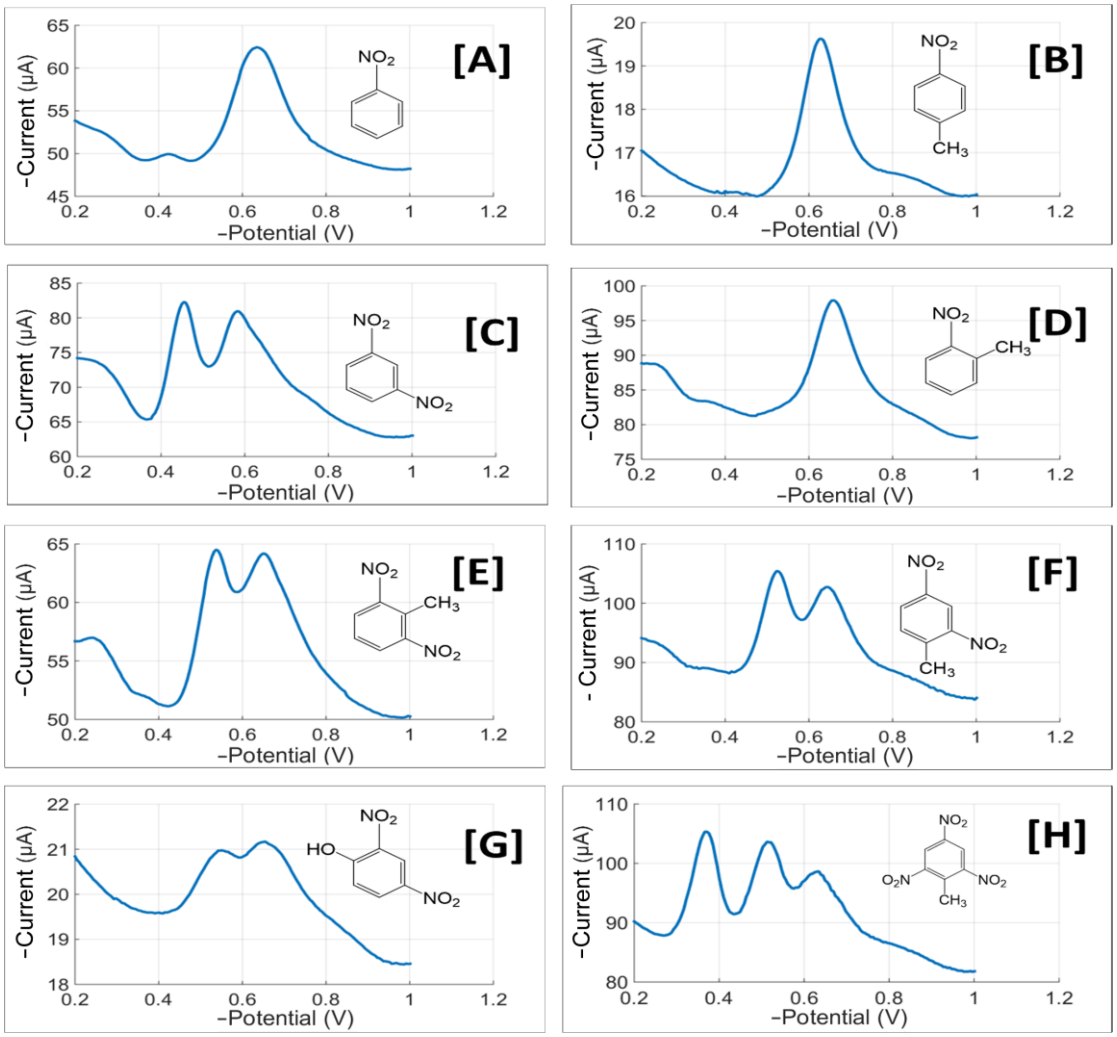

Figure S8. Differential pulse voltammograms for 10 mol L^{-1} of [**A**] NB [**B**] NT [**C**] 1,3-DNB, [**D**] 2-NT, [**E**] 2,6-DNT, [**F**] 2,4-DNT, [**G**] 2,4-DNP, [**H**] TNT employed in the discrimination study of nitroaromatic compounds.